Naoto Nagaosa

Born 1958 Feb. 21 Male
Nationality: Japanese

Education
1980 Graduate from the Department of Applied Physics, The University of Tokyo
1986 Ph.D Physics, The Univ. Tokyo

Job
1983 Research associate Theory division
Institute for Solid State Physics, Univ. Tokyo
1988-1990 Post Doctoral Fellow Physics Department MIT
1991 Associate Professor Dept. Applied Physics, Univ. Tokyo
1998- Professor Dept. Applied Physics, Univ. Tokyo
2007- also Team Leader, ASI, RIKEN

Research interest -- Condensed matter theory
Strongly correlated electronic systems
(gauge theory of high Tc superconductors, CMR manganites,
quantum spin system, spin textures)
Spintronics (spin-orbit interaction, anomalous Hall effect, spin Hall effect)
Quantum transport (localization, Tomonaga-Luttinger liquid)

Topological aspects of electronic states in solids
- Gauge fields in condensed matter physics -

Aug 15-17, 2012@FIRST-QIPP

Naoto Nagaosa
Department of Applied Physics
The University of Tokyo
and
CMRG,CERG, ASI, RIKEN

Plan of this lecture

1. Introduction
   - Berry phase
   - Haldane problem in 1D antiferromagnet

2. Topological Hall effects
   - Quantum Hall effect, Anomalous Hall effect
   - Spin Hall effect, Hall effect of light
   - Magnon Hall effect

3. Topological materials
   - Topological insulators
   - Topological superconductors
   - Topological periodic table

4. Physics of non-collinear spin structures
   - Multiferroics
   - Spin textures
   - Skyrmions

Why topology matters ?

1. Gauge structure of electrons in solids

   electron wavefunction is often "constrained" in sub-Hilbert space → connection and curvature

2. Two sources of "conservation law"

   symmetry is related to conservation – Noether

   topological index and quantum protectorate




Symmetry v.s. Topology

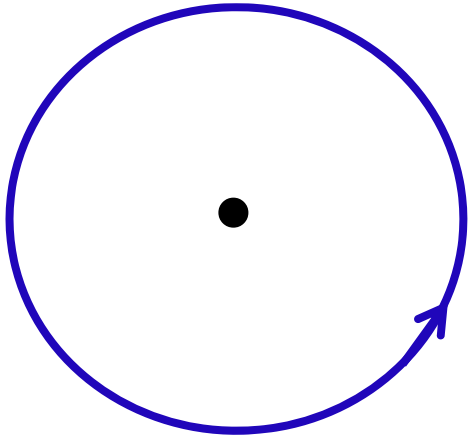

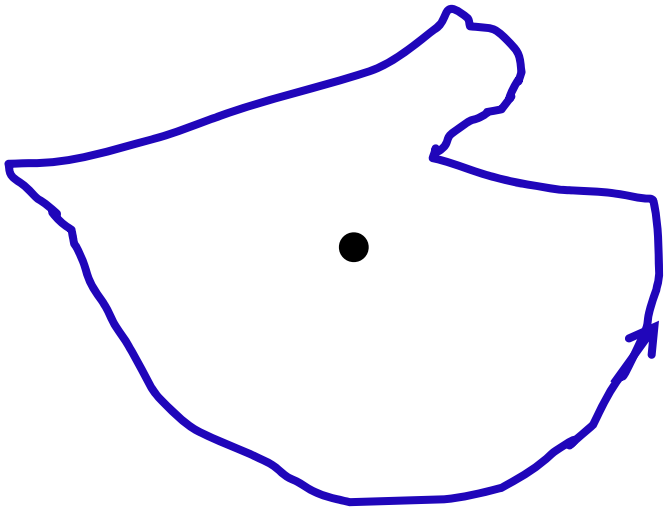

Rotational symmetry

⇩

Noether's theorem

⇩

Conservation of L_z

Winding number N_w

⇩

Connectivity of the loop

⇩

Conservation of N_w

Introduction

From Ryogo Kubo “Progress in Solid State Physics” 1962

Before “atomism”
-19th century

Mechanics — elasticity
Electromagnetism — Maxwell equation
e.m. properties of materials
Thermodynamics — gas/solution metallurgy
Crystallography — Bravais (1848), space group
Optics

Atomism
Late 19th cen.

Statistical mechanics — Maxwell, Boltzmann, Gibbs
electron (Lorentz) theory of metals
Puzzles : thermal radiation, Palmer series, specific heat

20th century
1900-1925

1905 Special relativity, 1915 General relativity
Planck (h) , Einstein (photon, specific heat) , Bohr (atom model)
Low temp. phys. Onnes (Liquid He 1908, Superconductivity 1911)
Laue, Bragg (X-ray crystallography 1912)
Born (Lattice dynamics 1915)

1925-1940 Quantum mechanics Schroedinger, Heisenberg
chemical bonds, metallic bonds
1927- Quantum field theory
1940 Seitz Modern Theory of Solids

1941-1945 World War II
Quantum electro-dynamics (Tomonaga, Feynman, Schwinger)

1945 Magnetic resonance
1947 Transistor
1953 Laser
1957 BCS, Kubo formula
1958 Anderson localization
1959 Super-exchange interaction, Anderson, Kanamori-Goodenough
1962 Josephson effect
1964 Kondo effect, DFT
1970- Renormalization group critical phenomena
Synthetic metals polyacethylene soliton
Charge/spin density wave

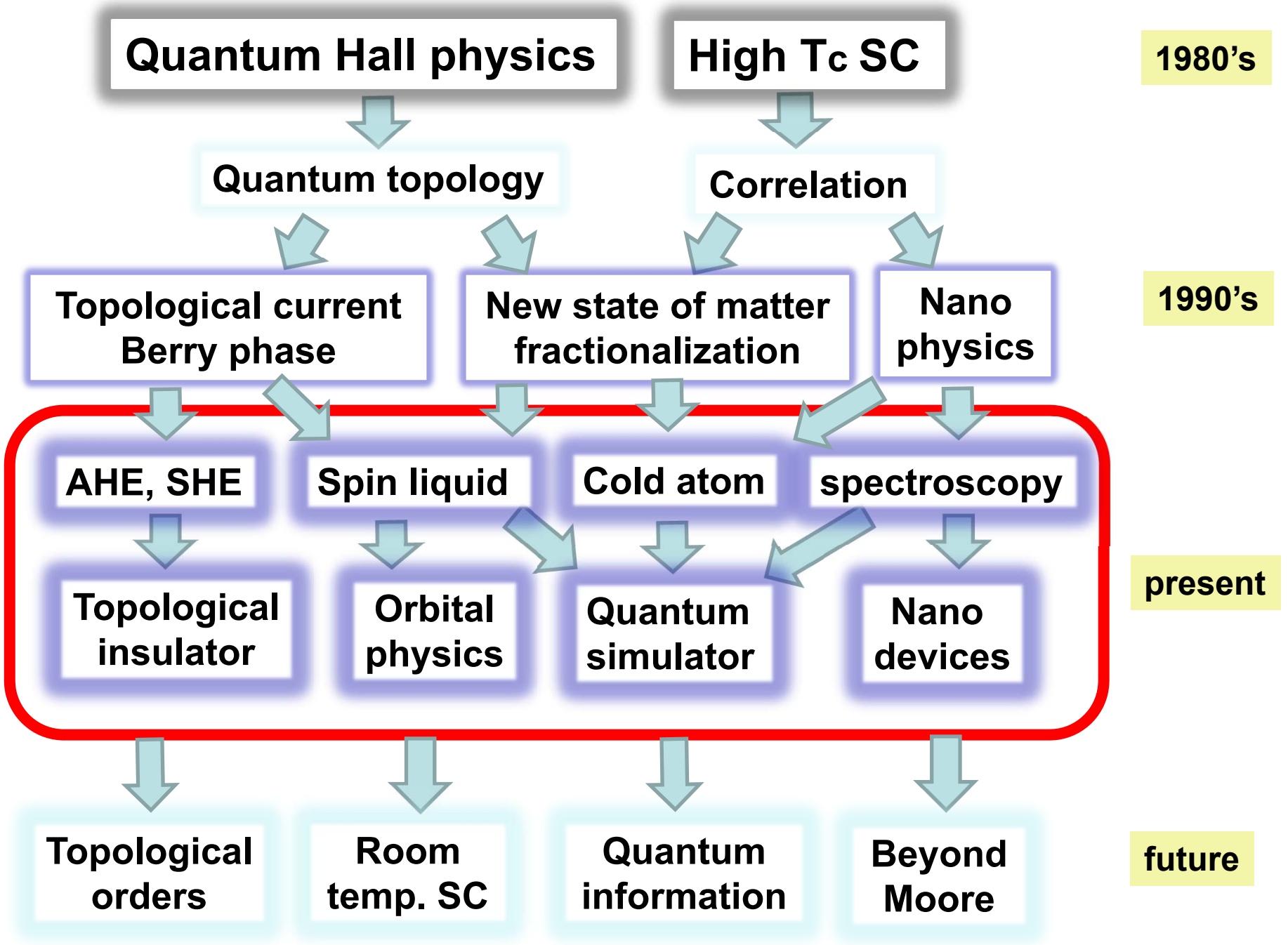
Quantum Hall physics
High Tc SC
1980's
Quantum topology
Correlation
Topological current
Berry phase
New state of matter
fractionalization
Nano
physics
1990's
AHE, SHE
Spin liquid
Cold atom
spectroscopy
Topological
insulator
Orbital
physics
Quantum
simulator
Nano
devices
present
Topological
orders
Room
temp. SC
Quantum
information
Beyond
Moore
future

Berry Phase

Berry phase

M.V.Berry, Proc. R.Soc. Lond. A392, 45(1984)

$H(X)$ Hamiltonian,

$X = (X_1, X_2, , , X_n)$ Parameters → adiabatic change

$$i\hbar\partial_t \psi(t) = H(X(t))\psi(t)$$

$$H(X)\phi_n(X) = E_n(X)\phi_n(X)$$

eigenvalue and eigenstate for each parameter set X

Transitions between eigenstates are forbidden during the adiabatic change

→ Projection to the sub-space of Hilbert space constrained quantum system

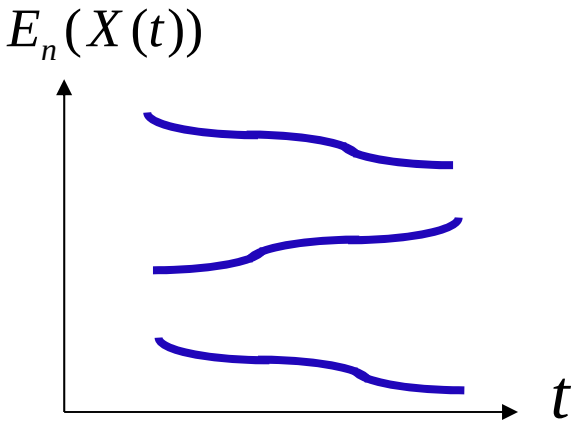

Berry phase

M.V.Berry, Proc. R.Soc. Lond. A392, 45(1984)

$$i\hbar\partial_t\psi(t) = H(X(t))\psi(t)$$

$$H(X)\phi_n(X) = E_n(X)\phi_n(X)$$

$$\psi(t) = e^{i\gamma_n(t)}e^{-(i/\hbar)\int_0^t dt' E_n(X(t'))}\phi_n(X(t))$$

$$\Rightarrow \quad \frac{d\gamma_n(t)}{dt} = i < \phi_n(X(t)) | \frac{\partial\phi_n(X(t))}{\partial X} > \cdot \frac{dX(t)}{dt}$$

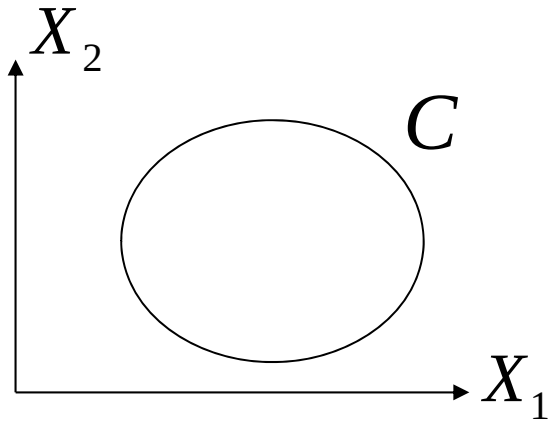

$$\psi(T) = e^{i\gamma_n(C)}e^{-(i/\hbar)\int_0^T dt E_n(X(t))}\psi(0)$$

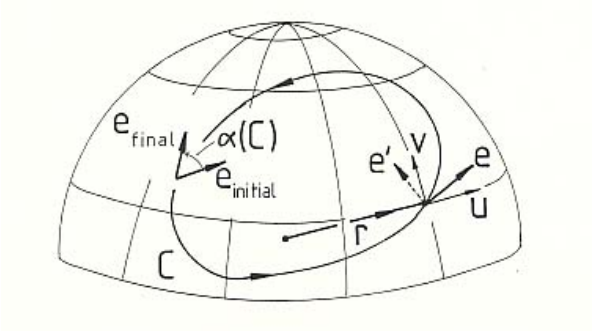

$$\gamma_n(C) = i\oint_C dX \bullet < \phi_n(X) | \nabla_X \phi_n(X) >$$

$$= \oint_C dX \bullet A_n(X) = \int\int dS \bullet B_n(X)$$

Berry Phase

Connection of the wave-function in the parameter space

→Berry phase curvature

Path integral and Aharonov-Bohm effect

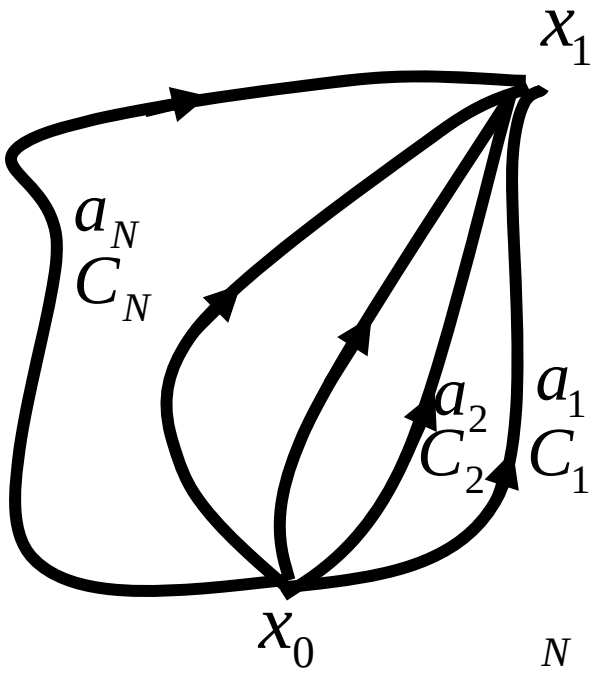

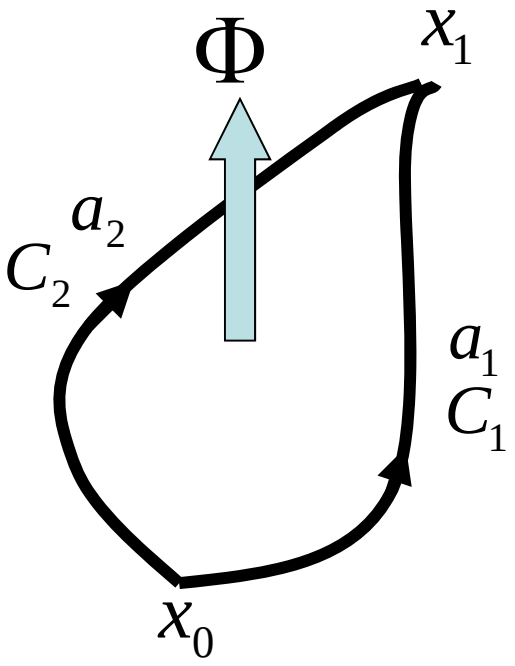

Amplitude from A to B $= \sum_{j=1}^{N} a_j$

$$a_1^* a_2 \,|_{\Phi} = a_1^* a_2 \,|_{\Phi=0}\; e^{ie\Phi/c\hbar}$$

$$r \Rightarrow r, k, X_1, X_2, \cdots, X_n$$

Generalized space

Berry Phase

Berry phase of 2x2 system - a spin

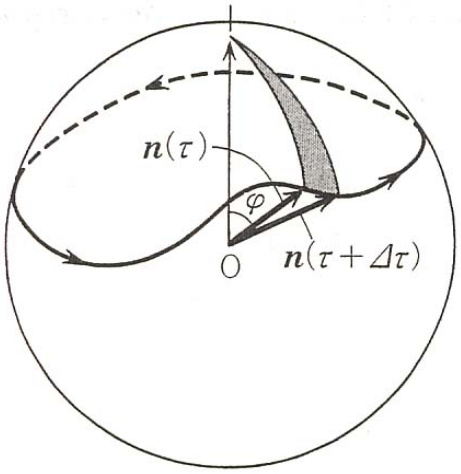

$$Z = \int D\vec{n}(\tau) \exp[-A(\{\vec{n}(\tau)\})]$$

$$|\vec{n}(\tau)> = [\cos(\theta(\tau)/2), e^{i\phi(\tau)} \sin(\theta(\tau)/2)]$$

$$A = \int_0^\beta d\tau [< \vec{n}(\tau) | \frac{d}{d\tau} | \vec{n}(\tau) > + \int_0^\beta d\tau < \vec{n}(\tau) | H | \vec{n}(\tau) >$$

$$A = iS \int_0^\beta d\tau (1 - \cos\theta(\tau)) \dot{\phi}(\tau) + \int_0^\beta d\tau H(\vec{n}(\tau))$$

$$= iS\omega$$

Berry phase
= solid angle enclosed by the path

$$\delta\omega = iS \int_0^\beta d\tau \delta\vec{n}(\tau) \cdot \left[\frac{d\vec{n}(\tau)}{d\tau} \times \vec{n}(\tau) \right]$$

$$S \frac{d\vec{n}(t)}{dt} = \vec{n}(t) \times \frac{\partial H(\vec{n}(t))}{\partial \vec{n}(t)}$$

Dirac Magnetic monopole

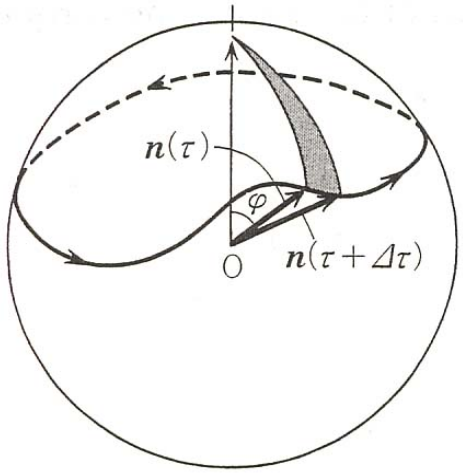

$$\vec{B}(\vec{n}) = S\frac{\vec{n}}{|\vec{n}|^3} = \nabla_{\vec{n}} \times \vec{A}(\vec{n})$$ Berry curvature

$$\vec{A}_I(\vec{n}) = \left[\frac{S(1-\cos\theta)}{n\sin\theta}\right]\hat{\phi} \qquad \vec{A}_{II}(\vec{n}) = -\left[\frac{S(1+\cos\theta)}{n\sin\theta}\right]\hat{\phi}$$

Berry connection

$$\vec{A}_{II}(\vec{n}) - \vec{A}_I(\vec{n}) = -\left[\frac{2S}{n\sin\theta}\right]\hat{\phi} = \nabla_{\vec{n}}\Lambda(\vec{n})$$

connected by gauge tr.

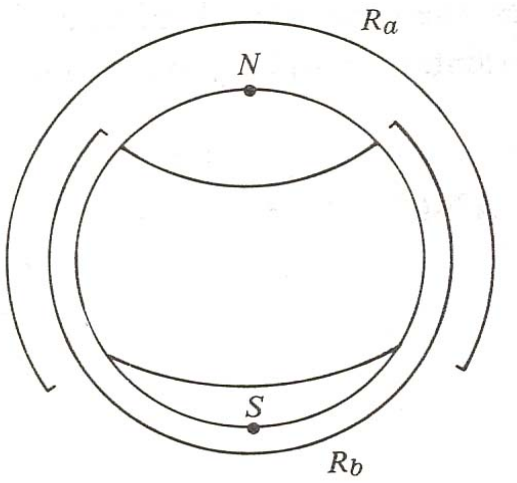

$$\Delta[\Lambda(\vec{n})]_C = 4\pi S = 2\pi \times \text{integer}$$

Dirac quantization condition

Yang-Wu construction

Haldane problem

1D quantum antiferromagnet - Haldane gap problem

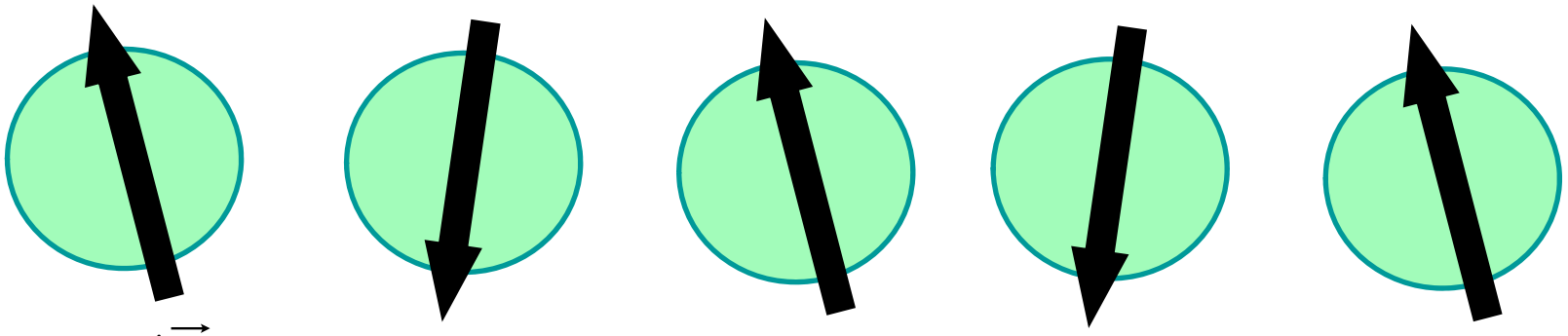

$$\vec{n}_i = (-1)^i \vec{\Omega}(x_i)$$

$$A_{Berry} = iS \sum_{i=1,2N} \omega(\vec{n}_i) = iS \sum_{i=1,2N} (-1)^i \omega(\vec{\Omega}(x_i)) = iS \sum_{k=1,N} [\omega(\vec{\Omega}(2ka)) - \omega(\vec{\Omega}((2k-1)a))]$$

$$= i\frac{S}{2}\int_0^\beta d\tau \int dx \frac{\partial\vec{\Omega}(x,\tau)}{\partial\tau} \times \vec{\Omega}(x,\tau) \cdot \frac{\partial\vec{\Omega}(x,\tau)}{\partial x} = 2\pi Q$$

Q : Skymion number

How many times the mapping wraps the unit sphere

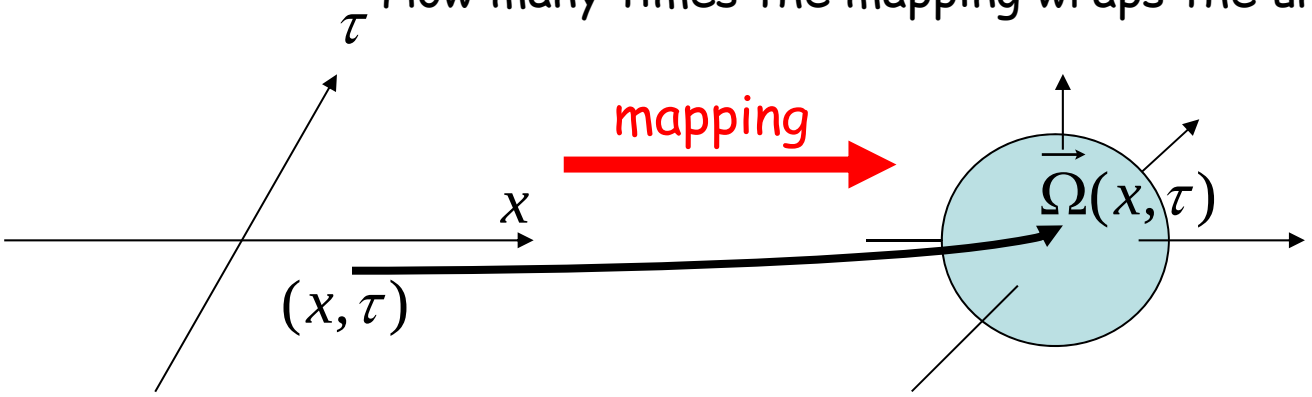

Gauge theory of 1D quantum antiferromagnet

$$A = i2\pi SQ + \int d\tau dx \frac{1}{g} |\partial_\mu \vec{\Omega}|^2$$ Non-linear sigma model

$$\vec{\Omega} = z^* \vec{\sigma} z \qquad z = (z_\uparrow, z_\downarrow) \qquad |z_\uparrow|^2 + |z_\downarrow|^2 = 1$$

$$L = i \frac{\theta}{2\pi} \varepsilon^{\mu\nu} \partial_\mu a_\nu + \frac{1}{g} |(\partial_\mu - i a_\mu) z_\sigma|^2$$ 1D QED with $\theta = 2\pi S$

$$a_\mu = i z_\sigma^* \partial_\mu z_\sigma$$ Emergent Gauge field

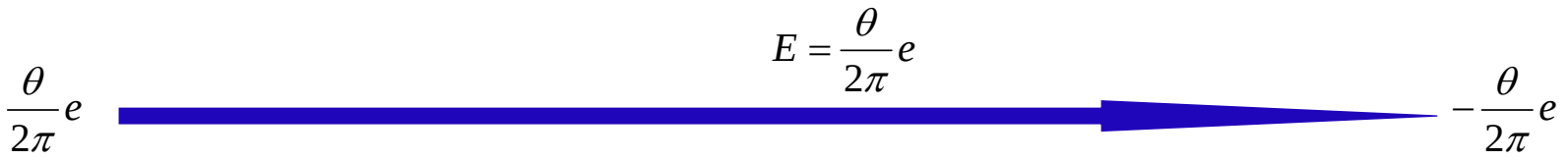

$S = 1/2$ deconfined spinons → gapless quantum liquid

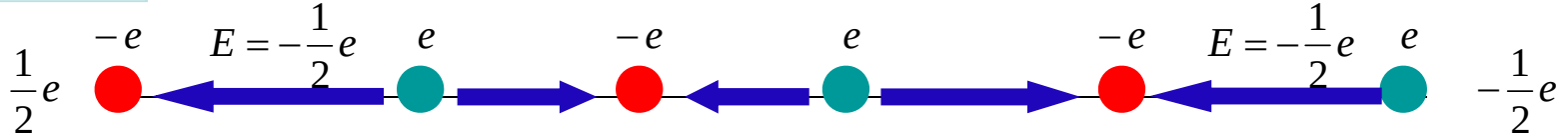

$S = 1$ confined spinons → gapful quantum liquid (Haldane gap)

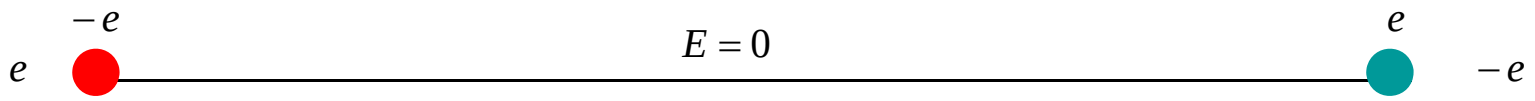

Journal of the Physical Society of Japan
Vol. 65, No. 9, September, 1996, pp. 3025-3031

Neutron Scattering Study of Magnetic Excitations in the Spin $S = 1$ One-Dimensional Heisenberg Antiferromagnet Y_2BaNiO_5

Takehiro SAKAGUCHI*, Kazuhisa KAKURAI, Tetsuya YOKOO[1] and Jun AKIMITSU[1]

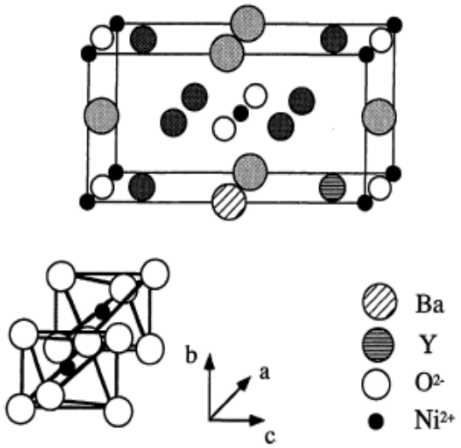

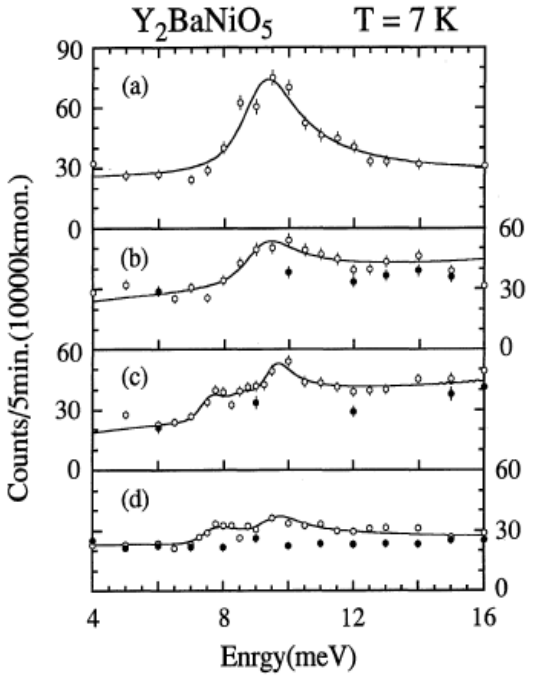

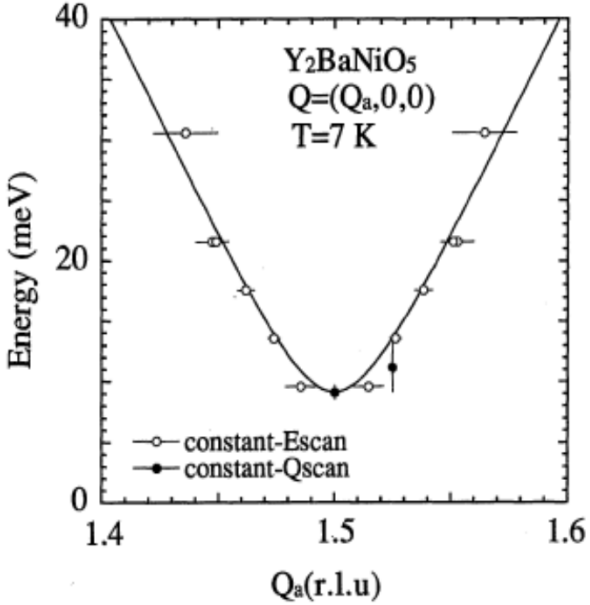

Fig. 6. Constant-Q scan at various wave vectors to observe the $\langle \widehat{S^z_Q} \widehat{S^z_{-Q}}(t) \rangle$ excitation at (a) $Q = (1.5, 0, 0)$, (b) $Q = (1.5, 0.835, 0)$, (c) $Q = (0.5, 1.1, 0)$ and (d) $Q = (0.5, 1.77, 0)$, represented by the open points. The closed points stand for the scans at (b) $Q = (1.65, 0.835, 0)$, (c) $Q = (0.65, 1.1, 0)$ and (d) $Q = (0.65, 1.77, 0)$, respectively. The solid lines in (b)–(d) represent least-square fits to three δ-like peaks convoluted with the instrumental resolution as described in the text. The samples were aligned with its a- and b-axis in the scattering plane.

S=1/2 spin at the edge of Haldane system

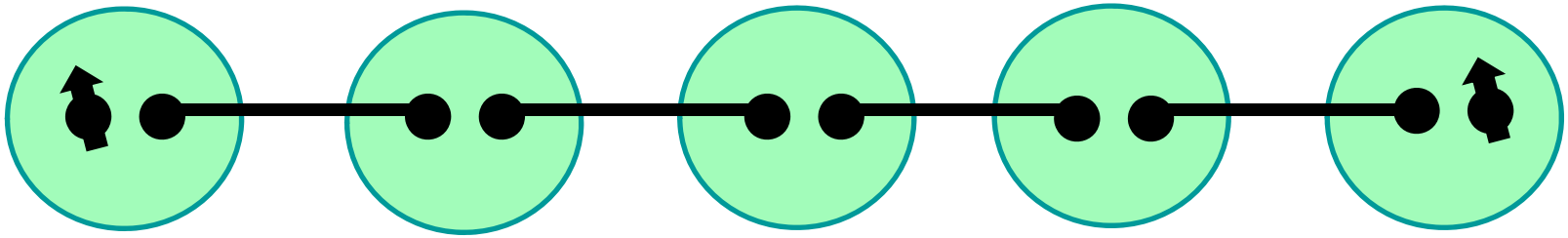

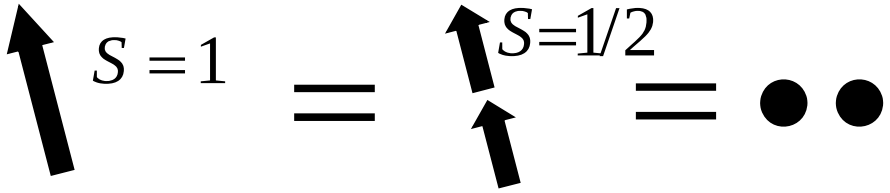

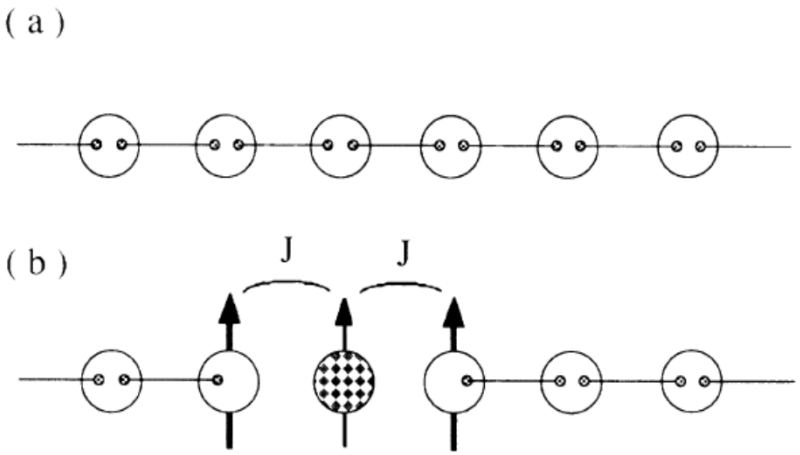

M. Hagiwara et al. 1990

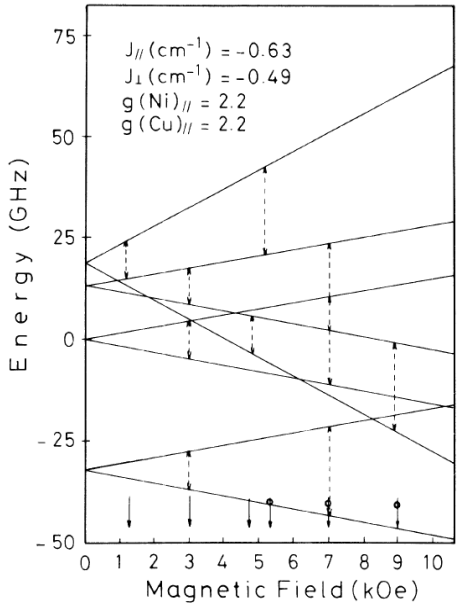

FIG. 4. ESR energy vs external magnetic-field diagram for the model shown in Fig. 1(b). The arrows show the experimental fields obtained at the frequency of 9.25 GHz and the arrows with circles those at 21.7 GHz. The broken arrows represent the theoretical transitions predicted for the frequencies of 9.25 and 21.7 GHz.

Topological Hall effects

Electrons with "constraint"

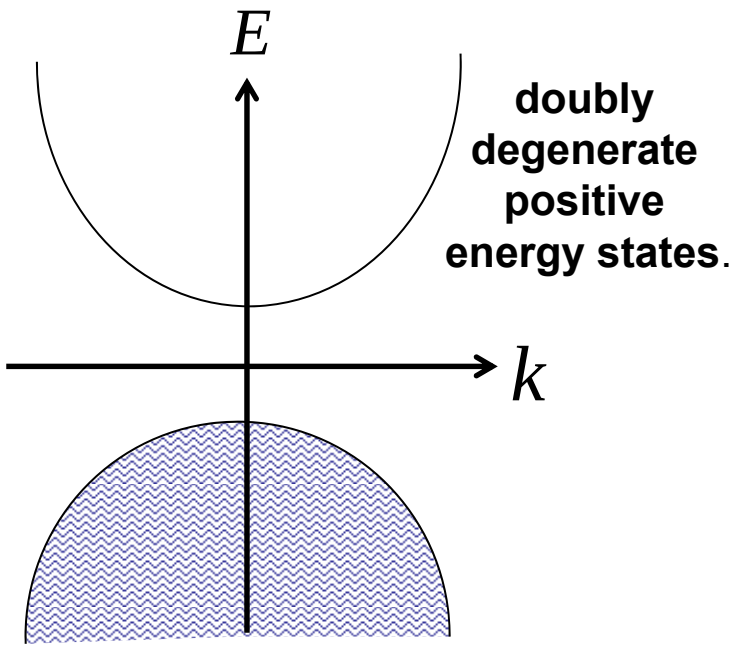

doubly degenerate positive energy states.

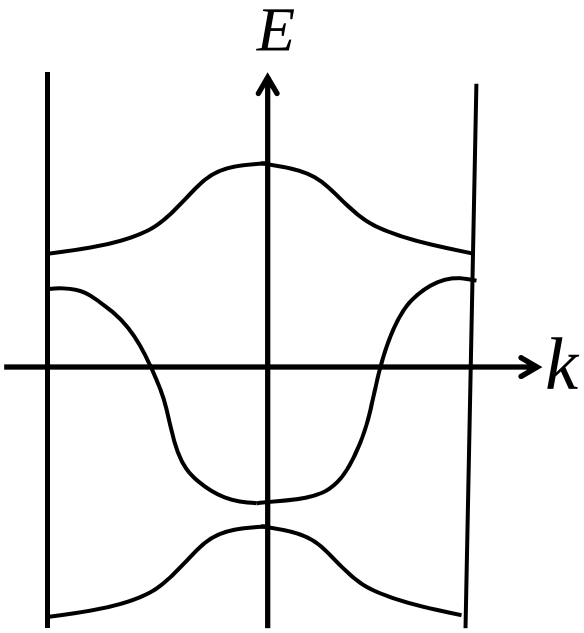

Dirac electrons

Projection onto positive energy state

→ Spin-orbit interaction as SU(2) gauge connection

Bloch electrons

Projection onto each band

→ Berry phase of Bloch wavefunction

Berry Phase Curvature in k-space

$$\psi_{nk}(r) = e^{ikr} u_{nk}(r)$$ Bloch wavefucntion

$$A_n(k) = -i < u_{nk} \mid \nabla_k \mid u_{nk} >$$ Berry phase connection in k-space

$$x_i = r_i + A_n(k) = i\partial_{k_i} + A_n(k)$$ covariant derivative

$$[x, y] = i(\partial_{k_x} A_{ny}(k) - \partial_{k_y} A_{nx}(k)) = iB_{nz}(k)$$ Curvature in k-space

$$\frac{dx(t)}{dt} = -i[x, H] = \frac{k_x}{m} - i[x, y]\frac{\partial V}{\partial y} = \frac{k_x}{m} + B_{nz}(k)\frac{\partial V}{\partial y}$$

Anomalous Velocity and Anomalous Hall Effect

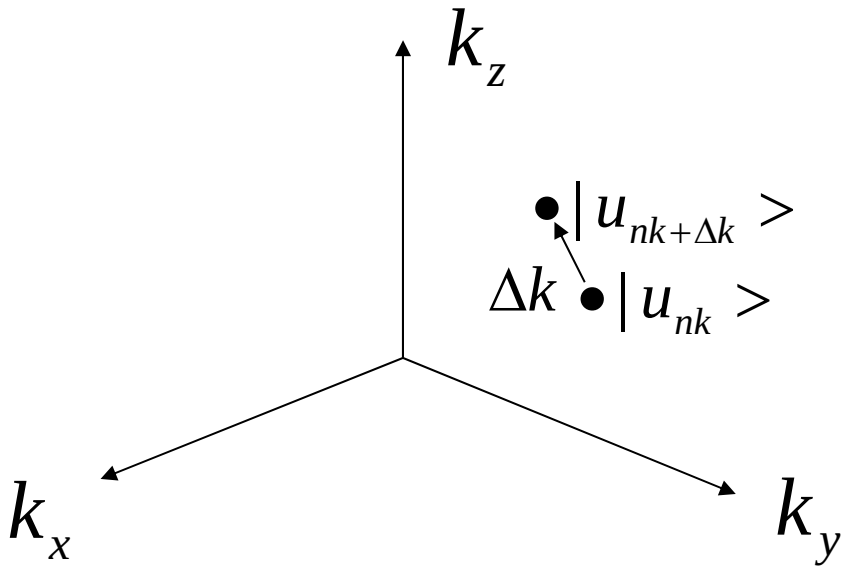

Electron Wavepacket Dynamics in solids

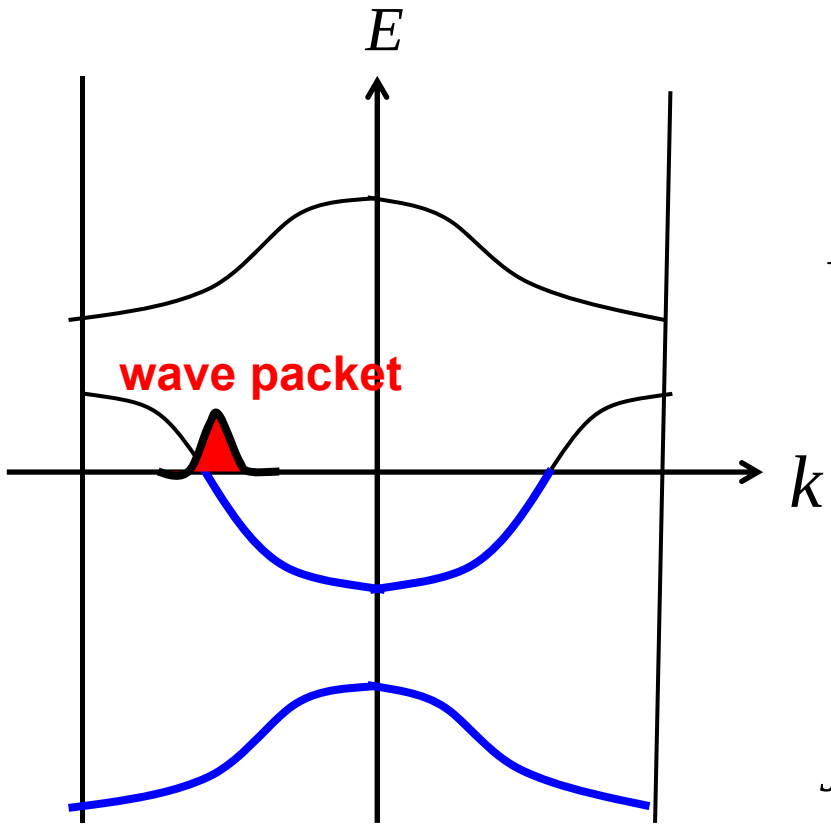

$$\frac{d\vec{r}(t)}{dt} = \frac{\partial \varepsilon_n(\vec{k})}{\partial \vec{k}} = \vec{v}_{nk}$$ **group velocity**

$$\frac{d\vec{k}(t)}{dt} = -\frac{\partial V(\vec{r})}{\partial \vec{r}} - \vec{B}(\vec{r}) \times \frac{d\vec{r}(t)}{dt}$$

Boltzmann transport equation

$$J = -e\int_{-\pi}^{\pi} \frac{dk}{2\pi} f_{nk} v_{nk}$$

$$J = -e\int_{-\pi}^{\pi} \frac{dk}{2\pi} \frac{\partial \varepsilon_{nk}}{\partial k} = \varepsilon_{n\pi} - \varepsilon_{n-\pi} = 0$$

Totally-filled band does not contribute to current.

Only energy dispersion $\varepsilon_n(\vec{k})$ ***matters ?***

Intra- and Inter-band matrix elements of current

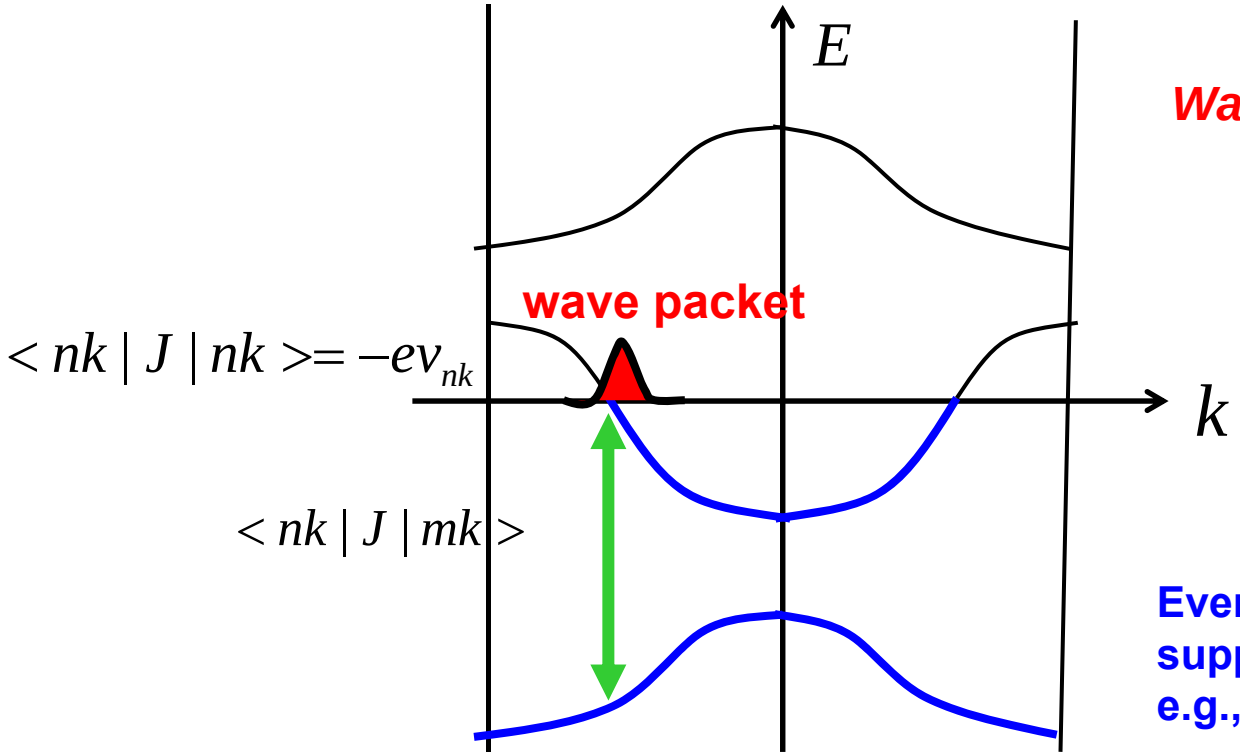

Wavefunction matters !!

Even a filled band can support current
e.g., polarization current
quantum Hall current

$$< nk \mid J \mid nk >= -e < nk \mid \frac{\partial H(k)}{\partial k} \mid nk >= -e \frac{\partial \varepsilon_n(k)}{\partial k}$$

$$< nk \mid J \mid mk >= -e < nk \mid \frac{\partial H(k)}{\partial k} \mid mk >= -e(\varepsilon_{nk} - \varepsilon_{mk}) < nk \mid \frac{\partial}{\partial k} \mid mk >$$

Correct equation of motion taking into account inter-band matrix element

$$\frac{d\vec{r}(t)}{dt} = \frac{\partial \varepsilon_n(\vec{k})}{\partial \vec{k}} - \vec{B}_n(\vec{k}) \times \frac{d\vec{k}(t)}{dt}$$

k-space curvature

anomalous velocity

Luttinger, Blount, Niu

$$\frac{d\vec{k}(t)}{dt} = -\frac{\partial V(\vec{r})}{\partial \vec{r}} - \vec{B}(\vec{r}) \times \frac{d\vec{r}(t)}{dt}$$

r-space curvature

Origin of the k-space curvature = interband current matrix

$$B_n(k) = \nabla \times A_n(k) \qquad A_n(k) = i < nk \,|\, \nabla \,|\, nk >$$

How the wavefunction is connected in k-space
→ Berry phase

Dirac's magnetic monopole in momentum space

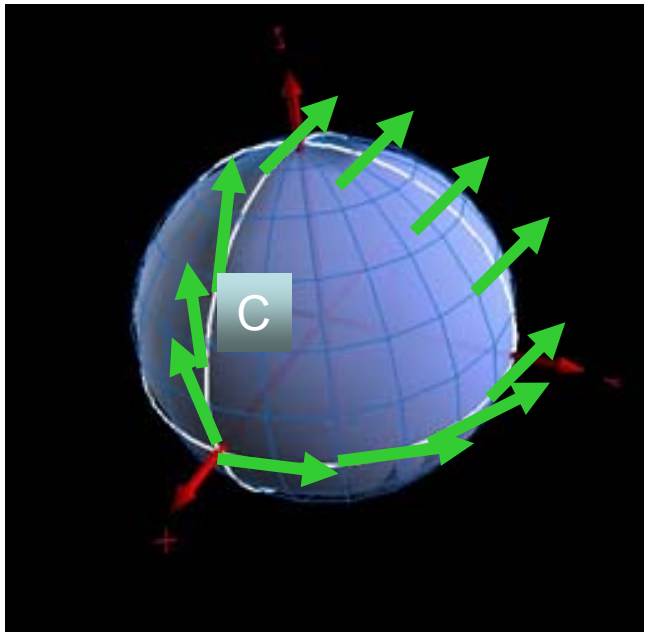

$$H = p_x\sigma_x + p_y\sigma_y + p_y\sigma_y$$

$$A_\mu(p) = i < \psi(p) | (\partial / \partial p_\mu) | \psi(p) >$$

$$\vec{B}(p) = \nabla_p \times \vec{A}(p) = \vec{p}/(2|\vec{p}|^3) = \text{solid angle}/2$$

$$\vec{p} \Rightarrow \vec{k} : \text{momentum}$$

$$\frac{d\vec{r}(t)}{dt} = \boxed{\frac{\partial \varepsilon_n(\vec{k})}{\partial \vec{k}}} - \boxed{\vec{B}_n(\vec{k}) \times \frac{d\vec{k}(t)}{dt}}$$

group velocity

k-pace-curvature anomalous velocity ➡ **AHE SHE QHE Pol. current**

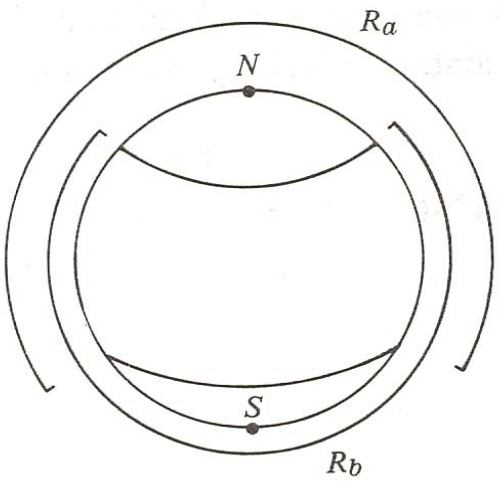

Quantal phase can not be determined self-consistently in a single gauge choice

We start with QED

$$L = \overline{\psi}(i\gamma^{\mu}[\partial_{\mu} - ieA_{\mu}] - m)\psi - \frac{1}{4}F_{\mu\nu}F^{\mu\nu}$$

ψ 4-component spinor

$j^{\mu} = e\overline{\psi}\gamma^{\mu}\psi$ charge current

Why do we care about spin current ?

Projection onto sub Hilbert space

$$L = \bar{\psi}(i\gamma^{\mu}[\partial_{\mu} - ieA_{\mu}] - m)\psi - \frac{1}{4}F_{\mu\nu}F^{\mu\nu}$$

$$j^{\mu} = e\bar{\psi}\gamma^{\mu}\psi$$

charge current

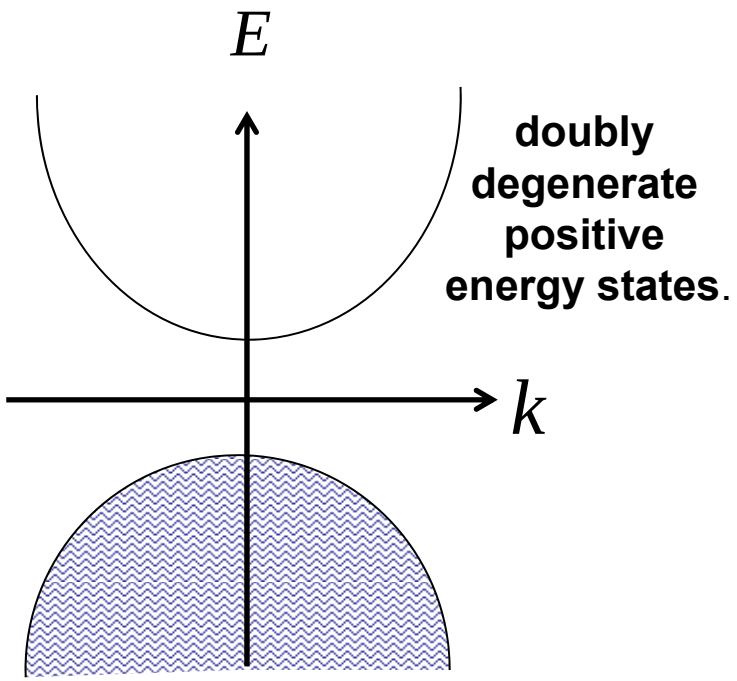

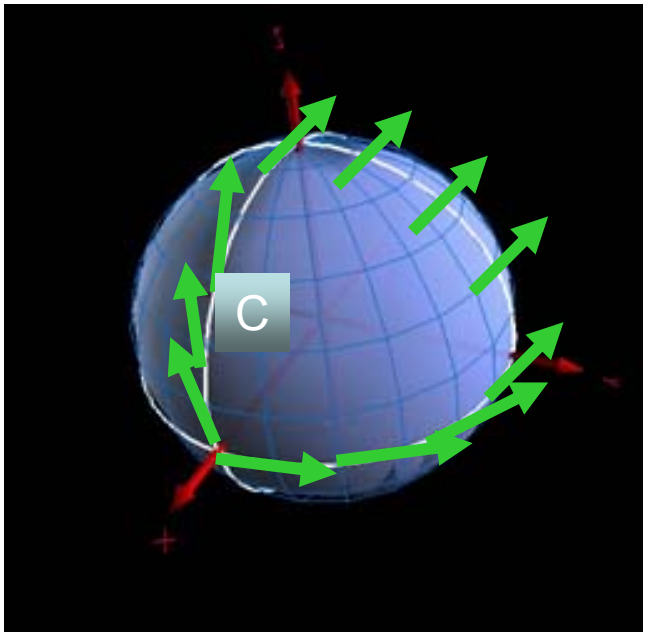

Dirac electrons

Projection onto positive energy state

Spin-orbit interaction

as SU(2) gauge connection

Non-relativistic approximation as Non-Abelian gauge theory

Froelich et al.,

1/mc2-expansion non-relativistic approximation

$$\mathcal{L} = i\hbar\psi^\dagger D_0\psi + \psi^\dagger\frac{\hbar^2}{2m}\vec{D}^2\psi + \frac{1}{2m}\psi^\dagger\left(2eq\frac{\tau^a}{2}\vec{A}\cdot\vec{A}^a + \frac{q^2}{4}\vec{A}^a\cdot\vec{A}^a\right)\psi + \frac{1}{8\pi}\left(E^2 - B^2\right).$$

$$D_i = \partial_i - i\frac{q}{\hbar}A_i^a\frac{\tau^a}{2} - i\frac{e}{\hbar}A_i$$

$$D_0 = \partial_0 + i\frac{q}{\hbar}A_0^a\frac{\tau^a}{2} + i\frac{e}{\hbar}A_0$$

ψ 2-component spinor

A_μ^a is coupled to spin current j_μ^a

SU(2) gauge field U(1) e.m. coupling

$A_0^a = B^a$ $A_i^a = \epsilon_{ial}E_l$ → No SU(2) gauge symmetry !! $\partial^\mu A_\mu^a = 0$

QED

Project out the positron states

Non-rel. approx. SU(2) gauge coupled to spin current

Project onto spin wavefunction

$(\psi^+ = f^+ z)$ z : spin w.f.

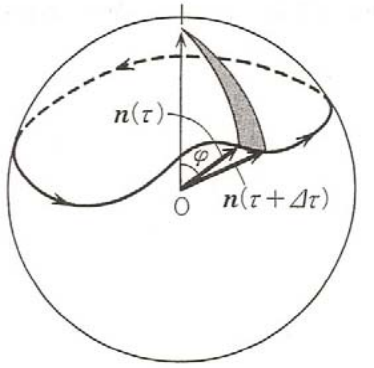

U(1) electromagnetism

$$\psi^+ \partial_0 \psi = f^+ \partial_0 f + f^+ f z^+ \partial_0 z = \frac{d\vec{n}}{dt} \cdot \vec{A}_S(\vec{n})$$

Spin Berry phase
→ Spin motive force

$$\psi_i^+ \psi_j = f_i^+ f_j < z_i | z_j > \quad < z_i | z_j > \propto e^{ia_{ij}}$$

"e.m.f." from non-collinear spins

$$\psi^+ (A_\mu^a \tau_a) \psi = f^+ f A_\mu^a < z | \tau_a | z >$$

"e.m.f." from spin-orbit int.

$$\psi^+ A_\mu \psi = f^+ f A_\mu$$

Maxwell e.m.f.

Solid angle by spins acting as a gauge field

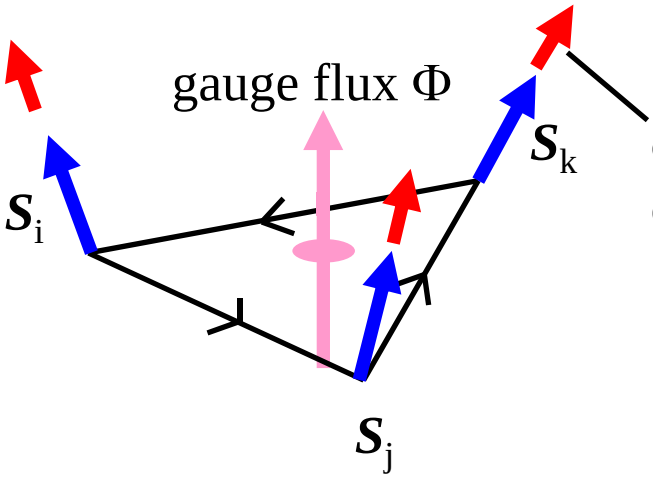

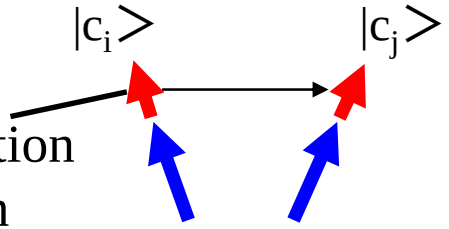

conduction electron

$$
\begin{aligned}
t_{ij} &= t\langle\chi_j|\chi_i\rangle \\
&= t\left(\cos\frac{\theta_i}{2}\cos\frac{\theta_j}{2} + \sin\frac{\theta_i}{2}\sin\frac{\theta_j}{2}\exp(i(\phi_j-\phi_i))\right) \\
&= t\cos\frac{\theta_{ij}}{2}\exp(ia_{ij})
\end{aligned}
$$

acquire a phase factor

Fictitious flux (in a continuum limit)

$$\Phi \propto \frac{\mathbf{S}_i \cdot (\mathbf{S}_j \times \mathbf{S}_k)}{2} = \frac{\Omega}{2}$$

scalar spin chirality

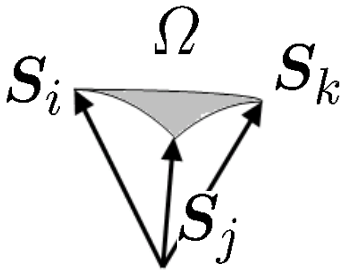

Gauge theory of strongly correlated electrons
- fluctuating spin field -

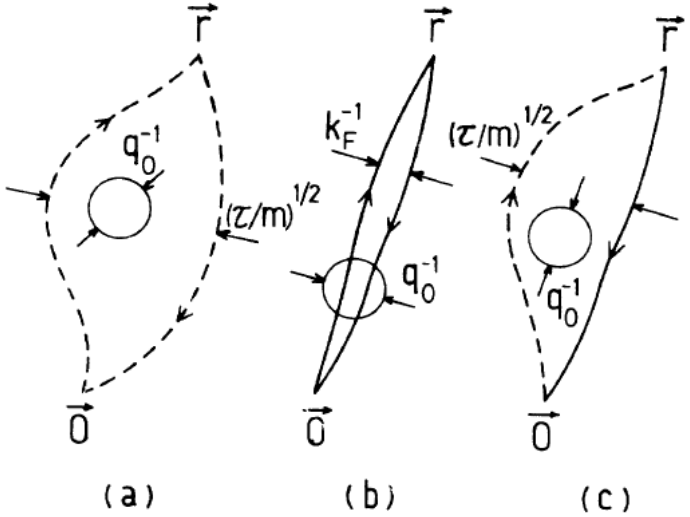

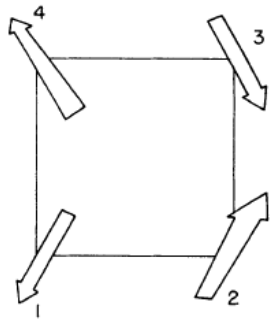

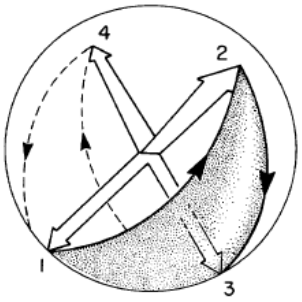

FIG. 1. Typical Feynman paths, projected onto the two-dimensional plane, which contribute to (a) the boson polarization Π_B, (b) the fermion polarization Π_F, and (c) the electron Green's function G_σ. Dashed and solid lines refer to boson and fermion paths. The circle with radius q_0^{-1} represents the scale of the fluctuating gauge-field flux.

N.N. and P.A.Lee PRL 1990
P.A.Lee, X.G. Wen, and N.N. RMP2006

3 Kinds of Current in Solids

1. Ohmic (transport) Current

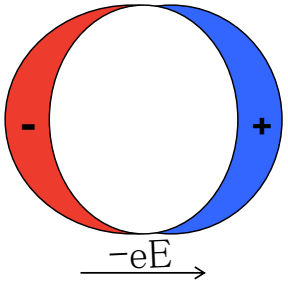

Dissipation/Joule heating
in nonequilibrium state

$$\propto -\frac{\partial f(\varepsilon)}{\partial \varepsilon}$$

2. Topological Current

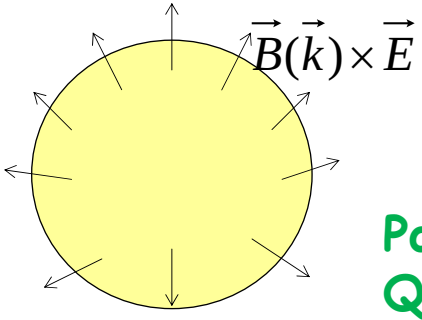

Berry phase

Due to multi-band effect/Berry phase
Dissipationless in equilibrium
The occupied states contribute

Polarization current
Quantum Hall current
Anomalous Hall current, Spin Hall current

$$\propto f(\varepsilon)$$

3. Superconducting Current

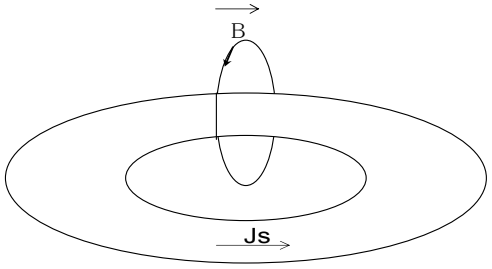

Dissipationless in equilibrium
Responding to ***A***

$$\propto \rho_s$$

Quantum Hall Effect

Quantum Hall effect

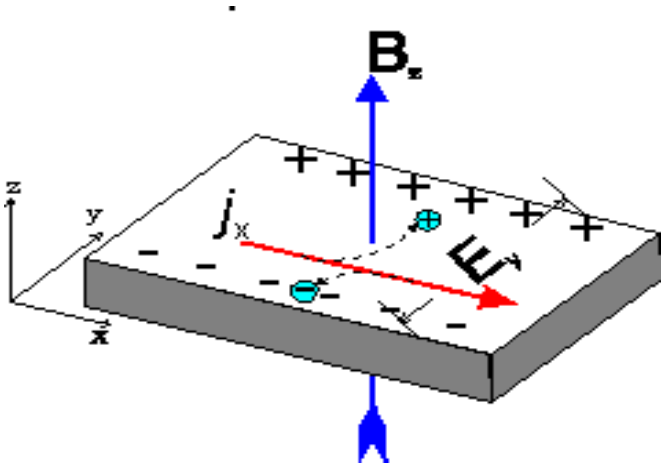

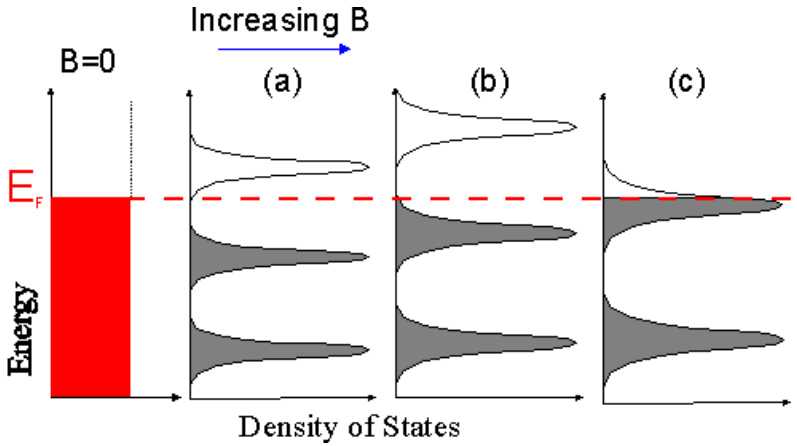

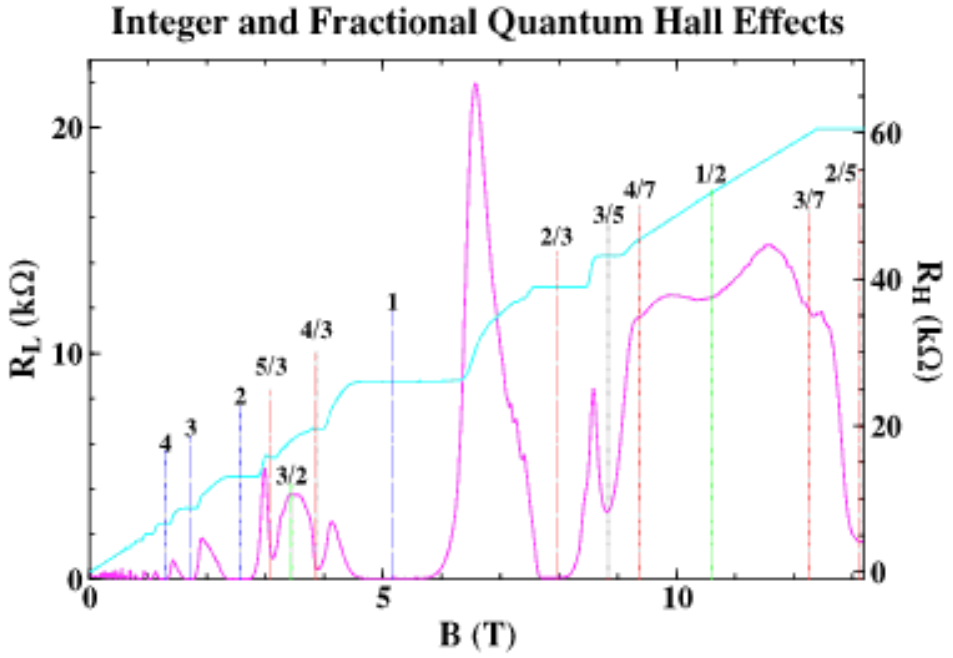

Topological nature of Hall effect - TKNN formula

$$\sigma_{xy} = i\sum_{n,\vec{k}} f(\varepsilon_n(\vec{k}))\sum_{m\neq n}\frac{\left\langle n\vec{k}\middle|J_y\middle|m\vec{k}\right\rangle\left\langle m\vec{k}\middle|J_x\middle|n\vec{k}\right\rangle - (J_x \leftrightarrow J_y)}{\left[\varepsilon_n(\vec{k}) - \varepsilon_m(\vec{k})\right]^2}$$

$$= e^2\sum_{n,\vec{k}} f(\varepsilon_n(\vec{k}))\left[\nabla_k \times \vec{A}_n(\vec{k})\right]_z$$

$$\vec{A}_n(\vec{k}) = -i\left\langle n\vec{k}\middle|\nabla_k\middle|n\vec{k}\right\rangle$$

$$\sum_{\vec{k}\in 1\text{st BZ}} b_n(\vec{k}) = \frac{N_\phi}{2\pi} \qquad N_\phi \text{ : Chern number} \Rightarrow \sigma_{xy} = \frac{e^2}{h}N_\phi$$

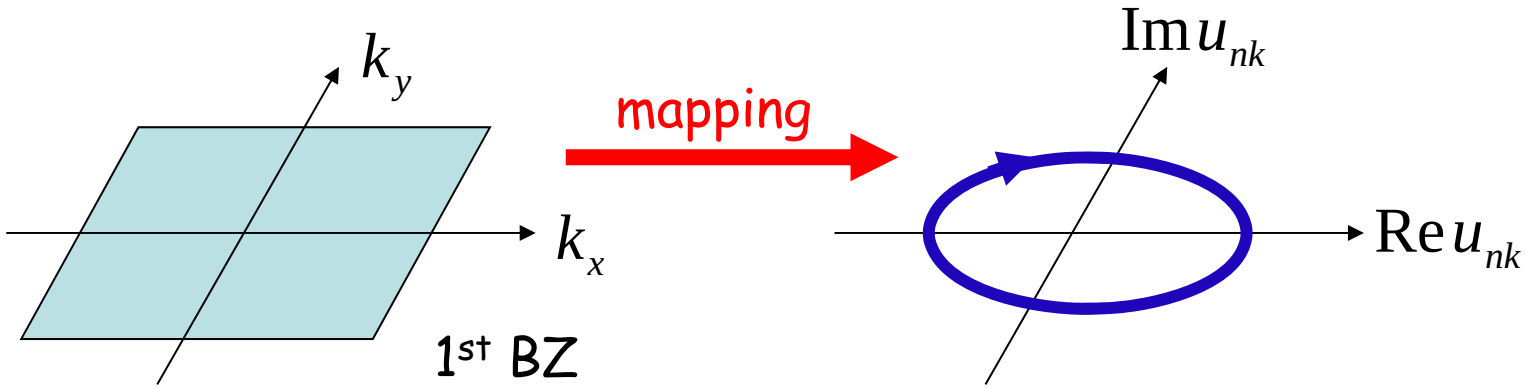

Bulk v.s. Edge in topological states

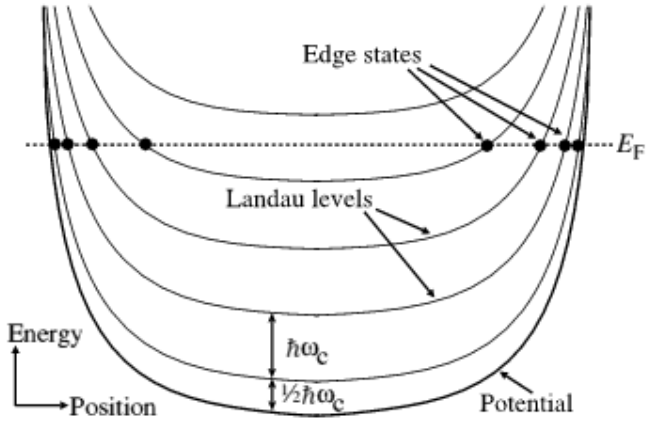

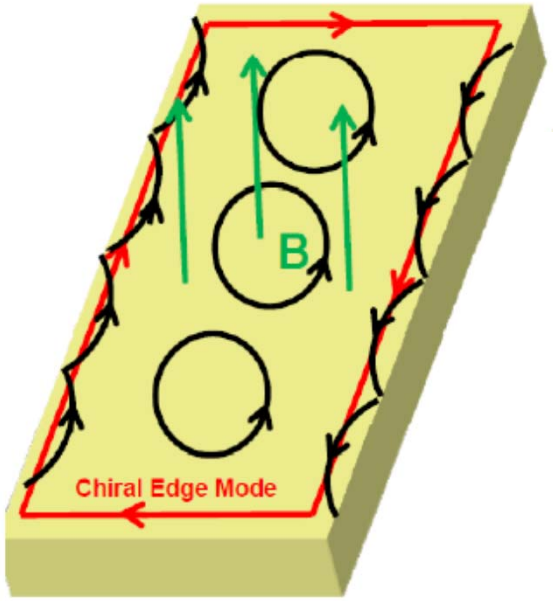

X.G.Wen

$$S_{Chern-Simons} = -\frac{m}{4\pi}\int d^2xdt\varepsilon^{\mu\nu\lambda}a_\mu\partial_\nu a_\lambda$$

$$S_{Edge} = -\frac{m}{4\pi}\int dxdt(\partial_t + v\partial_x)\phi\partial_x\phi = \frac{m}{2\pi}\int dt\sum_{k>0}(i\dot{\phi}_k\phi_{-k} - vk^2\phi_k\phi_{-k})$$

Fractional charge and Spin-Charge separation in 1D

$$H = -\sum_i t_i (c_i^+ c_{i+1} + c_{i+1}^+ c_i)$$

1/2 electrons per site

$\pm \frac{e}{2}$

E

anti-bonding

isolated

bonding

$$H = \int dx \psi^+(x)(-i\sigma^x \partial_x + m(x)\sigma^z)\psi(x)$$

Localized state
Zero mode

x

m(x)

Spinful case: 1 electrons per site

charge soliton

Spin soliton

Anomalous Hall Effect

Anomalous Hall Effect

$(La,Ca)MnO_3$ S. H. Chun et al. Phys. Rev. B 61, R9225 (2000).

$$\rho_{xy} = \underbrace{R_0 H}_{\text{ordinary term}} + \underbrace{4\pi R_S M}_{\text{anomalous term}}$$

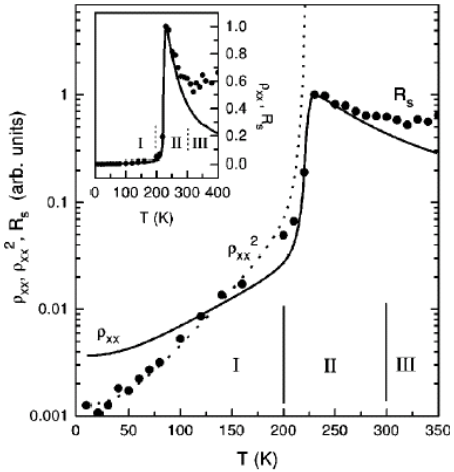

Conventional theory

Karplus and Luttinger $R_S \propto \rho^2$

intrinsic

J. Kondo $R_S \propto \langle (m - \langle m \rangle)^3 \rangle$

extrinsic

$$T \rightarrow 0 \quad R_S \rightarrow 0$$

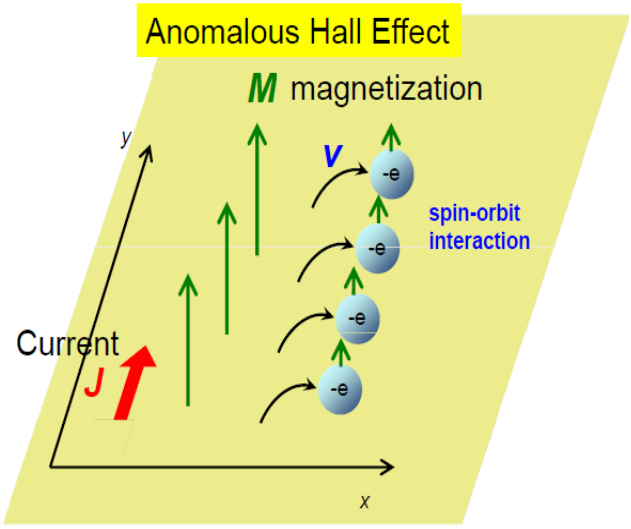

Intrinsic AHE - Topological nature

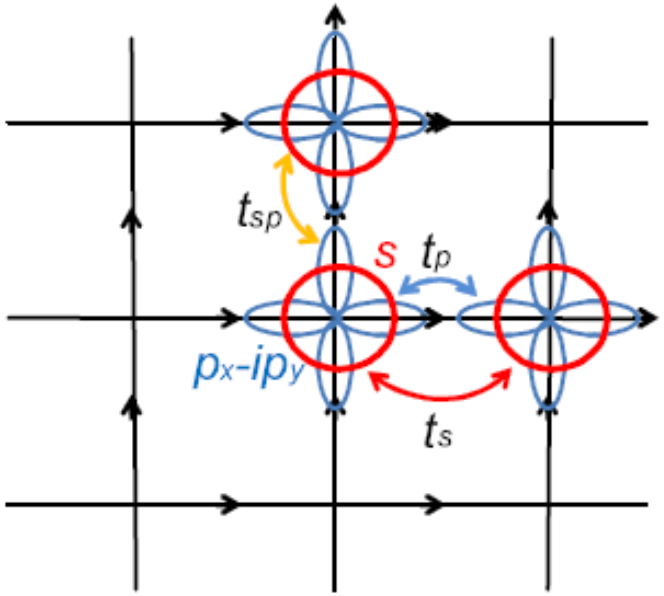

$$\sigma_{xy} = i\sum_{n,\vec{k}} f(\varepsilon_n(\vec{k}))\sum_{m\neq n}\frac{\left\langle n\vec{k}\middle|J_y\middle|m\vec{k}\right\rangle\left\langle m\vec{k}\middle|J_x\middle|n\vec{k}\right\rangle-(J_x\leftrightarrow J_y)}{\left[\varepsilon_n(\vec{k})-\varepsilon_m(\vec{k})\right]^2}$$

$$= e^2\sum_{n,\vec{k}} f(\varepsilon_n(\vec{k}))\left[\nabla_k\times\vec{A}_n(\vec{k})\right]_z$$

$$\vec{A}_n(\vec{k}) = -i\left\langle n\vec{k}\middle|\nabla_k\middle|n\vec{k}\right\rangle$$

$$\begin{aligned}
H &= -\sum_{i,\sigma,a=x,y} t_s s^\dagger_{i,\sigma} s_{i+a,\sigma} + h.c. \\
&+ \sum_{i,\sigma,a=x,y} t_p p^\dagger_{i,a,\sigma} s_{i+a,a,\sigma} + h.c. \\
&+ \sum_{i,\sigma,a=x,y} t_{sp} s^\dagger_{i\sigma} p_{i+a,a,\sigma} + h.c. \\
&+ \lambda\sum_{i,\sigma}\sigma(p^\dagger_{i,x,\sigma} - i\sigma p^\dagger_{i,y,\sigma})(p_{i,x,\sigma} + i\sigma p_{i,y,\sigma}).
\end{aligned}$$

$$h(\boldsymbol{k}) = \begin{bmatrix} \varepsilon_s - 2t_s(\cos k_x + \cos k_y) & \sqrt{2}t_{sp}(i\sin k_x + \sin k_y) \\ \sqrt{2}t_{sp}(-i\sin k_x + \sin k_y) & \varepsilon_p + t_p(\cos k_x + \cos k_y) \end{bmatrix}$$

$$h(\boldsymbol{k}) = \bar{\varepsilon} + m\sigma_z + \sqrt{2}t_{sp}(k_y\sigma_x - k_x\sigma_y)$$

Spin - Orbit Interaction

$$\mathcal{H}_{s\text{-}o} = \frac{-e\hbar}{2m^2c^2}(\vec{p} \times \nabla V)\cdot\vec{s}$$

$$= \frac{e\hbar}{2m^2c^2}(\vec{s} \times \nabla V)\cdot\vec{p}$$

$V = V(r)$: $\mathcal{H}_{s\text{-}o} = \frac{\hbar^2}{2m^2c^2}\cdot\frac{1}{r}\cdot\frac{dV}{dr}\,\vec{l}\cdot\vec{s}$

$\mathcal{H}_{s\text{-}o} = \vec{A}\cdot\vec{p}$ $\quad$ $\vec{A}$: vector potential

$$\boxed{\vec{A} = \frac{e\hbar}{2m^2c^2}\vec{s} \times \nabla V}$$

DM interaction

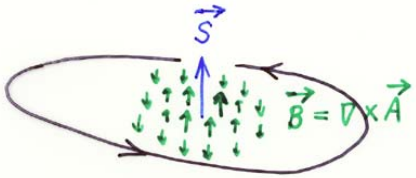

$$\Phi_D = \int_D d\vec{D}\cdot\nabla\times\vec{A}$$

$$= \oint_C d\vec{r}\cdot\vec{A}$$

$\longrightarrow 0$ (infinite D)

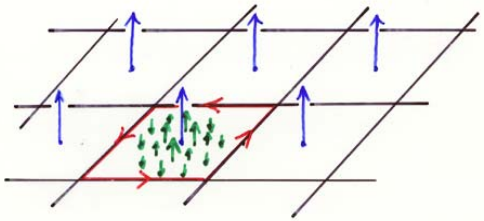

$$\Phi_{\text{Unit Cell}} = \int_{\text{Unit Cell}} d\vec{D}\cdot\nabla\times\vec{A}$$

$$= \oint_C d\vec{r}\cdot\vec{A} = 0$$

V: periodic function

Classification of Order Parameters

Inversion \ Time reversal	even	odd
even	ρ charge density	Spin $\vec{M}$ magnetization
odd	$\vec{j}_s$, $\vec{P}$ **spin current** polarization	$\vec{j}$, $\vec{T}$ current **toroidal moment**

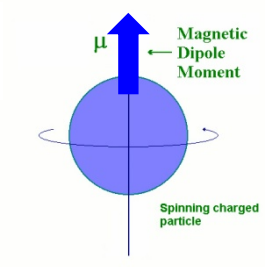

Spin current

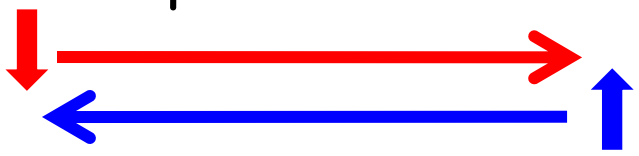

Model

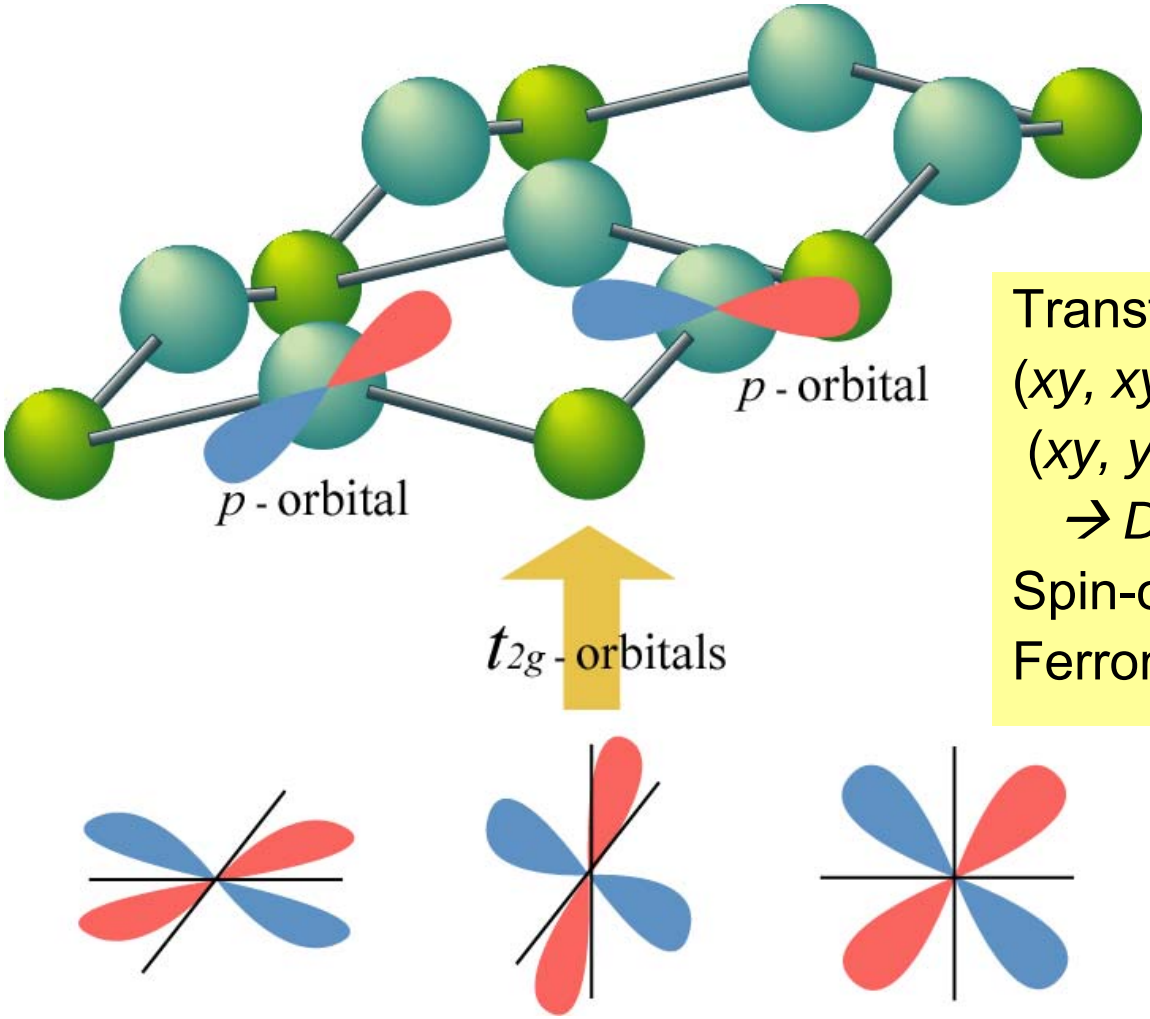

Transfer integrals

(*xy*, *xy*) = (*yz*, *yz*) = (*zx*, *zx*)=*t0*

(*xy*, *yz*)= (*xy*, *zx*)=+*t1*, -*t1*

→ *DM interaction*

Spin-orbit coupling λ

Ferromagnetic moment *Umz*

Dispersion

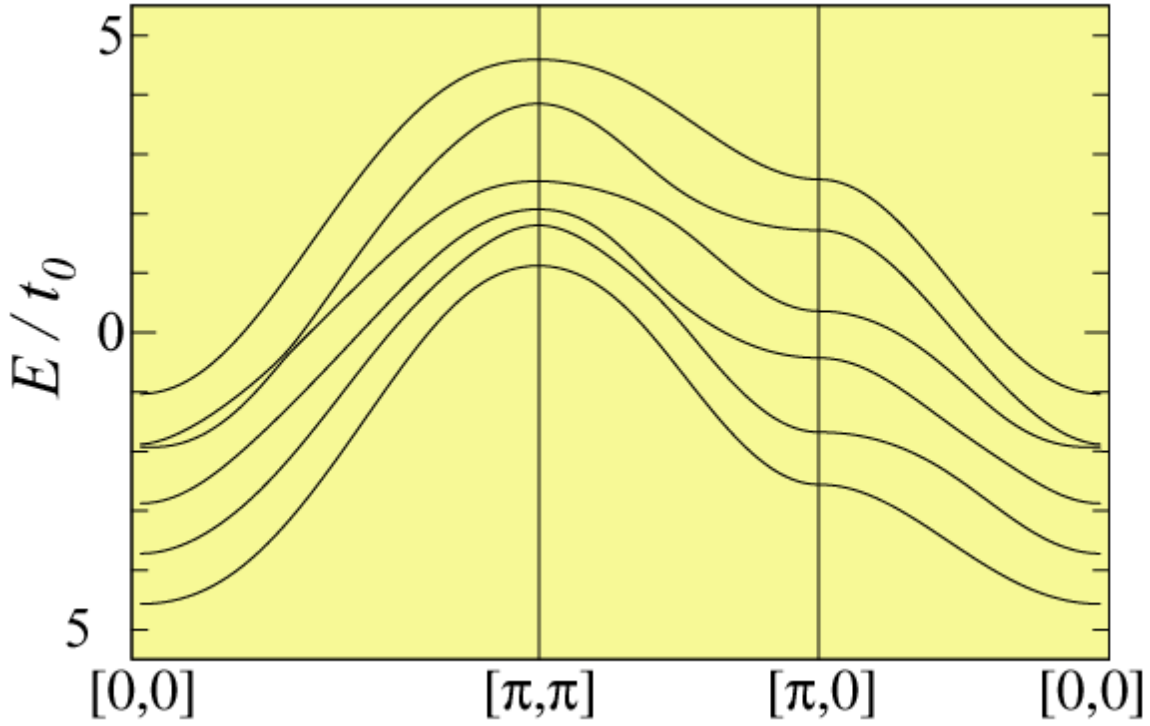

t1 =0.5t0, l = 0.4t0, Umz = 0.95t0.

The 4th and 5th bands are nearly degenerate at k = [0,0] and [π/2, π/2].

Chn's : (-1, -2, 3, -4, 5 -1).

Gauge flux density

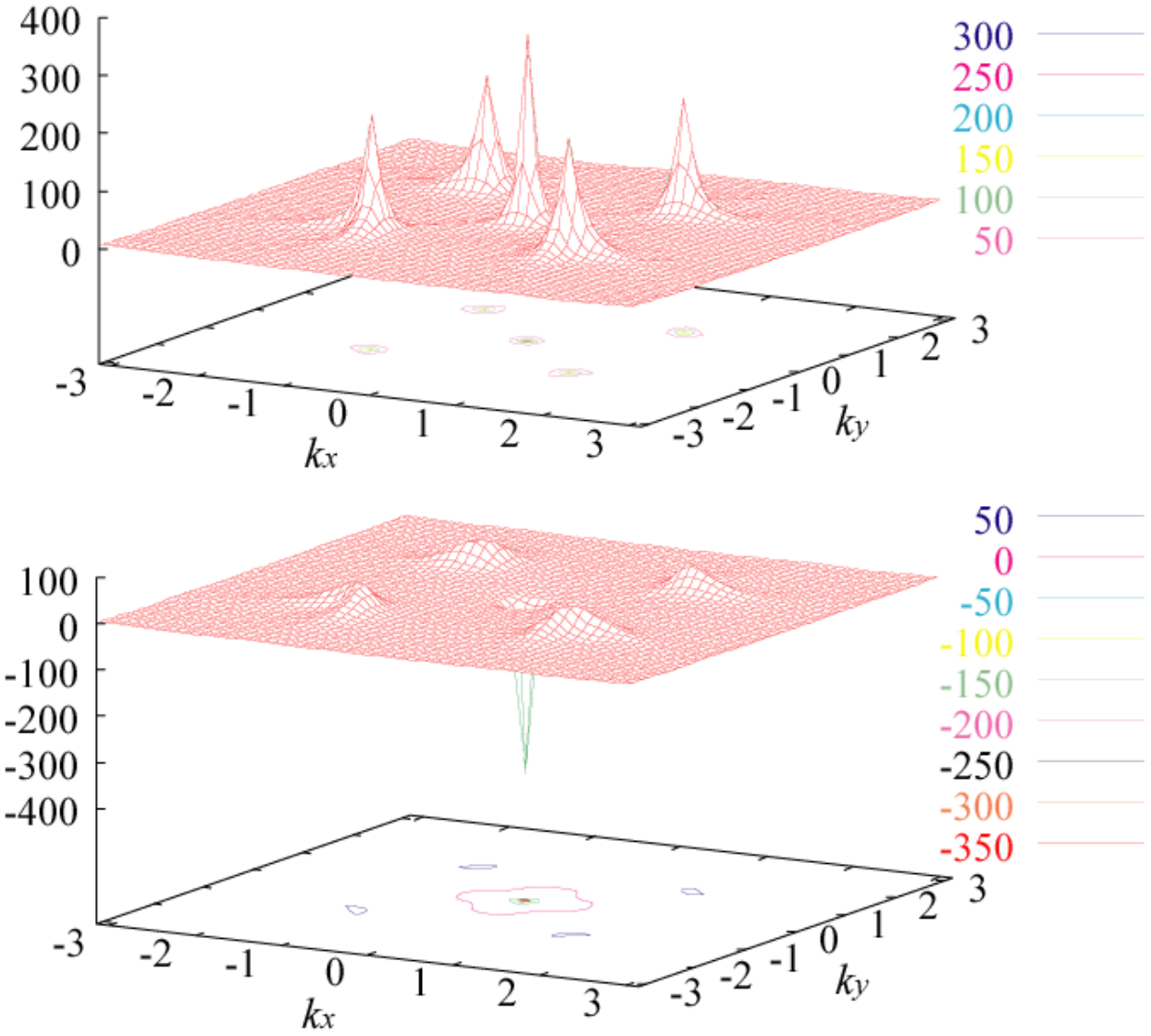

Gauge flux density in ***k***-space of the 5th band

t1=0.5*t0*, λ=0.4*t0*,*Umz*=0.95*t0* for the upper *Umz*=1.05*t0* for the lower

The transfer of *Chn* : 4th ⇔ 5th bands at (*Umz*)c ~ 1.0*t0*.

(The transfer occurs only at ***k*** = [0,0] in this case.)

Parity Anomaly

- Parity transformation in 2D

  (x, y) → (-x, y)

- Dirac fermion

$$H \cong \int \frac{d^2k}{(2\pi)^2} \psi^+(\vec{k}) h(\vec{k}) \psi(\vec{k}) \qquad h(\vec{k}) = \begin{bmatrix} V(\vec{k}) + m & k_D(\kappa_x - i\kappa_y)^p \\ k_D(\kappa_x + i\kappa_y)^p & V(\vec{k}) - m \end{bmatrix}$$

$$\varepsilon_\pm(\vec{k}) = \pm\sqrt{(k_D\kappa^p)^2 + m^2} \qquad \vec{\kappa} = \frac{\vec{k} - \vec{k}_0}{k_D}$$

$$b_\pm(\vec{k}) = \left[\nabla_k \times \vec{A}_n(\vec{k})\right]_z = \pm \frac{(p\kappa^{p-1})^2 m}{2\left[(k_D\kappa^p)^2 + m^2\right]^{\frac{3}{2}}}$$

- Mass term breaks P-symmetry → New Energy Scale

  m is a function of (λ, *Umz*) and can change the sign at the critical lines in (λ, *Umz*)-plane

Dirac's magnetic monopole in momentum space

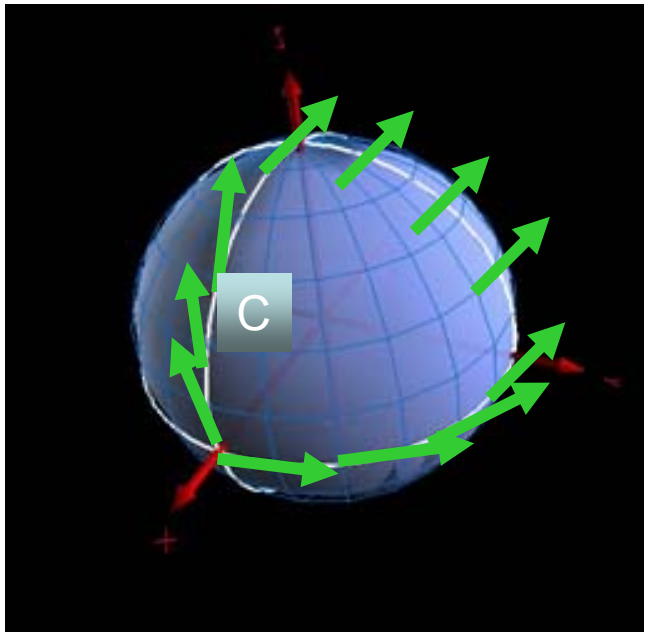

$$H = p_x\sigma_x + p_y\sigma_y + p_y\sigma_y$$

$$A_\mu(p) = i < \psi(p) | (\partial / \partial p_\mu) | \psi(p) >$$

$$\vec{B}(p) = \nabla_p \times \vec{A}(p) = \vec{p}/(2|\vec{p}|^3) = \text{solid angle}/2$$

$$\vec{p} \Rightarrow \vec{k} : \text{momentum}$$

$$\frac{d\vec{r}(t)}{dt} = \boxed{\frac{\partial \varepsilon_n(\vec{k})}{\partial \vec{k}}} - \boxed{\vec{B}_n(\vec{k}) \times \frac{d\vec{k}(t)}{dt}}$$

group velocity

k-pace-curvature anomalous velocity ➡ **AHE SHE QHE Pol. current**

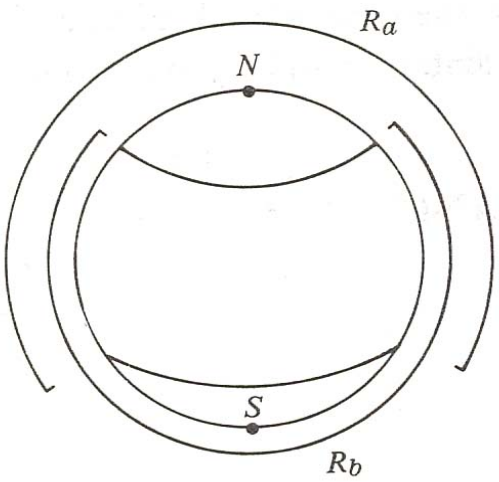

Quantal phase can not be determined self-consistently in a single gauge choice

Electron fractionalization in 2D

$$H = \psi^{+}[\sigma^{x} p_{x} + \sigma^{y} p_{y} + \sigma^{z} m(x)]\psi$$

$$\sigma_{xy} = \frac{e^2}{2h} sign(m)$$

$$(x \to \pm\infty)$$

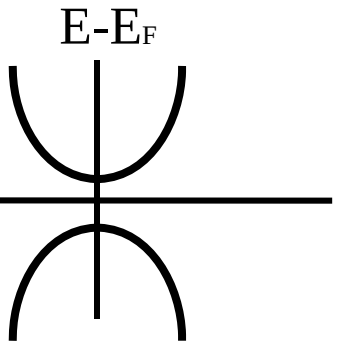

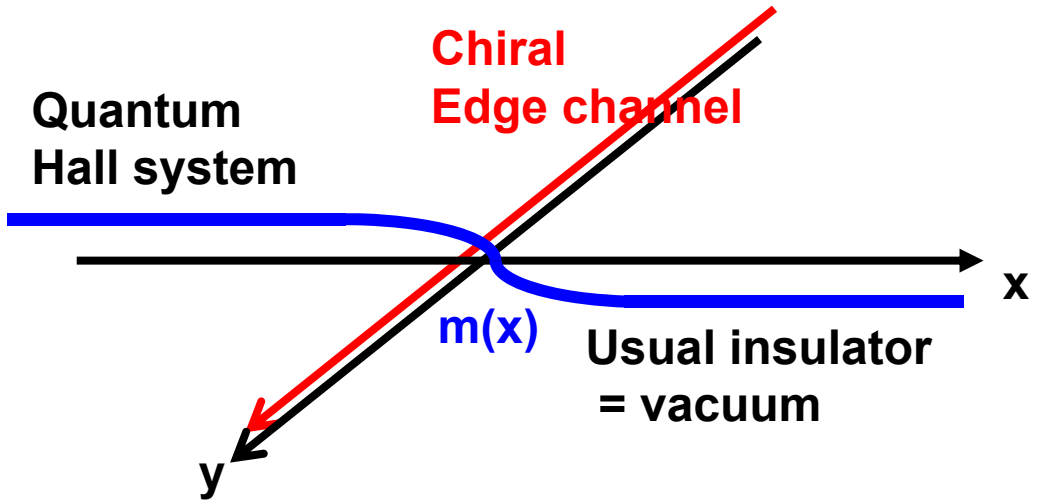

Anomalous Hall Effect of $SrRuO_3$

$SrRuO_3$ thin film on STO substrate

$T_C = 140$ K $\rho_0 = 50$ μΩcm

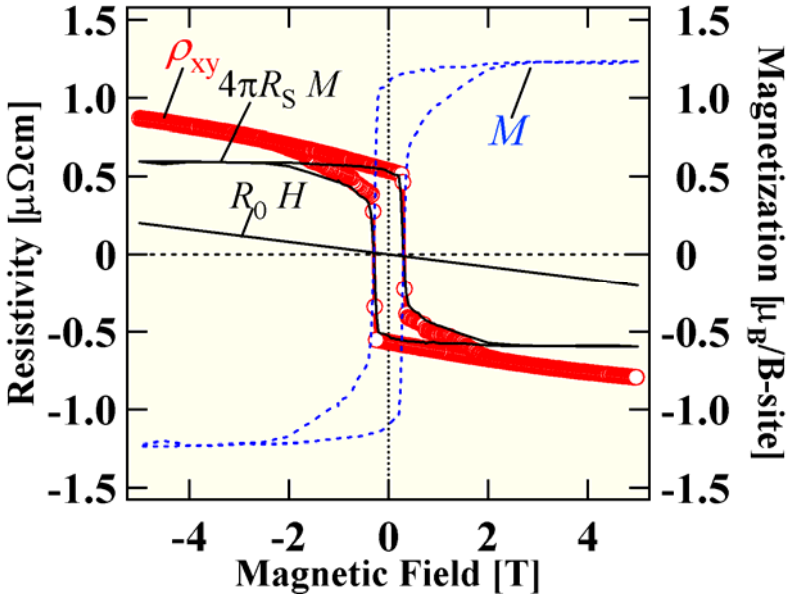

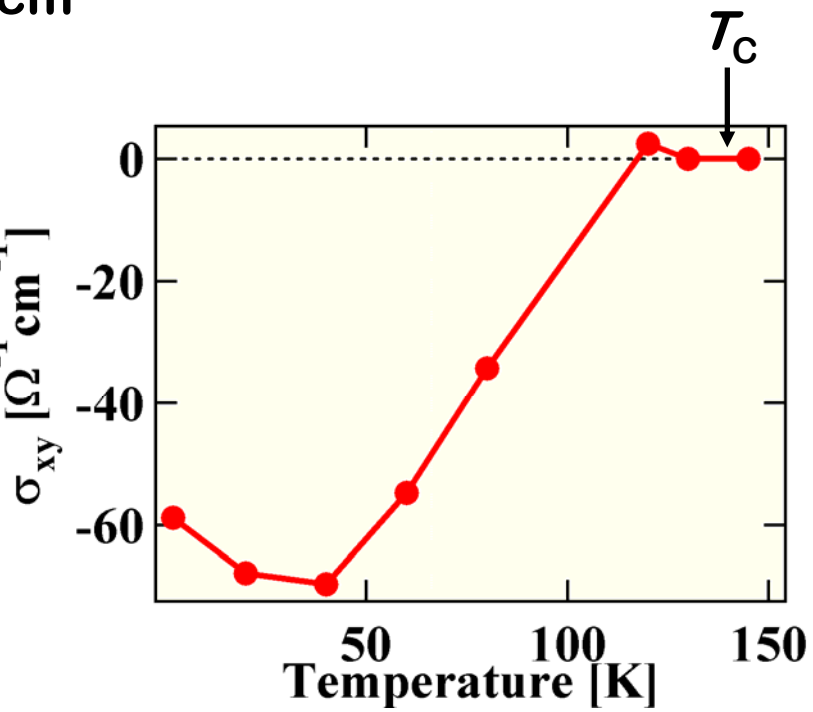

Large value at low temperature

Anomalous temperature dependence

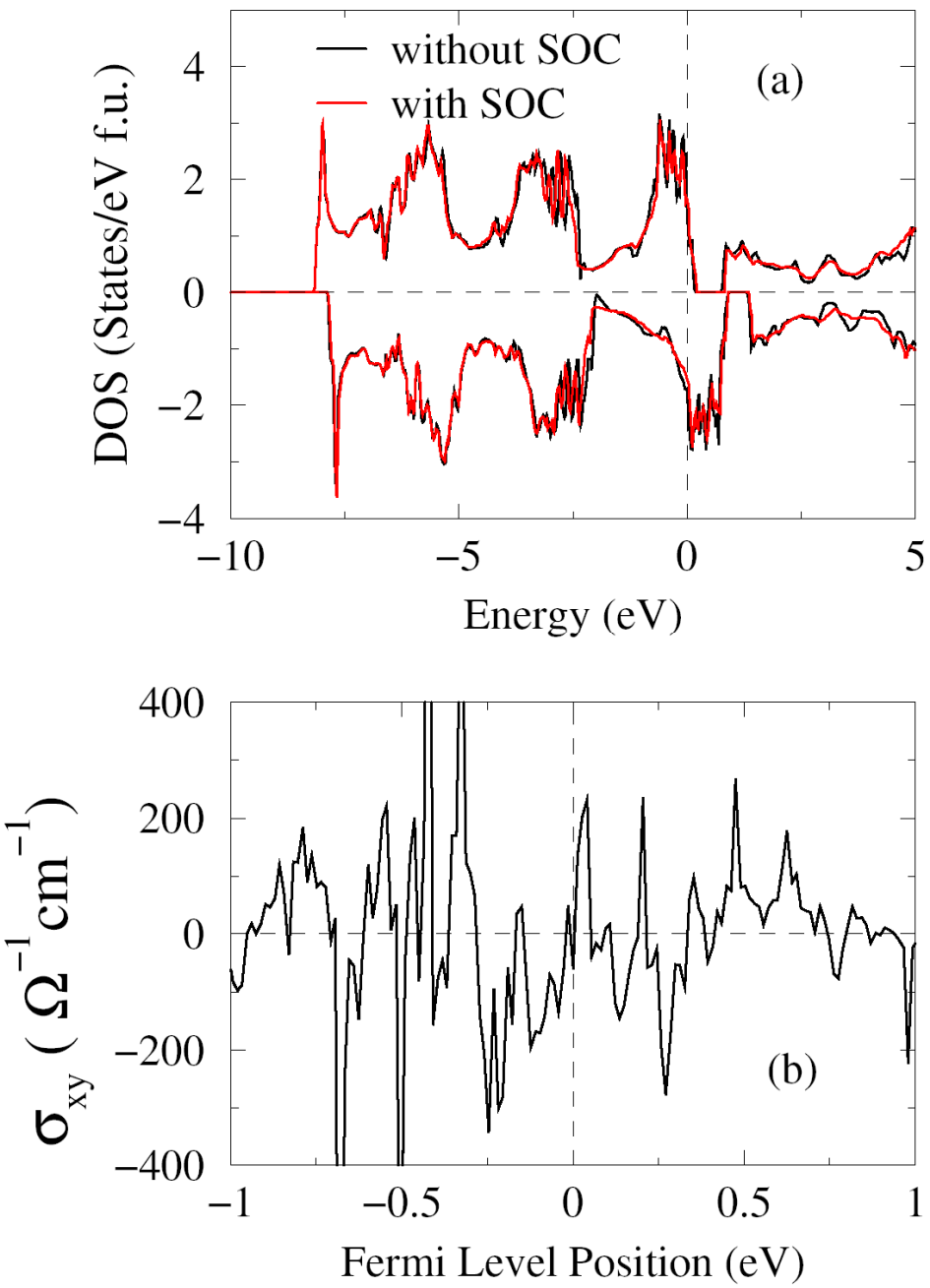
without SOC
with SOC
(a)
DOS (States/eV f.u.)
4
2
0
−2
−4
−10
−5
0
5
Energy (eV)
400
200
0
−200
−400
σxy (Ω−1 cm−1)
(b)
−1
−0.5
0
0.5
1
Fermi Level Position (eV)

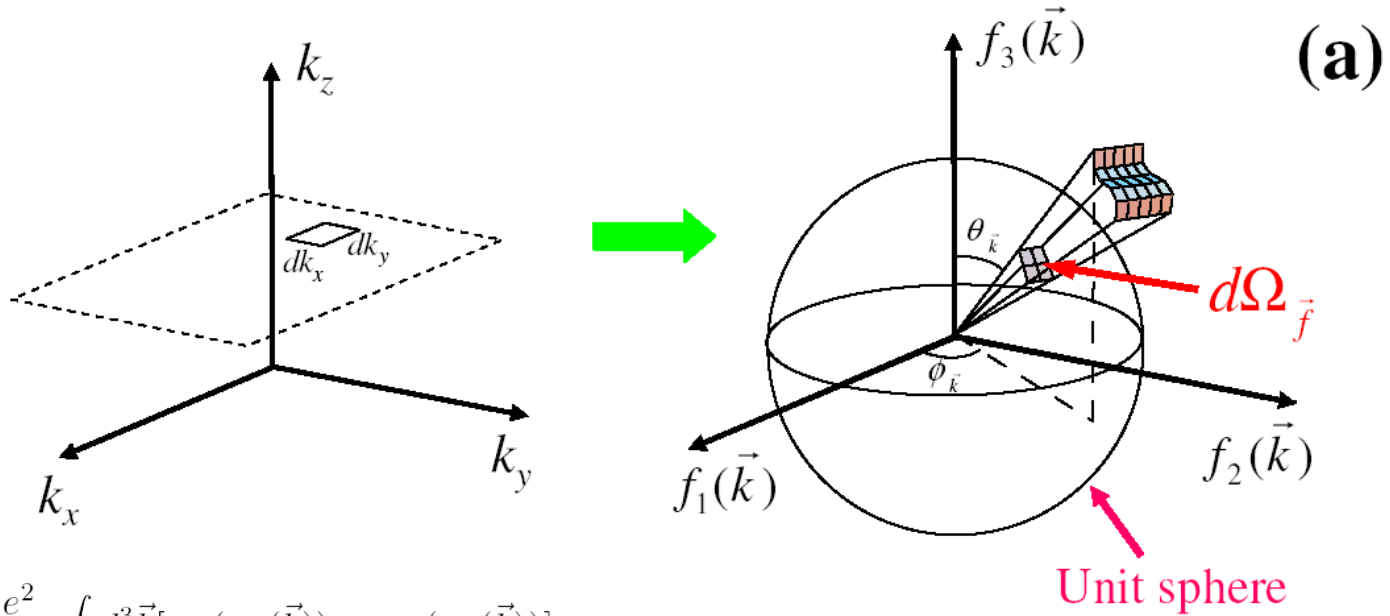

$$\sigma_{xy}^{2-\text{bands}} = \frac{e^2}{8\pi h}\int d^3\vec{k}[n_F(\varepsilon_-(\vec{k})) - n_F(\varepsilon_+(\vec{k}))]$$
$$\times \left(\frac{\partial\varphi_{\vec{f}}}{\partial k_x}\frac{\partial\theta_{\vec{f}}}{\partial k_y} - \frac{\partial\varphi_{\vec{f}}}{\partial k_y}\frac{\partial\theta_{\vec{f}}}{\partial k_x}\right)\sin\theta_{\vec{f}}$$
$$= \frac{e^2}{8\pi h}\int dk_z d\Omega_{\vec{f}}[n_F(\varepsilon_-(\vec{k})) - n_F(\varepsilon_+(\vec{k}))]$$

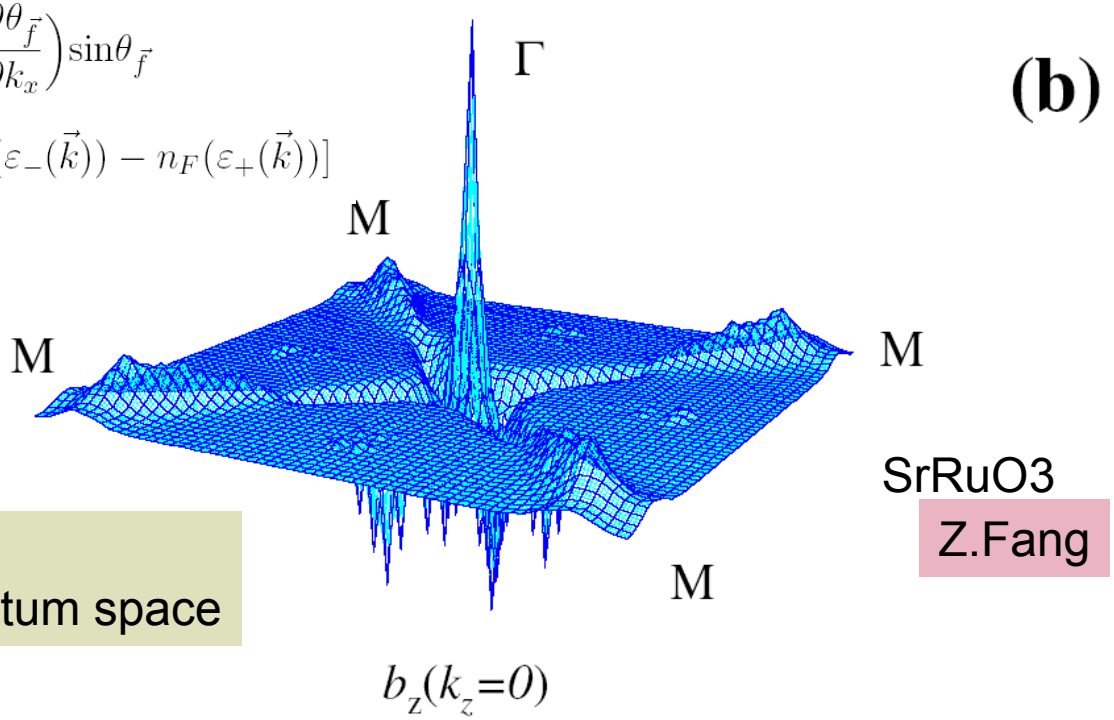

SrRuO3

Z.Fang

Degeneracy point
→ Monopole in momentum space

Anomalous Hall Effect in SrRuO3 - Magnetic Monopole in k-Space

Z.Fang et al.

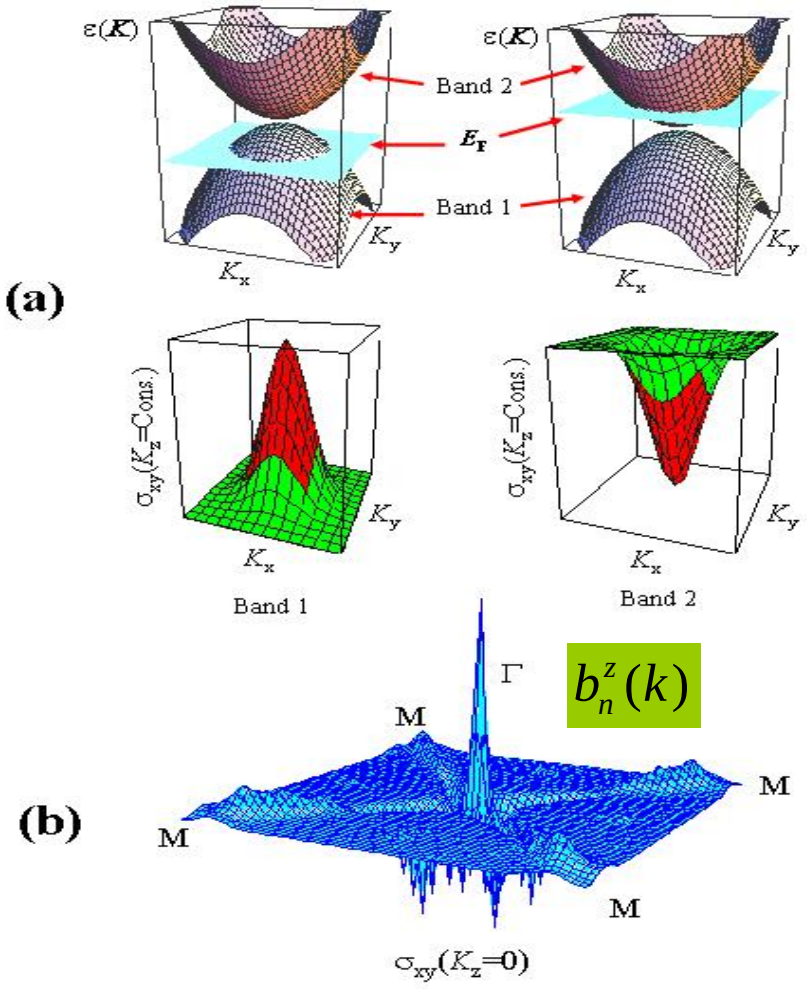

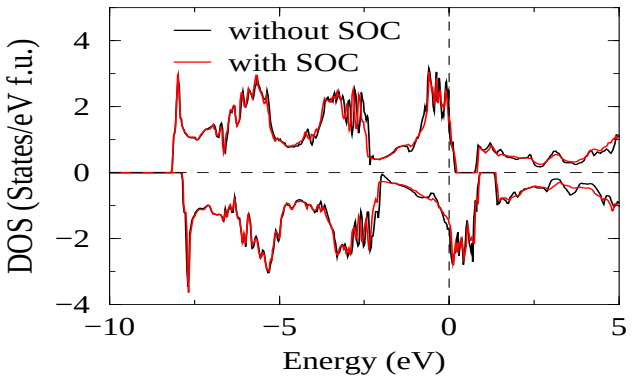

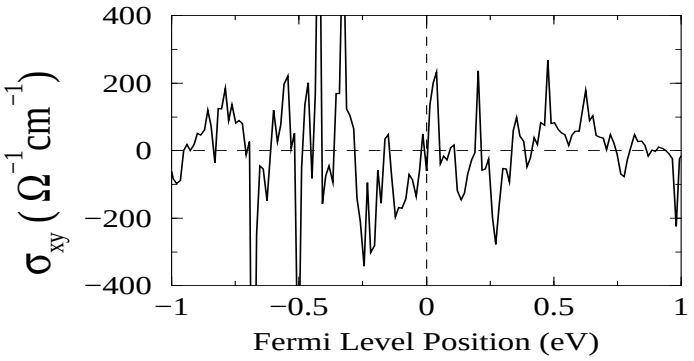

$$\sigma_{ij}^{TKNN} = -\epsilon_{ij\ell} e^2 \hbar \sum_n \int \frac{d^d \boldsymbol{p}}{(2\pi\hbar)^2} b_n^\ell(\boldsymbol{p}) f(\varepsilon_n(\boldsymbol{p}))$$

Small energy scale 0.02eV
Behavior like quantum chaos

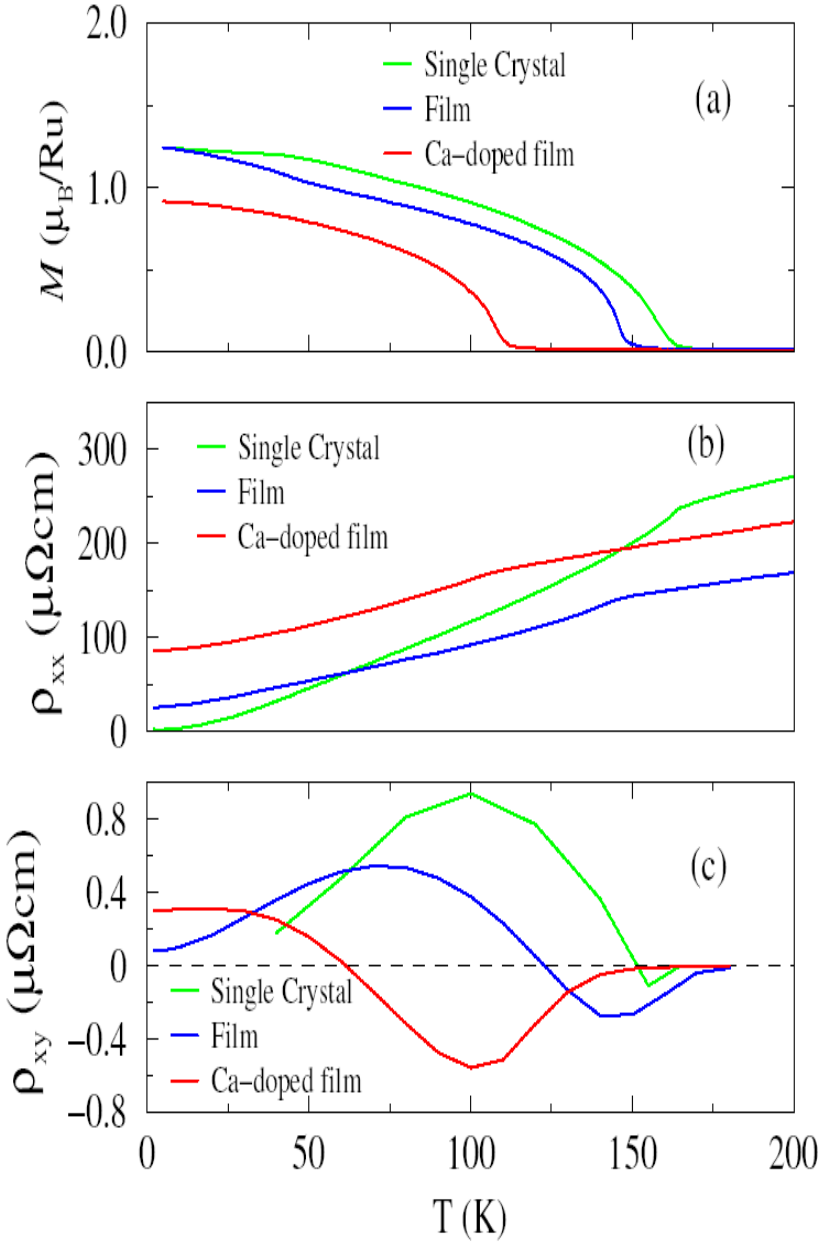

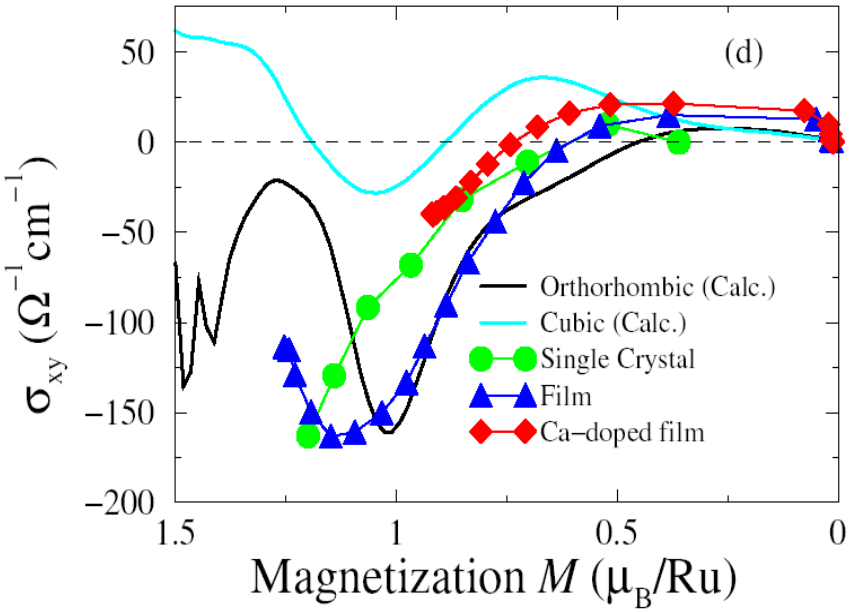

c.f. T. Jungwirth et al
(Ga,Mn)As

Another system of dissipationless AHE -- (Ga,Mn)As

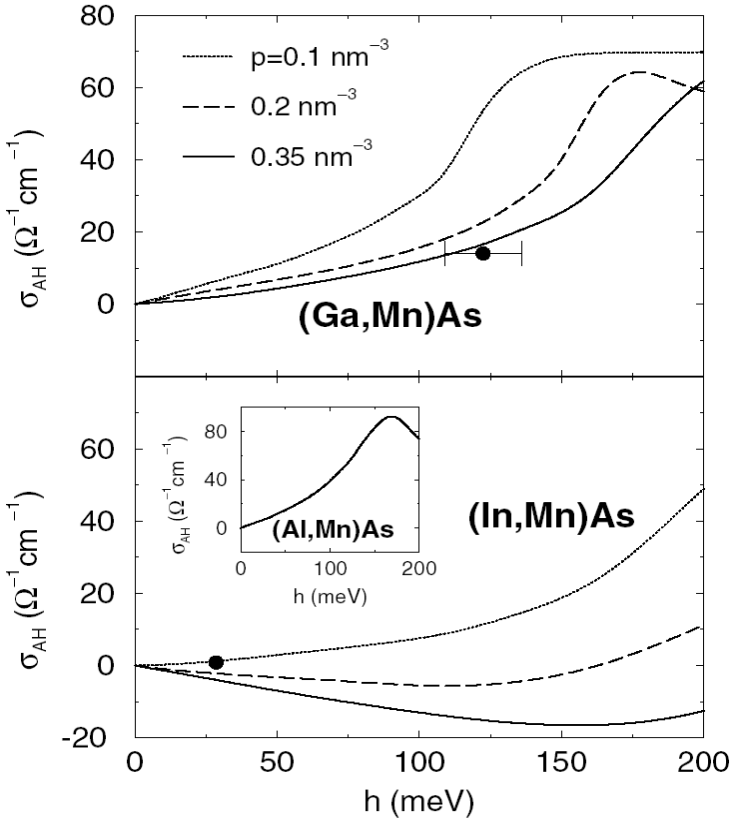

Jungwirth et al (2002)

Hopping transport
-- random network model

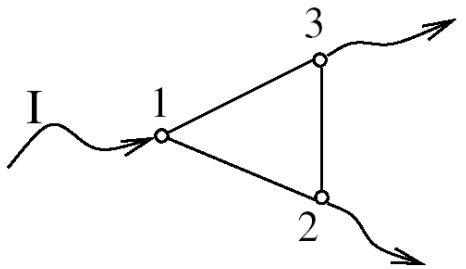

$$\sigma_{xy}^{\mathrm{AH}} \sim L\sigma_{xx}^{2}\frac{d\ln\varrho_0}{d\epsilon}\frac{hT}{e^2 t_{3/2}}(T_0/T)^{1/4}\, e^{-(T_0/T)^{1/4}},$$

Burkov-Balents (2003)

It turns that the intrinsic (Berry phase) mechanism dominates !!

Anderson Localization and Quantized Anomalous Hall Effect

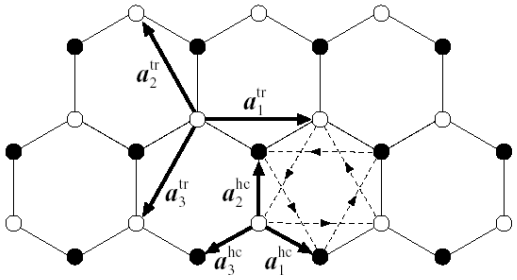

FIG. 1: Haldane's model defined on honeycomb lattice [12]. Open and closed c
respectively. The
tice vectors of ho
lattice respectivel
neighbor hopping.

D.F.M. Haldane (1988)
Zero field QHE

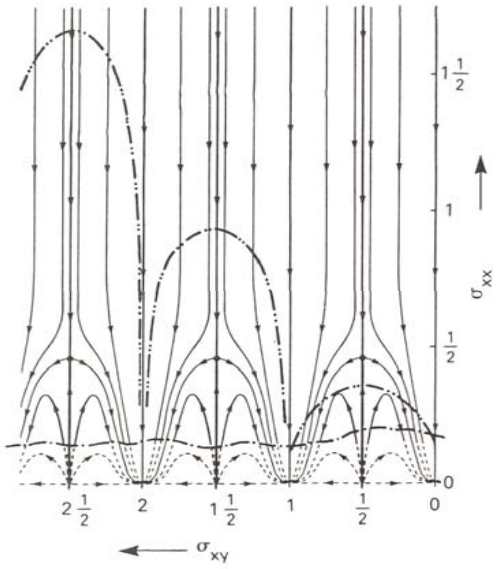

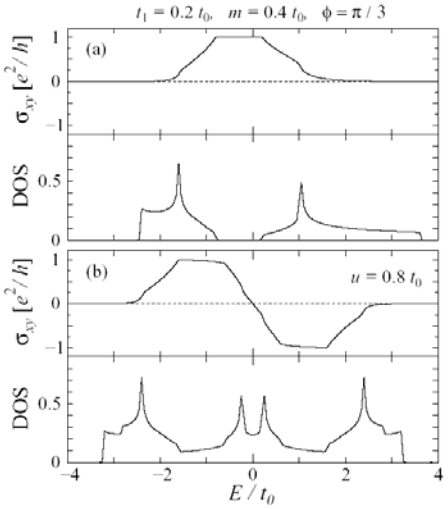

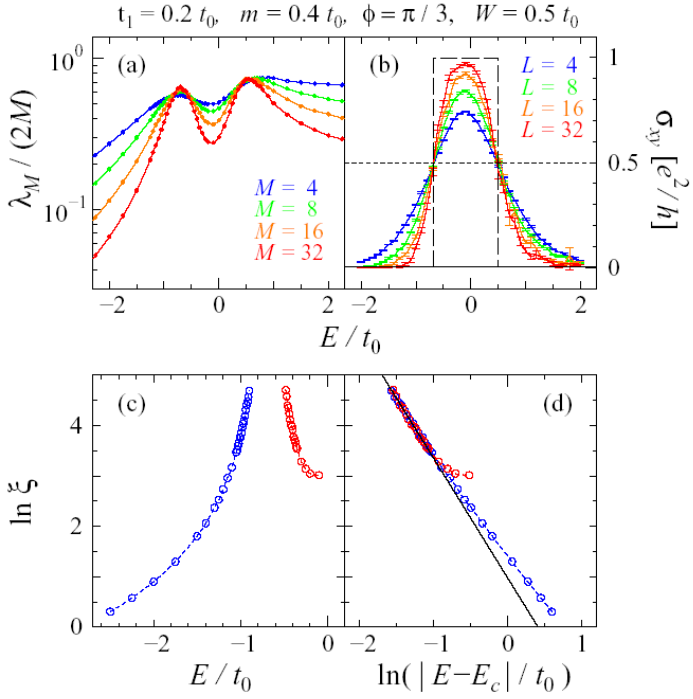

Spin Hall Effect

Classification of Order Parameters

Inversion \ Time reversal	even	odd
even	ρ charge density	Spin $\vec{M}$ magnetization
odd	$\vec{j}_s$, $\vec{P}$ **spin current** polarization	$\vec{j}$, $\vec{T}$ current **toroidal moment**

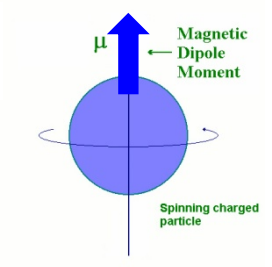

Spin current

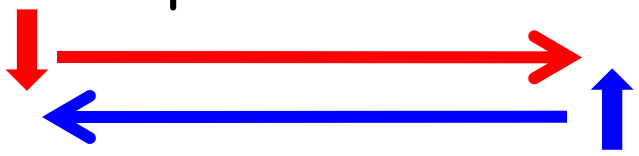

Time-reversal symmetry in quantum mechanics

$\Theta = e^{-i\pi S_y/\hbar} K$ Time-reversal operation

K complex conjugation

$\Theta[\alpha\psi] = \alpha^* \Theta\psi \quad <\Theta\psi|\Theta\phi> = <\phi|\psi>$ anti-unitary

$\Theta^2 = (-1)^{2S}$

Kramers theorem

$\Theta H = H\Theta$ Time-reversal symmetric Hamiltonian

ψ and $\Theta\psi$ are two orthogonal degenerate states

$<\psi|\Theta\psi> = <\Theta^2\psi|\Theta\psi> = -<\psi|\Theta\psi> = 0$

Barry phase and Kramers theorem

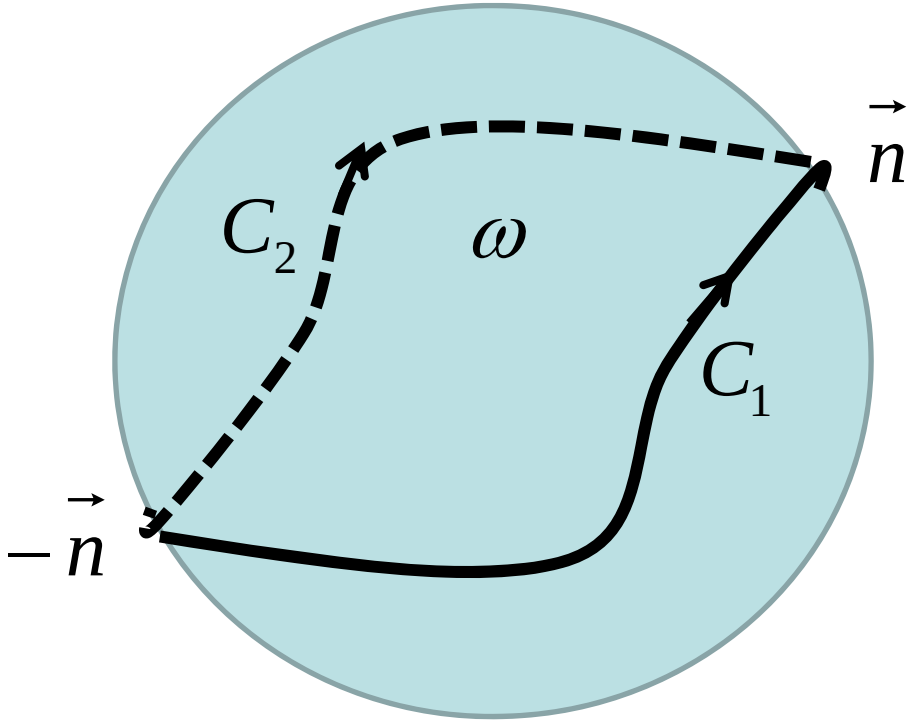

$$\exp[i \oint_{C_1+(-C_2)} d\vec{n}\cdot\vec{A}_s(\vec{n})] = e^{iS\omega}$$

$$A_j = \exp\left[i\int_{C_j} d\vec{n}\cdot\vec{A}_s(\vec{n}) \right]$$

Amplitude for Cj

$$\omega = 2\pi \quad S = 1/2$$

➡ $A_1 A_2^* = -1 \quad A_1 = -A_2$

➡ Tunneling amplitude from n to -n is zero $A_1 + A_2 = 0$

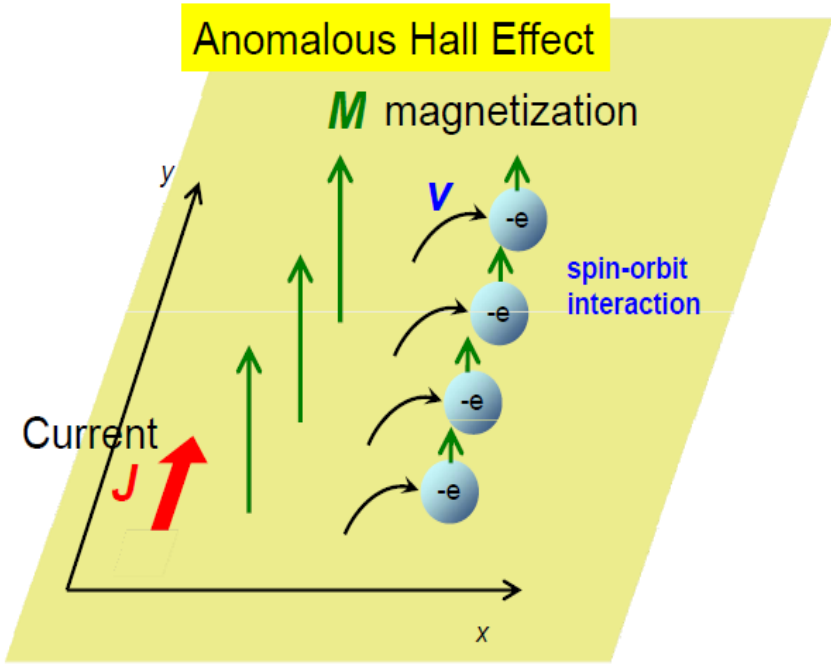
Anomalous Hall Effect
M magnetization
y
v
-e
-e
-e
-e
spin-orbit
interaction
Current
J
x

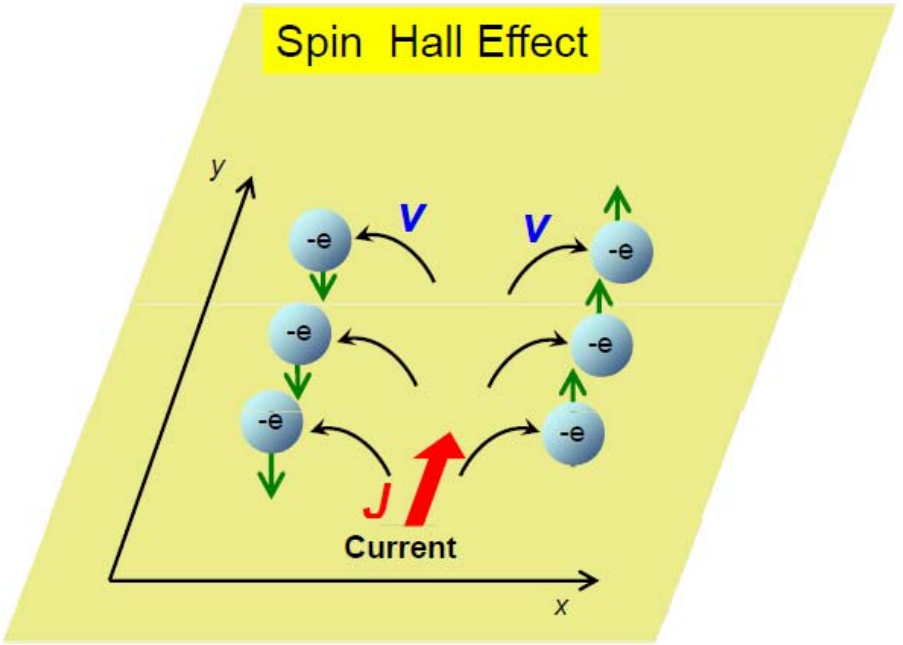
Spin Hall Effect
y
v
v
-e
-e
-e
-e
-e
-e
J
Current
x

Spin Hall effect in semiconductors

$$j_{xy} = \frac{eE_z}{12\pi^2\hbar}\left(k_F^H - k_F^L\right) \equiv \frac{1}{2e}\sigma_s E_z$$

x: current direction
y: spin direction
z: electric field

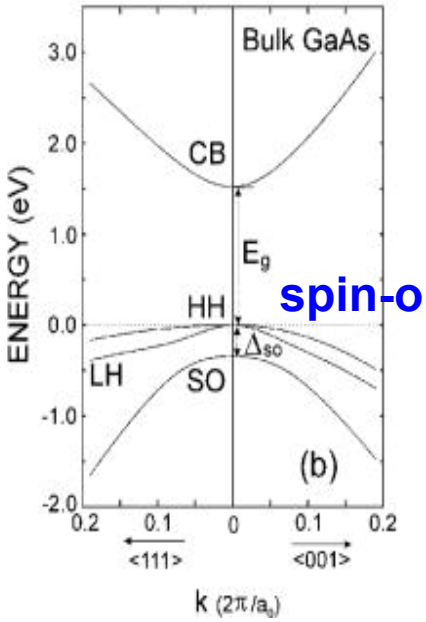

spin-orbit int.

SU(2) analog of the QHE

- topological origin
- dissipationless
- All occupied states in the valence band contribute.

External electric field does not break time-reversal symmetry.
Spin current is allowed in this system with time-reversal symmetry

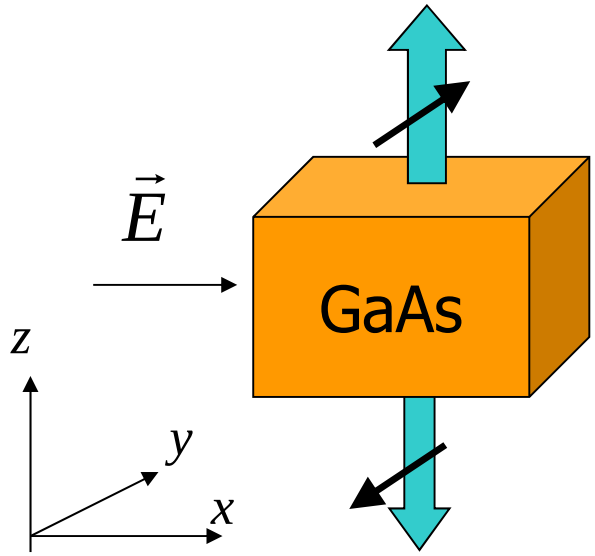

Wave-packet formalism in systems with Kramers degeneracy

Let us extend the wave-packet formalism to the case with time-reversal symmetry.

Adiabatic transport

= The wave-packet stays in the same band, but can transform inside the Kramers degeneracy.

$$\left|\psi_n(t)\right\rangle = \int d^3q \left(a_1(\vec{q},t)\left|\psi_{n1}(\vec{q},\vec{x}_c,t)\right\rangle + a_2(\vec{q},t)\left|\psi_{n2}(\vec{q},\vec{x}_c,t)\right\rangle\right) \quad (n=H,L)$$

$$\begin{pmatrix} z_1(\vec{q},t) \\ z_2(\vec{q},t) \end{pmatrix} = \frac{1}{\sqrt{a_1^2+a_2^2}} \begin{pmatrix} a_1(\vec{q},t) \\ a_2(\vec{q},t) \end{pmatrix}$$

Eq. of motion

$$\begin{cases} \dot{\vec{k}} = -e\vec{E} \\ \dot{x}_l = \dfrac{\partial E^n}{\partial k_l} - \dot{\vec{k}}_j \left(z^+ F^n_{lj} z\right) \quad n=H,L \\ \dot{z} = i\left(\dot{\vec{k}}\cdot\vec{A}^n\right) z \end{cases}$$

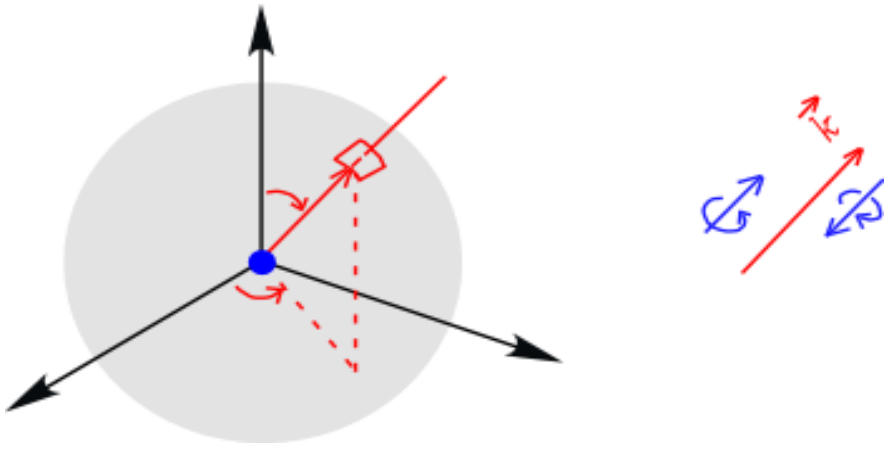

Real-space trajectory within Abelian approximation

Eq. of motion: $\dot{k}_i = -E_i$, $\dot{x}_i = \frac{k_i}{m_\lambda} + \frac{\lambda}{k^3}\varepsilon_{ijk}\dot{k}_j k_k$

It can be integrated:

$$\vec{k}(t) = (k_{x0}, k_{y0}, k_{z0} - E_z t),$$

$$z(t) = z_0 + \frac{k_{z0}}{m_\lambda}t - \frac{E_z}{2m_\lambda}t^2,$$

$$x(t) = x_0 + \frac{k_{x0}}{m_\lambda}t + \frac{\lambda k_{y0}}{k_{x0}^2 + k_{y0}^2}\frac{E_z t - k_{z0}}{\sqrt{k_{x0}^2 + k_{y0}^2 + (E_z t - k_{z0})^2}},$$

$$y(t) = x_0 + \frac{k_{y0}}{m_\lambda}t - \frac{\lambda k_{x0}}{k_{x0}^2 + k_{y0}^2}\frac{E_z t - k_{z0}}{\sqrt{k_{x0}^2 + k_{y0}^2 + (E_z t - k_{z0})^2}}$$

Side jump ($\perp \vec{k}\ (// \vec{S})$)

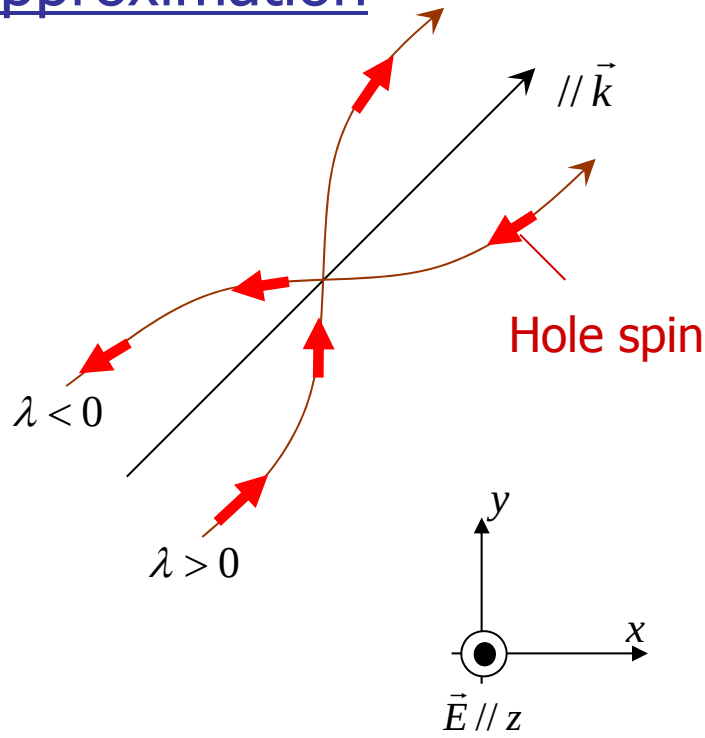

Spin motion can be known from orbital motion since $\vec{S} = \lambda\hat{k}$.

Spin current (spin // y, velocity // x)

$$j_{xy}^H = \frac{1}{3}\sum_{\lambda=\pm\frac{3}{2},\vec{k}} \dot{x}S_y n^\lambda(\vec{k}) = \frac{E_z k_F^H}{4\pi^2\hbar},$$

$$j_{xy}^L = \frac{1}{3}\sum_{\lambda=\pm\frac{1}{2},\vec{k}} \dot{x}S_y n^\lambda(\vec{k}) = \frac{E_z k_F^L}{36\pi^2\hbar},$$

Spin accumulation at the boundary

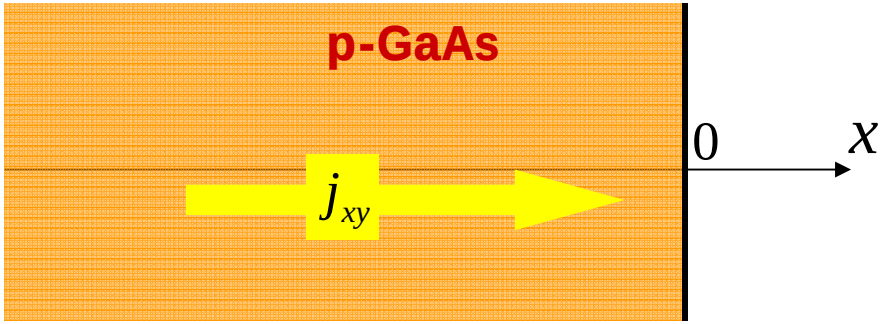

p-GaAs : $x \le 0$

Spin current : $j_{xy}(x) = j_{xy}\theta(-x)$

Diffusion eq.

$$\frac{\partial s^y(x,t)}{\partial t} - D\frac{\partial^2 s^y(x,t)}{\partial x^2} = -\frac{\partial j_{xy}(x,t)}{\partial x} - \frac{s^y(x,t)}{\tau_s}$$

Steady-state solution: $s^y(x) = j_{xy}\sqrt{\frac{\tau_s}{D}}e^{x/L}, \quad L \equiv \sqrt{D\tau_s}$

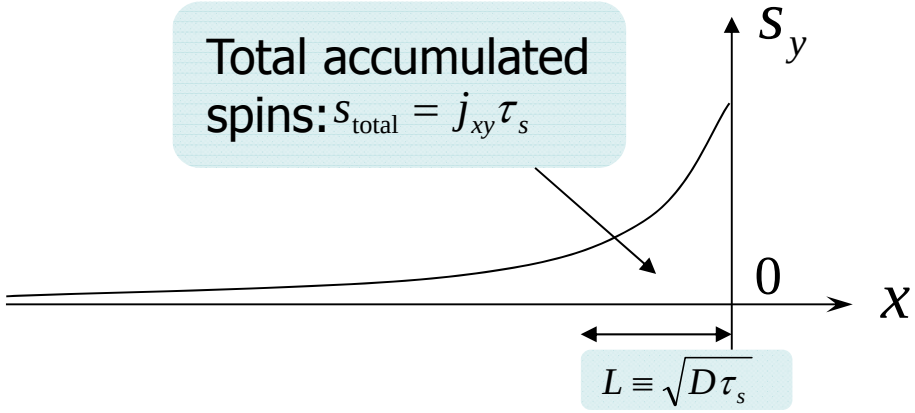

Spin injection by ferromagnetic semiconductor $Ga_{1-x}Mn_xAs$

Ohno et al., Nature 402,790 (1999)

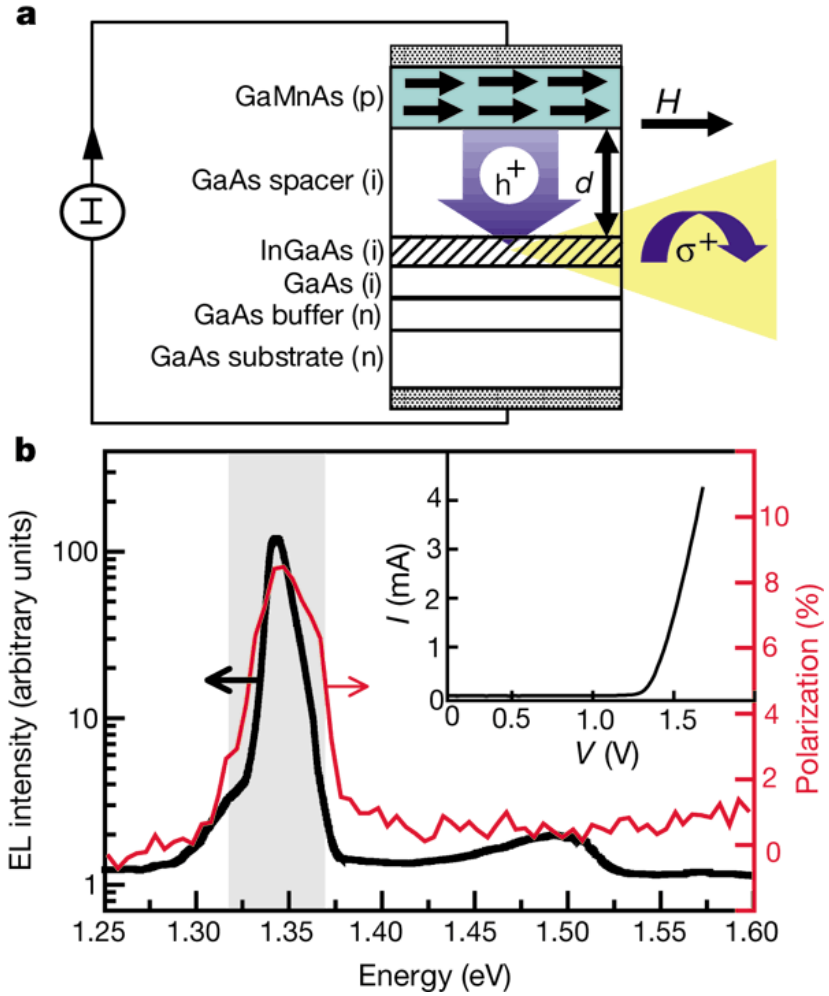

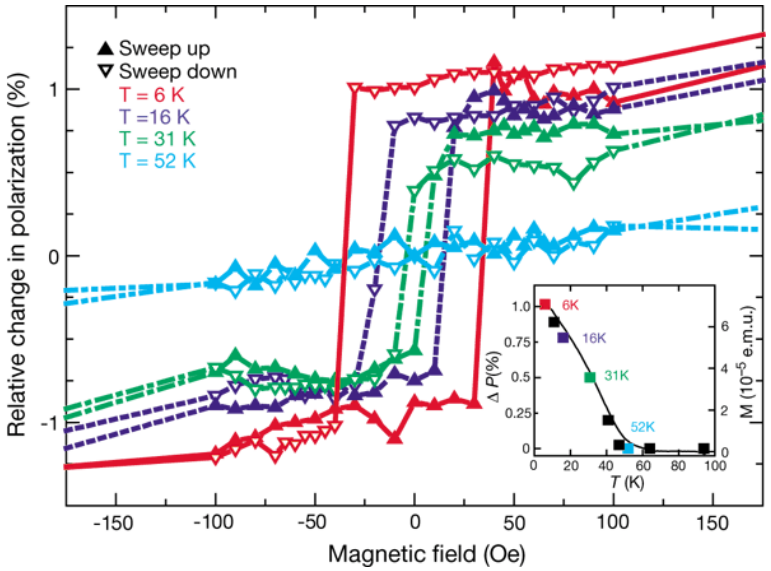

Experimental confirmation of spin Hall effect in GaAs

D.D.Awschalom (n-type) UC Santa Barbara

J.Wunderlich (p-type) Hitachi Cambridge

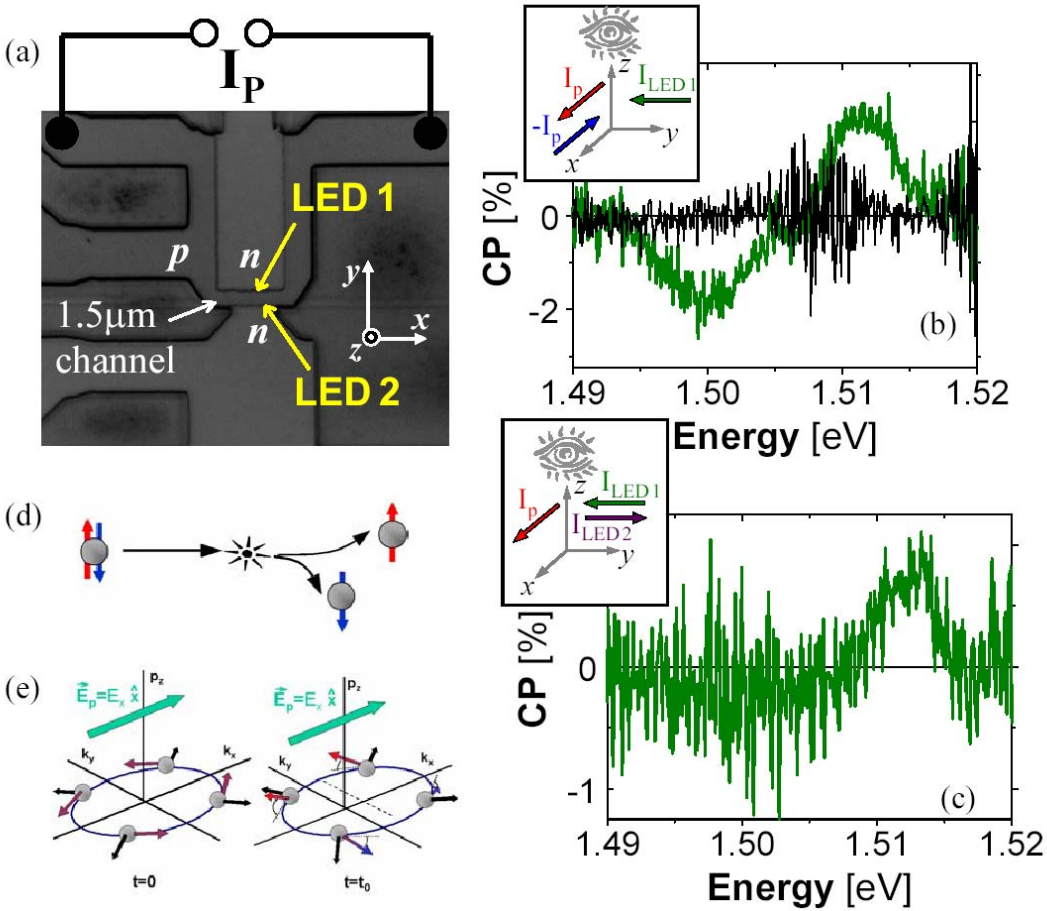

Wunderlich et al. 2004

Hall Effect of Light

Can neutral particle show Hall effect ?

Hall effect of photon

M. Onoda et al, Phys. Rev. Lett. **93,** 083901 (2004).
K.Y. Bliokh and Y.P. Bliokh
Phys. Rev. Lett. **96**, 073903 (2006).
F. D. M. Haldane and S. Raghu,
Phys. Rev. Lett. **100**, 013904 (2008)
O. Hosten, P. Kwiat, Science **319,** 787 (2008).

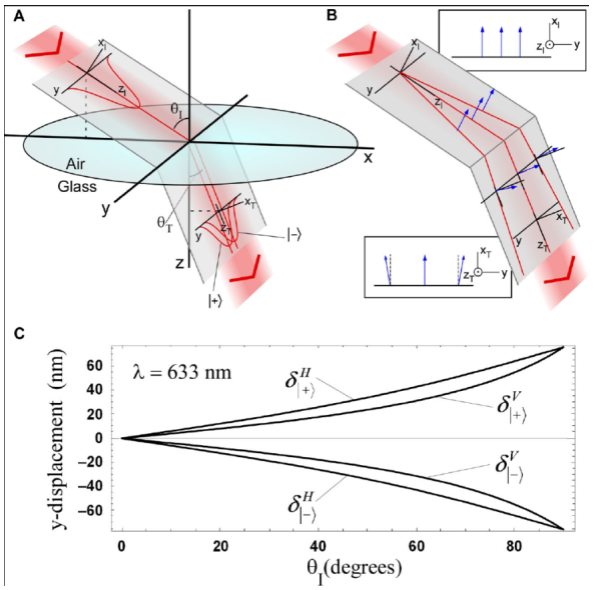

Thermal Hall effect by phonon : $Tb_3Ga_5O_{12}$

Strohm, Rikken, & Wyder, PRL **95** ('05).

Thermal Hall angle: $\alpha(B) = \kappa_{xy}(B)/\kappa_{xx}(B) \sim 10^{-4}\mathrm{rad\ T}^{-1}$ at 5K.

Thermal Hall effect by magnons

H. Kastura, N.N., and P.A. Lee, PRL **104** ('10).

Y. Onose et al., Science (2010)

gravitational lens

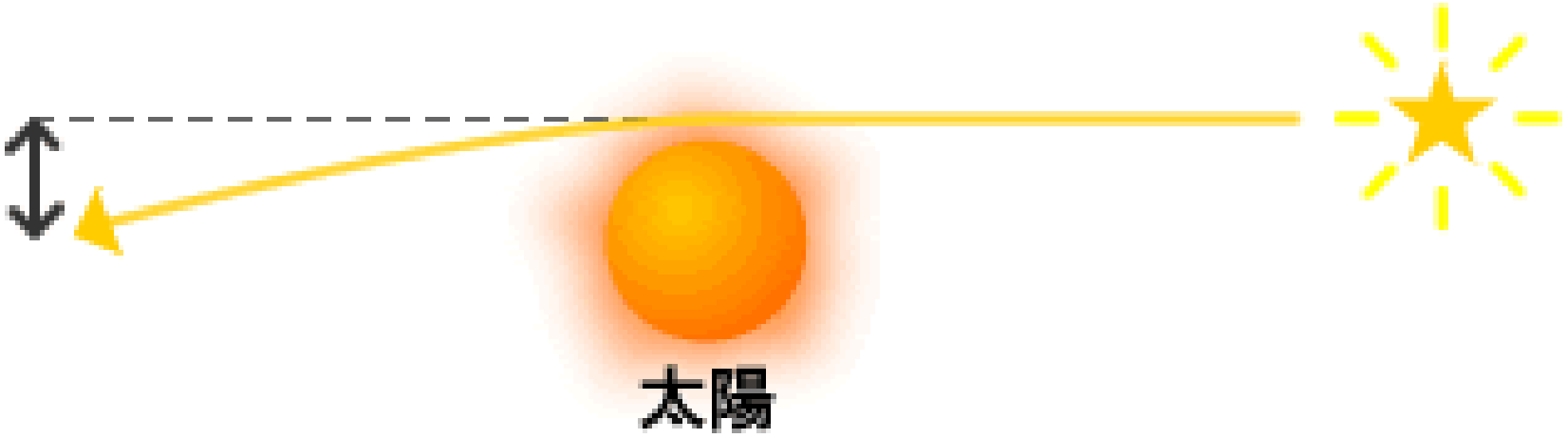

Curvature in momentum space changes the trajectory of light

Hall Effect of Light

Photon also has "spin"

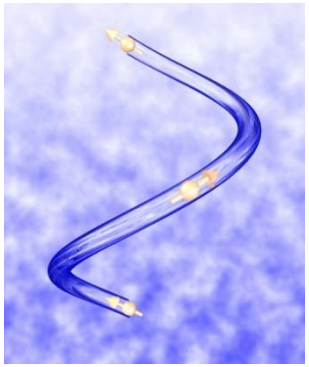

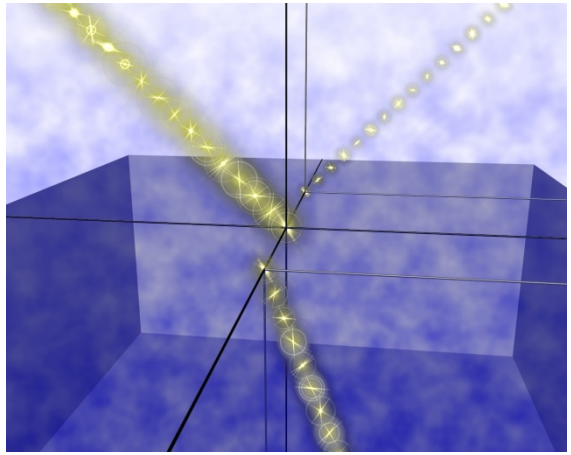

Extended equation of geometrical optics

$$velocity: \dot{\vec{r}}_c = v(\vec{r}_c)\frac{\vec{k}_c}{k_c} + \dot{\vec{k}}_c \times (z_c \,|\, \vec{\Omega}_{\vec{k}_c} \,|\, z_c)$$

$$force: \dot{\vec{k}}_c = -[\vec{\nabla} v(\vec{r}_c)]k_c$$

$$polarization: |\, \dot{z}_c) = -i\dot{\vec{k}}_c \cdot \vec{\Lambda}_{\vec{k}_c} \,|\, z_c)$$

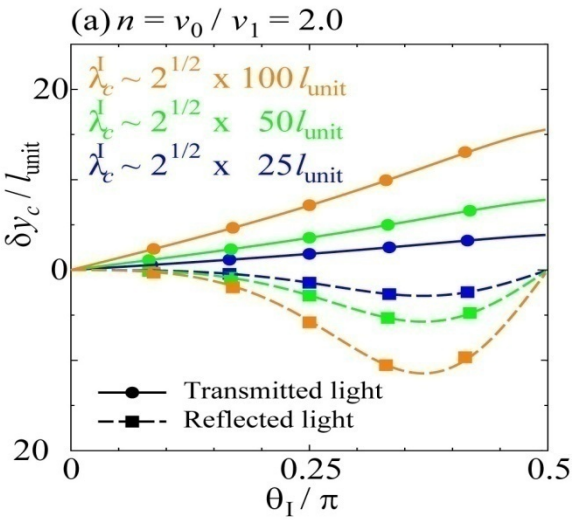

M.Onoda, S.Murakami, N.N. (PRL2004)

K.Y. Blikoh, Y.P.Blikoh

Rotation of polarization in optical fiber

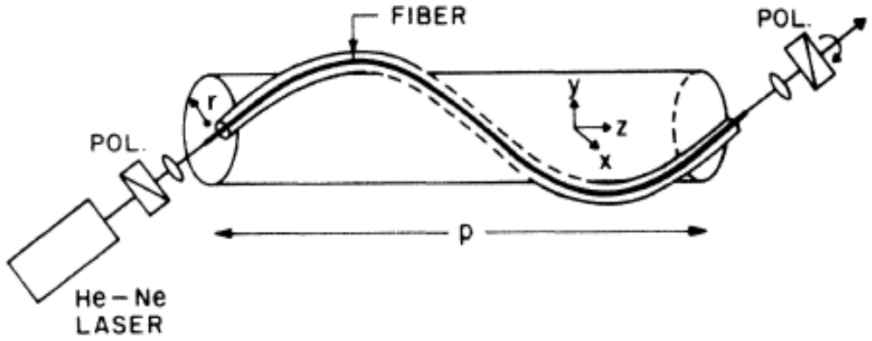

polarization
rotation

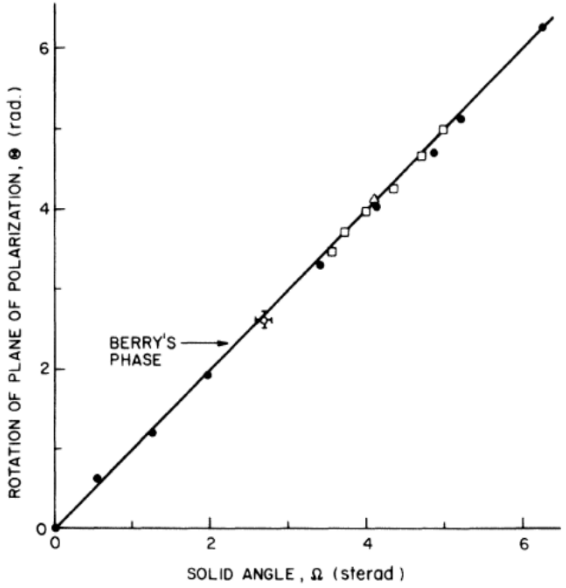

solid angle

Tomita-Chiao 1986
M.V.Berry

Sciencexpress Report

Observation of the Spin Hall Effect of Light via Weak Measurements

Onur Hosten* and Paul Kwiat

Department of Physics, University of Illinois at Urbana-Champaign, Urbana, IL 61801, USA.

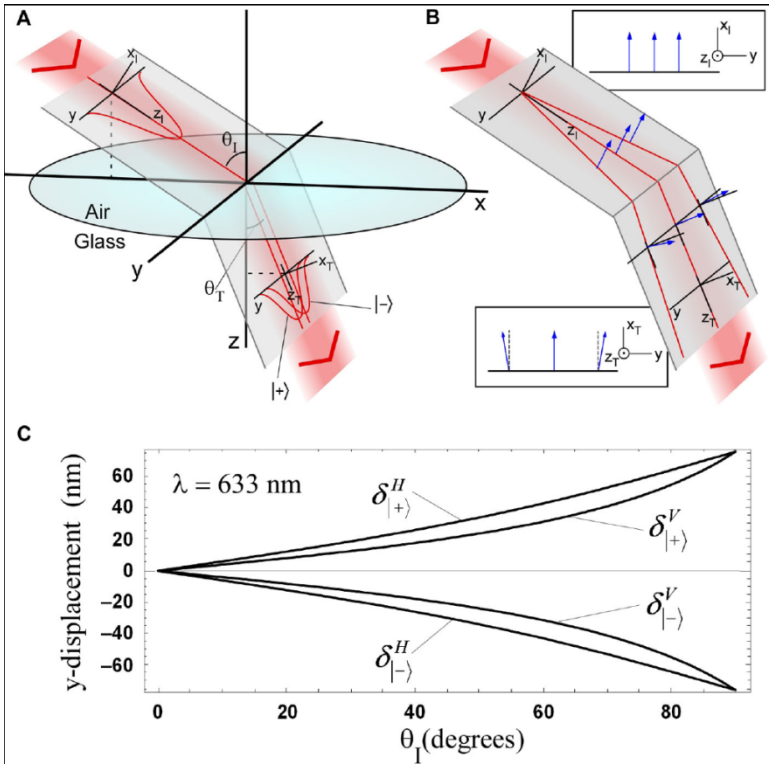

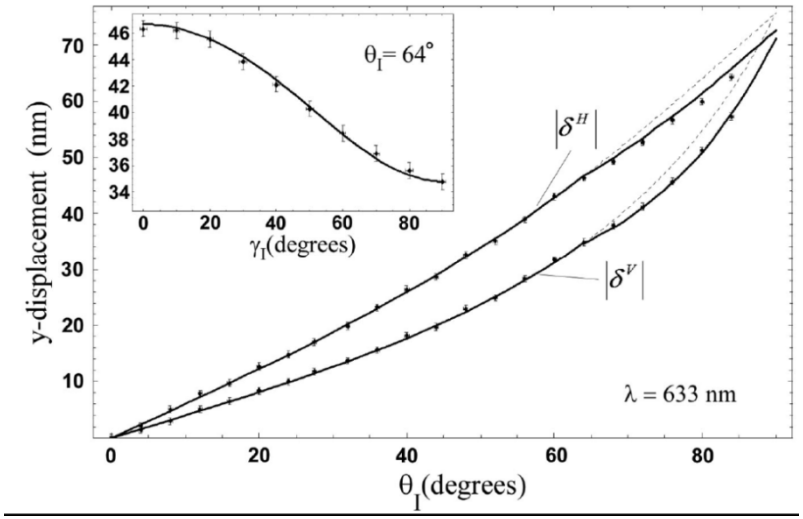

1 angstrom accuracy by quantum "weak measurement"

$$A_w = \frac{\langle \psi_2 | \hat{\mathbf{A}} | \psi_1 \rangle}{\langle \psi_2 | \psi_1 \rangle}$$

Giant shift of X-ray beam in deformed crystal

Sawada-Murakami-Nagaosa PRL06

Berry curvature in r-k space

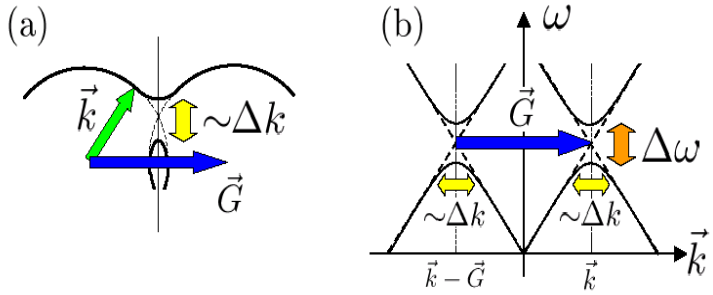

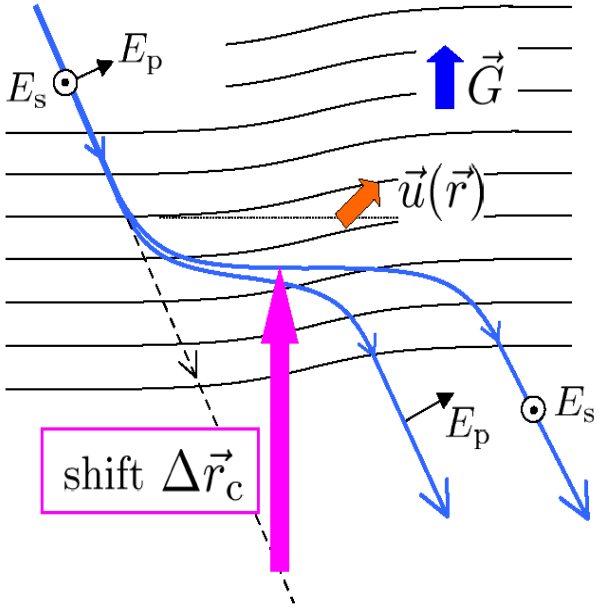

$\approx 10^6$ enhancement

PRL2010

PRL 104, 244801 (2010) — Selected for a Viewpoint in *Physics* — PHYSICAL REVIEW LETTERS — week ending 18 JUNE 2010

Berry-Phase Translation of X Rays by a Deformed Crystal

Yoshiki Kohmura, Kei Sawada, and Tetsuya Ishikawa

RIKEN, SPring-8 Center, 1-1-1, Kouto, Sayo-cho, Sayo-gun, Hyogo 679-5148, Japan

(Received 21 December 2009; published 14 June 2010)

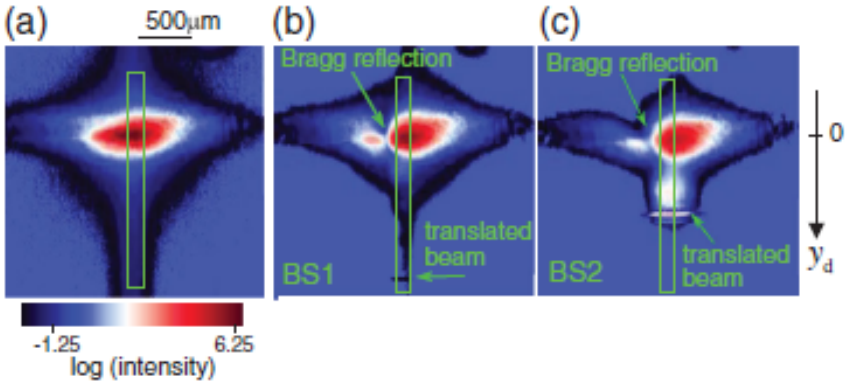

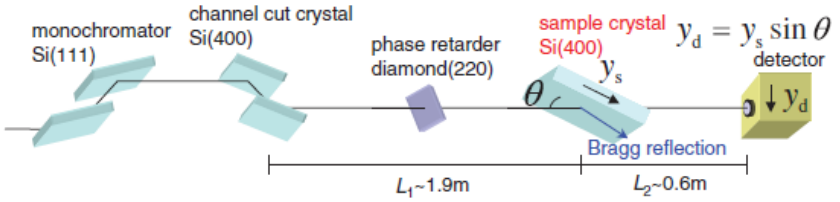

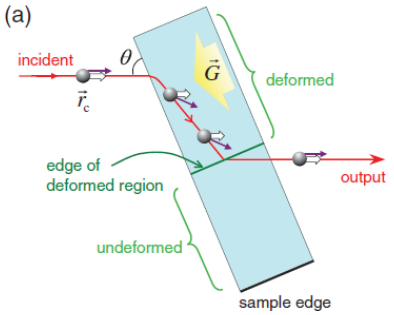

Magnon Hall Effect

Kubo formula for thermal Hall conductivity

$$\kappa^{xy} = \frac{V}{T}\int_0^\infty dt \int_0^\beta d\lambda \langle j_E^x(-i\lambda) j_E^y(t)\rangle_{\rm th}$$

$$\kappa^{xy} = -i\frac{1}{4T}\frac{1}{V}\sum_{\vec{k}} n_\alpha(\vec{k})[\Theta^x_{\alpha\beta}(\vec{k})(\omega_\alpha(\vec{k})+\omega_\beta(\vec{k}))^2\Theta^y_{\beta\alpha}(\vec{k}) - (x\leftrightarrow y)]$$

$$= -\frac{1}{2}\frac{1}{T}{\rm Im}\sum_\alpha \int_{\rm BZ}\frac{d^2k}{(2\pi)^2} n_\alpha(k)\left\langle \frac{\partial u_\alpha(k)}{\partial k_x}\middle|(\mathcal{H}(k)+\omega_\alpha(k))^2\middle|\frac{\partial u_\alpha(k)}{\partial k_y}\right\rangle$$

Berry curvature

Bose distribution function $n_\alpha(\vec{k}) = 1/(e^{\beta\omega_\alpha(\vec{k})}-1)$

$$\mathcal{H}(\vec{k})|u_\alpha(\vec{k})\rangle = \omega_\alpha(\vec{k})|u_\alpha(\vec{k})\rangle$$

c.f. Matsumoto- Murakami

$$L_z^{\rm self} \simeq m_1^* l_z^{\rm self} = -\frac{16JSm_1^*}{\hbar V}{\rm Im}\sum_{\boldsymbol{k}}\rho(\varepsilon_{1\boldsymbol{k}})\left\langle\frac{\partial u_1}{\partial k_\alpha}\middle|\frac{\partial u_1}{\partial k_\beta}\right\rangle$$

Thermal Hall effect in Kagome ferromagnet

Spin Wave Hamiltonian

$$\mathcal{H}(\vec{k}) = 4JS - 2JS\Lambda(\vec{k},\phi)/\cos(\phi/3)$$

$$\Lambda(\vec{k},\phi) = \begin{pmatrix} 0 & \cos k_1 e^{-i\phi/3} & \cos k_3 e^{i\phi/3} \\ \cos k_1 e^{i\phi/3} & 0 & \cos k_2 e^{-i\phi/3} \\ \cos k_3 e^{-i\phi/3} & \cos k_2 e^{i\phi/3} & 0 \end{pmatrix}$$

$$(k_j \equiv \vec{k}\cdot\vec{a}_j)$$

Magnon dispersion $JS = 1,\ \phi = \pi/3$

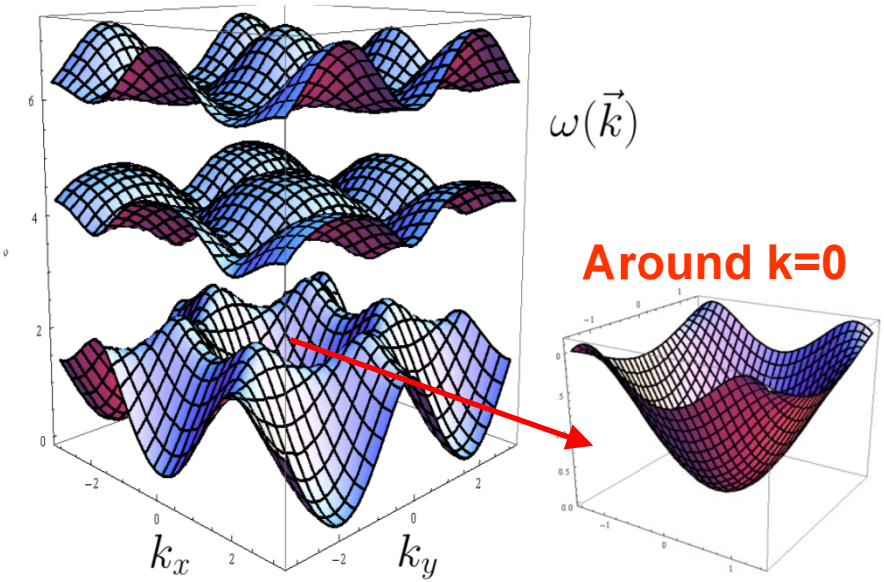

TKNN-like formula:

$$\kappa^{xy} \sim -\frac{(6JS)^2}{2T}\int_{\mathrm{BZ}}\frac{d^2k}{(2\pi)^2}n_1(\vec{k})\ \mathrm{Im}\langle\partial_{k_x}u_1(\vec{k})|\partial_{k_y}u_1(\vec{k})\rangle$$

$$\sim -\frac{(6JS)^2}{2T}\int_0^\infty\frac{dk}{2\pi}\frac{k}{e^{\beta JSk^2}-1}\left(\frac{-\phi k^2}{27\sqrt{3}}\right) = \boxed{\frac{\pi\phi}{36\sqrt{3}}T}$$

$$\omega_1(\vec{k}) \sim JS(k_x^2+k_y^2)$$

T-linear & B-linear!

$$\phi \propto \Phi = \frac{eBA_\triangle}{\hbar c}$$

Skew scattering ? Small in the scattering of low energy limit (s-wave).

Target material -$Lu_2V_2O_7$

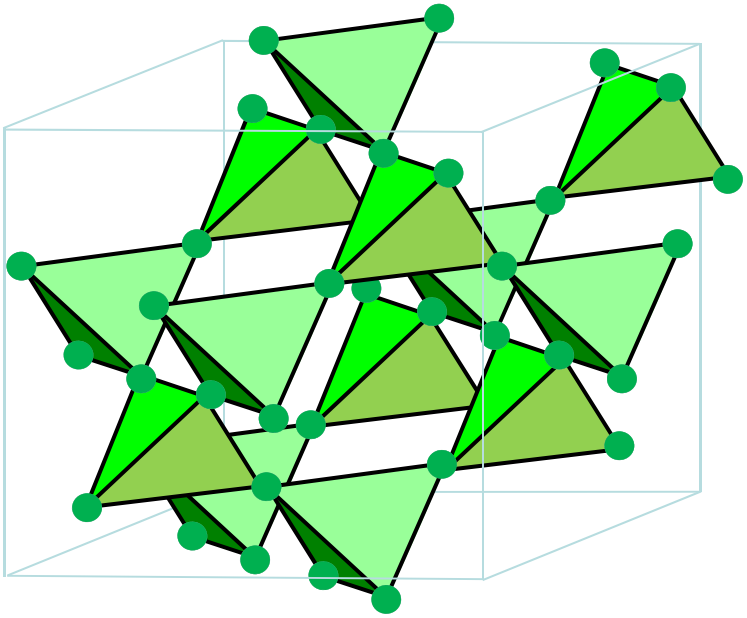

- ✓Pyrochlore Lattice
- (111) Plane is Kagome
- ✓Collinear ferromagnet
- ✓insulator

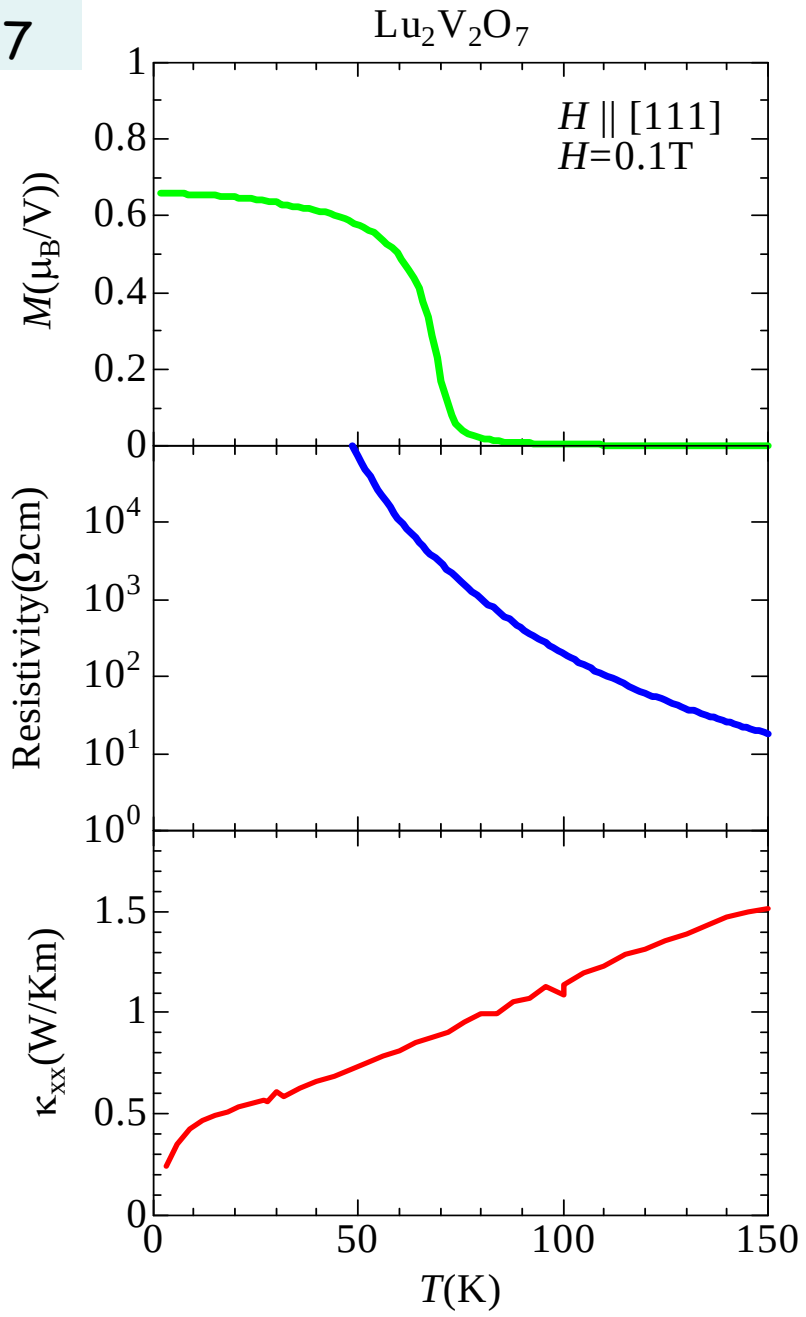

Thermal Hall conductivity for $Lu_2V_2O_7$

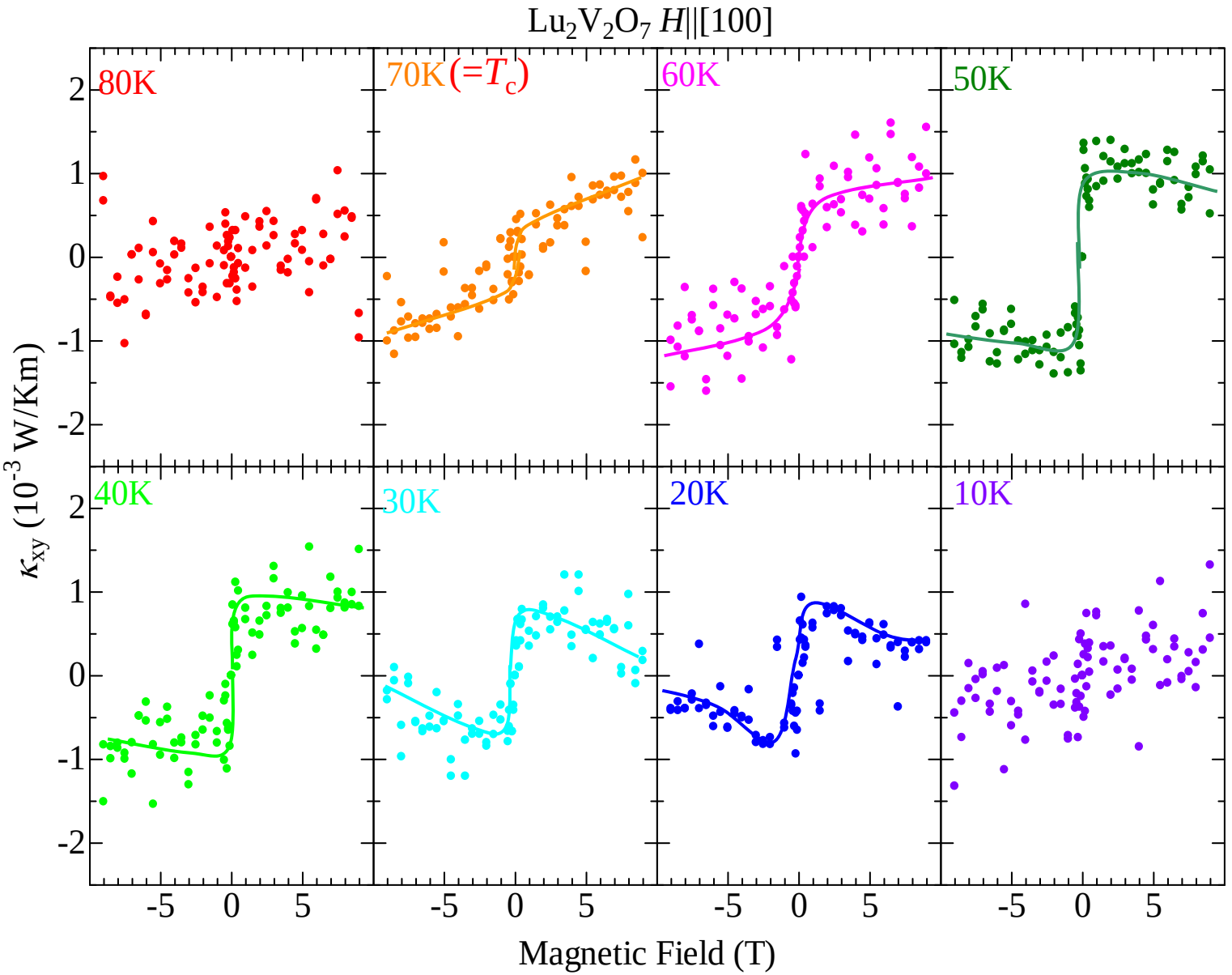

Theory of magnon Hall effect based on DM interaction

Katsura & Nagaosa

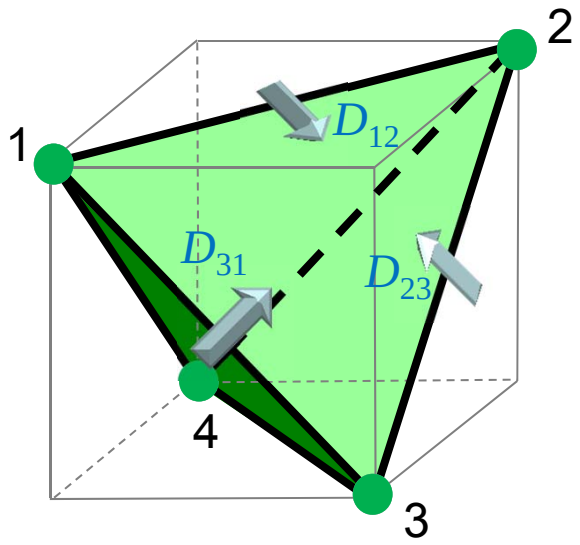

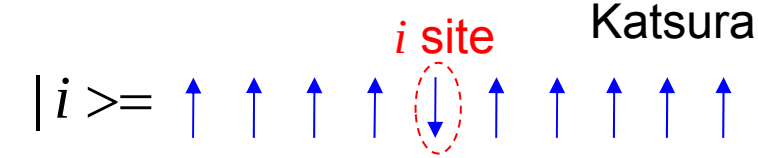

$$< j|-J\vec{S}_i\cdot\vec{S}_j+\vec{D}_{ij}\cdot(\vec{S}_i\times\vec{S}_j)|i>=-(\tilde{J}/2)e^{i\phi_{ij}}$$

$$\tilde{J}e^{i\phi_{ij}}=J+i\vec{D}_{ij}\cdot\vec{n}$$

Magnons acquire Berry phase owing to DM interaction.

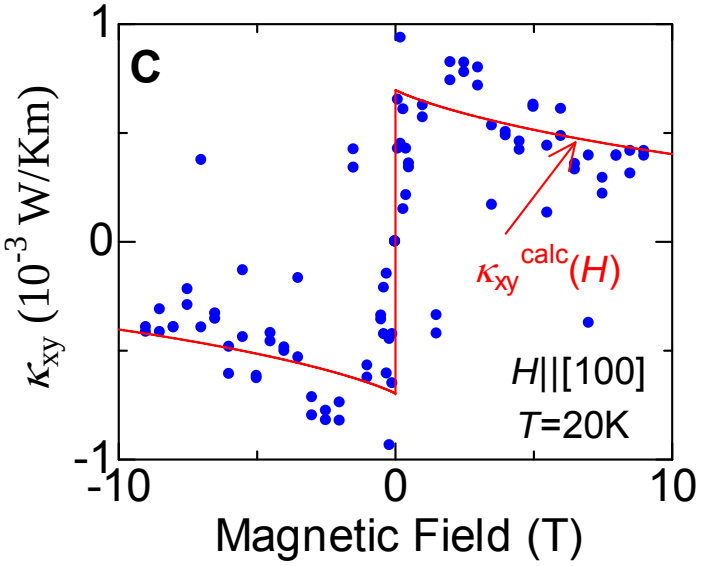

$$\kappa_{\alpha\beta}(H,T)=\Phi_{\alpha\beta}\frac{k_B^2T}{\pi^{3/2}\hbar a}\left(2+\frac{g\mu_BH}{2JS}\right)^2\sqrt{\frac{k_BT}{2JS}}\mathrm{Li}_{5/2}\left[\exp\left(-\frac{g\mu_BH}{k_BT}\right)\right],$$

(isotropic)

$$\mathrm{Li}_n(z)=\sum_{k=0}^{\infty}\frac{z^k}{k^n}$$

D/J=0.32

Cf. D/J=0.19 for $CdCr_2O_4$

c.f. Matsumoto -Murakami

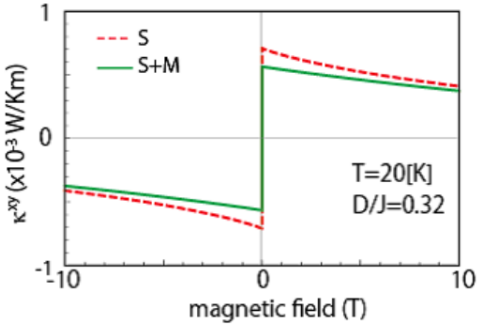

Various ferromagnetic insulators

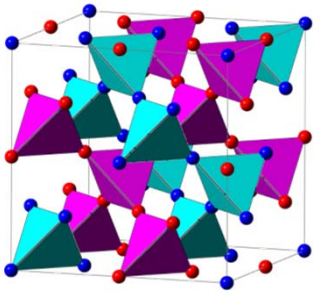

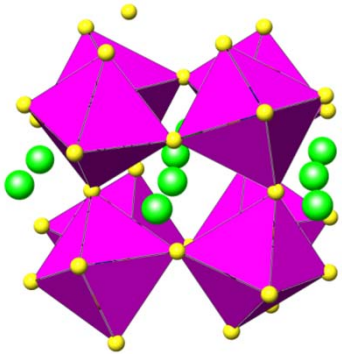

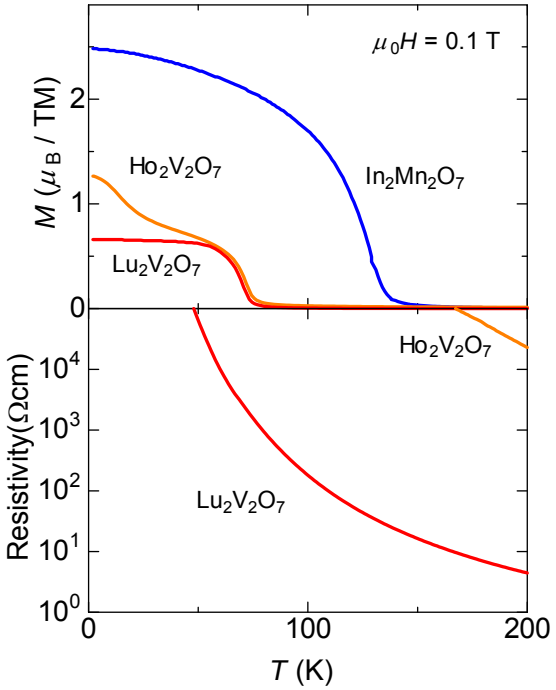

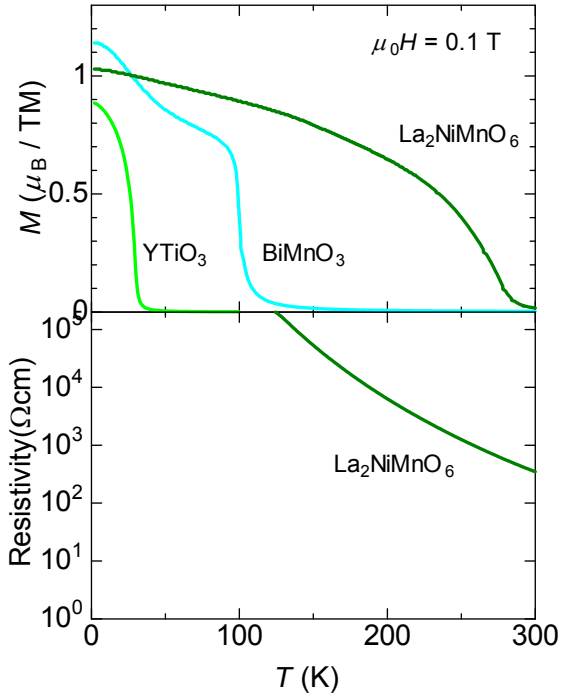

La_2NiMnO_6:

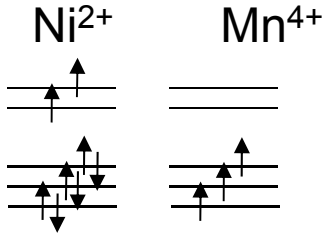

$YTiO_3$ Akimitsu *et al.*, 2001

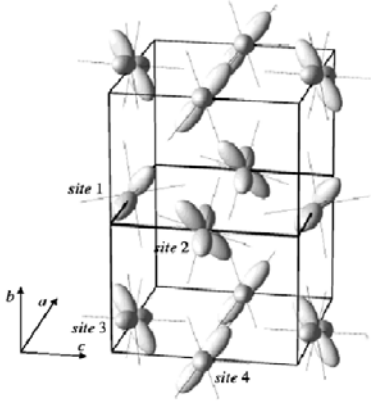

$BiMnO_3$ Atou *et al.* 1999

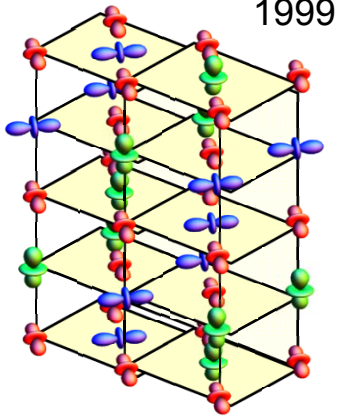

Pyrochlore ferromagnet

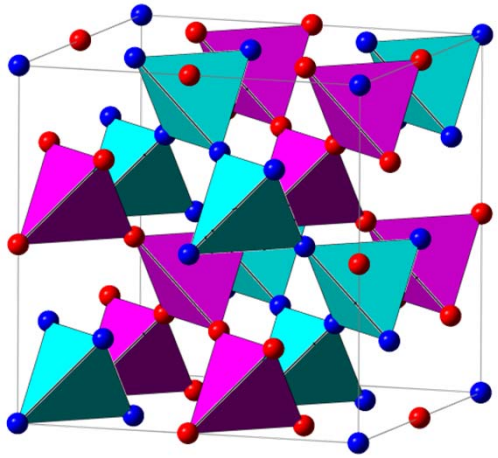

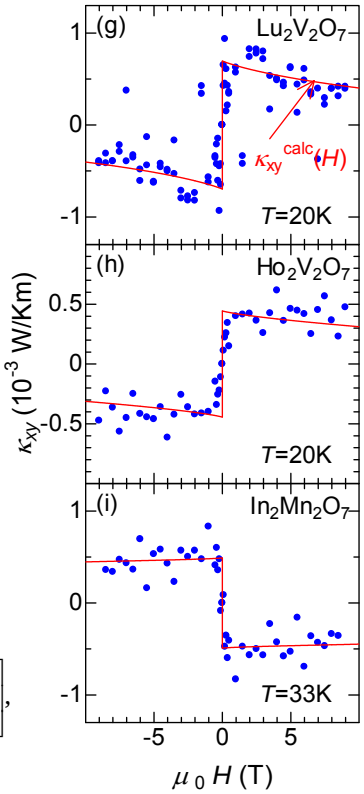

Theoretical formula

$$\kappa_{\alpha\beta}(H,T) = \Phi_{\alpha\beta}\frac{k_B^2 T}{\pi^{3/2}\hbar a}\left(2+\frac{g\mu_B H}{2JS}\right)^2\sqrt{\frac{k_B T}{2JS}}\,\mathrm{Li}_{5/2}\left[\exp\left(-\frac{g\mu_B H}{k_B T}\right)\right],$$

material	κ_{xy} (10^{-3} W/Km)	$\lvert D/J\rvert$
$Lu_2V_2O_7$ (20K)	1	0.32
$Ho_2V_2O_7$ (20K)	0.05	0.15
$In_2Mn_2O_7$ (33K)	-0.05	0.08

Perovskite ferromagnet

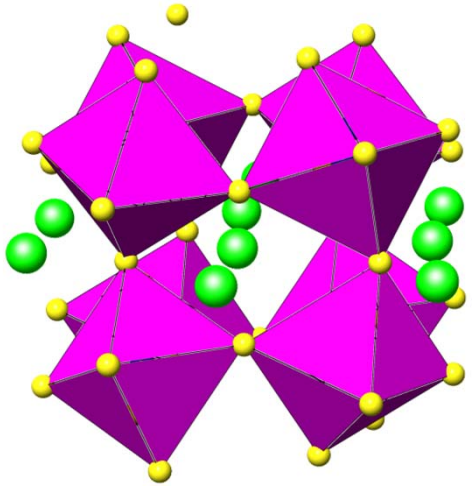

material	κ_{xy} (10^{-3} W/Km)
La_2NiMnO_6	indiscernible
$YTiO_3$	indiscernible
$BiMnO_3$ (31K)	-0.02~-0.04

Effect of lattice geometry on DM-induced magnon Hall effect

$Lu_2V_2O_7$
$Ho_2V_2O_7$
$In_2Mn_2O_7$

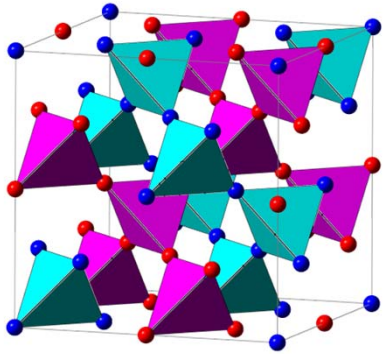

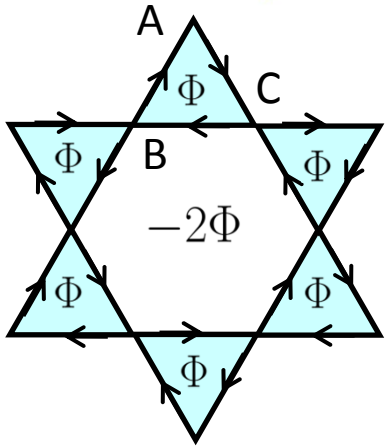

$\kappa_{xy} \neq 0$

La_2NiMnO_6
$YTiO_3$

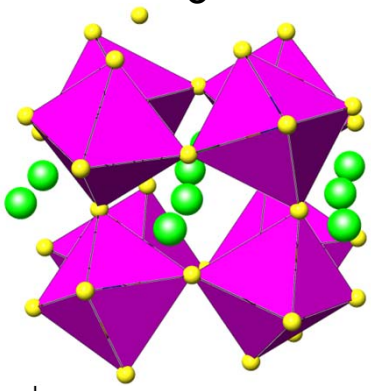

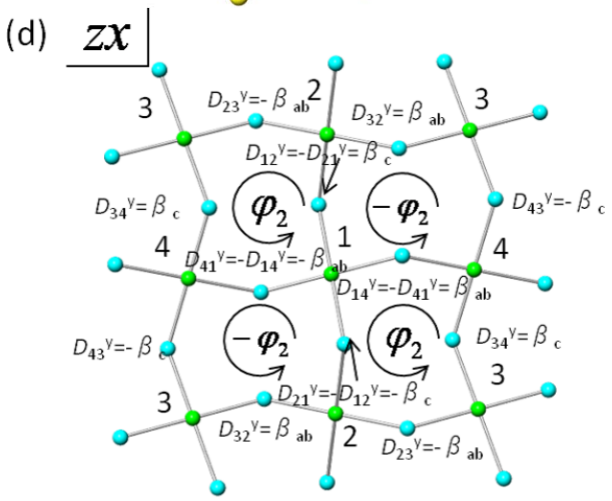

$\kappa_{xy} = 0$

$BiMnO_3$

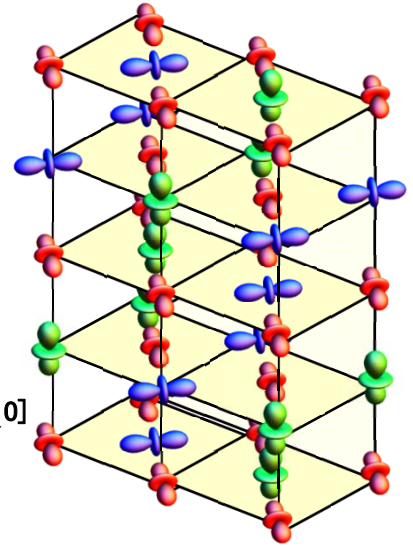

$\kappa_{xy} \neq 0$

Topological Materials

Quantum Hall effect

Haldane model for quantum Hall effect

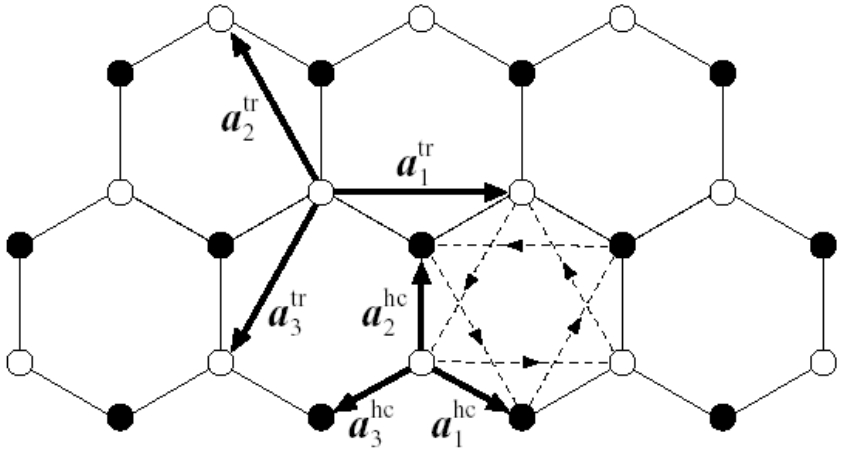

Complex transfer integral
between next nearest neighbor sites

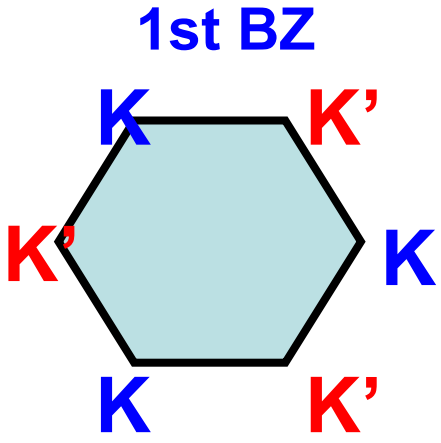

Dirac fermion at
K and K' points

⇨ Generation of the mass m with the same sign
at K and K' points

⇨ Quantized Hall effect
without Landau level formation

Anderson Localization and Quantized Anomalous Hall Effect

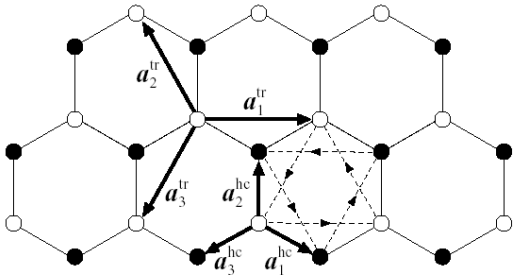

FIG. 1: Haldane's model defined on honeycomb lattice [12]. Open and closed c
respectively. The
tice vectors of ho
lattice respectivel
neighbor hopping.

D.F.M. Haldane (1988)
Zero field QHE

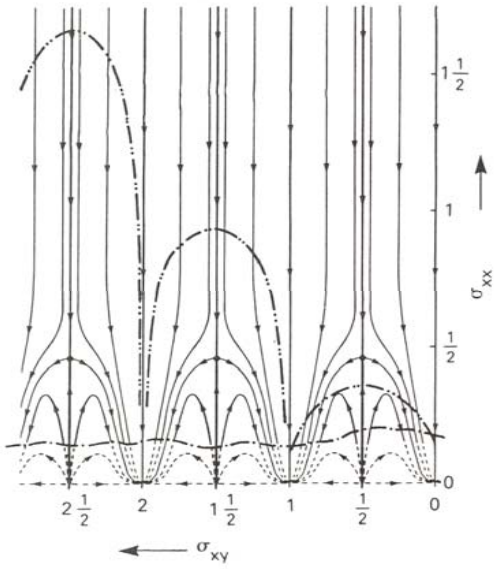

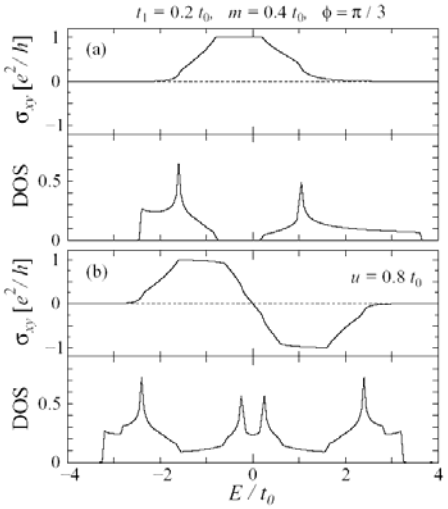

M.Onoda, N.N. (2005)
Quantized AHE

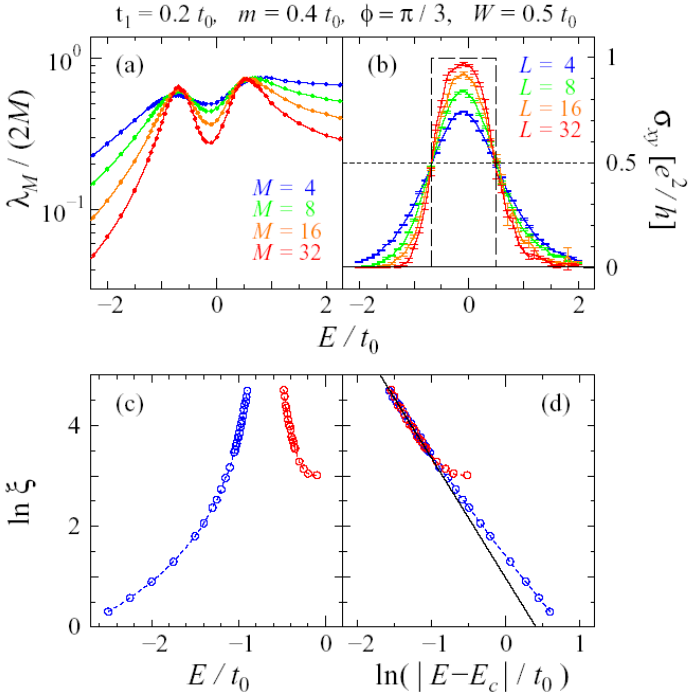

Quantized Anomalous Hall effect

Kubo formula

$$\sigma_{xy} = -\frac{i\hbar e^2}{L^2}\sum_{\mathbf{k}}\sum_{n\neq m} f(E_{n\mathbf{k}})\frac{\langle u_{n\mathbf{k}}|v_x|u_{m\mathbf{k}}\rangle\langle u_{m\mathbf{k}}|v_y|u_{n\mathbf{k}}\rangle - \langle u_{n\mathbf{k}}|v_y|u_{m\mathbf{k}}\rangle\langle u_{m\mathbf{k}}|v_x|u_{n\mathbf{k}}\rangle}{(E_{n\mathbf{k}} - E_{m\mathbf{k}})^2}$$

$$v_\mu = \frac{\partial \mathcal{H}(\mathbf{k})}{\hbar \partial k_\mu} \qquad \text{velocity}$$

$$\langle u_{m\mathbf{k}}|v_\mu|u_{n\mathbf{k}}\rangle = \frac{1}{\hbar}(E_{n\mathbf{k}} - E_{m\mathbf{k}})\langle u_{m\mathbf{k}}|\frac{\partial}{\partial k_\mu}|u_{n\mathbf{k}}\rangle \qquad \text{Feynman theorem}$$

$$\sigma_{xy} = -\frac{ie^2}{\hbar L^2}\sum_{\mathbf{k}}\sum_{n} f(E_{n\mathbf{k}})\left(\frac{\partial}{\partial k_x}\langle u_{n\mathbf{k}}|\frac{\partial}{\partial k_y}u_{n\mathbf{k}}\rangle - \frac{\partial}{\partial k_y}\langle u_{n\mathbf{k}}|\frac{\partial}{\partial k_x}u_{n\mathbf{k}}\rangle\right)$$

$$\sigma_{xy} = \nu\frac{e^2}{h}, \qquad \nu = \sum_n \int_{\mathrm{BZ}} \frac{d^2\mathbf{k}}{2\pi}\left(\frac{\partial a_{n,y}}{\partial k_x} - \frac{\partial a_{n,x}}{\partial k_y}\right) \in \mathbb{Z} \qquad \text{TKNN}$$

First Chern number as a winding number

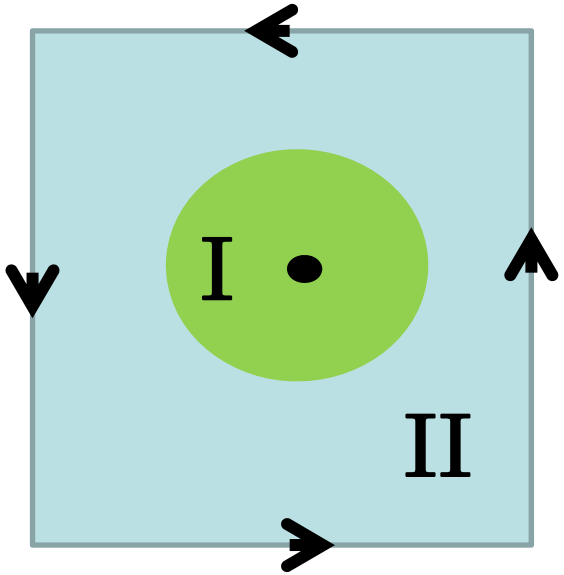

$$\nu_n = \frac{1}{2\pi}\oint_{\partial \mathrm{BZ}} d\mathbf{k}\cdot \boldsymbol{a}_n(\mathbf{k})$$
$$= \frac{1}{2\pi i}\oint_{\partial \mathrm{BZ}} d\mathbf{k}\cdot \langle u_n\mathbf{k}|\frac{\partial}{\partial \mathbf{k}}|u_n\mathbf{k}\rangle$$

Singularity of $a_n(k)$

⇨ Patch structure to define the gauge choice (Yang-Wu)

Single value-ness of the wave function ⇨ $\nu_n = \text{integer}$

$$< u_n(k)\,|\,u_n(k+dk)\,> = 1 + < u_n\,|\,\partial_k\,|\,u_n\,> \cdot dk = e^{i a_n(k)\cdot dk}$$

Laughlin's pumping argument

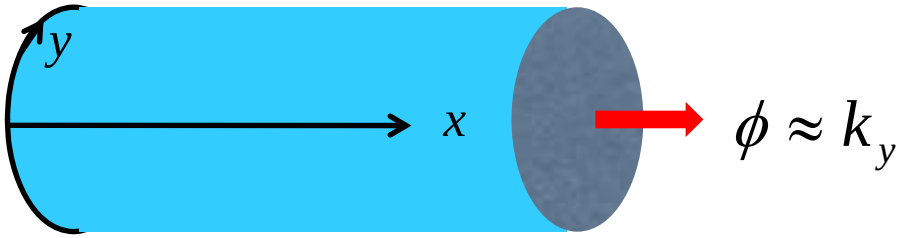

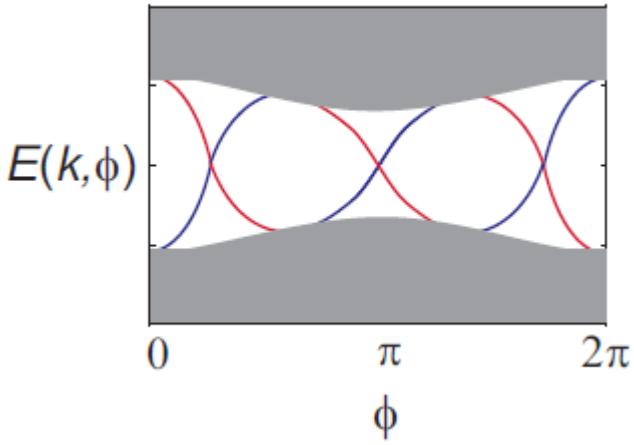

Edge channel

$$|\psi_{n,k}\rangle = \frac{1}{\sqrt{N_c}} e^{ikx} |u_{n,k}\rangle \qquad |R,n\rangle = \frac{1}{2\pi}\int dk e^{-ik(R-r)} |u_{k,n}\rangle$$

Wannier function

$$P_\rho(\phi=\phi_0) - P_\rho(\phi=0) = \iint \frac{dk d\phi}{2\pi}(\partial_\phi A_x - \partial_k A_\phi)$$

$$= \iint \frac{dk d\phi}{2\pi} F_{\phi x} = \text{Chern number}$$

Polarization
=pumped charge

$$A_\mu = i < u | \partial_\mu | u >$$

Berry connection

Effective theory - Chern Simons term

$$A_\mu(t,x) = (A_0, A_x, \phi) \Rightarrow S_{CS} = \iint dtdx \frac{\phi}{2\pi} \varepsilon^{\mu\nu} \partial_\mu A_\nu$$

Dimensional reduction

$$\phi \Rightarrow \theta(t,x) \Rightarrow S_{1D} = \iint dtdx \frac{\theta(t,x)}{2\pi} \varepsilon^{\mu\nu} \partial_\mu A_\nu$$

$$j^\mu = -\frac{\delta S_{1D}}{\delta A_\mu} \Rightarrow \rho = -\frac{1}{2\pi}\frac{\partial\theta}{\partial x} \qquad j = \frac{1}{2\pi}\frac{\partial\theta}{\partial t}$$

Particle-hole symmetry $\Rightarrow \theta = -\theta \mod 2\pi$

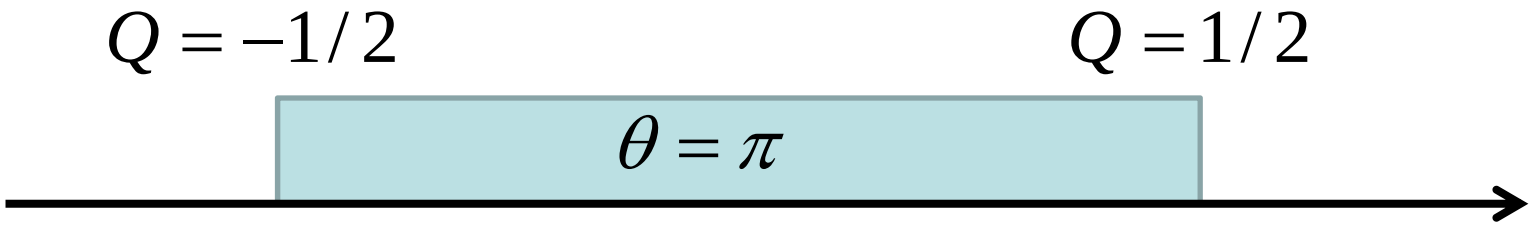

Topological Insulator

Global properties of manifolds and topological order

Gauss-Bonnet

$$\int_S K\sigma_1 \wedge \sigma_2 = 2\pi\chi(S)$$

$$\chi(S) = 2 - 2g$$

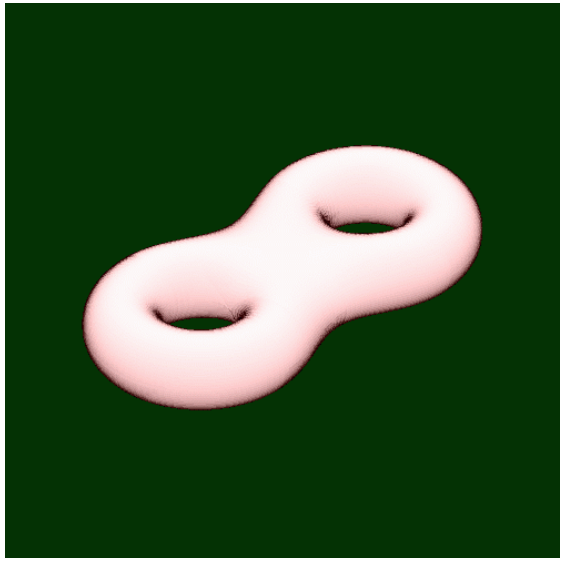

Spin Hall Insulator

S.Murakami, N.N., S.C.Zhang (2004)

Zero gap semiconductors HgTe, HgSe, HgS, alpha-Sn

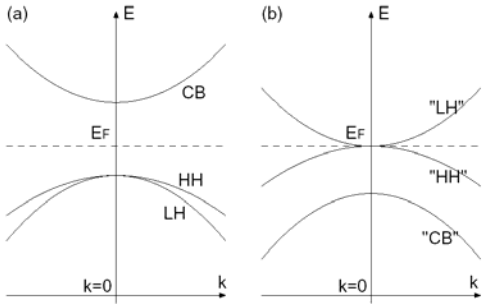

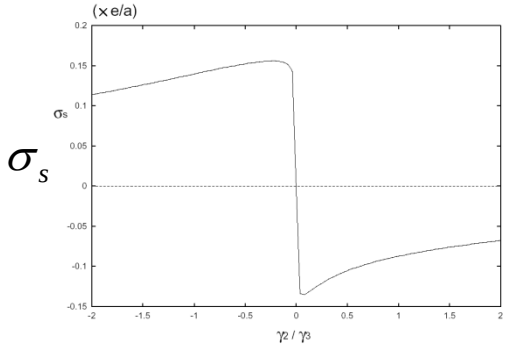

Narrow gap semiconductors Rocksalt structure: PbTe, PbSe, PbS

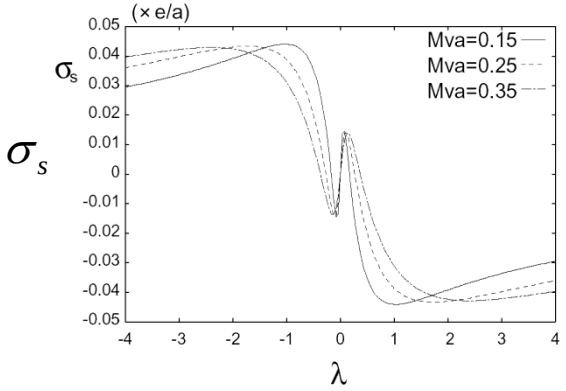

Fradkin-Dagotto -Boyanovsky

$$H = v\mathbf{k}\cdot\hat{p}\tau_1 + \lambda v\mathbf{k}\cdot(\hat{p}\times\boldsymbol{\sigma})\tau_2 + Mv^2\tau_3.$$

Tchernyshyov

$$H = \epsilon(\mathbf{k}) + \sum_{a=1}^{5} d_a(\mathbf{k})\Gamma_a,$$

Geometrical meaning of σ_s in 5d space

$$\sigma^l_{ij(c)} = \frac{4}{2V}\sum (n_L(\mathbf{k}) - n_H(\mathbf{k}))\eta^l_{ab}G^{ab}_{ij},$$

$$G^{ab}_{ij} = \frac{1}{4d^3}\epsilon_{abcde}d_c\frac{\partial d_d}{\partial k_i}\frac{\partial d_e}{\partial k_j}.$$

Quantum Spin Hall insulator system

© C.L.Kane

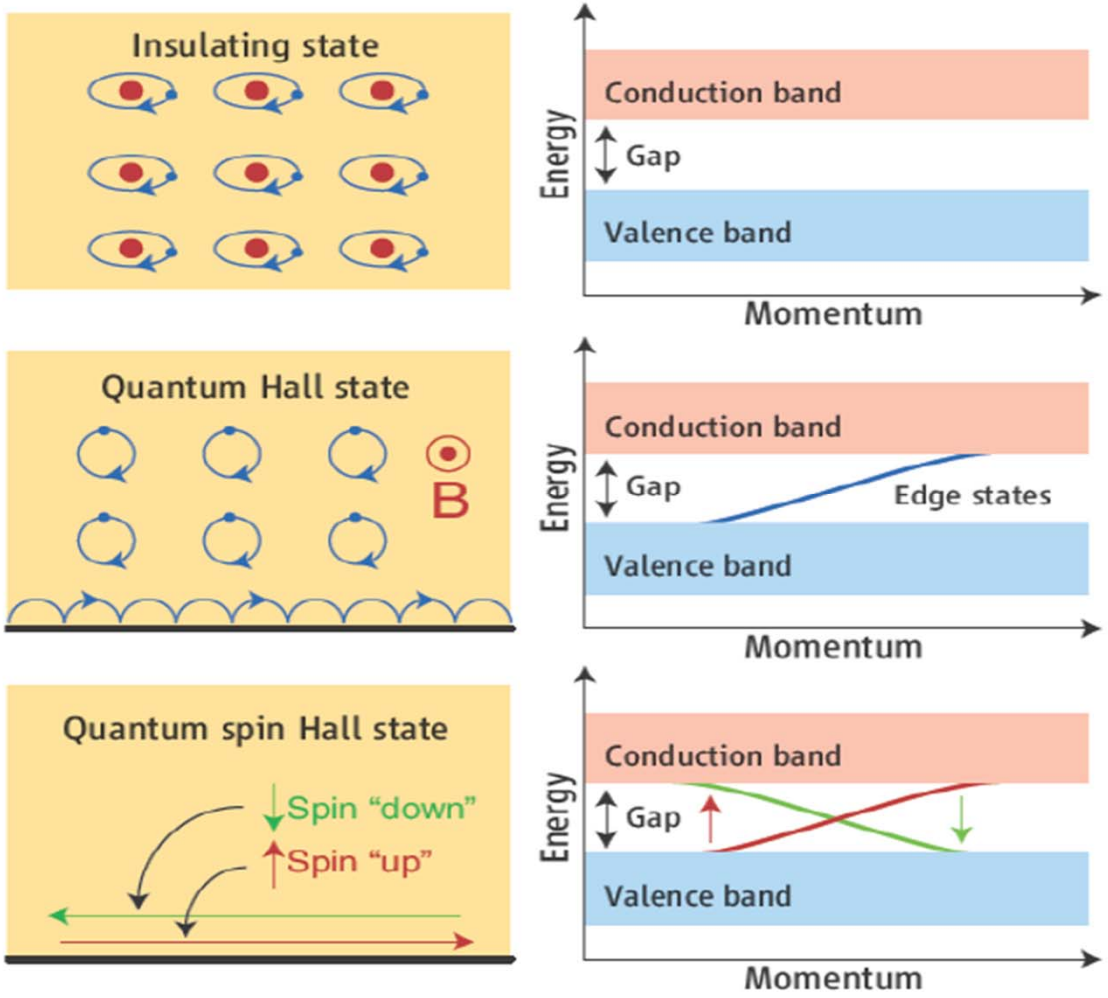

Backward scattering is forbidden
by time-reversal symmetry

Xu-Moore
Wu-Berbevig-Zhang

Haldane model for quantum Hall effect

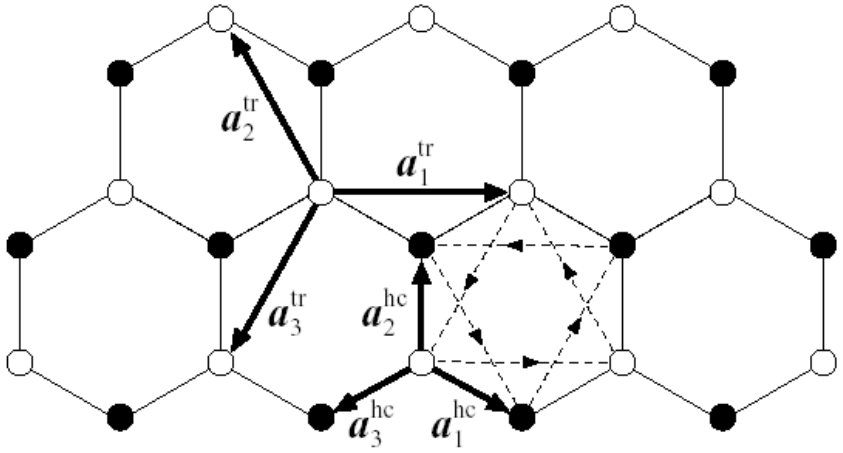

Complex transfer integral
between next nearest neighbor sites

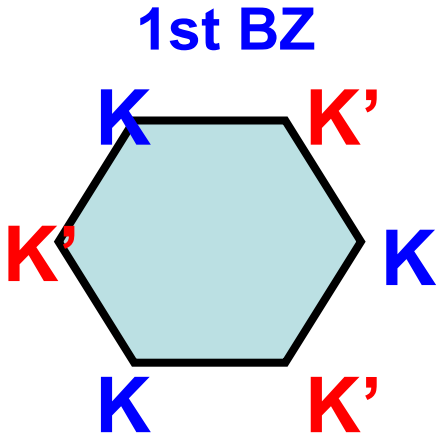

Dirac fermion at
K and K' points

⇨ Generation of the mass m with the same sign
at K and K' points

⇨ Quantized Hall effect
without Landau level formation

Quantum spin Hall phases

Bernevig and Zhang, PRL (2005)
Kane and Mele, PRL (2005),

- bulk = gapped (insulator)
- gapless edge states -- carry spin current, topologically protected

Quantum spin Hall state ≈ Quantum Hall state × 2

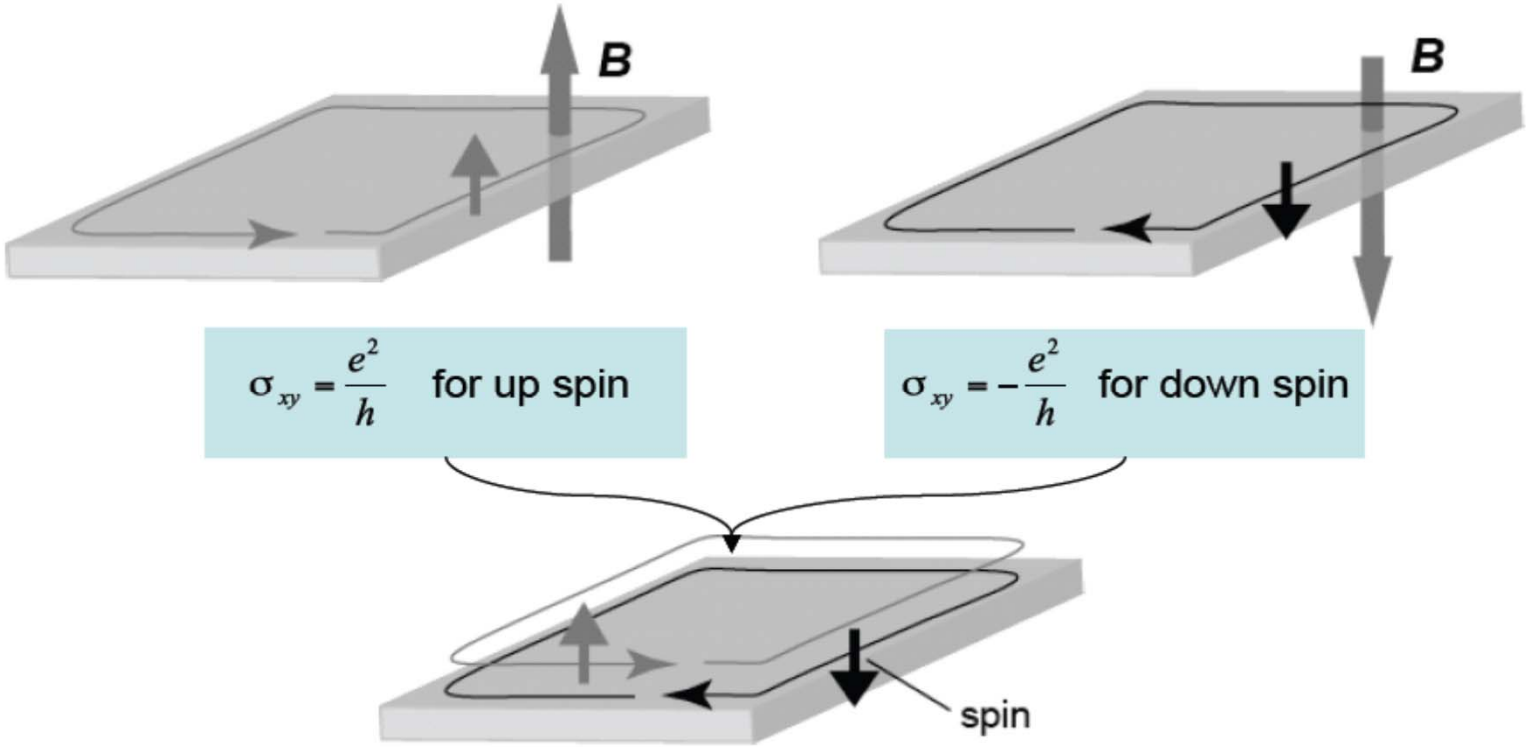

Emergence of the helical edge mode

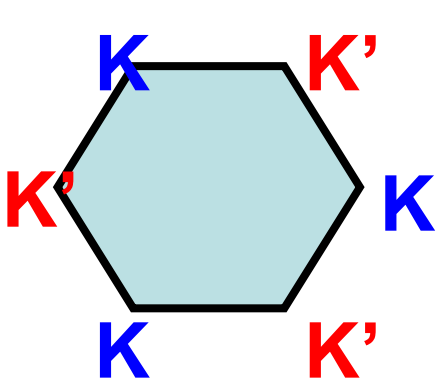

Two Dirac Fermions at K and K' → 8 components

$$\mathcal{H}_0 = -i\hbar v_F \psi^\dagger (\sigma_x \tau_z \partial_x + \sigma_y \partial_y)\psi.$$

$$\mathcal{H}_{SO} = \Delta_{so} \psi^\dagger \sigma_z \tau_z s_z \psi.$$

$$\mathcal{H}_R = \lambda_R \psi^\dagger (\sigma_x \tau_z s_y - \sigma_y s_x)\psi.$$

helical edge modes

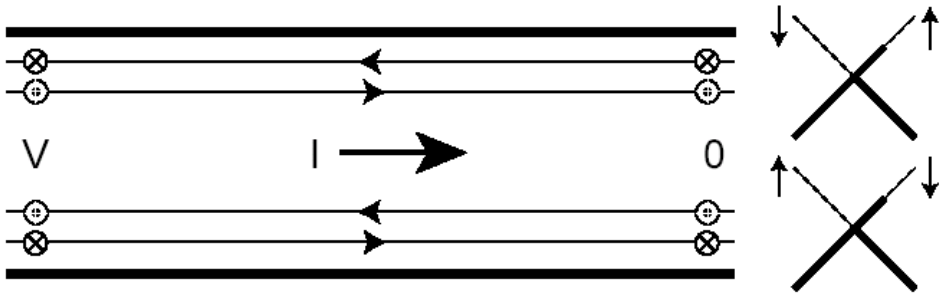

Stability against the T-invariant disorder due to Kramer's theorem

Kane-Mele, Xu-Moore, Wu-Bernevig-Zhang

$$|-k\downarrow> = \Theta\,|k\uparrow> \qquad H\Theta = \Theta H$$

$$<k\uparrow|H|-k\downarrow> = <k\uparrow|H\Theta|k\uparrow> = [H|k\uparrow>]^{+}\Theta|k\uparrow>$$

$$= [\Theta^2|k\uparrow>]^{+}[\Theta H|k\uparrow>] = -<k\uparrow|H\Theta|k\uparrow> = 0$$

Charge pumping

$$|\psi_{n,k}\rangle = \frac{1}{\sqrt{N_c}} e^{ikx} |u_{n,k}\rangle \qquad |R,n\rangle = \frac{1}{2\pi}\int dk e^{-ik(R-r)} |u_{k,n}\rangle$$

Wannier function

$$P_\rho = \sum_n \langle 0,n|r|0,n\rangle = \frac{1}{2\pi}\oint dk\ \mathcal{A}(k)$$

polarization

$$\mathcal{A}(k) = i\sum_n \langle u_{k,n}|\nabla_k|u_{k,n}\rangle$$

Berry connection

$$P_\rho[t_2] - P_\rho[t_1] = \frac{1}{2\pi}\left[\oint_{c2} dk\ \mathcal{A}(t,k) - \oint_{c1} dk\ \mathcal{A}(t,k)\right]$$

$$P_\rho[t_2] - P_\rho[t_1] = \frac{1}{2\pi}\int_{\tau_{12}} dtdk\ \mathcal{F}(t,k)$$

$$\mathcal{F}(t,k) = i\sum_n \left(\langle \nabla_t u_{k,n}(t)|\nabla_k u_{k,n}(t)\rangle - c.c\right)$$

Berry curvature

Charge pumping and electric polarization

$$|\psi_{n,k}\rangle = \frac{1}{\sqrt{N_c}} e^{ikx} |u_{n,k}\rangle$$ Bloch function

r unbounded operator

$$J = -e\dot{r} = \dot{P}$$

Polarization current

$$P(t_2) - P(t_1) = \int_{t_1}^{t_2} dt J$$

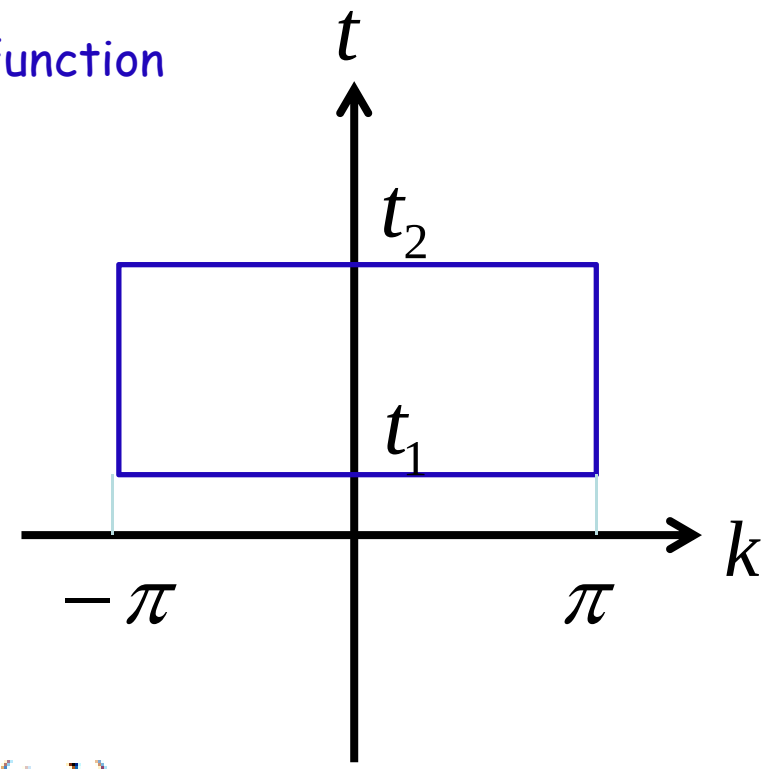

$$P_\rho[t_2] - P_\rho[t_1] = \frac{1}{2\pi} \int_{\tau_{12}} dt dk \, \mathcal{F}(t,k)$$

$$\mathcal{F}(t,k) = i \sum_n \left(\langle \nabla_t u_{k,n}(t) | \nabla_k u_{k,n}(t) \rangle - c.c \right)$$

Berry curvature

Z2 pseudo spin pumping

Fu-Kane

$$|u^{I}_{-k,\alpha}\rangle = e^{i\chi_{k,\alpha}}\Theta|u^{II}_{k,\alpha}\rangle$$
$$|u^{II}_{-k,\alpha}\rangle = -e^{i\chi_{-k,\alpha}}\Theta|u^{I}_{k,\alpha}\rangle$$

Time-reversal pair

$$P^{s} = \frac{1}{2\pi}\int_{-\pi}^{\pi} dk\mathcal{A}^{s}(k), \quad s = I \text{ or } II$$

"spin" selective polarization

$$\mathcal{A}^{s}(k) = i\sum_{\alpha}\langle u^{s}_{k,\alpha}|\nabla_{k}|u^{s}_{k,\alpha}\rangle$$

$$\Rightarrow \mathcal{A}^{I}(-k) = \mathcal{A}^{II}(k) - \sum_{\alpha}\nabla_{k}\chi_{k,\alpha}$$

$$\Rightarrow P^{I} = \frac{1}{2\pi}\left[\int_{0}^{\pi} dk\mathcal{A}(k) - \sum_{\alpha}(\chi_{\pi,\alpha} - \chi_{0,\alpha})\right]$$

$$\frac{\mathrm{Pf}[w(\pi)]}{\mathrm{Pf}[w(0)]} = \exp[i\sum_{\alpha}(\chi_{\pi,\alpha} - \chi_{0,\alpha})]$$

$$w_{mn}(k) = \langle u_{-k,m}|\Theta|u_{k,n}\rangle$$

$$P_\theta = P^I - P^{II}$$

$$P_\theta = \frac{1}{2\pi i}\left[\int_0^\pi dk \nabla_k \log\mathrm{Det}[w(k)] - 2\log\left(\frac{\mathrm{Pf}[w(\pi)]}{\mathrm{Pf}[w(0)]}\right)\right]$$

$$(-1)^{P_\theta} = \frac{\sqrt{\mathrm{Det}[w(0)]}}{\mathrm{Pf}[w(0)]}\frac{\sqrt{\mathrm{Det}[w(\pi)]}}{\mathrm{Pf}[w(\pi)]}$$

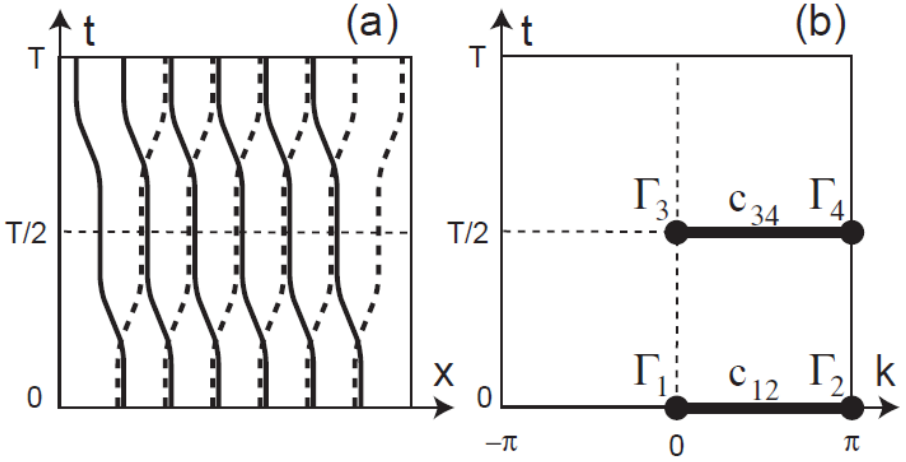

$$\Delta = P_\theta(T/2) - P_\theta(0) \mod 2$$

$$(-1)^{\Delta} = \prod_{i=1}^{4}\frac{\sqrt{\mathrm{Det}[w(\Gamma_i)]}}{\mathrm{Pf}[w(\Gamma_i)]}$$

Z2 topological invariant

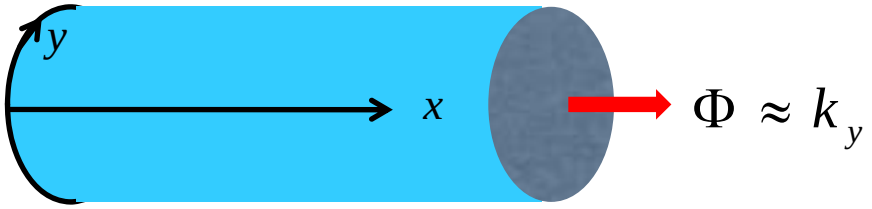

$\Phi \approx k_y$

$$(-1)^{\Delta} = \prod_{i=1}^{4} \frac{\sqrt{\mathrm{Det}[w(\Gamma_i)]}}{\mathrm{Pf}[w(\Gamma_i)]}$$

Kane-Mele-Fu
Z2 number and helical edge modes

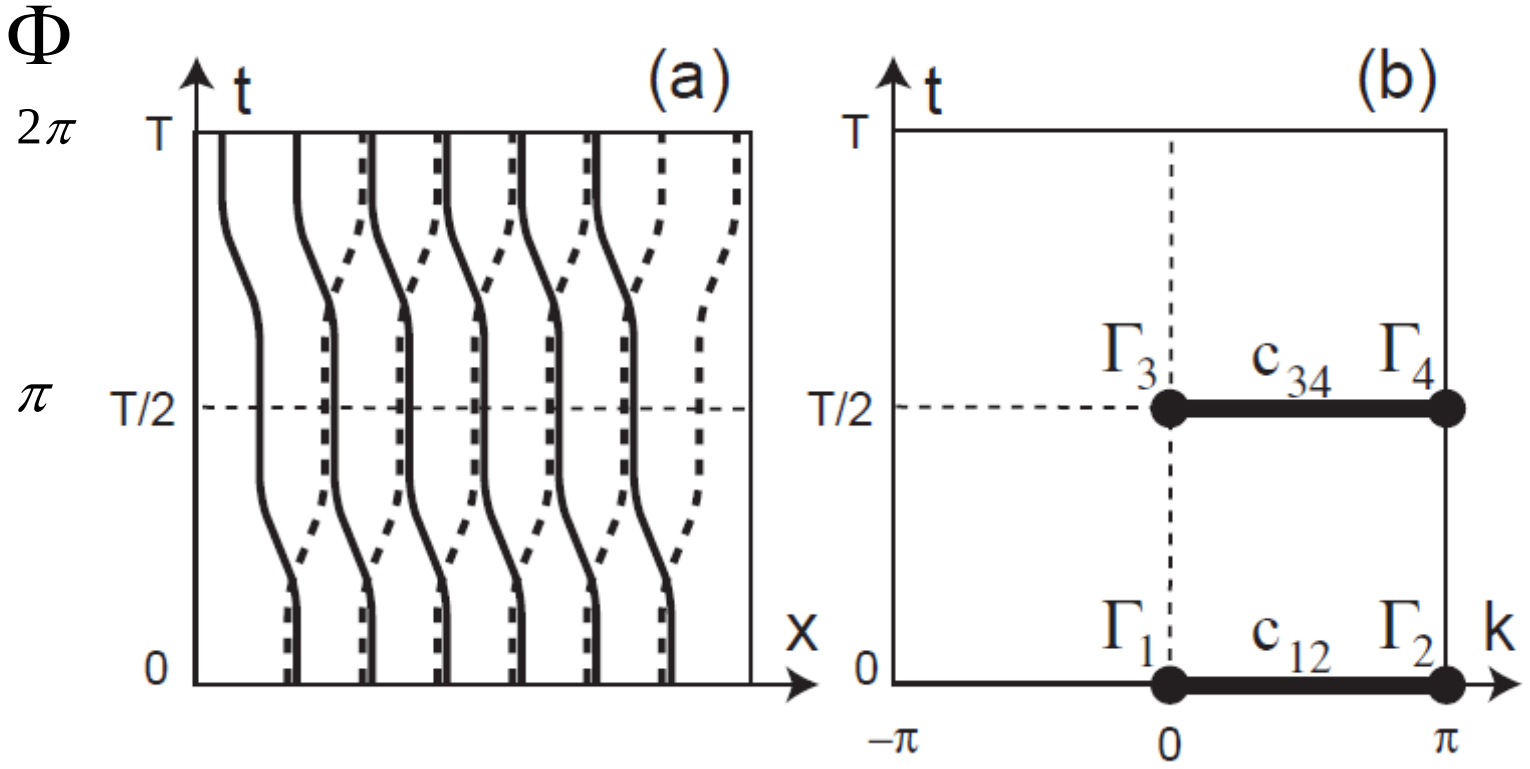

Electron fractionalization in 2D

$$H = \psi^{+}[\sigma^{x} p_{x} + \sigma^{y} p_{y} + \sigma^{z} m(x)]\psi$$

$$\sigma_{xy} = \frac{e^2}{2h} sign(m)$$

$$(x \to \pm\infty)$$

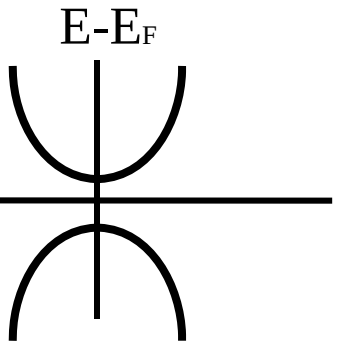

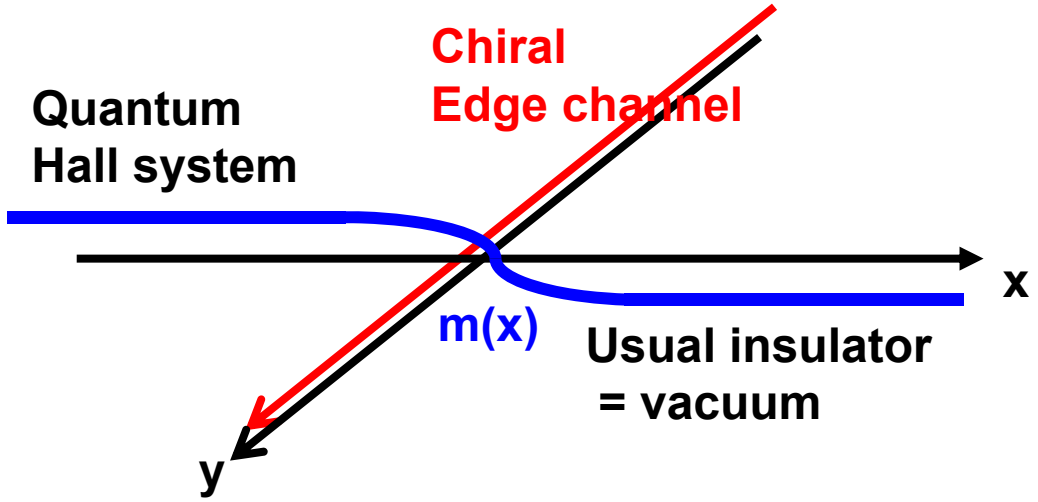

Effective Theory for the phase transition between QSHS and Insulator in 2D

Murakami et al. 07

$$H(\vec{k}) = \begin{pmatrix} h_{\uparrow\uparrow}(\vec{k}) & h_{\uparrow\downarrow}(\vec{k}) \\ h_{\downarrow\uparrow}(\vec{k}) & h_{\downarrow\downarrow}(\vec{k}) \end{pmatrix}$$

$$H(\vec{k}) = \sigma_y H^T(-\vec{k})\sigma_y$$

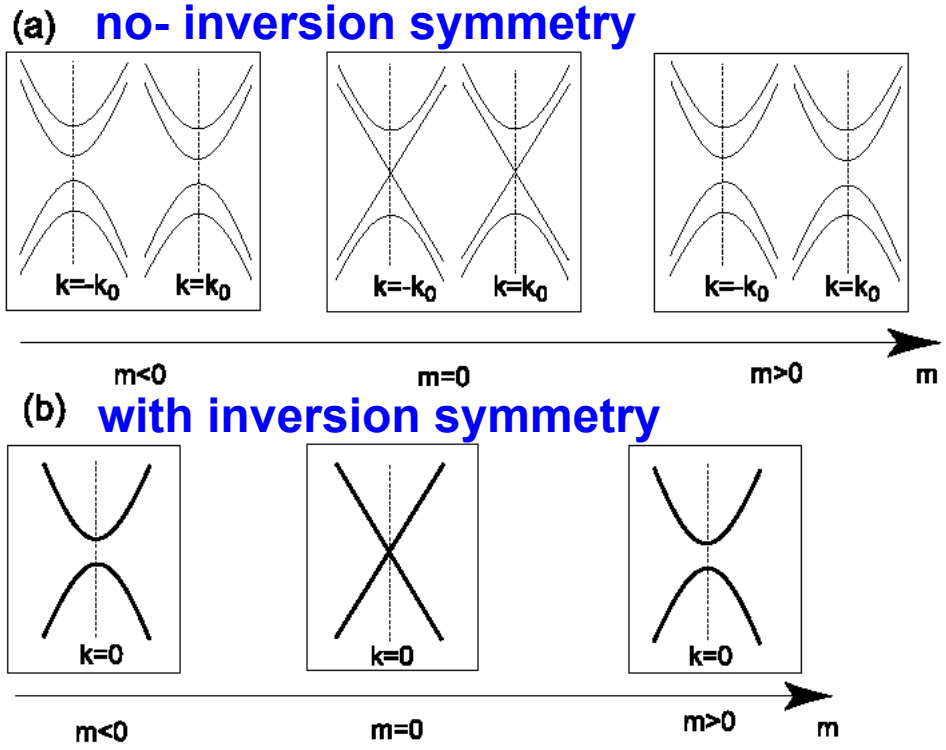

$$\begin{aligned} H(0) &= E_0 + \begin{pmatrix} a_3 & a_1 - ia_2 & 0 & -a_4 - ia_5 \\ a_1 + ia_2 & -a_3 & a_4 + ia_5 & 0 \\ 0 & a_4 - ia_5 & a_3 & a_1 + ia_2 \\ -a_4 + ia_5 & 0 & a_1 - ia_2 & -a_3 \end{pmatrix} \\ &= E_0 + \sum_{i=1}^{5} a_i \Gamma_i, \end{aligned} \tag{8}$$

CdTe/HgTe/CdTe quantum well

Bernevig et al.

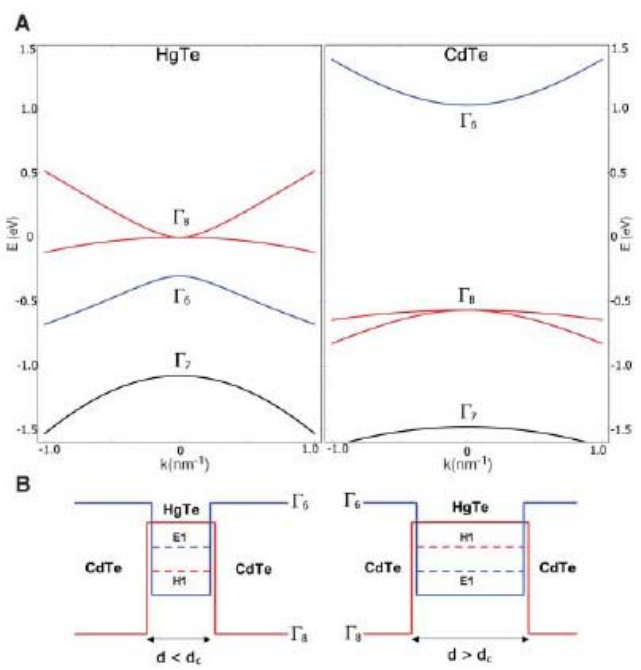

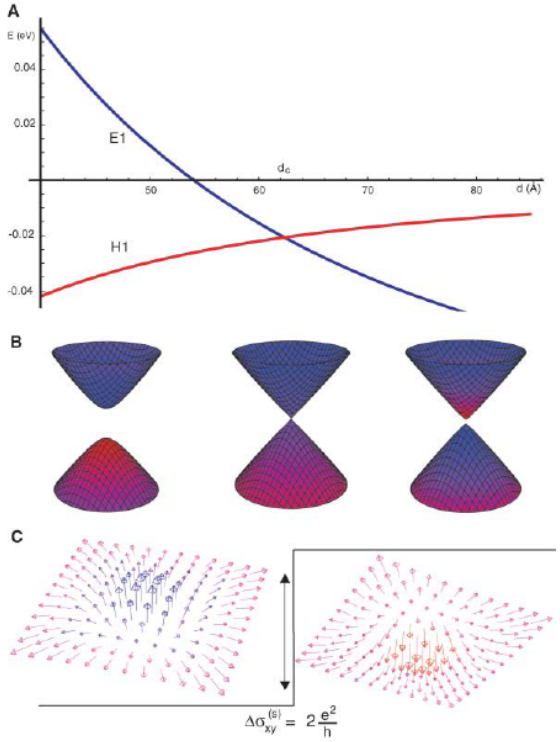

Experimental observation of QSHE

Molenkampf group

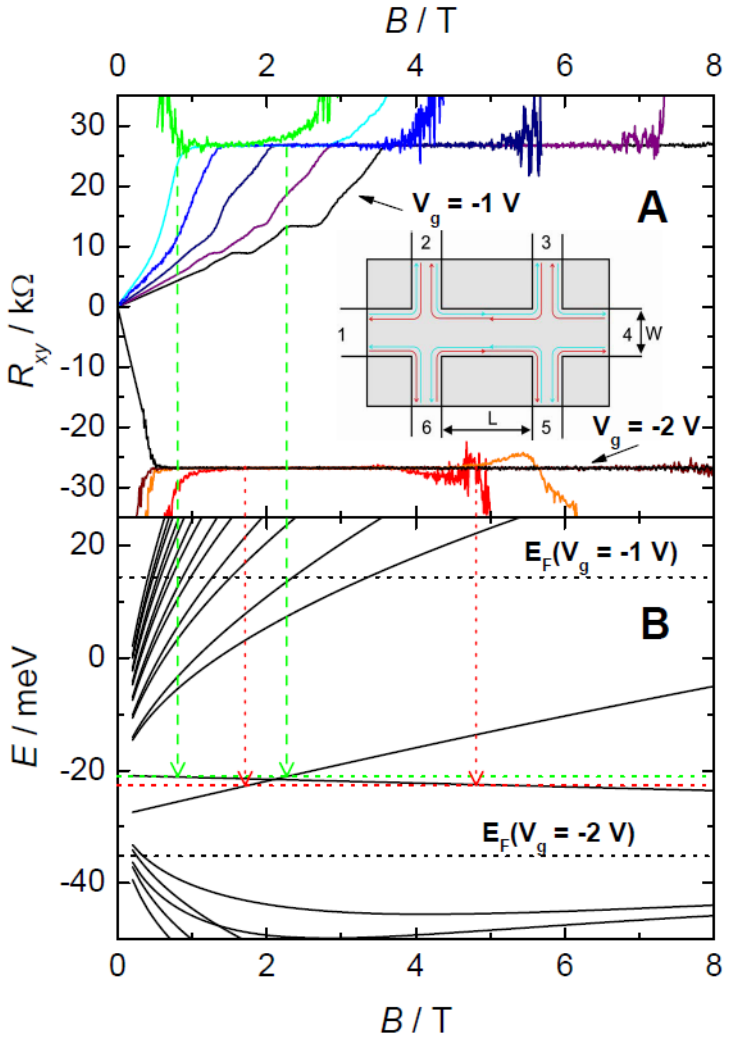

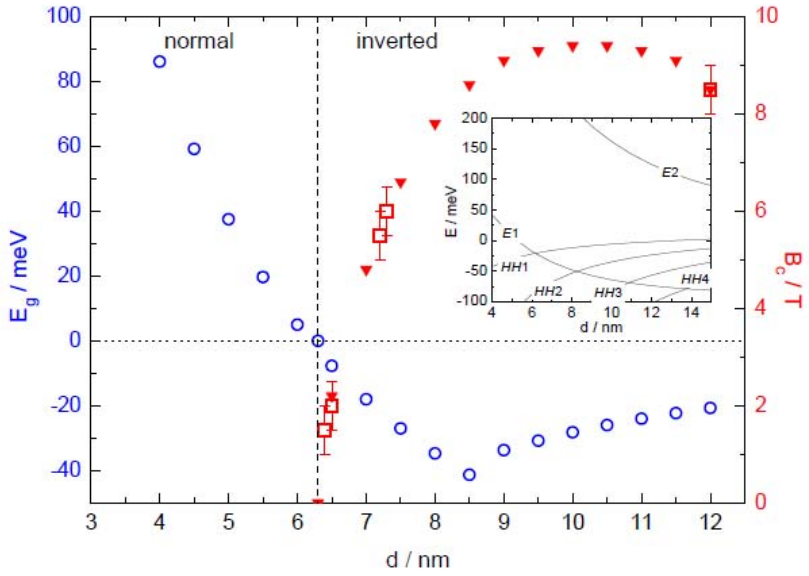

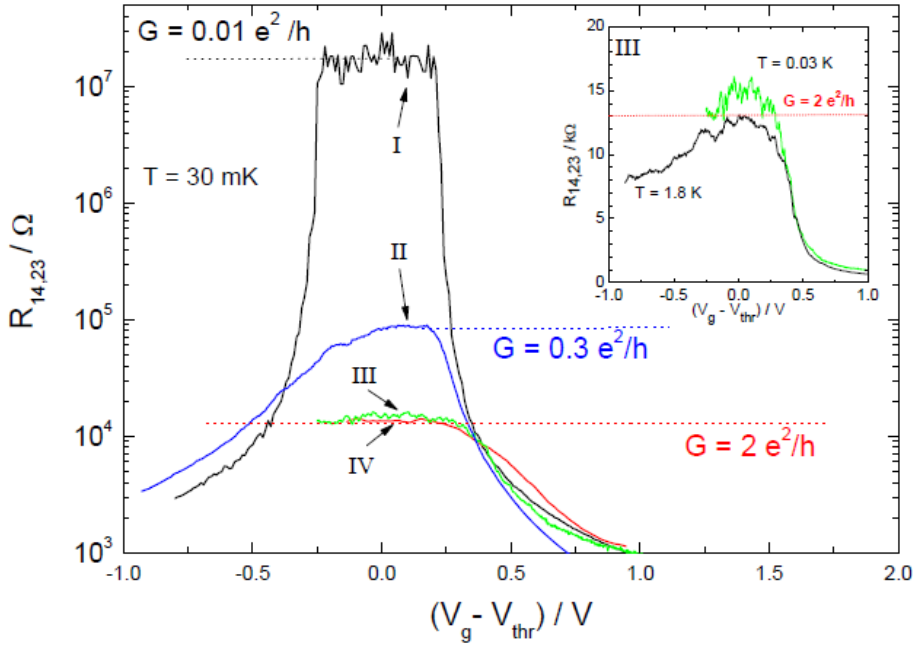
G = 0.01 e² /h
T = 30 mK
I
II
III
IV
G = 0.3 e²/h
G = 2 e²/h
R14,23 / Ω
(Vg - Vthr) / V
III
T = 0.03 K
G = 2 e²/h
T = 1.8 K
R14,23 / kΩ
(Vg - Vthr) / V

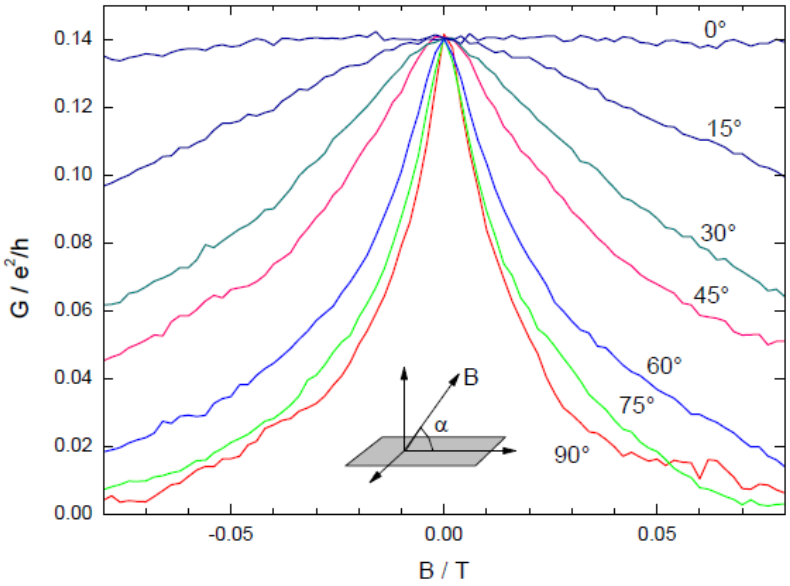
0°
15°
30°
45°
60°
75°
90°
B
α
G / e²/h
B / T

Electron fractionalization in 3D

$$H = \psi^{+}[\tau^{x}(\vec{\sigma}\cdot\vec{p}) + \tau^{z}m(x)]\psi$$ 4x4 Dirac

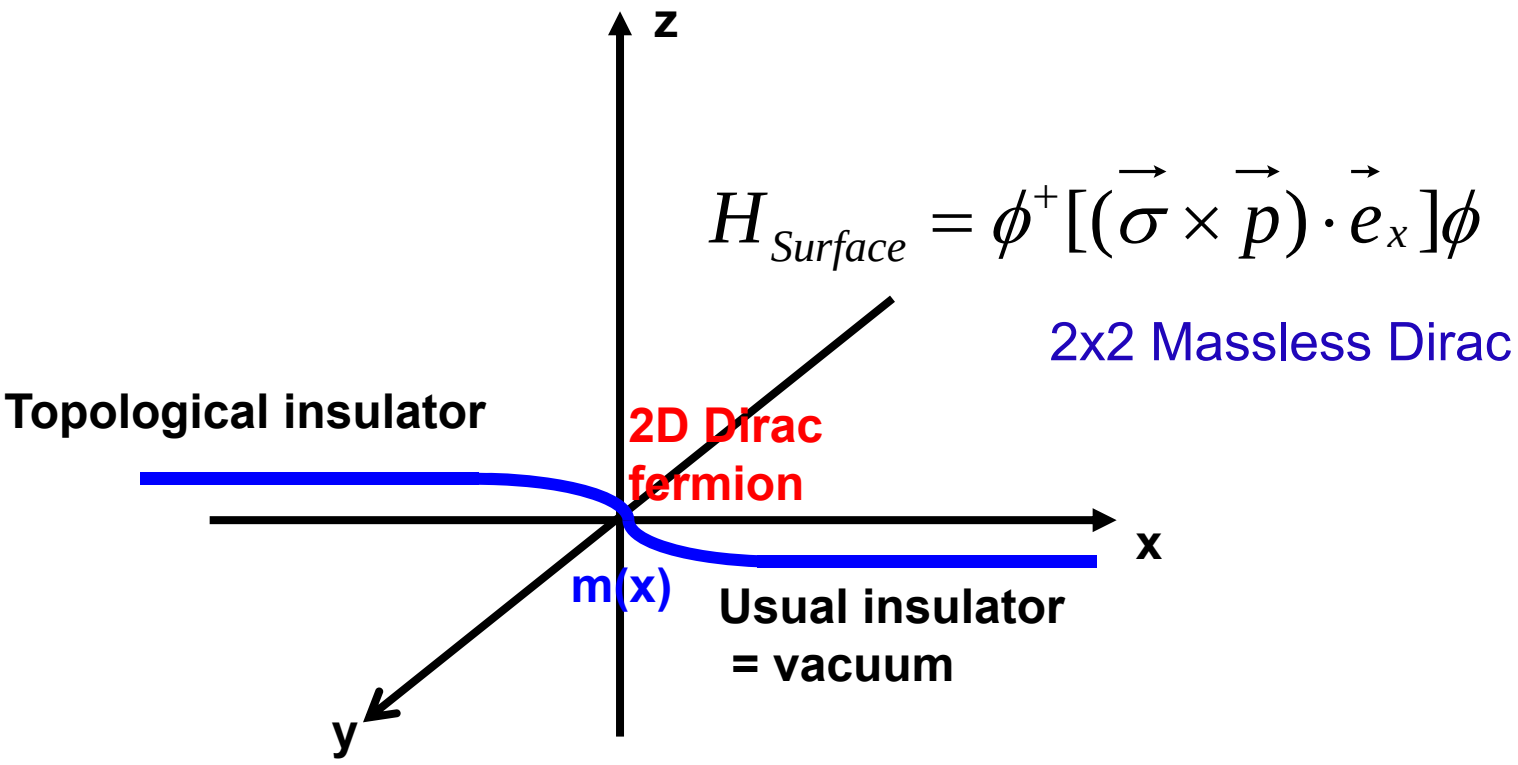

Generalization to 3D system

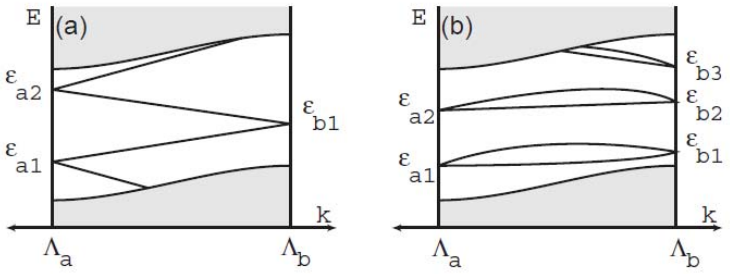

$$H = \psi^{+}[\rho^{x}(\vec{\sigma}\cdot\vec{p}) + \rho^{z} m(x)]\psi$$

$$(-1)^{\nu_0} = \prod_{n_j=0,1} \delta_{n_1 n_2 n_3}$$

$$(-1)^{\nu_{i=1,2,3}} = \prod_{n_{j\neq i}=0,1;n_i=1} \delta_{n_1 n_2 n_3}$$

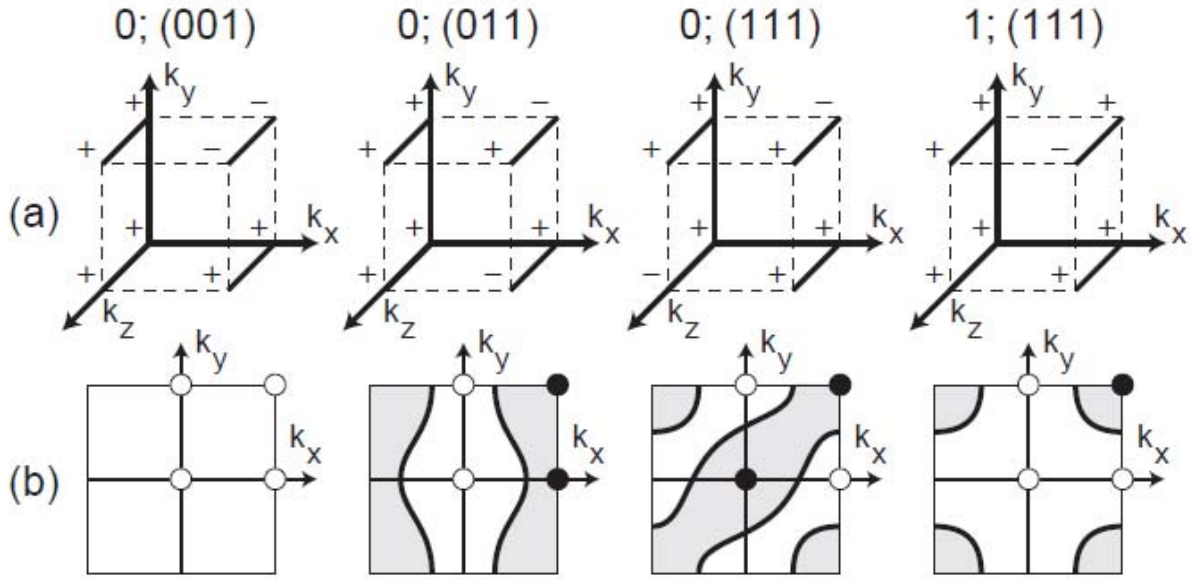

$\nu_0 = 1$ Strong TI

$\nu_0 = 0;\ \nu_i = 1$

Weak TI

$Bi_{1-x}Sb_x$

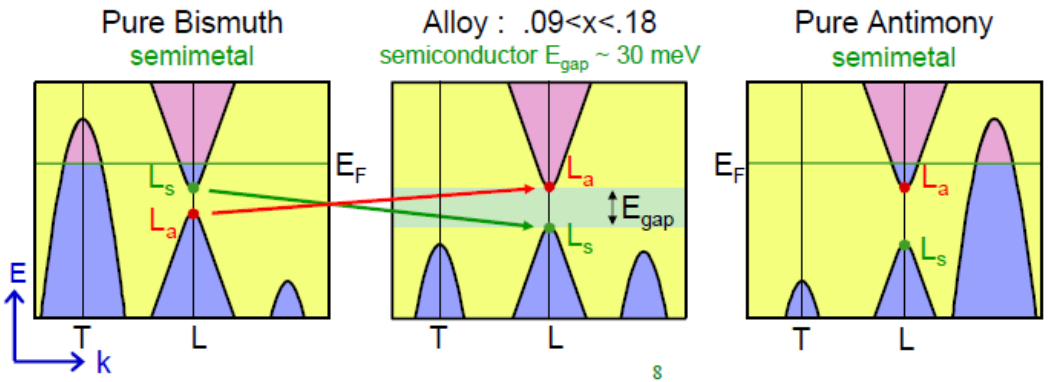

Inversion symmetry $\Rightarrow$ $(-1)^{\nu_0} = \prod_{i=1}^{8} \prod_{n} \xi_{2n}(\Gamma_i)$

Experiments on Bi_{1-x} Sb_x

Map $E(k_x,k_y)$ for (111) surface states below E_F using Angle Resolved Photoemission Spectroscopy

D. Hsieh, D. Qian, L. Wray, Y. Xia, Y. S. Hor, R. J. Cava and M. Z. Hasan, Nature (08) in press

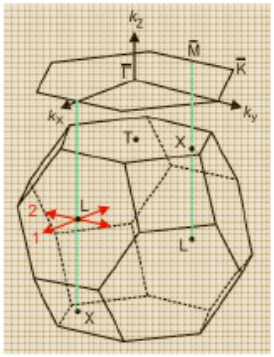

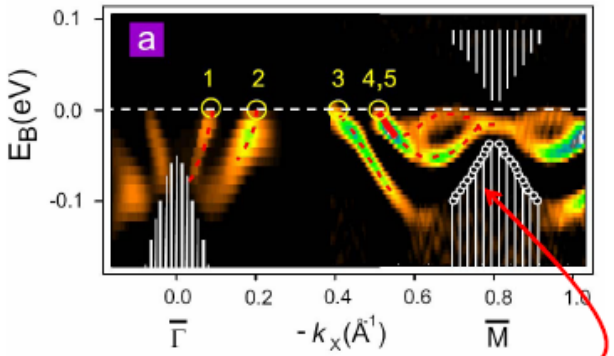

- Bulk Dirac points at L project to M in surface Brillouin Zone
- Observe 5 surface state bands crossing E_F between Γ and M and Kramers degenerate surface Dirac point at M.
- Bi_{1-x} Sb_x is a Strong Topological Insulator

From C.L.Kane's homepage

3D generalization of QSH system
Topological insulator

helical edge channels

$\Rightarrow H = \psi^{+}(\vec{\sigma} \times \vec{p}) \cdot \vec{e}_z \psi$

odd # of 2D chiral Dirac surface metal
- Robust against disorder
- Superconductivity ?

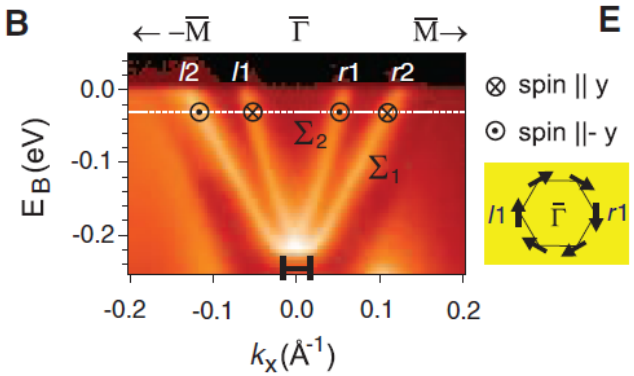

Field theory of topological insulator

Qi et al., PRB78, 195424(2008)

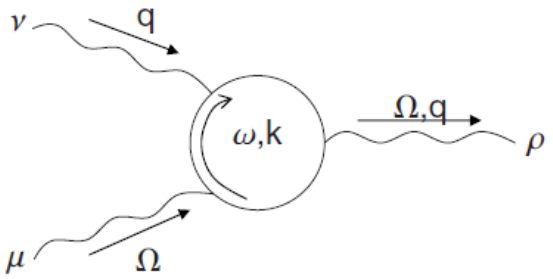

$$S_{\text{eff}} = \frac{C_2}{24\pi^2}\int d^4x dt \epsilon^{\mu\nu\rho\sigma\tau} A_\mu \partial_\nu A_\rho \partial_\sigma A_\tau$$

$$C_2 = -\frac{\pi^2}{15}\epsilon^{\mu\nu\rho\sigma\tau}\int \frac{d^4k d\omega}{(2\pi)^5}\mathrm{Tr}\left[\left(G\frac{\partial G^{-1}}{\partial q^\mu}\right)\left(G\frac{\partial G^{-1}}{\partial q^\nu}\right)\left(G\frac{\partial G^{-1}}{\partial q^\rho}\right)\right.$$
$$\left.\times\left(G\frac{\partial G^{-1}}{\partial q^\sigma}\right)\left(G\frac{\partial G^{-1}}{\partial q^\tau}\right)\right],$$

Bloch wave in (4+1)D

$$C_2 = \frac{1}{32\pi^2}\int d^4k \epsilon^{ijk\ell}\,\mathrm{tr}[f_{ij}f_{k\ell}]$$

$$f_{ij}^{\alpha\beta} = \partial_i a_j^{\alpha\beta} - \partial_j a_i^{\alpha\beta} + i[a_i, a_j]^{\alpha\beta} \qquad a_i^{\alpha\beta}(\mathbf{k}) = -i\langle\alpha,\mathbf{k}|\frac{\partial}{\partial k_i}|\beta,\mathbf{k}\rangle$$

Current density

$$j_\mu(\mathbf{x}) = \frac{\delta S_{\text{eff}}[A]}{\delta A_\mu(\mathbf{x})} \qquad j^\mu = \frac{C_2}{8\pi^2}\epsilon^{\mu\nu\rho\sigma\tau}\partial_\nu A_\rho \partial_\sigma A_\tau$$

$$A_x = 0, \quad A_y = B_z x, \quad A_z = -E_z t, \quad A_w = A_t = 0, \quad \Rightarrow \quad j_w = \frac{C_2}{4\pi^2} B_z E_z$$

Dimensional reduction: From (4+1)D to (3+1)D

$$k_w \to \theta(\vec{x}) = \theta_0 + \delta\theta(\vec{x}) \quad \Rightarrow \quad S_{3D} = \frac{G_3(\theta_0)}{4\pi}\int d^3x dt \epsilon^{\mu\nu\sigma\tau}\delta\theta\partial_\mu A_\nu \partial_\sigma A_\tau$$

$$G_3(\theta_0) = -\frac{\pi}{6}\int \frac{d^3k d\omega}{(2\pi)^4}\text{Tr}\,\epsilon^{\mu\nu\sigma\tau}\left[\left(G\frac{\partial G^{-1}}{\partial q^\mu}\right)\left(G\frac{\partial G^{-1}}{\partial q^\nu}\right)\right.$$
$$\left.\times\left(G\frac{\partial G^{-1}}{\partial q^\sigma}\right)\left(G\frac{\partial G^{-1}}{\partial q^\tau}\right)\left(G\frac{\partial G^{-1}}{\partial \theta_0}\right)\right],$$

$$G_3(\theta_0) = \frac{1}{8\pi^2}\int d^3k \epsilon^{ijk}\,\text{tr}[f_{\theta i} f_{jk}]$$

$$\partial_A \mathcal{K}^A = \frac{1}{32\pi^2}\epsilon^{ABCD}\,\mathrm{tr}[f_{AB}f_{CD}] \Rightarrow G_3(\theta_0) = \int d^3k\,\partial_A \mathcal{K}^A$$

$$\mathcal{K}^A = \frac{1}{16\pi^2}\epsilon^{ABCD}\,\mathrm{Tr}\left[\left(f_{BC} - \frac{1}{3}[a_B, a_C]\right)\cdot a_D\right]$$

$$P_3(\theta_0) = \int d^3k\,\mathcal{K}^\theta$$

$$\Rightarrow\quad S_{3D} = \frac{1}{4\pi}\int d^3x dt\,\epsilon^{\mu\nu\sigma\tau} A_\mu (\partial P_3/\partial\theta)\,\partial_\nu \delta\theta\,\partial_\sigma A_\tau$$

$$\Rightarrow\quad S_{3D} = \frac{1}{4\pi}\int d^3x dt\,\epsilon^{\mu\nu\sigma\tau} P_3(x,t)\,\partial_\mu A_\nu \partial_\sigma A_\tau$$

Axion electrodynamics

Time-reversal symmetry $\Rightarrow$ $P_3 = 1/2 \text{ or } 0 \mod 1$

Prediction for phenomena

1. Hall effect induced by spatial gradient of P_3

$$j^{\mu} = \frac{\partial_z P_3}{2\pi}\epsilon^{\mu\mu\rho}\partial_{\nu}A_{\rho}$$

$$J_y^{2D} = \int_{z_1}^{z_2} dz j_y = \frac{1}{2\pi}\left(\int_{z_1}^{z_2} dP_3\right)E_x$$

$$\sigma_{xy}^{2D} = \int_{z_1}^{z_2} dP_3/2\pi = \pm\frac{e^2}{2h}$$

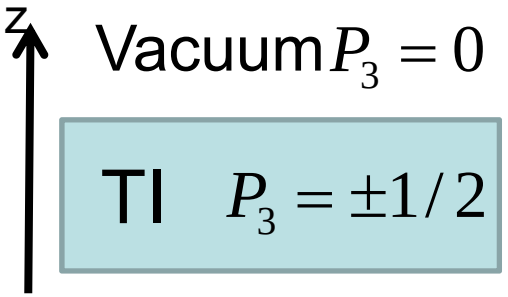

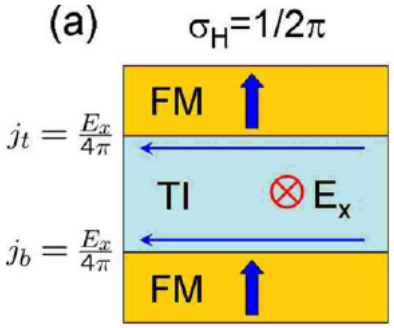

2. TME induced by temporal gradient of P_3

$$\mathbf{P}_t = \left(n + \frac{1}{2}\right)\frac{e^2}{hc}\mathbf{B}$$

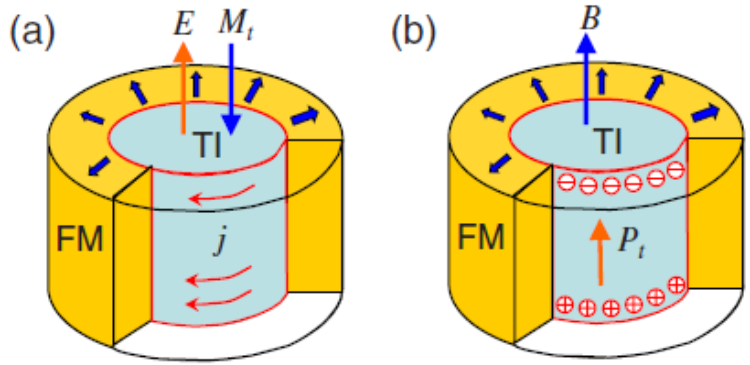

Bulk v.s. surface in topological ME effect

$$S_\theta = \int d^3x dt \left(\frac{\theta(x,t)}{2\pi}\right)\left(\frac{\alpha}{2\pi}\right)\vec{E}\cdot\vec{B}$$

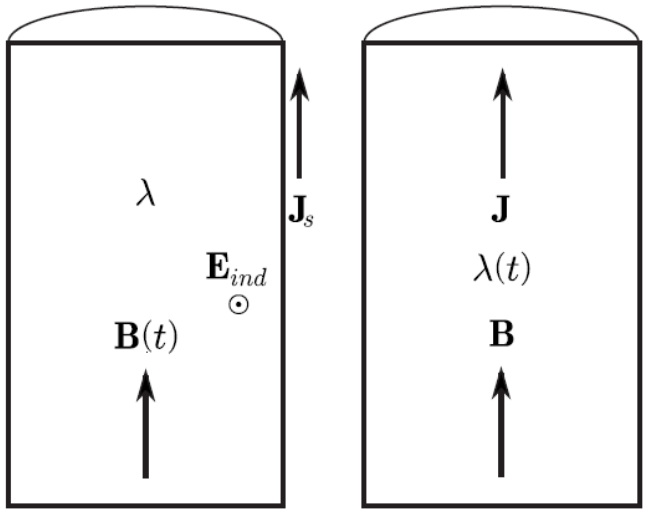

$$J \propto \nabla\theta \times E + \dot{\theta}B$$

$$\rho \propto -\nabla\theta \cdot B$$

θ appears in the form of $\partial_\mu \theta$ for charge and current densities

$\nabla\theta$ produces the surface current

$\dot{\theta}$ requires the bulk T-symmetry breaking

Qi et al., Essin et al.

$\theta = 0 \mod 2\pi$ or $\theta = \pi \mod 2\pi$

due to the time-reversal symmetry

Magnetic impurities in topological insulators

Z. Hasan's group 2008
Y.L. Chen et al. 2010

Magnetic impurities could form insulating ferromagnet on TI through localization

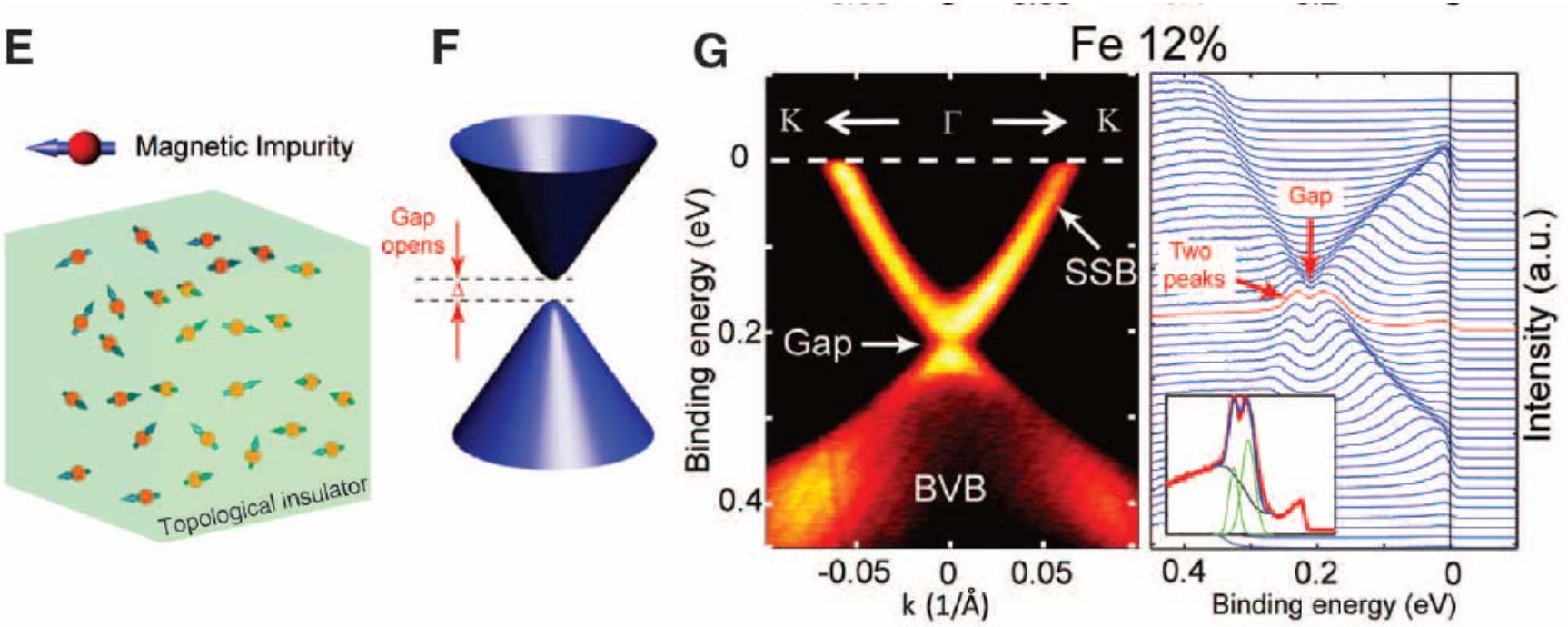

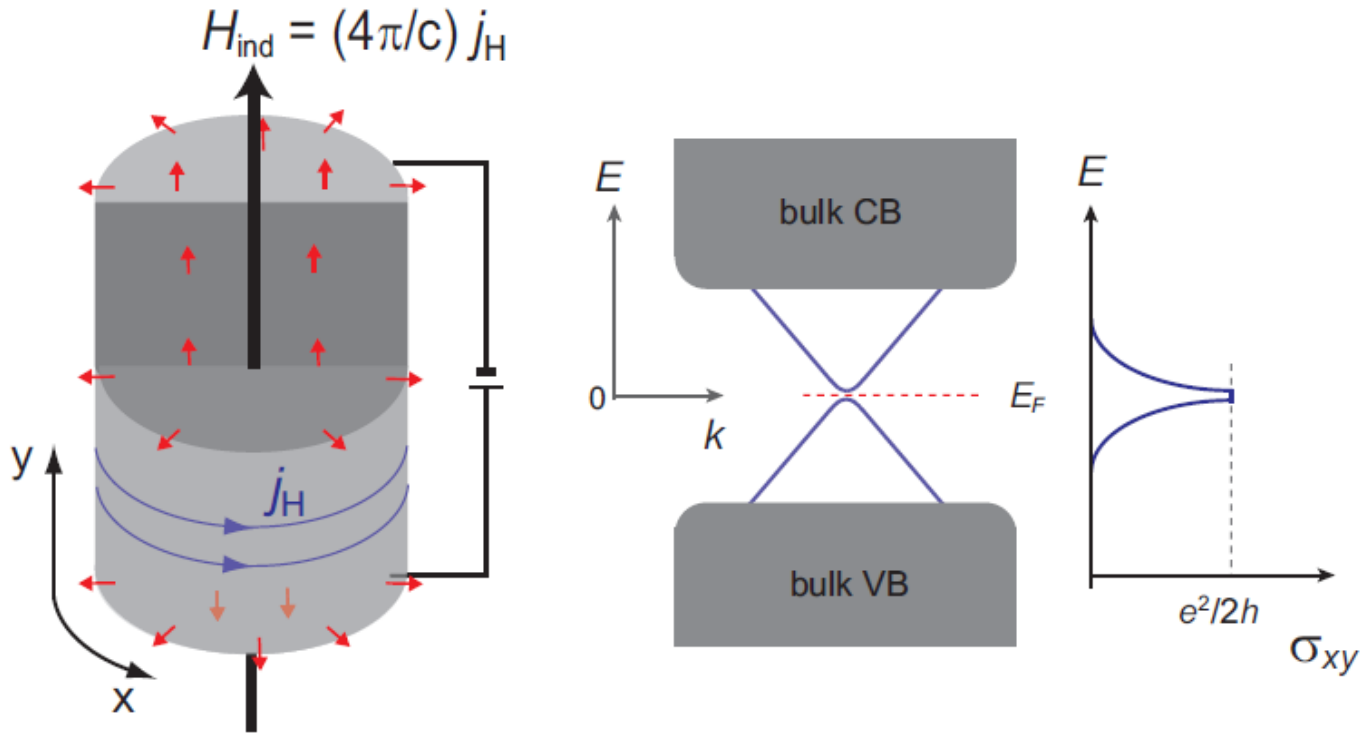

Difficulties to realize TME

1. Get rid of carriers in the bulk
2. Attach the insulating ferromagnetic layer with the magnetization perpendicular to the surface
3. Tune the Fermi energy within the gap of surface Dirac

Localization of surface states by magnetic impurities

$$\mathcal{H}^{2D}_{\rm Dirac} = -i\hbar v_F \hat{\mathbf{z}} \times \boldsymbol{\sigma} \cdot \boldsymbol{\nabla} + m\sigma_3$$

$$\mathcal{V} = \sum_{\mu=0}^{3} \sigma_\mu V_\mu(\boldsymbol{r})$$ Disorder

K.Nomura and N.N. PRL2011
c.f. Q.Niu, arXiv:1011.4083

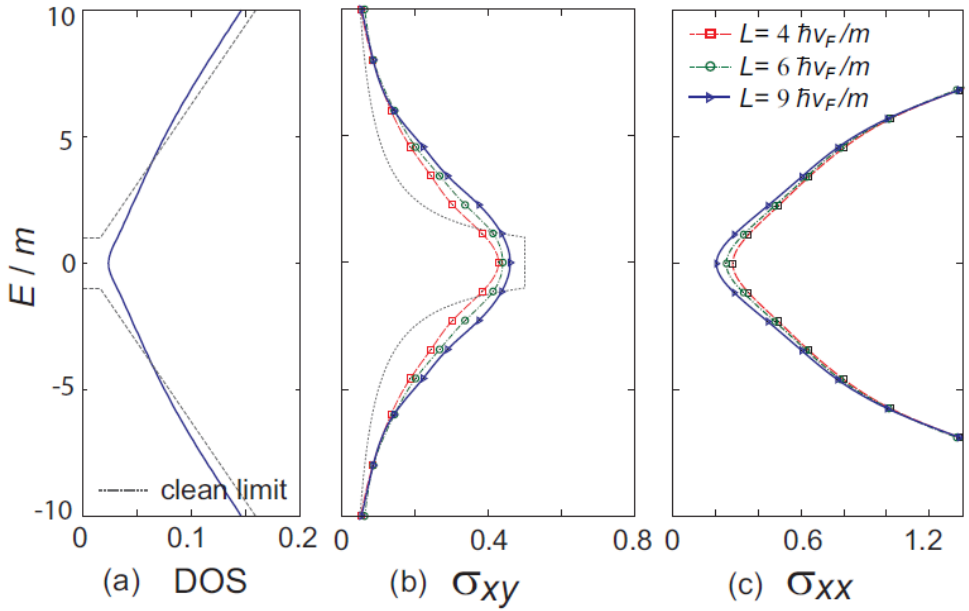

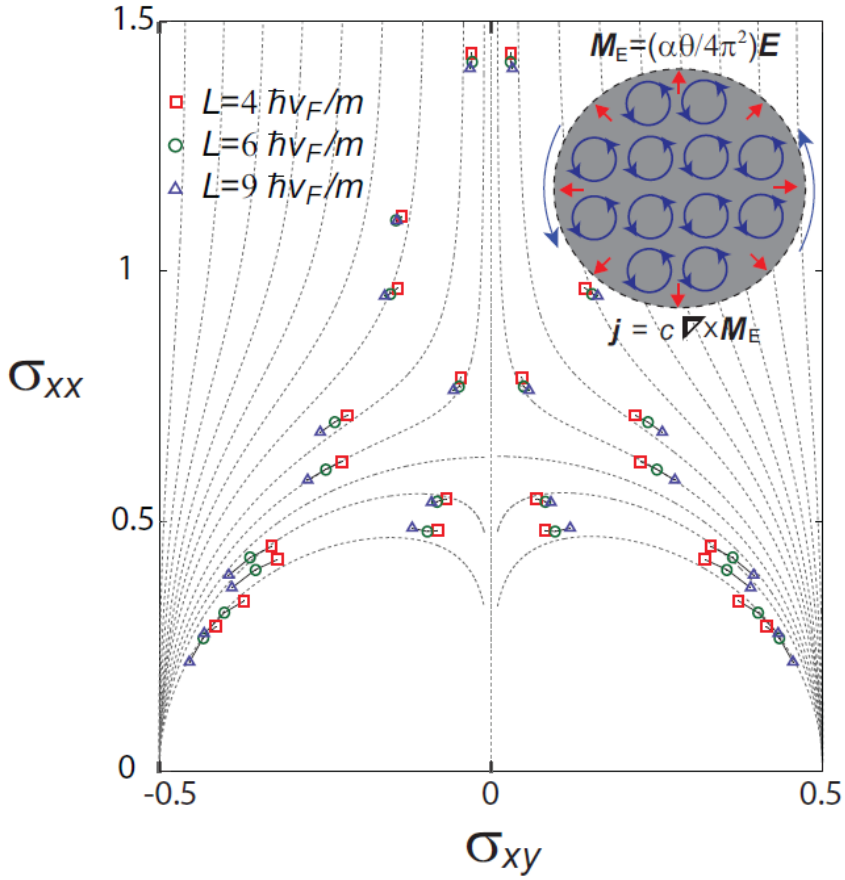

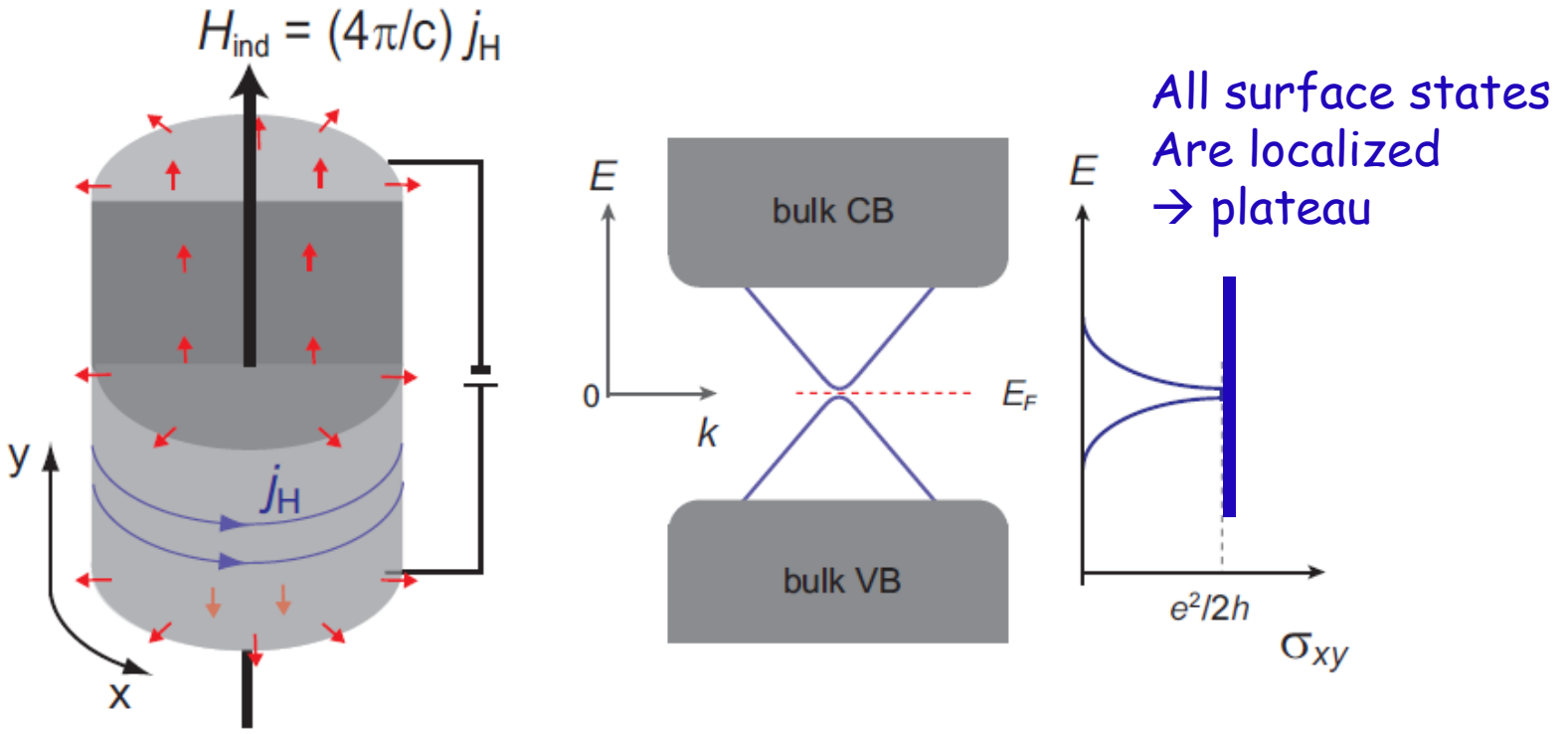

All surface states
Are localized
→ plateau

ME control of surface magnetization

K. Nomura and N.N. PRL2011

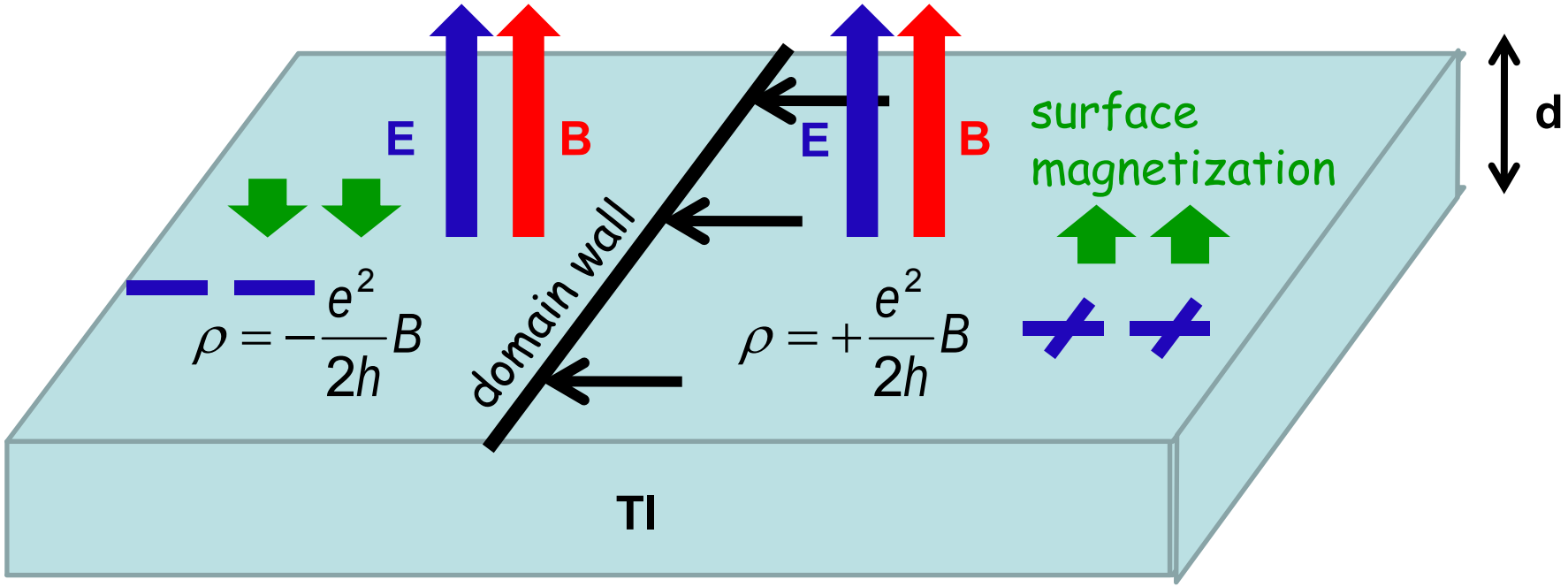

$$\rho = \pm\frac{e^2}{2h}B \qquad E = \rho Ed = \pm\frac{e^2}{2h}BEd$$ per unit area

Bulk energy gain controlled by surface magnetization

B=10T E=10^3 V/cm d=1mm

$B_{eff} \approx 10^3 T$

acting on surface magnetization

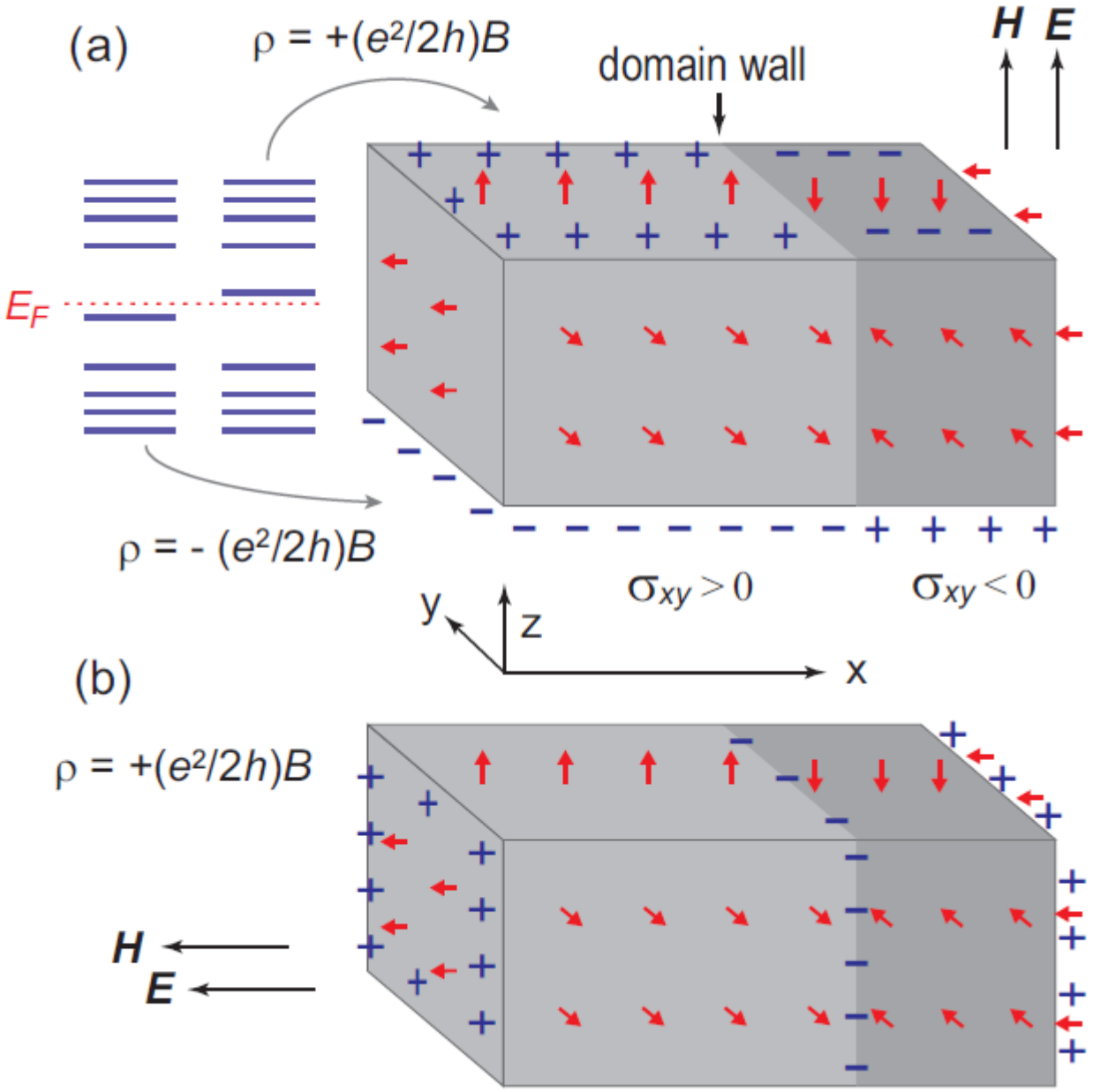
(a)
ρ = +(e²/2h)B
domain wall
H E
E_F
ρ = - (e²/2h)B
σxy > 0
σxy < 0
y
z
x
(b)
ρ = +(e²/2h)B
H
E

Spintronics on Topological insulator

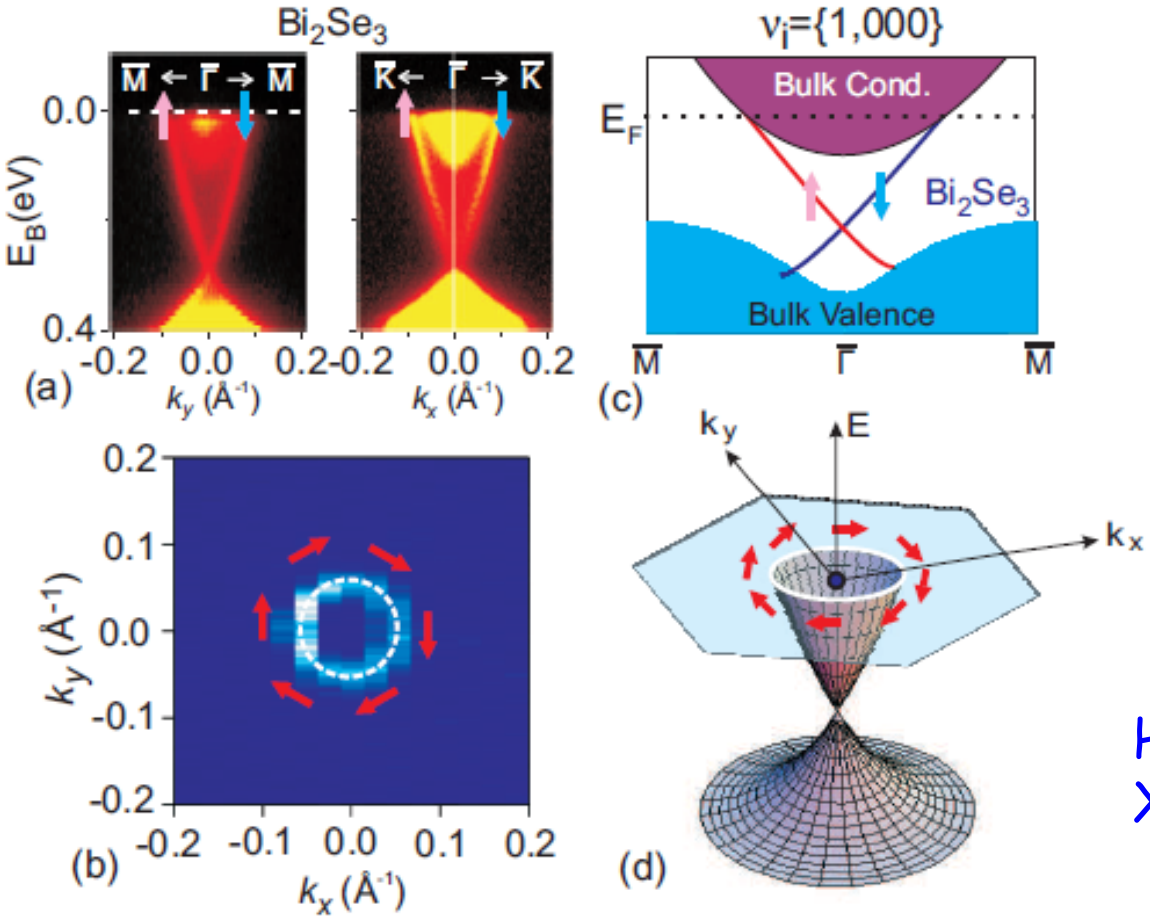

Hsieh et al.
Xia et al.

2D Dirac Hamiltonian $H = \psi^{+}\vec{\sigma}\cdot(\vec{e}_z \times \vec{p})\psi$

Spin textures are charged on topological insulator

K. Nomura and N.N. PRB Rapid 2010

Assume that the Fermi energy is within the gap ➔ QHS

$$n_x \leftrightarrow A_y$$
$$n_y \leftrightarrow -A_x$$

$$\nabla \cdot \vec{n} \leftrightarrow (\nabla \times \vec{A})_z = B_z$$

$$\rho_e \propto \sigma_H B_z \quad \Rightarrow \quad \rho_e^{\mathrm{ind}} = -\left(\frac{\sigma_H \Delta}{e v_F}\right) \boldsymbol{\nabla} \cdot \boldsymbol{n}$$

$$\Delta = M$$

exchange coupling

$$j_x = \sigma_H E_y = -\sigma_H \dot{A}_y \quad \Rightarrow \quad \boldsymbol{j}_e^{\mathrm{ind}} = \left(\frac{\sigma_H \Delta}{e v_F}\right) \frac{\partial \boldsymbol{n}}{\partial t}$$

$$P_\perp = \frac{\sigma_H \Delta}{e v_F} n_\perp$$

in-plane magnetization is equivalent to in-plane polarization

Spin textures are charged on topological insulator

K. Nomura and N.N.

$$\rho_e^{\rm ind} = -\left(\frac{\sigma_H \Delta}{e v_F}\right) \boldsymbol{\nabla}\cdot \boldsymbol{n}, \quad \boldsymbol{j}_e^{\rm ind} = \left(\frac{\sigma_H \Delta}{e v_F}\right) \frac{\partial \boldsymbol{n}}{\partial t} \qquad \rho_e^{\rm ind} = -\left(\frac{\gamma_e}{\gamma_m}\right) \rho_m^{\rm ind}$$

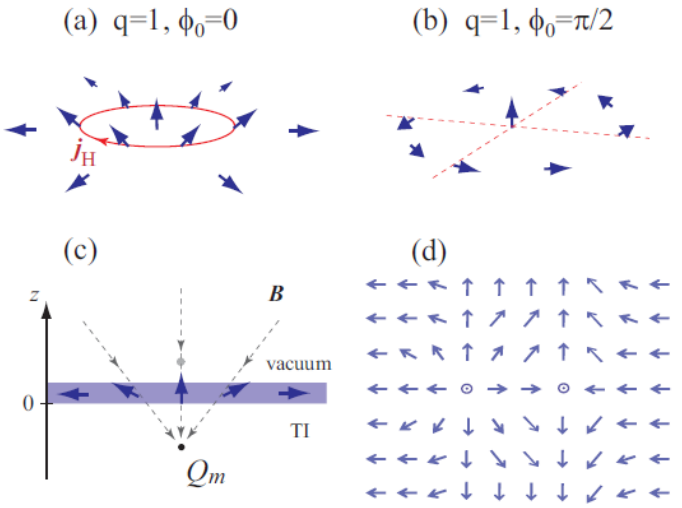

Vortex

Vortex creation/manipulation by gating

c.f. Haldane, Qi et al.

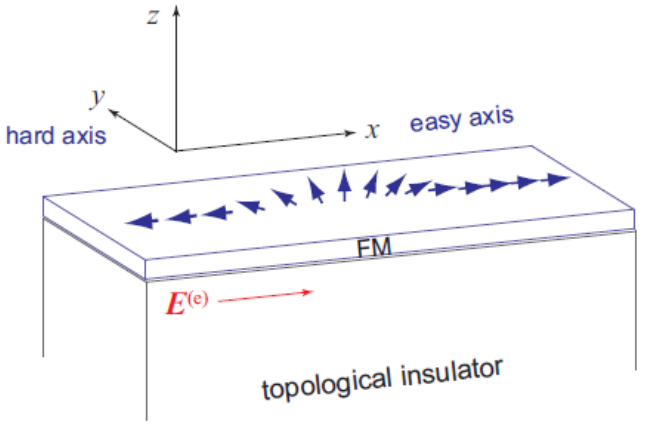

Domain wall

Charge density along the DW $\approx e/\xi$

$\xi \approx a(E_{gap}/\Delta)$ Δ exchange coupling

$\alpha \approx 0.01$ Gilbert damping

$$\left|\frac{dX}{dt}\right| \simeq \tilde{E}^{(e)} \times 10^{-2}[\mathrm{m/s}]$$

Similarity between d- and p-orbitals

$$d_{xy}, d_{yz}, d_{zx} \leftrightarrow p_z, p_x, p_y$$

$$-\vec{L} \leftrightarrow \vec{L}$$

$$(\vec{J}')^2 = (\vec{L} - \vec{S})^2 \leftrightarrow (\vec{J})^2 = (\vec{L} + \vec{S})^2$$

$$= const. - 2\vec{L}\cdot\vec{S} \qquad = const. + 2\vec{L}\cdot\vec{S}$$

STO **GaAs**

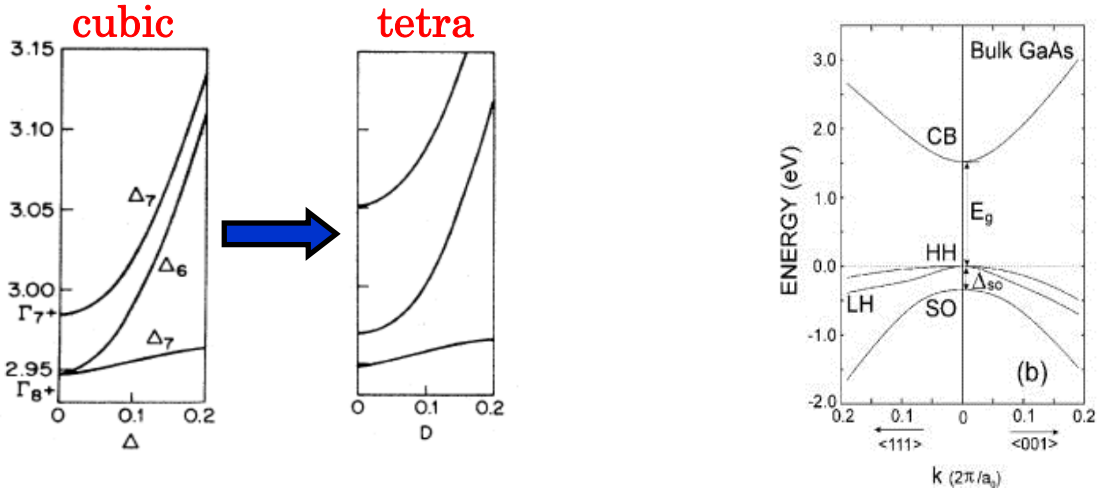

$$J_{eff} = 1/2 \text{ and } 3/2$$

Transition-metal oxide

c.f. Topological Mott insulator
S. Raghu, X-L. Qi, C. Honerkamp, and S.C. Zhang

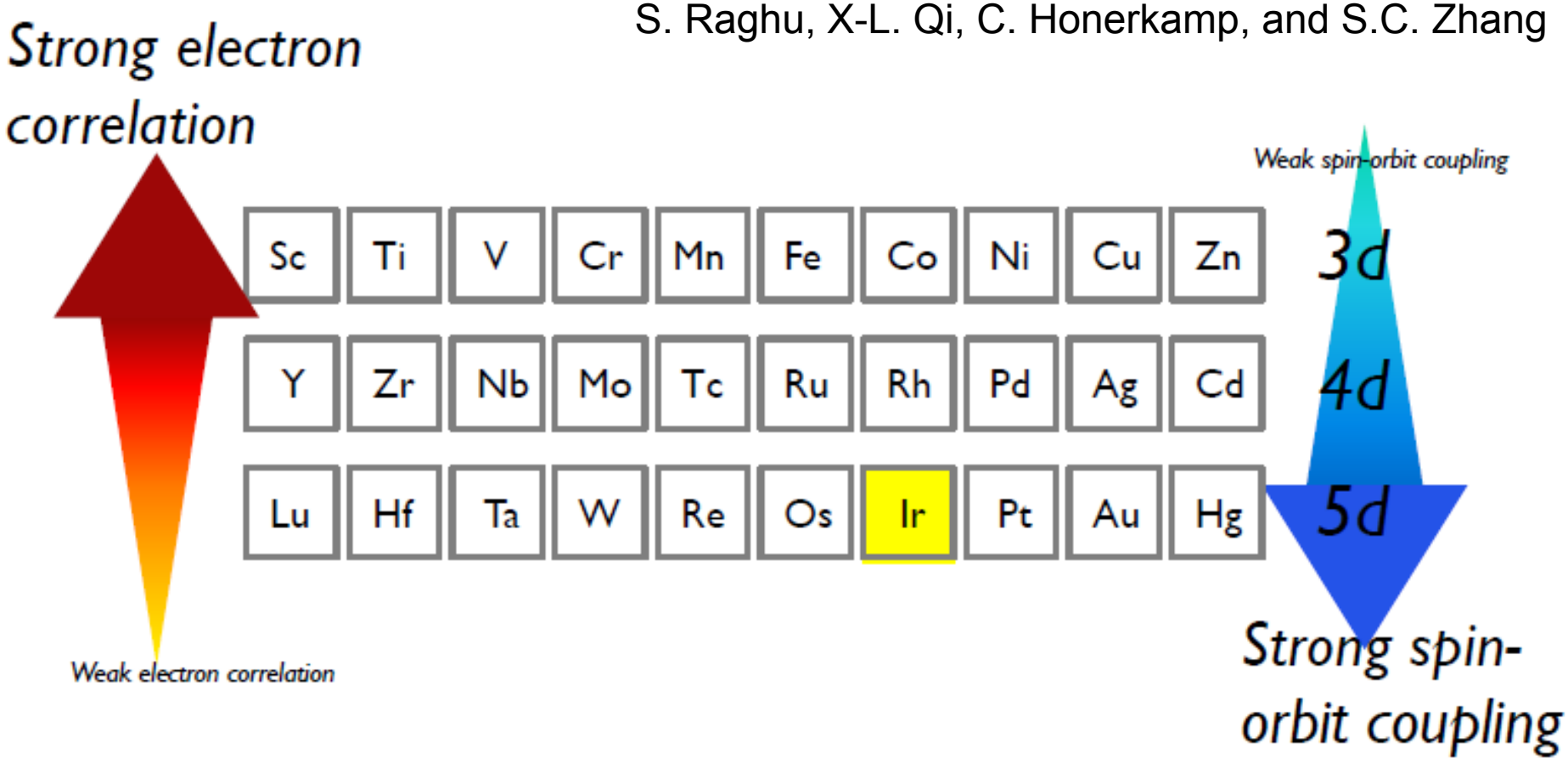

For Sr_2IrO_4: $U \sim 0.5eV$

$\zeta_{SO} \sim 0.45eV$

B.J. Kim

SOC induced Mott state – schematic picture

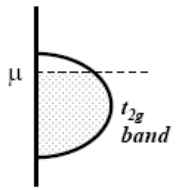

wide t_{2g}–band Metal

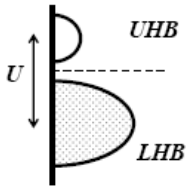

$S = 1/2$ Mott ground state

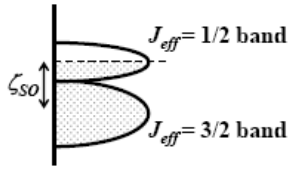

J_{eff} band split due to SO

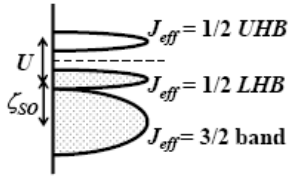

J_{eff}= 1/2 Mott ground state

$$U \approx \zeta_{SO} \approx 0.5eV \quad \text{for} \quad Sr_2IrO_4$$

$$Ir^{4+} : 5d^5$$

$J_{eff} = 1/2$

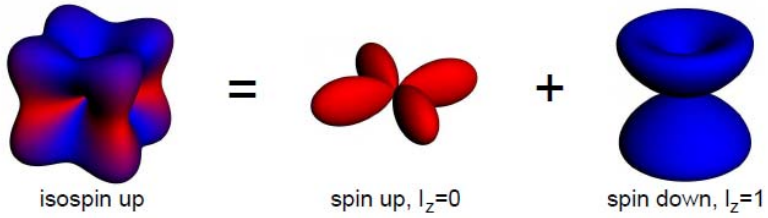

$$|1/2\rangle = (|xy\uparrow\rangle + |yz\downarrow\rangle + i|zx\downarrow\rangle)/\sqrt{3}$$

$$|-1/2\rangle = (-|xy\downarrow\rangle + |yz\uparrow\rangle - i|zx\uparrow\rangle)/\sqrt{3}$$

B.J. Kim T.W. Noh

Optical spectroscopy

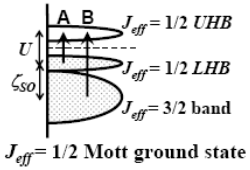

J_{eff}= 1/2 Mott ground state

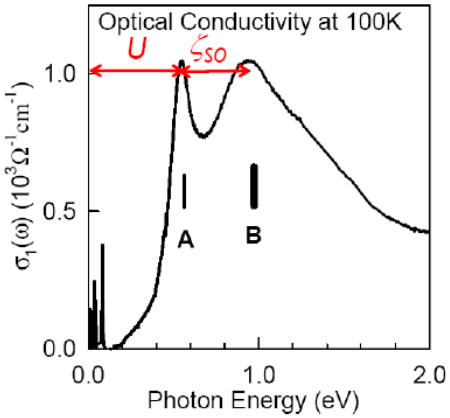

Double peak feature in optical conductivity
A: $J_{1/2}$(lower) → $J_{1/2}$(upper)
B: $J_{3/2}$ → $J_{1/2}$

X-ray Absorption Spectroscopy

$$J_{eff1/2} = \frac{1}{\sqrt{3}}\left(|xy,\pm 1/2\rangle \pm |yz,\mp 1/2\rangle + i|zx,\mp 1/2\rangle\right)$$

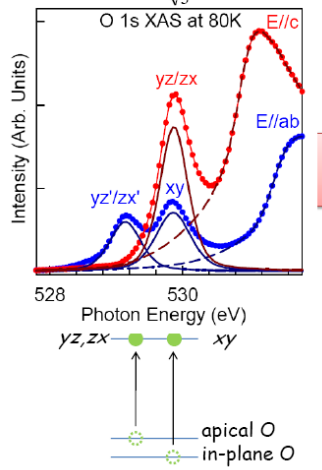

Characteristic orbital state with xy:yz:zx=1:1:1 ratio of J_{eff}=1/2 is confirmed by O K-edge XAS

Crystal Structure of Na_2IrO_3

Ir^{4+} $(5d^5)$ H. Takagi

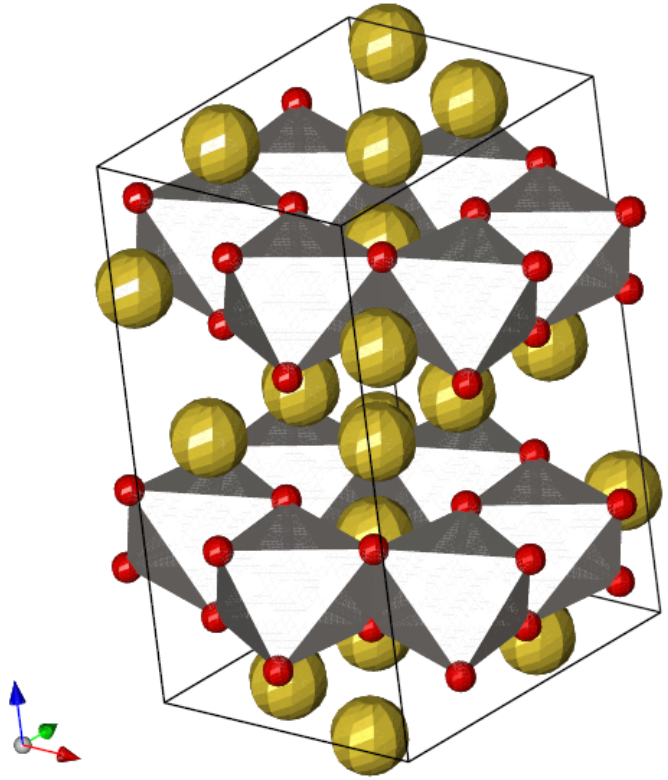

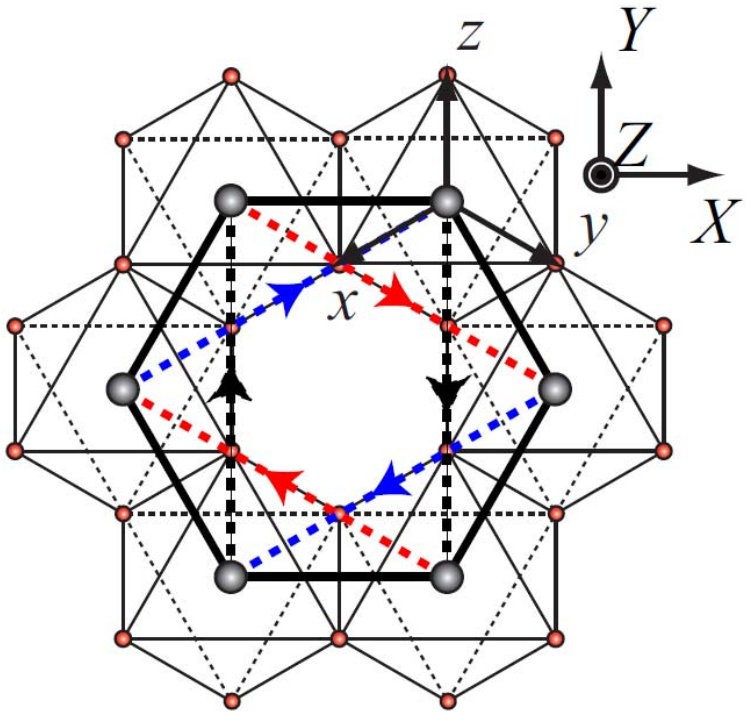

Complex orbitals produce complex transfer integrals

$$H = \sum_{ij\sigma} t_{ij} e^{i\sigma a_{ij}} c^{+}_{i\sigma} c_{j\sigma} + U \sum_{i} n_{i\uparrow} n_{i\downarrow}$$

$$< p_z, \uparrow | H | 1/2 >= te^{i\theta} \qquad < p_z, \downarrow | H | -1/2 >= te^{-i\theta}$$

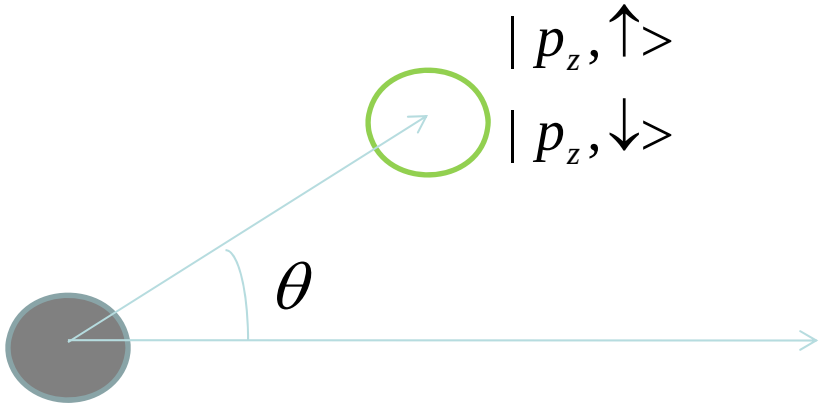

$J_{eff} = 1/2, \ |\pm 1/2>$

$$|1/2\rangle = (|xy\uparrow\rangle + |yz\downarrow\rangle + i|zx\downarrow\rangle)/\sqrt{3}$$
$$|-1/2\rangle = (-|xy\downarrow\rangle + |yz\uparrow\rangle - i|zx\uparrow\rangle)/\sqrt{3}$$

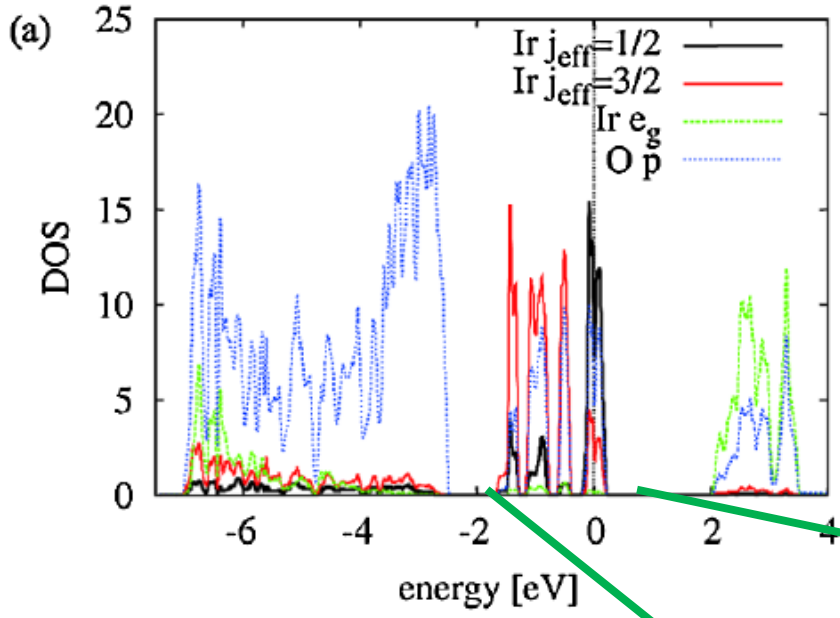

c.f. Jaejun Yu
trigonal X-tal field splitting 0.6eV
→Trivial insulator

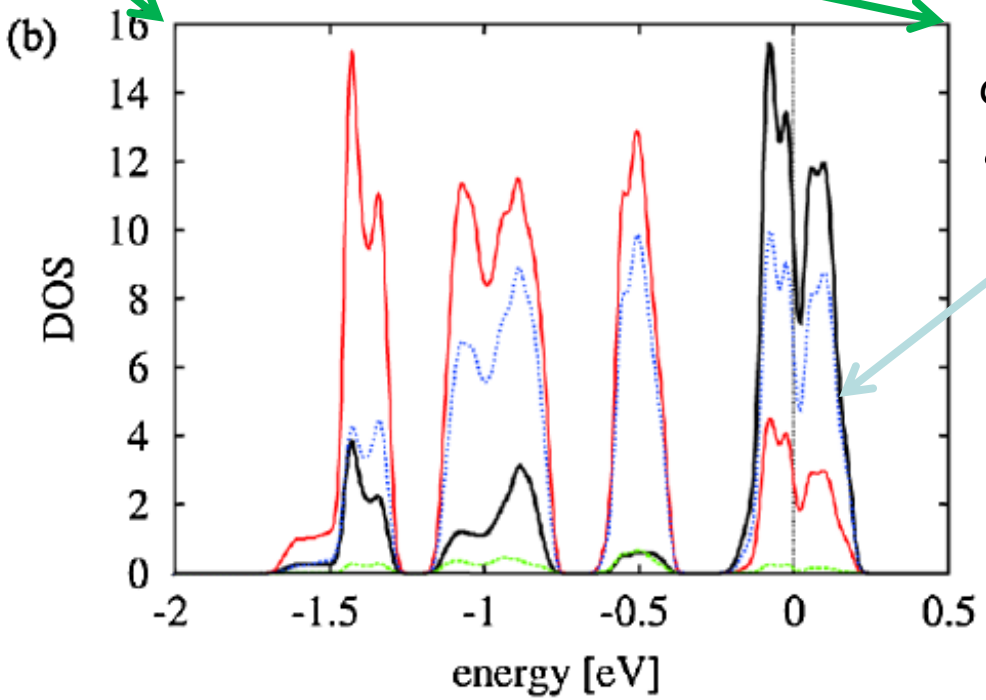

dominant
$J_{eff} = 1/2$

Correlated Kane-Mele model

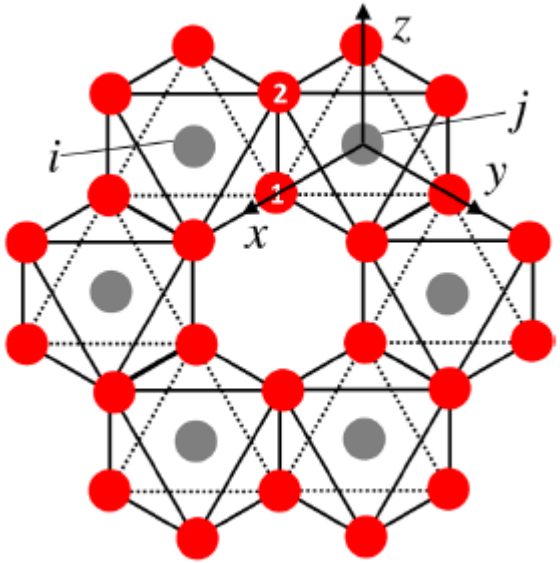

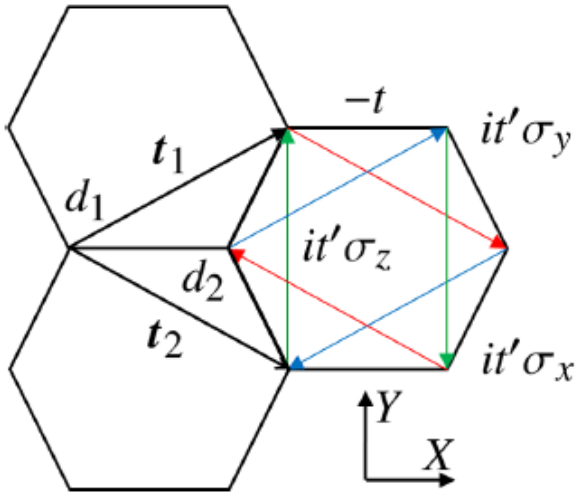

$(pd)^2/(\varepsilon_d - \varepsilon_p)$ -order processes cancel for 90-degree bonds

$$t = -\frac{1}{3}\frac{|(pd\pi)|^2}{\epsilon_d - \epsilon_p}\frac{(pp\sigma) + 3(pp\pi)}{\epsilon_d - \epsilon_p} \qquad t' \equiv \frac{1}{3}\frac{|(pd\pi)|^2}{\epsilon_d - \epsilon_p}\frac{(pp\sigma) - (pp\pi)}{\epsilon_d - \epsilon_p}$$

are of the order of room temperature

$$\Rightarrow \quad H_0 = \int d^2r\psi^\dagger(\boldsymbol{r})\left[3t'\eta_z\tau_z\sigma_Z - \frac{3}{2}t\eta_z[-i\partial_Y\tau_x + i\partial_X\tau_y]\right]\psi(\boldsymbol{r})$$

σ : spin

τ : sublattice

η : K or K'

nature materials

REVIEW ARTICLE

PUBLISHED ONLINE: 24 JANUARY 2012 | DOI: 10.1038/NMAT3223

Emergent phenomena at oxide interfaces

H. Y. Hwang[1,2,3*], Y. Iwasa[1,3,4], M. Kawasaki[1,3,4], B. Keimer[5], N. Nagaosa[1,4] and Y. Tokura[1,4,6*]

Artificial charge-modulation in atomic-scale perovskite titanate superlattices

A. Ohtomo, D. A. Muller, J. L. Grazul & H. Y. Hwang

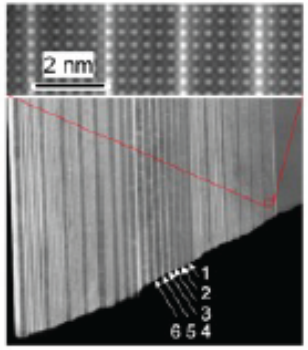

Strong polarization enhancement in asymmetric three-component ferroelectric superlattices

Ho Nyung Lee, Hans M. Christen, Matthew F. Chisholm, Christopher M. Rouleau & Douglas H. Lowndes

Condensed Matter Sciences Division, Oak Ridge National Laboratory, Oak Ridge,

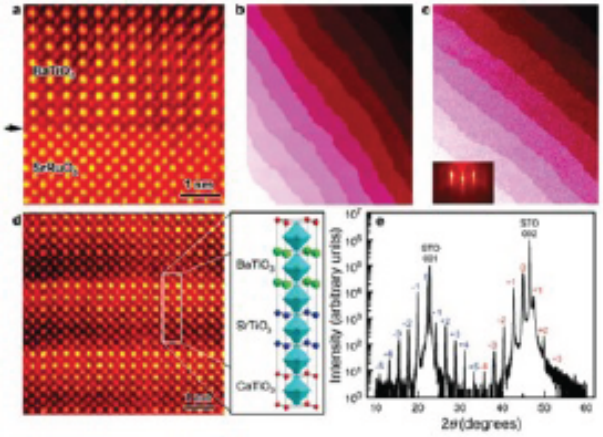

$[LaMnO_3]_n[SrTiO_3]_m$ superlattice

by courtesy of H. N. Lee, ORNL

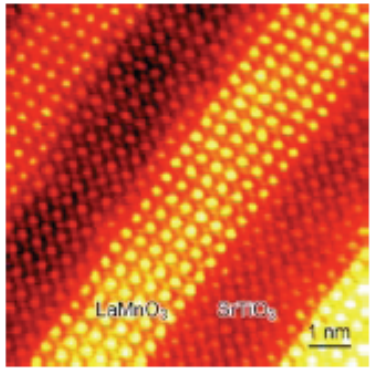

- Layered structure can be prepared with atomic precision
- Great flexibility: tunable lattice constant, carrier concentration, spin-orbit interaction, correlation strength

Topological insulator in oxide superlattice

D.Xiao et al
Nature Com. 2011

Perovskite (111)-bilayer

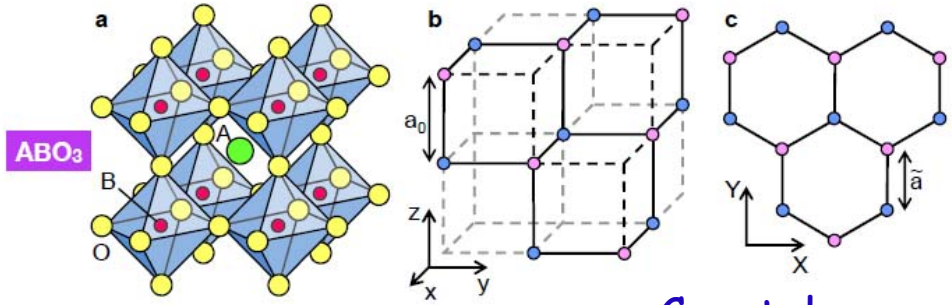

Crystal structure

Atomic Orbitals in Crystal Field + SO

Orbitals and symmetry

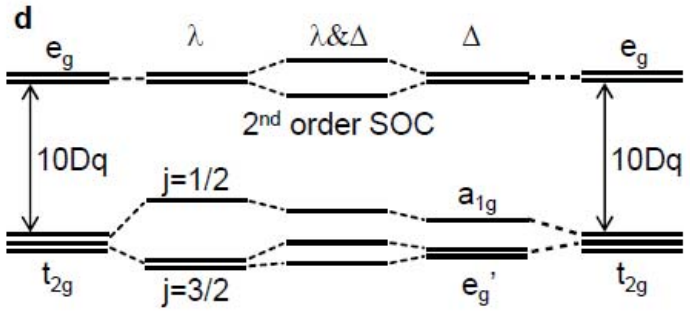

e_g Orbitals

e_g^1, e_g^2, e_g^3 are possible candidates

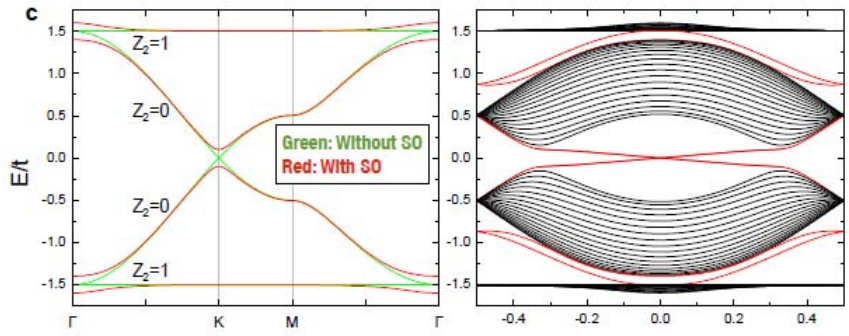

Nearly flat Z_2 band obtained if $V_{dd\delta}/V_{dd\sigma}$~0

e_g Systems

First-principles calc.

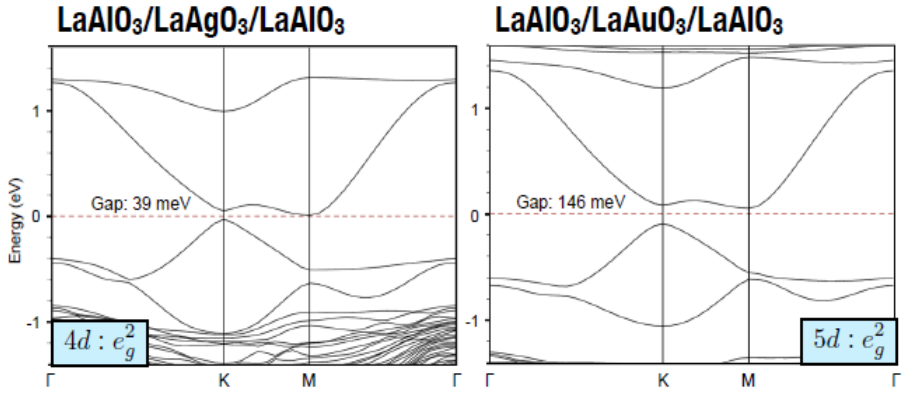

$LaAuO_3$ bilayer has an energy gap ~ 2000 K

Materials Consideration

$A=La^{3+}, Sr^{2+}$

$LaBO_3 \rightarrow B^{3+}$

$SrBO_3 \rightarrow B^{4+}$

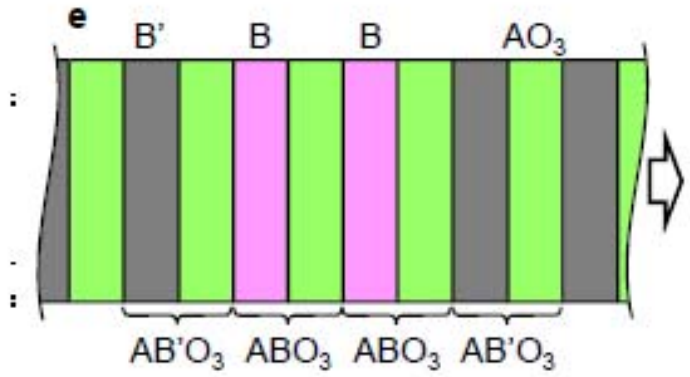

$AB'O_3$: $LaAlO_3$ and $SrTiO_3$

TABLE SI: List of candidate materials

	Configuration	Bulk	Superlattice
$LaReO_3$	t_{2g}^4	—	—
$LaRuO_3$	t_{2g}^5	metallic Ref. [2]	—
$SrRhO_3$	t_{2g}^5	metallic Ref. [3]	Ref. [4]
$SrIrO_3$	t_{2g}^5	metallic Refs. [5, 6]	metallic Ref. [7]
$LaOsO_3$	t_{2g}^5	—	—
$LaAgO_3$	e_g^2	metallic (band calc.) Ref. [8]	—
$LaAuO_3$	e_g^2	Refs. [9, 10]	—

t_{2g} Systems

metal

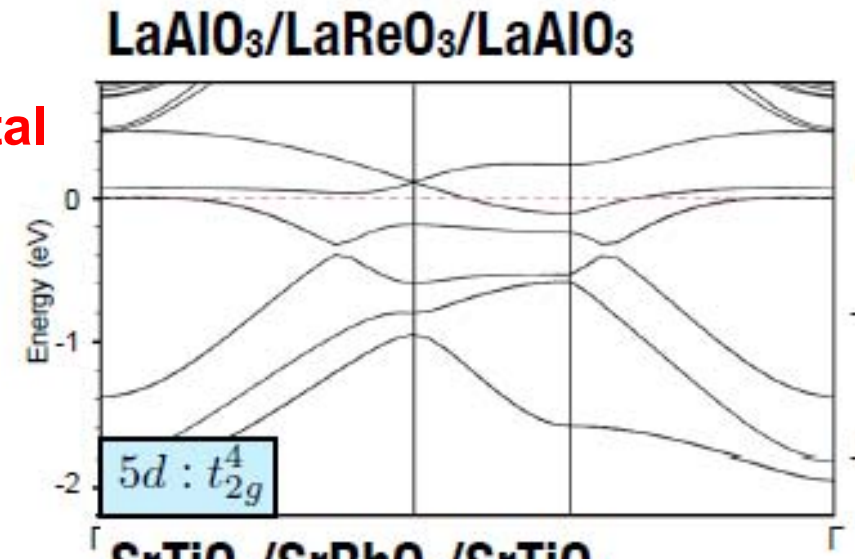

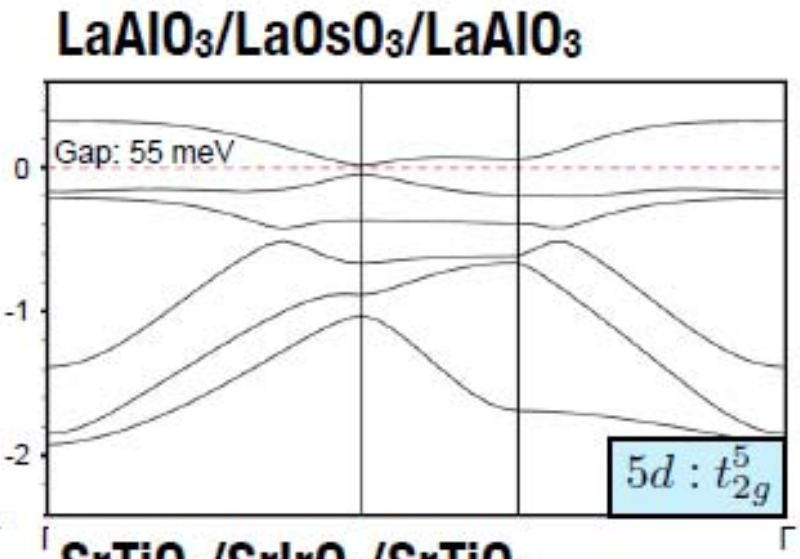

TI

metal

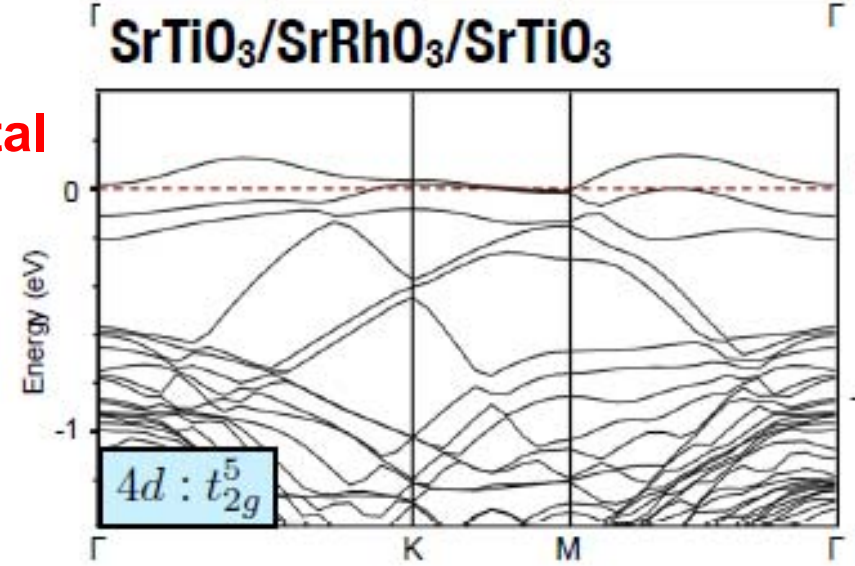

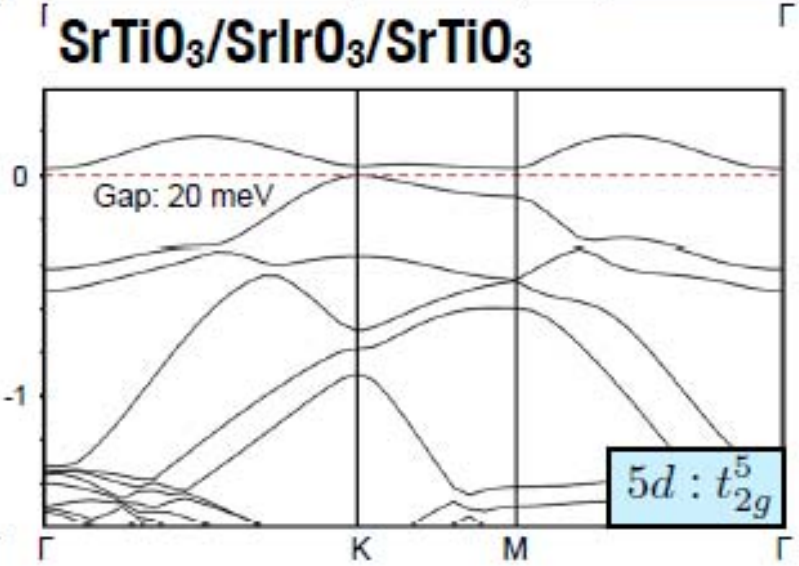

TI

Integer Quantum Hall Effect

How to break time-reversal symmetry?

- External: Ferromagnetic or G-type antiferromagnetic substrate
- Internal: Stoner instability (U/Bandwidth>>1)

Mean field Hamiltonian $H = H_{eg} + \vec{h} \cdot \vec{\sigma}$

$e_g^{0.5}, e_g^{3.5}$

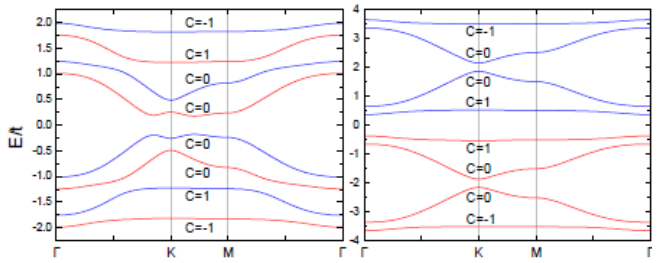

e_g^1

Small h Large h

Quantized Anomalous Hall effect

Correlation effect

Fractional quantized Anomalous Hall effect

Fractional Quantum Hall Effect

- 3-fold degenerate GS

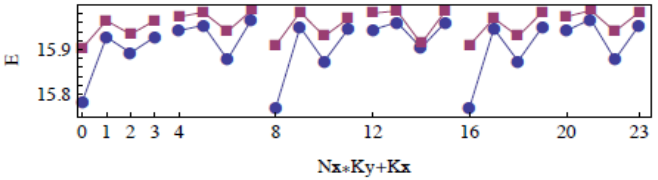

- Chern number

$$\sigma_{xy} = \frac{e^2}{hg} \sum_{K=1}^{g} \int_0^{2\pi} \int_0^{2\pi} d\phi_1 d\phi_2 \left(\left\langle \frac{\partial \Phi_0}{\partial \phi_1} \middle| \frac{\partial \Phi_0}{\partial \phi_2} \right\rangle - \left\langle \frac{\partial \Phi_0}{\partial \phi_2} \middle| \frac{\partial \Phi_0}{\partial \phi_1} \right\rangle \right)$$

g=3, C_1=0.3344, C_2=0.3311,C_3=0.3344

Other proposals, see Tang et al PRL; Neupert et al PRL; Sun et al PRL, 2011

BiTeI giant bulk Rashba system and TI under pressure

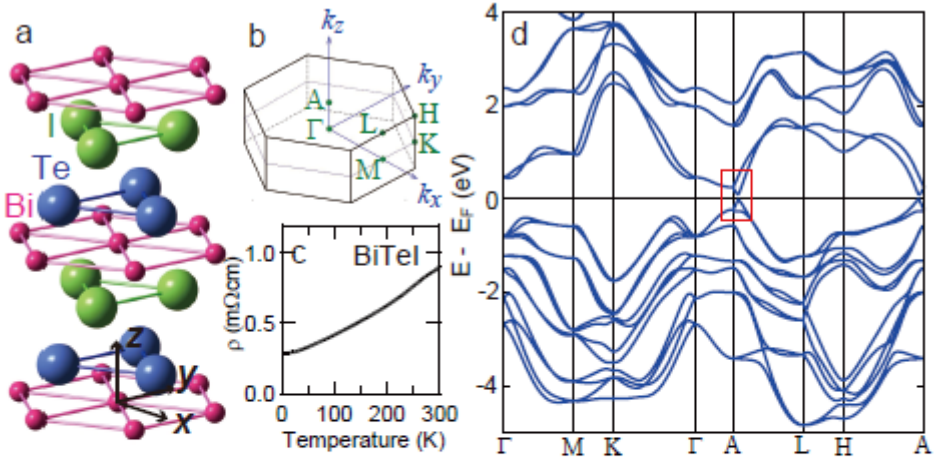

K. Ishizaka et al.
Nature Mat. (2011)

M. S. Bahramy, R.Arita,
B.J.Yang, N.Nagaosa
Nature Com. (2012)

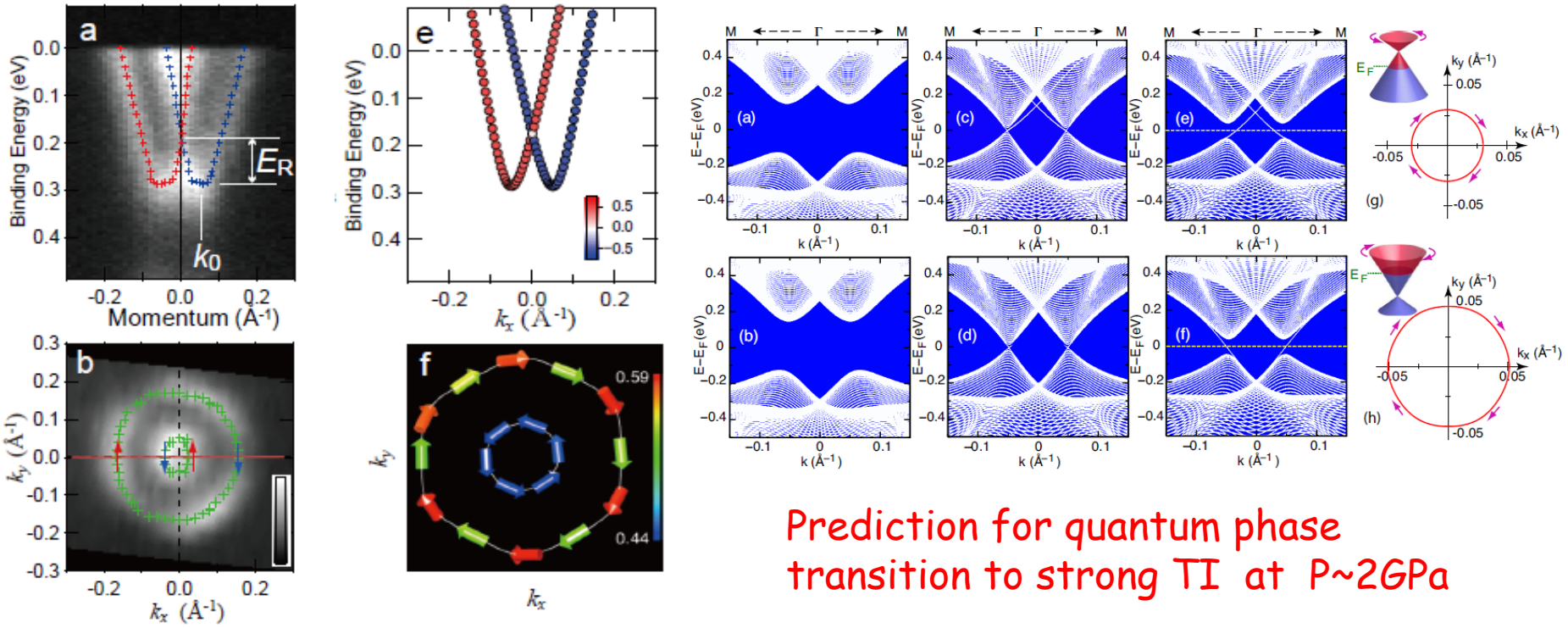

Prediction for quantum phase transition to strong TI at P~2GPa

Topological Superconductors

Majorana (real) Fermions

f^+, f Usual (complex) fermions

$\psi = (f^+ + f)/\sqrt{2}$ ➡ $\psi = \psi^+ \quad \psi^2 = 1$

"half" of the usual (complex) fermion
"real" fermion

$f = (\psi_1 + i\psi_2)/\sqrt{2}$

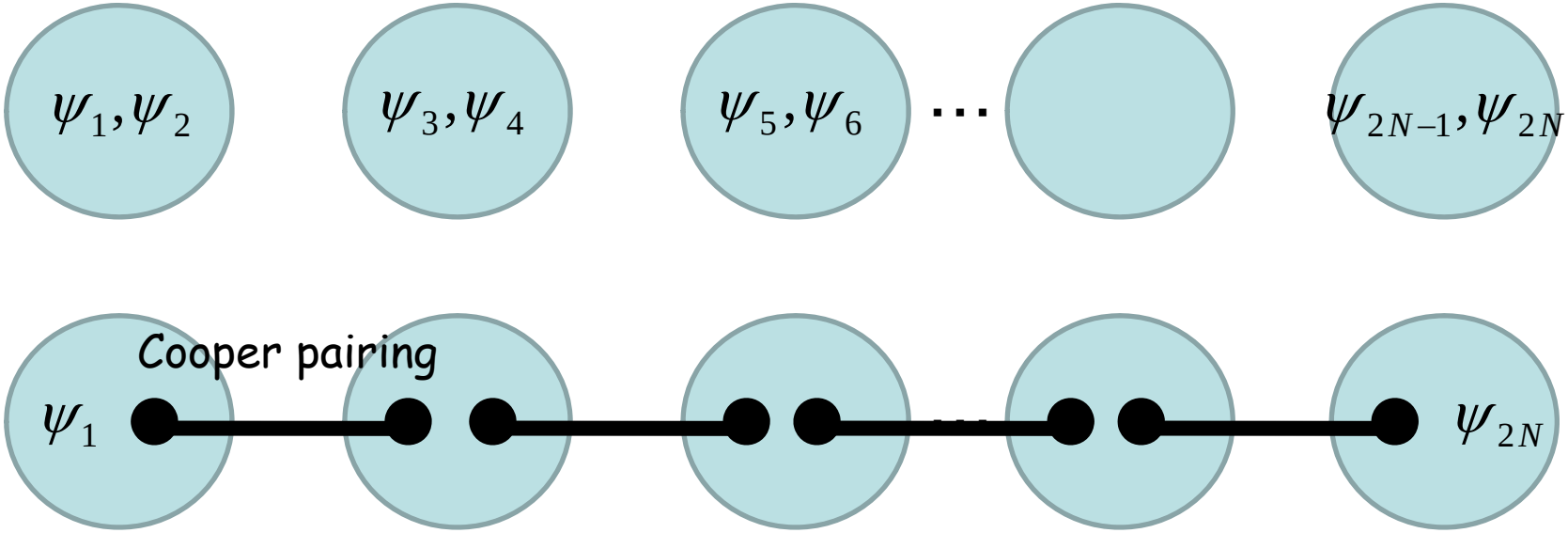

ψ_1, ψ_{2N} Single fermion → 1 q-bit

Kitaev model

Alicea 2012

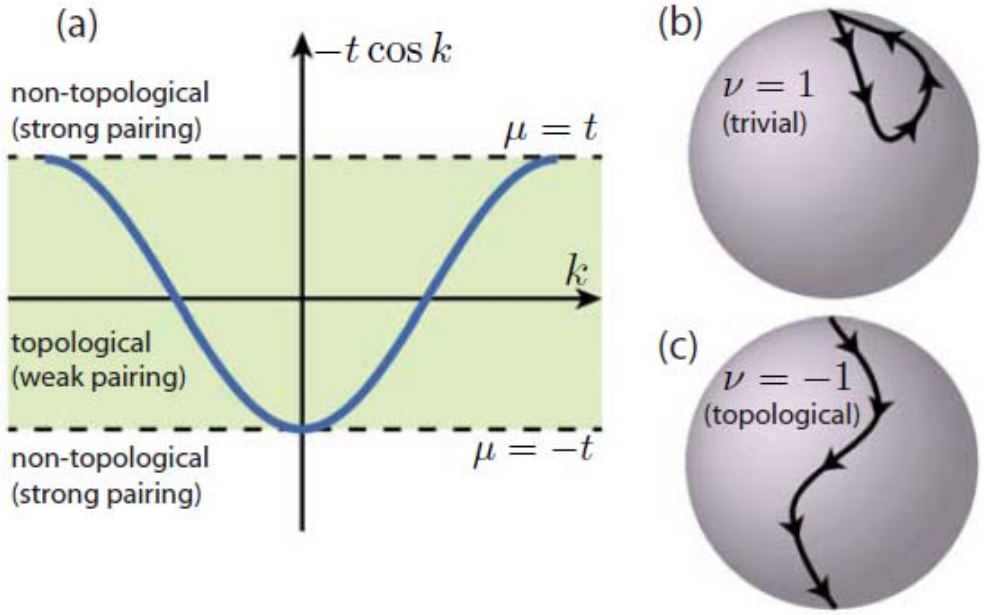

$$H = \frac{1}{2}\sum_{k\in BZ} C_k^\dagger \mathcal{H}_k C_k, \quad \mathcal{H}_k = \begin{pmatrix} \epsilon_k & \tilde{\Delta}_k^* \\ \tilde{\Delta}_k & -\epsilon_k \end{pmatrix} \qquad \Delta_k = i\Delta \sin k$$

$$\mathcal{H}_k = \mathrm{h}(k)\cdot\boldsymbol{\sigma} \qquad (C_{-k}^\dagger)^T = \sigma^x C_k$$

$$h_{x,y}(k) = -h_{x,y}(-k), \quad h_z(k) = h_z(-k)$$

$$\Rightarrow \quad \hat{\mathrm{h}}(0) = s_0\hat{\mathbf{z}}, \quad \hat{\mathrm{h}}(\pi) = s_\pi\hat{\mathbf{z}}$$

Sciencexpress Reports

Signatures of Majorana Fermions in Hybrid Superconductor-Semiconductor Nanowire Devices

V. Mourik,[1*] K. Zuo,[1*] S. M. Frolov,[1] S. R. Plissard,[2] E. P. A. M. Bakkers,[1,2] L. P. Kouwenhoven[1]†

Here we report the observation of such zero-energy peaks and show that they rigidly stick to zero-energy while changing B and gate voltages over large ranges. Furthermore, we show that this zero-bias peak is absent if we take out any of the necessary ingredients of the Majorana proposals, i.e., the rigid zero bias peak disappears for zero magnetic field, for a magnetic field parallel to the spin-orbit field, or

Majorana fermion
at the ends of Rashba
quantum wire
next to superconductor

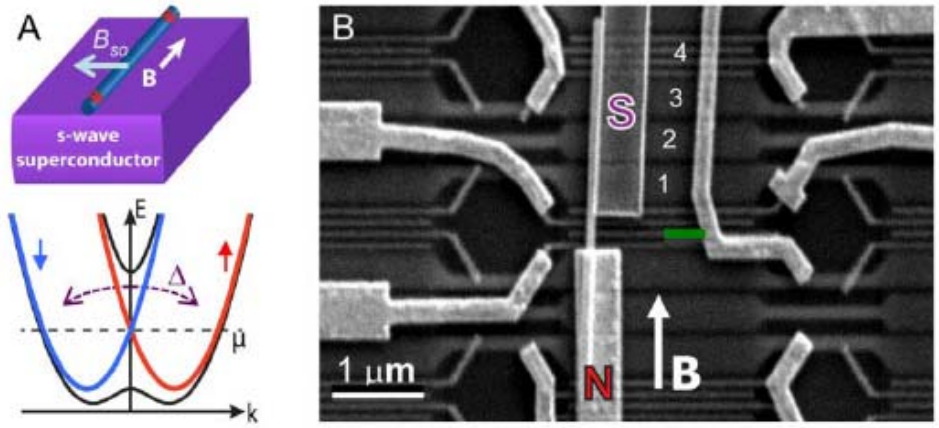

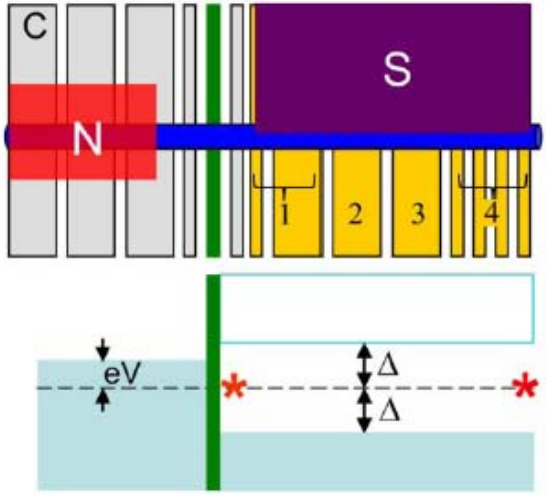

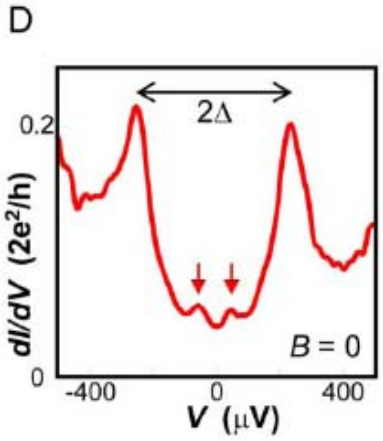

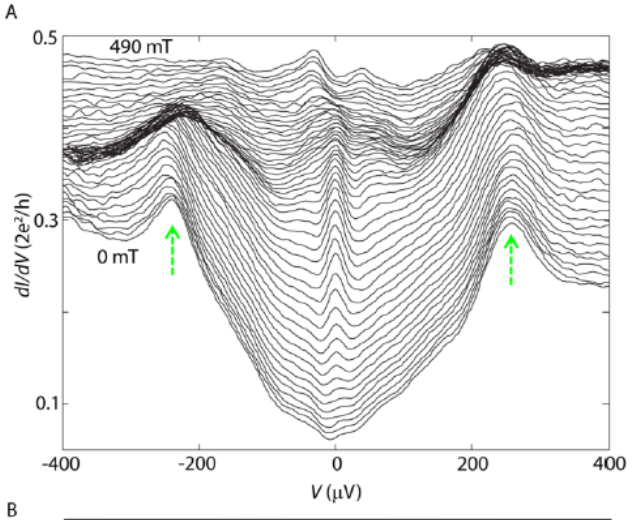

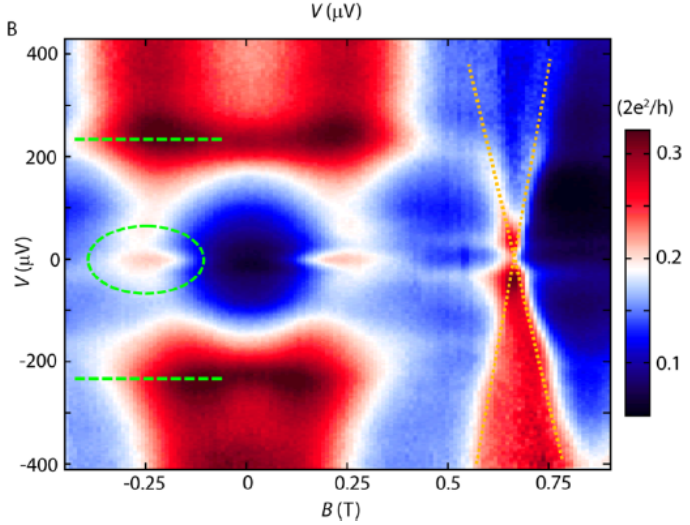

Analogy between chiral superconductor and QHS

Quantum Hall system

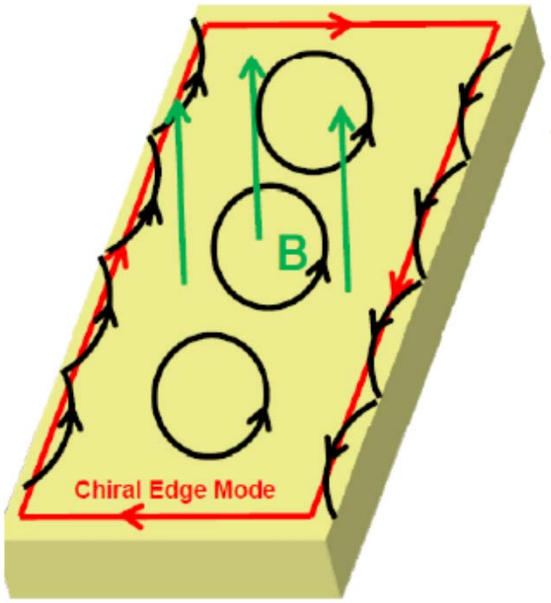

$\sigma_H = \frac{e^2}{h} n$ n : Topological integer

Chiral edge channels

Chiral superconductor

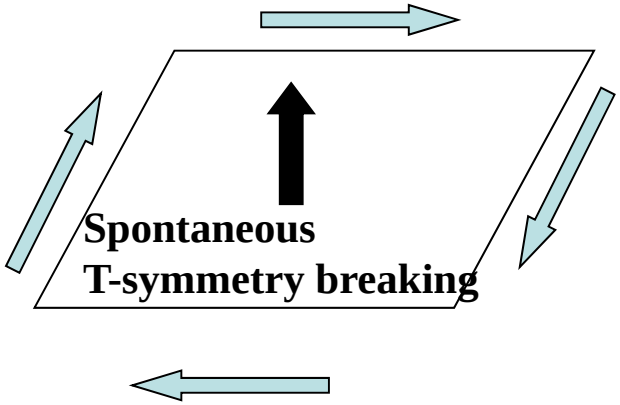

??

Chiral p-wave superconductors Sr_2RuO_4

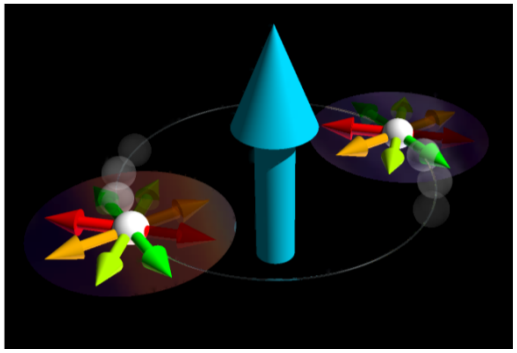

Maeno (1994), Sigrist-Rice

Spin-triplet p-wave

Time-reversal symmetry broken

Topological index for chirality

$$N=\frac{1}{4\pi}\int_{-\infty}^{\infty}dk_x\int_{-\infty}^{\infty}dk_y\hat{\boldsymbol{m}}\cdot\left(\frac{\partial\hat{\boldsymbol{m}}}{\partial k_x}\times\frac{\partial\hat{\boldsymbol{m}}}{\partial k_y}\right)$$

$$\hat{\boldsymbol{m}}=\frac{\boldsymbol{m}}{|\boldsymbol{m}|},\qquad \boldsymbol{m}=(\mathrm{Re}\,d_z,\mathrm{Im}\,d_z,\epsilon_k)$$

Volovik

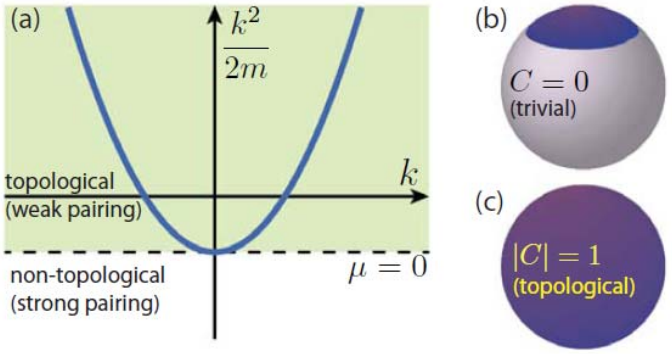

related to the # of edge channels but not to σ_H

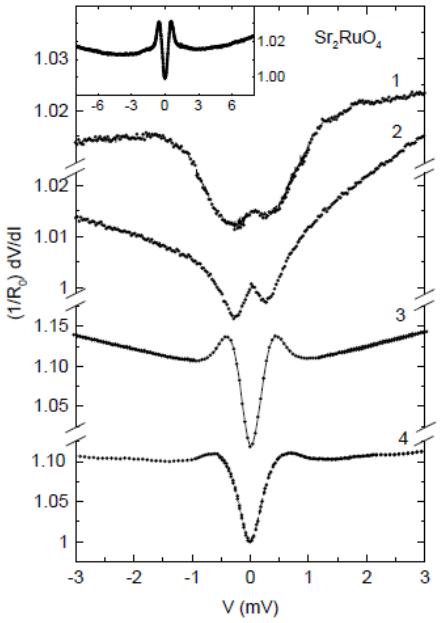

SRO-Pt point contact Andreev bound state

Laube et al. (00)

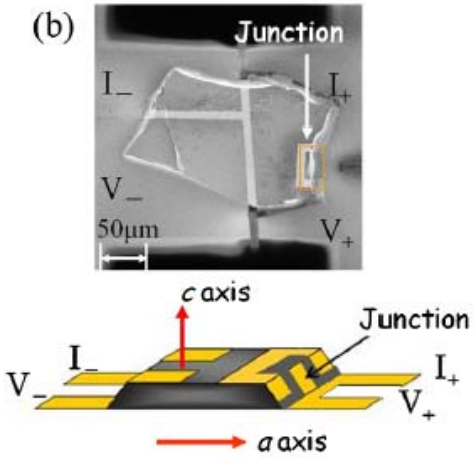

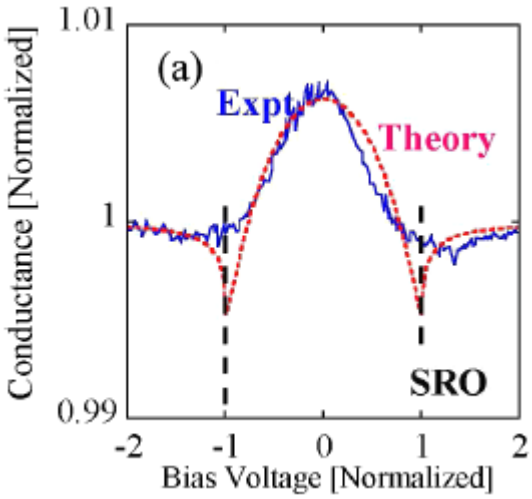

Kashiwaya-Tanaka-Maeno group (2011)

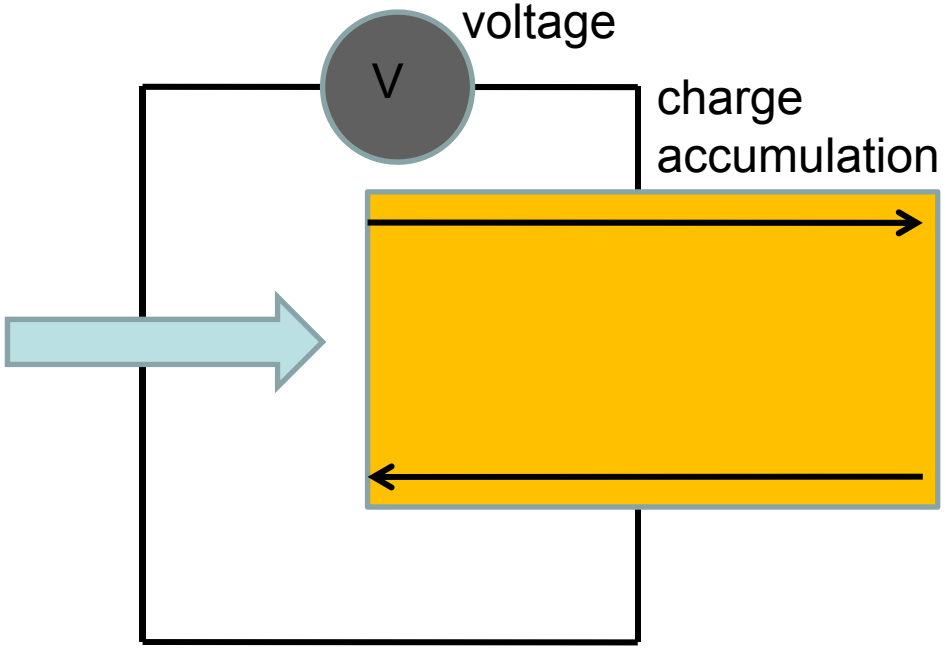

$$\sigma_H^s \approx \frac{e^2}{h} \cdot \frac{1}{(k_F \lambda)^2}$$

compressible ground state

Furusaki-Matsumoto-Sigrist (2000)

Current ***I***

Majorana (real) Fermions

f^+, f Usual (complex) fermions

$\psi = (f^+ + f)/\sqrt{2} \Rightarrow \psi = \psi^+ \quad \psi^2 = 1$

"half" of the usual (complex) fermion
"real" fermion

Chiral Majorana mode at the edge of spinless p+ip SC (A.Furusaki et al.)

$$\mathcal{H}_p = \psi^\dagger(\boldsymbol{r})\left(-\frac{\hbar^2}{2m}\nabla^2 - \mu\right)\psi(\boldsymbol{r}) + \frac{1}{\lambda}|\eta(\boldsymbol{r})|^2$$
$$-\frac{i}{2k_F}\eta(\boldsymbol{r})\cdot\psi^\dagger(\boldsymbol{r})\nabla\psi^\dagger(\boldsymbol{r}) - \frac{i}{2k_F}\eta^*(\boldsymbol{r})\cdot\psi(\boldsymbol{r})\nabla\psi(\boldsymbol{r})$$

$$\psi(y,t) = e^{i\pi/4+i\phi/2}\int_0^{k_F}\frac{dk}{\sqrt{4\pi}}\left(e^{ik(\epsilon y - vt)}\gamma_k + e^{-ik(\epsilon y - vt)}\gamma_k^\dagger\right)$$

$$H_p = \int_0^{k_F} dk\, vk\gamma_k^\dagger\gamma_k$$

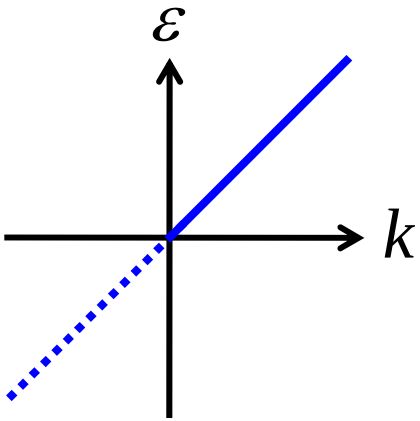

c.f. Majorna zero energy bound state at vortex
(Read-Green, Kitaev, Ivanov, D.H.Lee etc.)

Majorana interferometer on topological insulator

Fu-Kane, Beenacker et al., Ng-Lee et al.

$$c_L^+ = \gamma_1 + i\gamma_2 \qquad c_R^+ = \gamma_1 \pm i\gamma_2$$

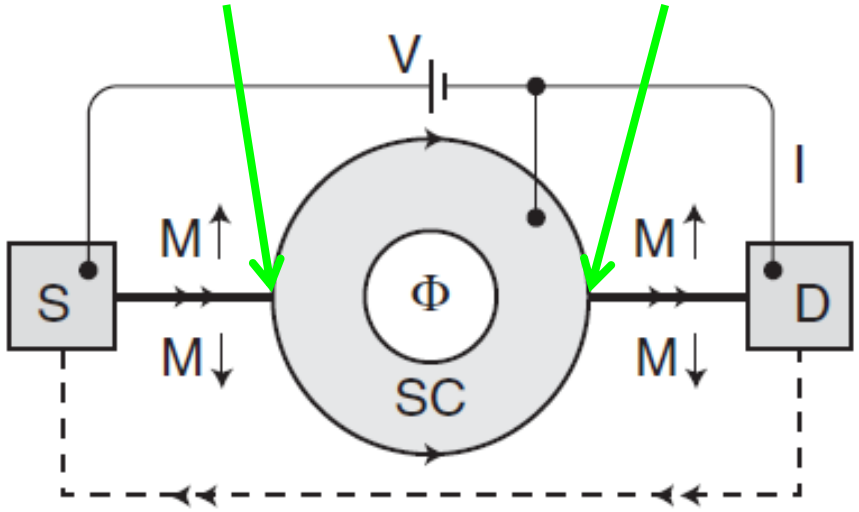

$$I = (-1)^n \frac{e}{h} \frac{\pi k_B T \sin(eV\delta L/v_M)}{\sinh(\pi k_B T \delta L/v_M)}, \qquad k_B T,\, eV \ll \Delta_0.$$

Topological periodic table

Kitaev, Schnyder *et al.* PRB 2008

	symmetry			d							
	$\mathcal{T}^2$	$\mathcal{C}^2$	$\mathcal{S}^2$	0	1	2	3	4	5	6	7
A	0	0	0	Z	0	Z	0	Z	0	Z	0
AIII	0	0	1	0	Z	0	Z	0	Z	0	Z
AI	1	0	0	Z	0	0	0	2Z	0	Z_2	Z_2
BDI	1	1	1	Z_2	Z	0	0	0	2Z	0	Z_2
D	0	1	0	Z_2	Z_2	Z	0	0	0	2Z	0
DIII	−1	1	1	0	Z_2	Z_2	Z	0	0	0	2Z
AII	−1	0	0	2Z	0	Z_2	Z_2	Z	0	0	0
CII	−1	−1	1	0	2Z	0	Z_2	Z_2	Z	0	0
C	0	−1	0	0	0	2Z	0	Z_2	Z_2	Z	0
CI	1	−1	1	0	0	0	2Z	0	Z_2	Z_2	Z

$\mathcal{T}$: time-reversal

$\mathcal{C}$: particle-hole

$\mathcal{S}$: chiral

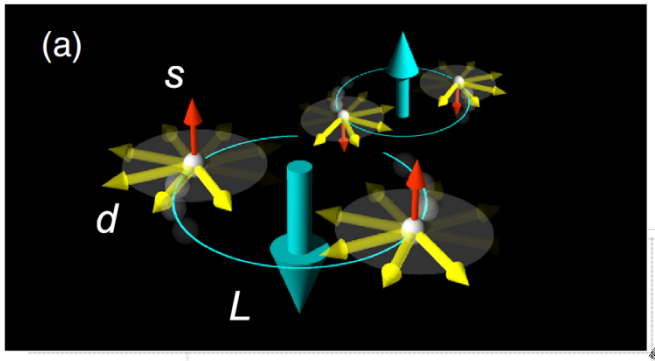

Sr_2RuO_4

Maeno *et al.* JPSJ 2012

$Cu_xBi_2Se_3(?)$

Sasaki *et al.* PRL 2011

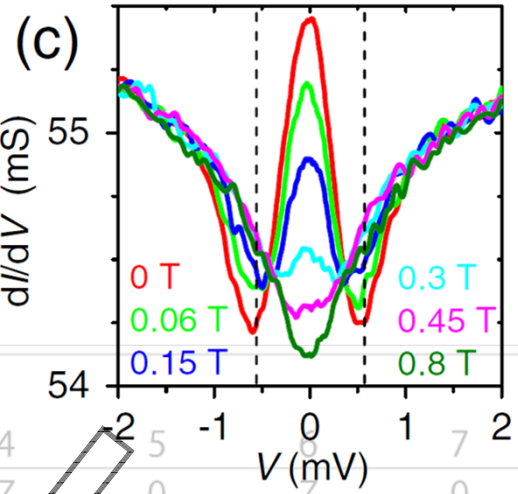

	d							
	0	1	2	3	4	5	6	7
A	0	0	0	Z	0	Z	0	Z
AIII	0	0	1	0	Z	0	Z	0
AI	1	0	0	Z	0	0	2Z	0
BDI	1	1	1	Z_2	Z	0	0	0
D	0	1	0	Z_2	Z_2	Z	0	0
DIII	1	0	1	0	Z_2	Z_2	Z	0
AII	0	1	0	2Z	0	Z_2	Z_2	Z
CII	−1	−1	1	0	2Z	0	Z_2	Z_2
C	0	−1	0	0	0	2Z	0	Z_2
CI	1	−1	1	0	0	0	2Z	0

Chiral superconductor
Helical superconductor
Topological Insulator

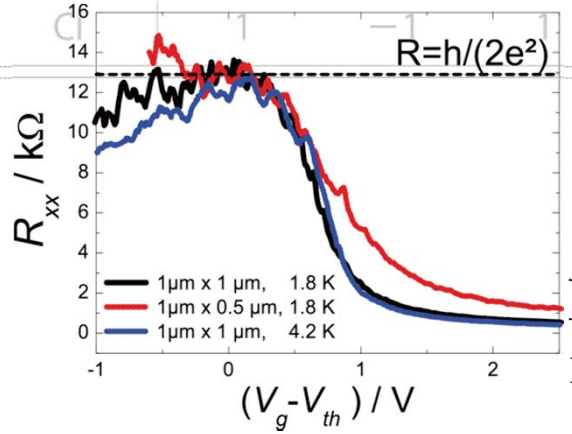

HgTe/CdTe

Koenig *et al.* JPSJ 2008

Bi_2Se_3

Xia *et al.* NatPhys 2009

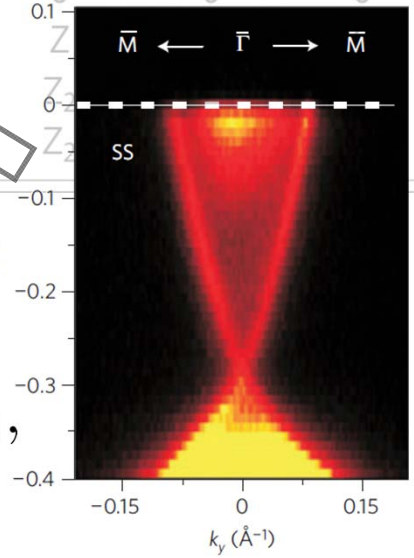

$Bi_{1-x}Sb_x$, Bi_2Te_3, $BiTlSe_2$ etc.

A model of chiral superconductors

Asahi-N.N. 2012 ArXiv:

$H = \sum_{\boldsymbol{k}} C^{\dagger}_{\boldsymbol{k}} H(\boldsymbol{k}) C_{\boldsymbol{k}}$ Spinless fermion pairing between sites

$$H(\boldsymbol{k}) = \begin{pmatrix} 2t_x \cos k_x + 2t_y \cos k_y - \mu & d_x \sin k_x - i d_y \sin k_y \\ d_x \sin k_x + i d_y \sin k_y & \mu - 2t_x \cos k_x - 2t_y \cos k_y \end{pmatrix}$$

$$\mathcal{H}_k = \mathrm{h}(k) \cdot \boldsymbol{\sigma} \qquad (C^{\dagger}_{-k})^T = \sigma^x C_k$$

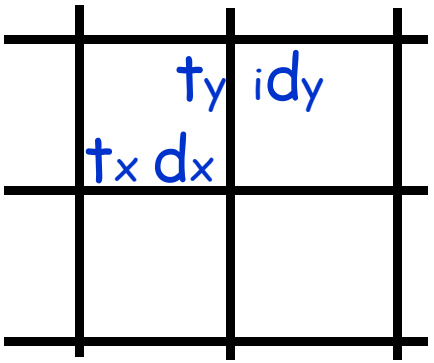

$$h_{x,y}(k) = -h_{x,y}(-k), \quad h_z(k) = h_z(-k)$$

Time-reversal symmetric momenta

$$k_m = (0,0),(0,\pi),(\pi,0),(\pi,\pi)$$

$$\hat{h}(k_m) = s(k_m)\hat{e}_z$$

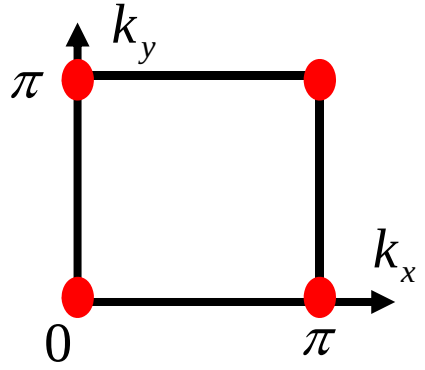

Z and Z2 topological invariants and phase diagram

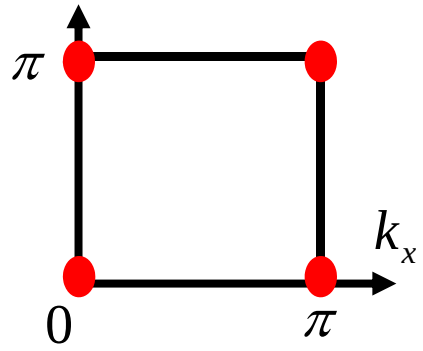

$$\hat{h}(k_m) = s(k_m)\hat{e}_z$$

$$\nu_x = s(\pi,0)s(\pi,\pi)$$

$$\nu_y = s(0,\pi)s(\pi,\pi)$$

$$(-1)^{\nu} = s(0,0)s(0,\pi)s(\pi,0)s(\pi,\pi)$$

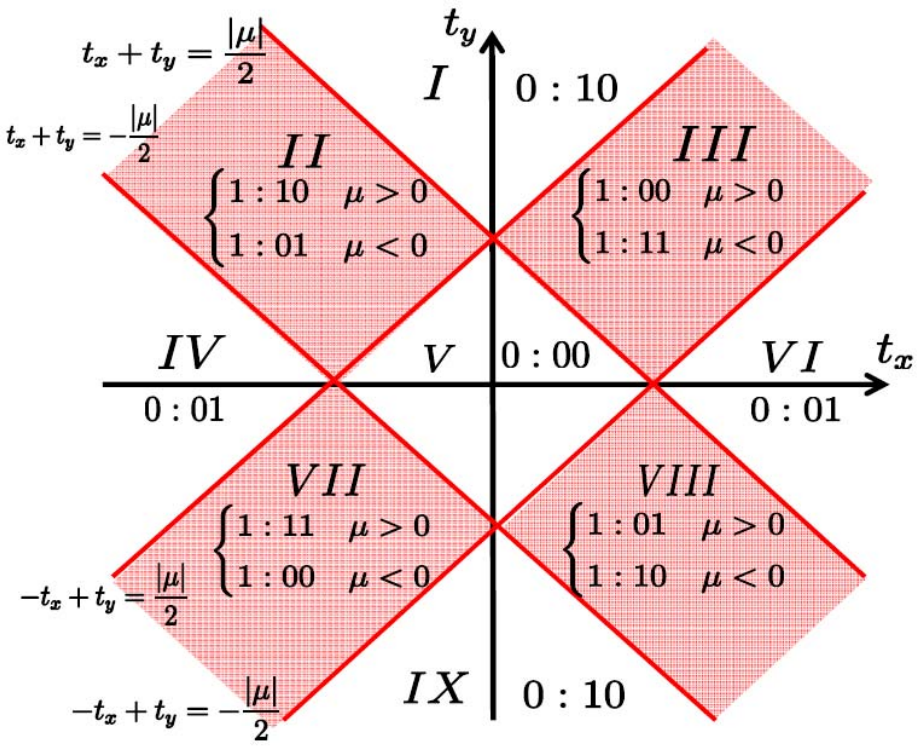

Generalization to include spatially dependent cases

Teo-Kane 2010

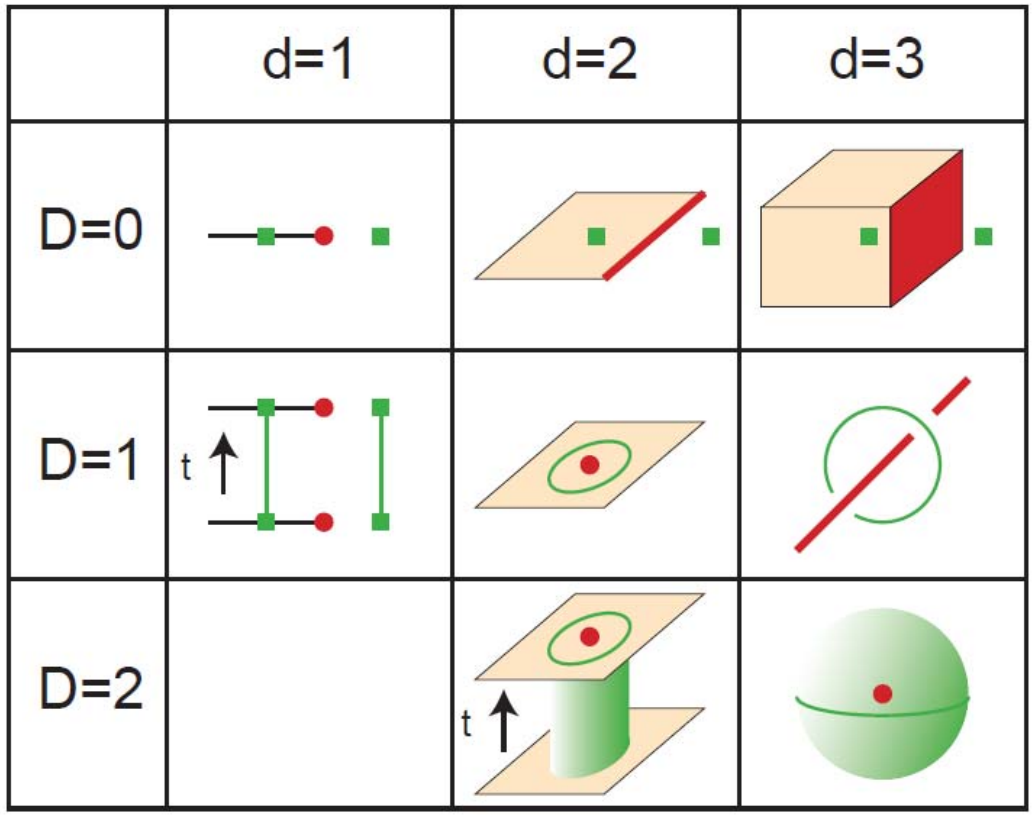

FIG. 1: Topological defects characterized by a D parameter family of d dimensional Bloch-BdG Hamiltonians. Line defects correspond to $d - D = 2$, while point defects correspond to $d - D = 1$. Temporal cycles for point defects correspond to $d - D = 0$.

Symmetry					$\delta = d - D$							
s	AZ	Θ^2	Ξ^2	Π^2	0	1	2	3	4	5	6	7
0	A	0	0	0	$\mathbb{Z}$	0	$\mathbb{Z}$	0	$\mathbb{Z}$	0	$\mathbb{Z}$	0
1	AIII	0	0	1	0	$\mathbb{Z}$	0	$\mathbb{Z}$	0	$\mathbb{Z}$	0	$\mathbb{Z}$
0	AI	1	0	0	$\mathbb{Z}$	0	0	0	$2\mathbb{Z}$	0	$\mathbb{Z}_2$	$\mathbb{Z}_2$
1	BDI	1	1	1	$\mathbb{Z}_2$	$\mathbb{Z}$	0	0	0	$2\mathbb{Z}$	0	$\mathbb{Z}_2$
2	D	0	1	0	$\mathbb{Z}_2$	$\mathbb{Z}_2$	$\mathbb{Z}$	0	0	0	$2\mathbb{Z}$	0
3	DIII	-1	1	1	0	$\mathbb{Z}_2$	$\mathbb{Z}_2$	$\mathbb{Z}$	0	0	0	$2\mathbb{Z}$
4	AII	-1	0	0	$2\mathbb{Z}$	0	$\mathbb{Z}_2$	$\mathbb{Z}_2$	$\mathbb{Z}$	0	0	0
5	CII	-1	-1	1	0	$2\mathbb{Z}$	0	$\mathbb{Z}_2$	$\mathbb{Z}_2$	$\mathbb{Z}$	0	0
6	C	0	-1	0	0	0	$2\mathbb{Z}$	0	$\mathbb{Z}_2$	$\mathbb{Z}_2$	$\mathbb{Z}$	0
7	CI	1	-1	1	0	0	0	$2\mathbb{Z}$	0	$\mathbb{Z}_2$	$\mathbb{Z}_2$	$\mathbb{Z}$

TABLE I: Periodic table for the classification of topological defects in insulators and superconductors. The rows correspond to the different Altland Zirnbauer (AZ) symmetry classes, while the columns distinguish different dimensionalities, which depend only on $\delta = d - D$.

K-Theory Bott periodicity

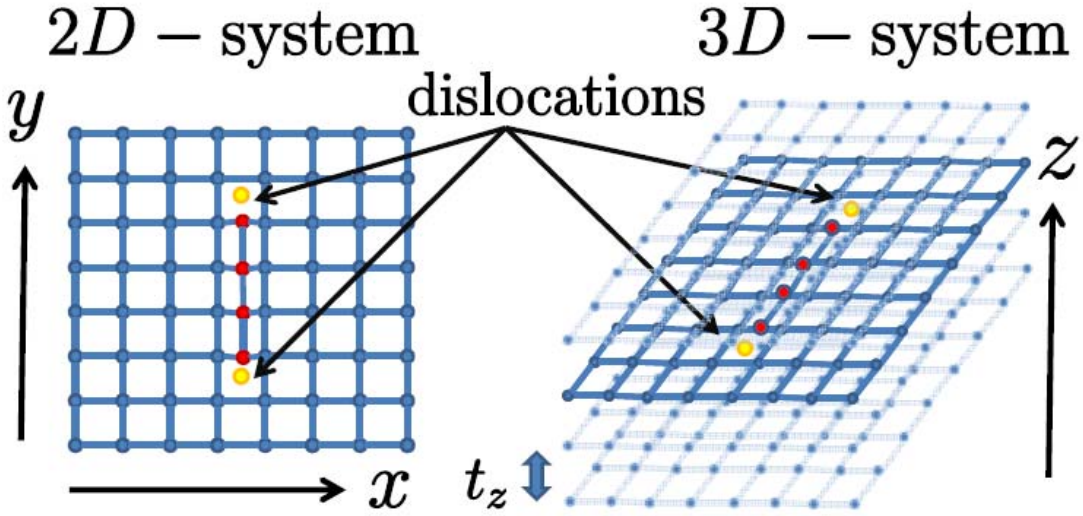
$2D-$ system
$3D-$ system
dislocations
y
x
z
t_z

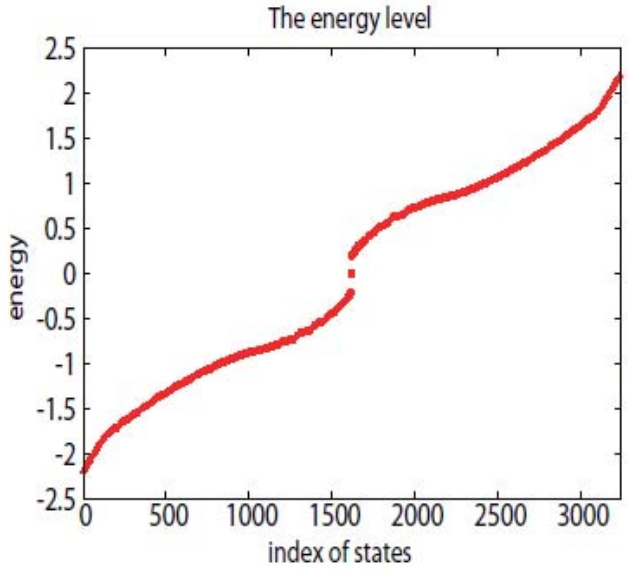
The energy level
energy
index of states
2.5
2
1.5
1
0.5
0
-0.5
-1
-1.5
-2
-2.5
0
500
1000
1500
2000
2500
3000

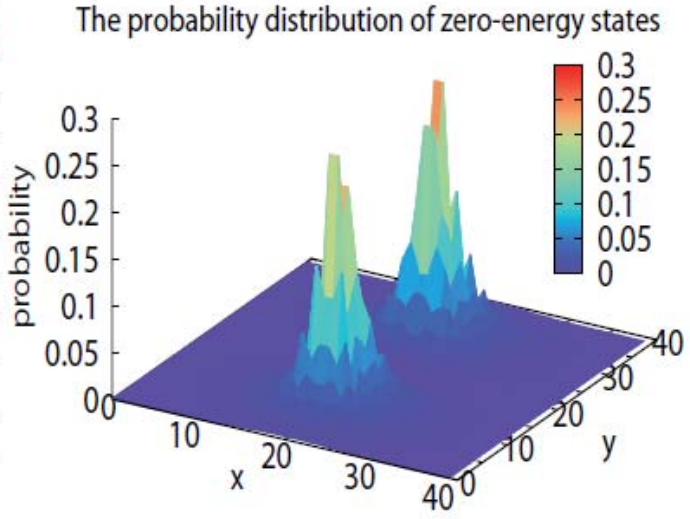
The probability distribution of zero-energy states
probability
x
y
0.3
0.25
0.2
0.15
0.1
0.05
0
10
20
30
40

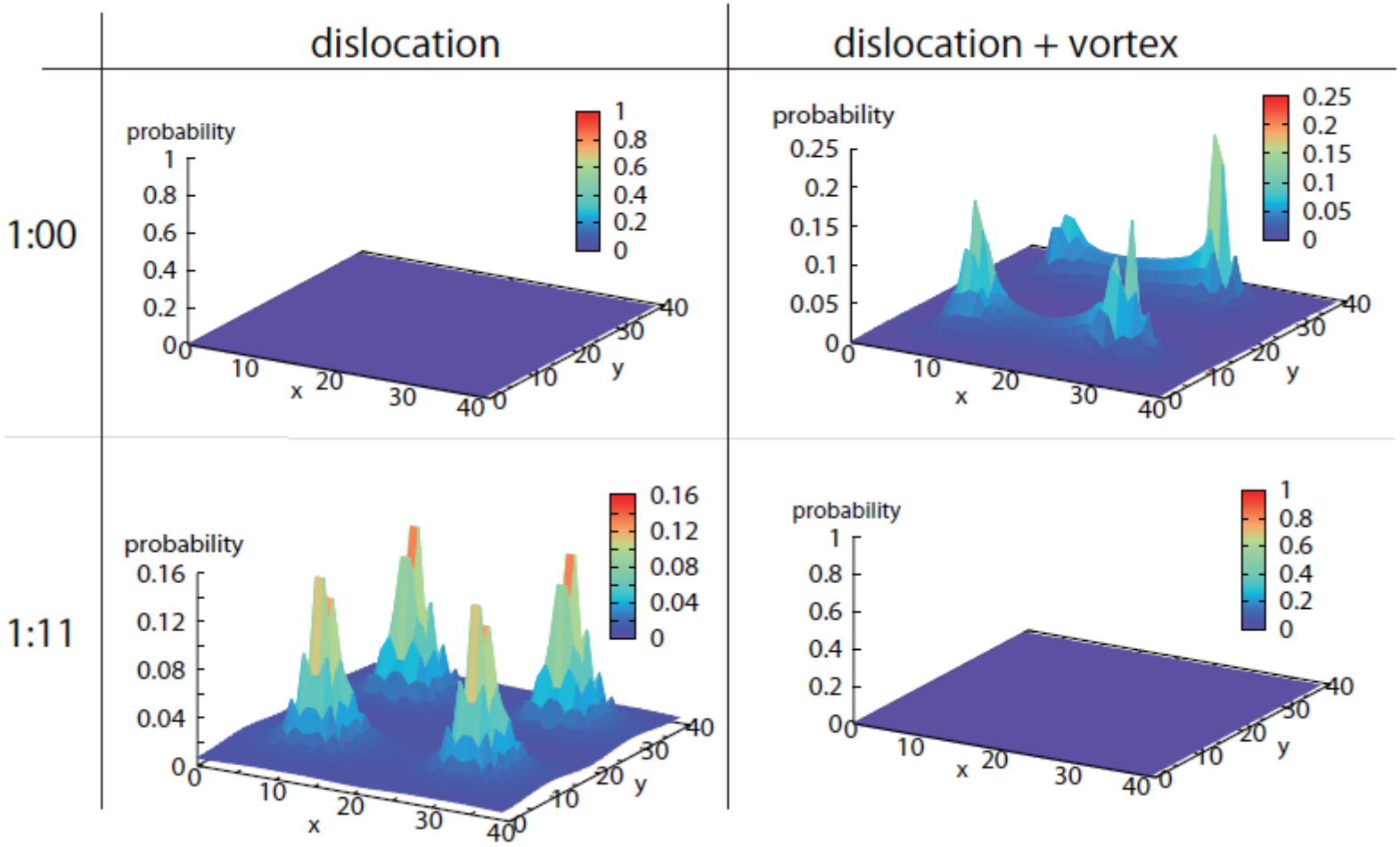
dislocation
dislocation + vortex
1:00
1:11
probability
x
y

Edge modes of various systems

Majorana fermion

$$\psi_k^+ = \psi_{-k}$$

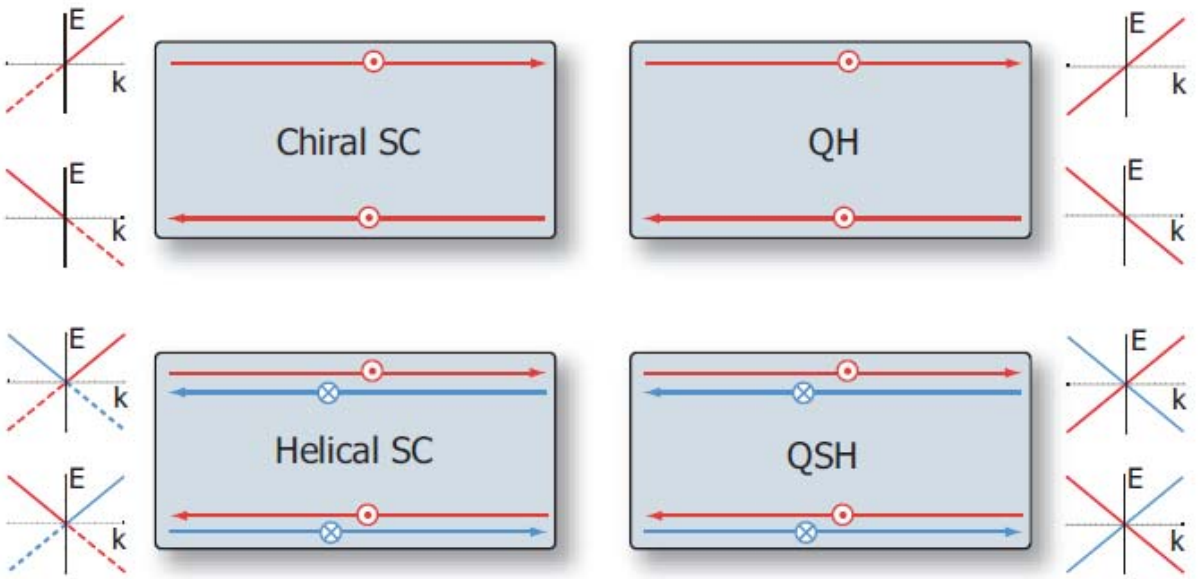

Topological Superconductivity and Superfluidity

Xiao-Liang Qi, Taylor L. Hughes, Srinivas Raghu and Shou-Cheng Zhang

robust ← → susceptible

Chiral Majorana	Chiral Fermion	Helical Majorana	Spinless Fermion	Helical Fermion	Spinful Fermion	2-Spinful Fermion
p+ip SC 5/2 FQH STI+SC	1/3 FQH	Helical SC	Ferro wire	QSHS	Q-wire	Ladder

Split electrons into fractions

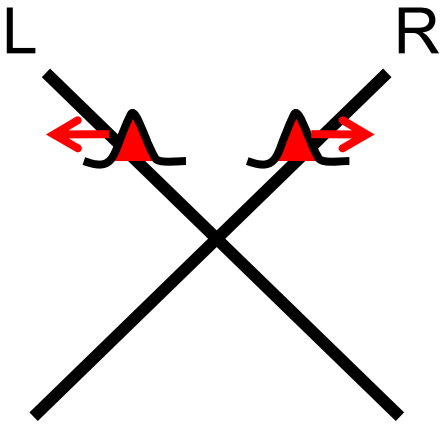

R or L

$\uparrow$ or $\downarrow$

positive or negative energy

➔8 pieces of fractions !!

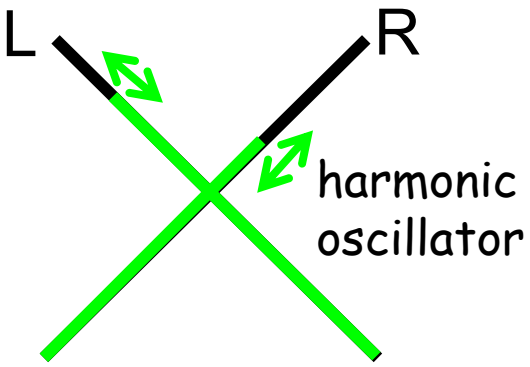

$\rho_{R\uparrow} = \partial_x \phi_{R\uparrow}$ etc.

Various combination of ϕ's

can be fixed by el - el interaction

➔Recombination of pieces

robust ⟵ ⟶ susceptible

Chiral Majorana	Chiral Fermion	Helical Majorana	Spinless Fermion	Helical Fermion	Spinful Fermion	2-Spinful Fermion
p+ip SC 5/2 FQH STI+SC	1/3 FQH	Helical SC	Ferro wire	QSHS	Q-wire	Ladder

Interactions are restricted when el. are fractionalized

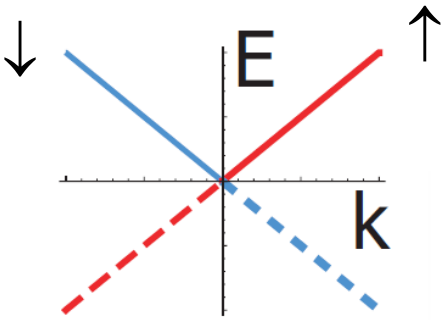

Two chiral Majoranas or one helical Majorana

$$g\psi_{\uparrow}\psi_{\uparrow}\psi_{\downarrow}\psi_{\downarrow} = g$$

No relevant interaction

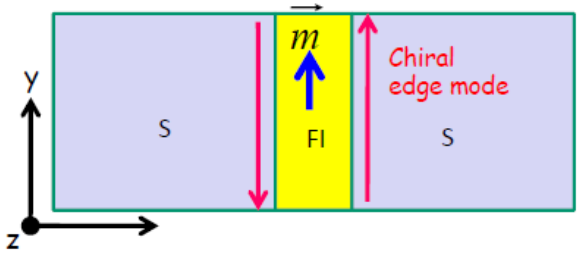

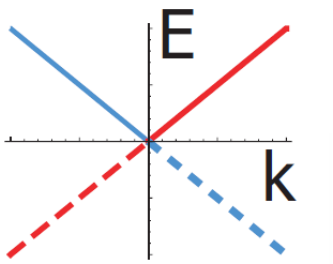

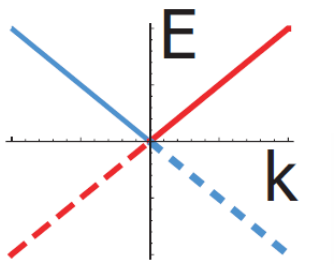

Two helical Majoranas

$$g\psi_{R\uparrow}\psi_{L\uparrow}\psi_{R\downarrow}\psi_{L\downarrow} \approx g\rho_R\rho_L$$

Forward scattering
Massless Thirring model

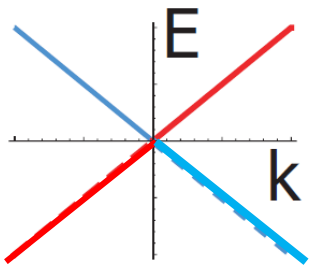

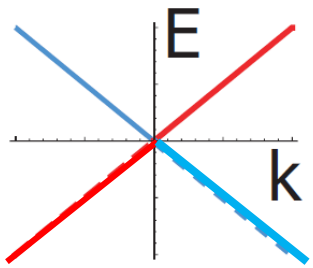

Two helical Fermions

Forward + backward scattering
→ Opening of the gap

Interface of oxides as 2D Rashba system

LaAlO3/SrTiO3 interface

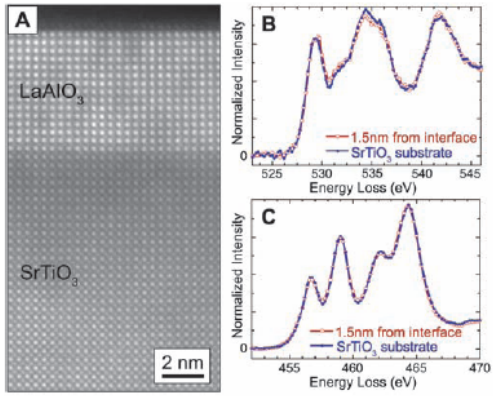

Fig. 1. STEM and EELS analysis of a $LaAlO_3/SrTiO_3$ heterostructure. **(A)** High-angle annular dark field image of a 15-uc-thick $LaAlO_3$ film grown on $SrTiO_3$ showing a coherent interface. **(B)** O-K EELS spectra of the $SrTiO_3$ close to (1.5 nm) and far away from the interface. Even at 1.5 nm from the interface, the O-K fine structure is only very slightly damped compared with the bulk. The damping could be caused by the presence of a low concentration of oxygen vacancies. **(C)** Small changes of the Ti-$L_{2,3}$ fine structure close to the interface are consistent with a small concentration of Ti^{3+}, which falls below the detection limit by 6 nm from the interface and beyond.

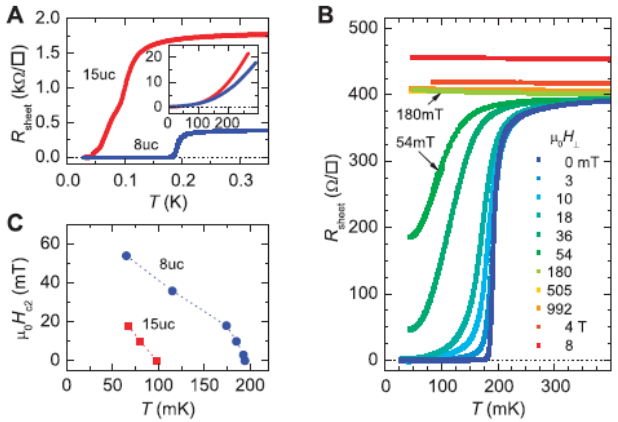

Fig. 2. Transport measurements on $LaAlO_3/SrTiO_3$ heterostructures. **(A)** Dependence of the sheet resistance on T of the 8-uc and 15-uc samples (measured with a 100-nA bias current). (Inset) Sheet resistance versus temperature measured between 4 K and 300 K. **(B)** Sheet resistance of the 8-uc sample plotted as a function of T for magnetic fields applied perpendicular to the interface. **(C)** Temperature dependence of the upper critical field H_{c2} of the two samples.

M. Reyren et al 2007

Rashba control of LaAlO3/SrTiO3 interface

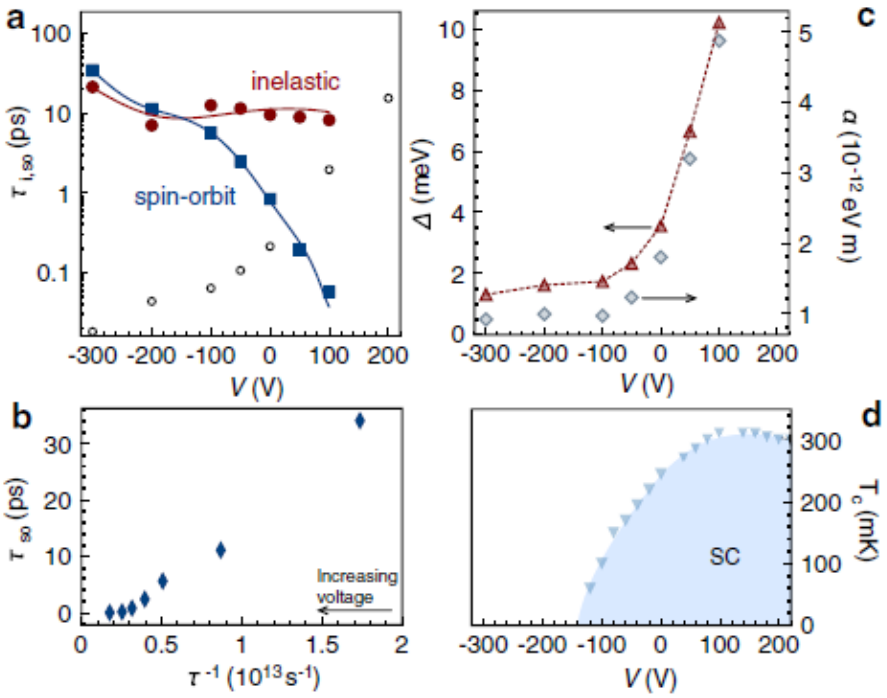

A.D.Caviglia et al. 2007

Novel FFLO state in Rashba interface

K. Michaeli, A.C. Potter, and P.A. Lee, arXiv:1107.4352v2

Bilayer Rashba superconductor

S. Nakosai-Y.Tanaka-N.N. PRL (2012)

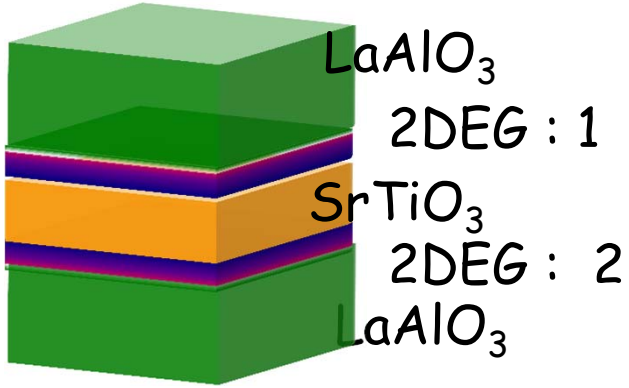

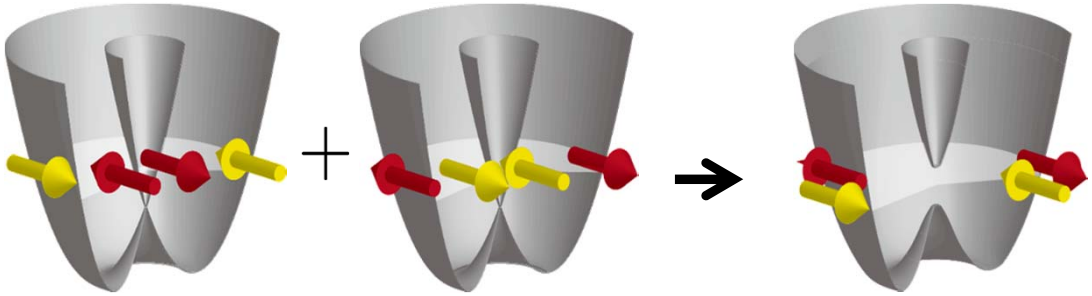

Hybridization

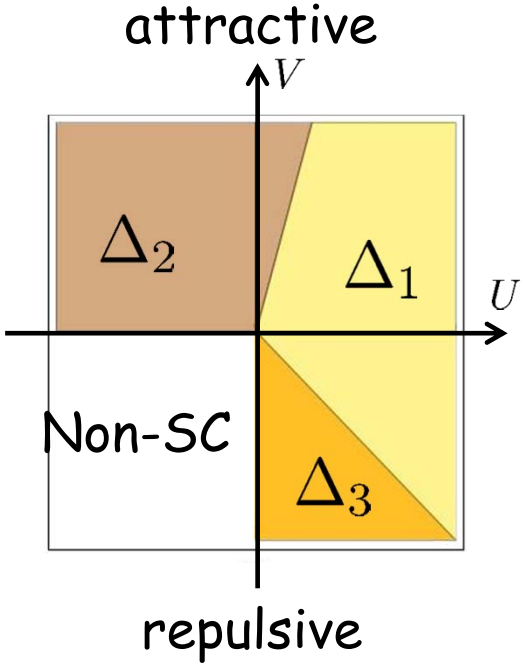

Inter-layer repulsive
Intra-layer attractive
interaction leads to
topological SC

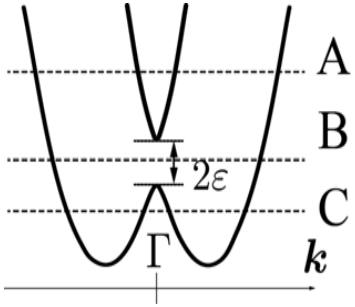

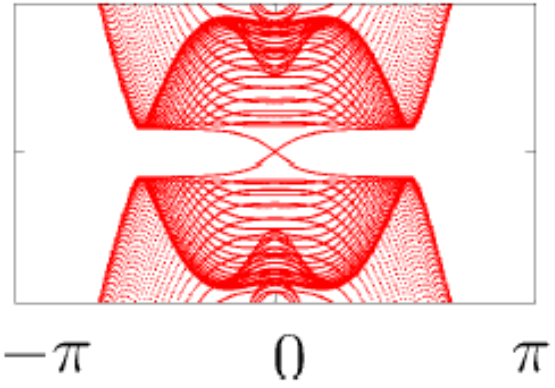

helical Majorana
edge channel

Physical properties of topological superconductors

Physical effects by helical Majorana edge channels

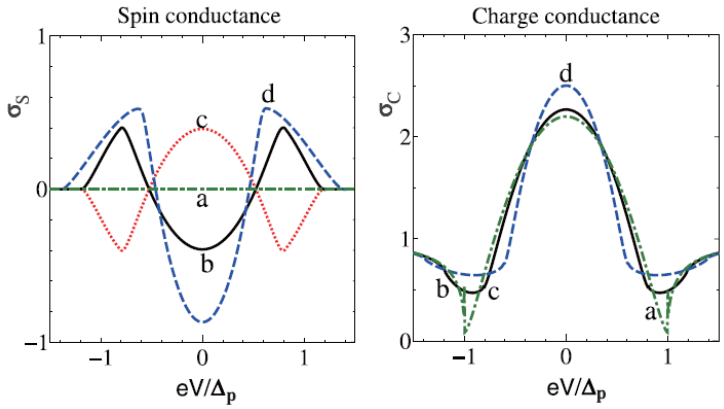

Andreev reflection

Y. Tanaka et al. PRB2009

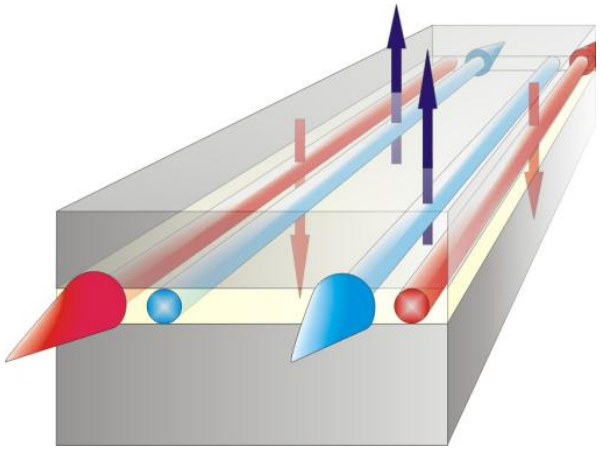

Ising Kondo effect

R. Shindou et al. PRB

TL effect in Josephson junction

Y.Asano et al. PRL2010

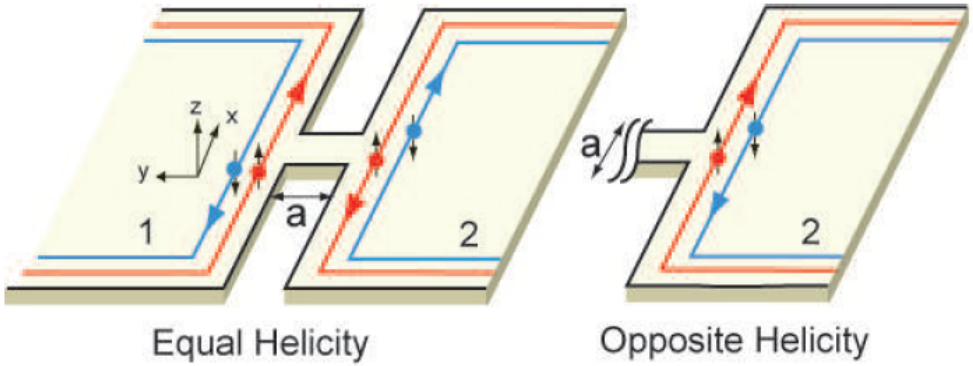

Interference with Majorana fermions in quasi-particle tunneling

$$\Psi_i = e^{i\pi/4 + i\varphi_i/2}\gamma_i \qquad \gamma_i^+ = \gamma_i \qquad \varphi = \varphi_2 - \varphi_1$$

$$t\Psi_1^+\Psi_2 + t^*\Psi_2^+\Psi_1 \quad (t = |t|e^{i\alpha})$$

$$\Rightarrow |t|[ie^{i\varphi/2+i\alpha}\gamma_1\gamma_2 - ie^{-i\varphi/2-i\alpha}\gamma_2\gamma_1 \propto i\cos(\varphi/2-\alpha)\gamma_1\gamma_2]$$

$$J = \frac{C}{2e}\frac{d^2\varphi}{dt^2} + \frac{1}{2eR(\varphi)}\frac{d\varphi}{dt} + J_0\sin(\varphi)$$

$$R^{-1}(\varphi) \propto \sin^2(\varphi/2-\alpha)$$

Interactions are restricted when el. are fractionalized

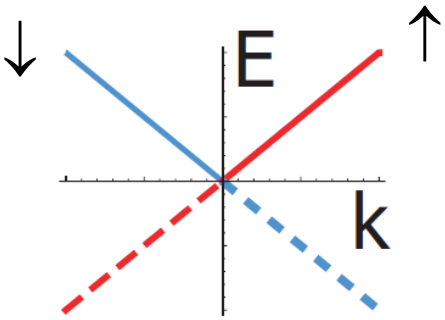

Two chiral Majoranas or one helical Majorana

$$g\psi_{\uparrow}\psi_{\uparrow}\psi_{\downarrow}\psi_{\downarrow} = g$$

No relevant interaction

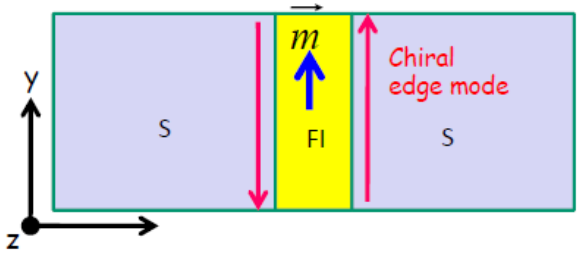

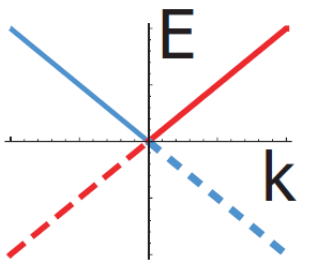

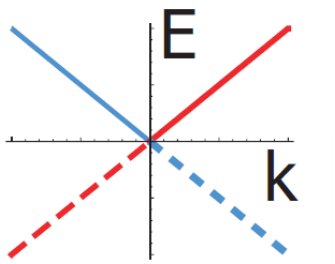

Two helical Majoranas

$$g\psi_{R\uparrow}\psi_{L\uparrow}\psi_{R\downarrow}\psi_{L\downarrow} \approx g\rho_R\rho_L$$

Forward scattering
Massless Thirring model

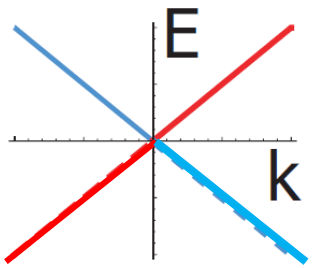

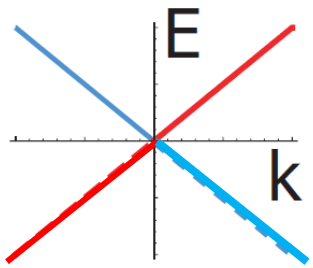

Two helical Fermions

Forward + backward scattering
→ Opening of the gap

Interacting two helical superconductors

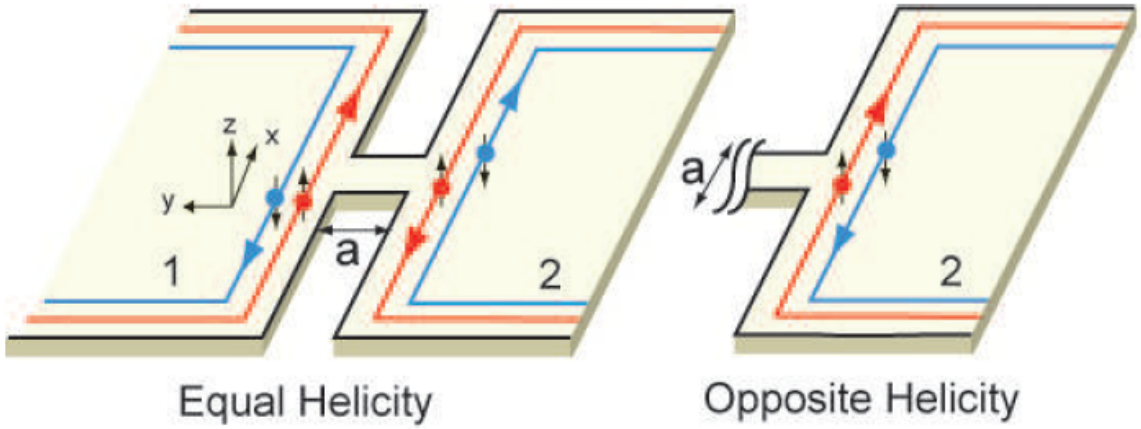

Asano
-Tanaka-NN
PRL 2010

$$H_0 = -iv \sum_{j=1,2} \int dx \left[\gamma_{Rj}(x) \partial_x \gamma_{Rj}(x) - \gamma_{Lj}(x) \partial_x \gamma_{Lj}(x) \right]$$

Helical Majorana
Edge channels

$$H_{\text{int.}} = g \int dx \gamma_{R1}(x) \gamma_{R2}(x) \gamma_{L2}(x) \gamma_{L1}(x)$$

Interaction

$$H_T = -ta \sum_{\sigma,\sigma'} \left[\Psi^\dagger_{1,\sigma}(0) \left\{ \sigma_0 + i\boldsymbol{\lambda} \cdot \boldsymbol{\sigma} \right\}_{\sigma,\sigma'} \Psi_{2,\sigma'}(0) + \Psi^\dagger_{2,\sigma}(0) \left\{ \sigma_0 - i\boldsymbol{\lambda} \cdot \boldsymbol{\sigma} \right\}_{\sigma,\sigma'} \Psi_{1,\sigma'}(0) \right],$$

Tunneling

Conductance due to quasi-particle tunneling

$$\frac{\sigma}{G_0} = \pi\frac{\lambda_+^2}{K}\cos^2\left(\frac{\varphi}{2}\right) + \sin^2\left(\frac{\varphi}{2}\right)D_\theta\left(\frac{T}{T_0}\right)^{2/K-2}$$
$$+ \pi\lambda_-^2 K\sin^2\left(\frac{\varphi}{2}\right) + \lambda_3^2\cos^2\left(\frac{\varphi}{2}\right)D_\phi\left(\frac{T}{T_0}\right)^{2K-2}$$

Each term is sensitive to The phase difference between the 2 SC's
→ Interference

		$\lambda = 0$	$\lambda \neq 0$
Equal helicity			
$\varphi = 0$	$K = 1$	0	const.
	$K < 1$	0	T^{2K-2}
	$K > 1$	0	const.
$\varphi \neq 0$	$K = 1$	const.	const.
	$K < 1$	$T^{2/K-2} \to 0$	T^{2K-2}
	$K > 1$	$T^{2/K-2}$	$T^{2/K-2}$
Opposite helicity			
$\varphi = 0$	$K = 1$	0	const.
	$K < 1$	0	const.
	$K > 1$	0	$T^{2/K-2}$
$\varphi \neq 0$	$K = 1$	const.	const.
	$K < 1$	const.	T^{2K-2}
	$K > 1$	const.	$T^{2/K-2}$

With SOI, the q.p. tunneling is always relevant as the temperature is lowered independent of the sign of the interaction

Quite different behavior between equal and opposite helicities

Kondo impurity at helical Majorana edge channels

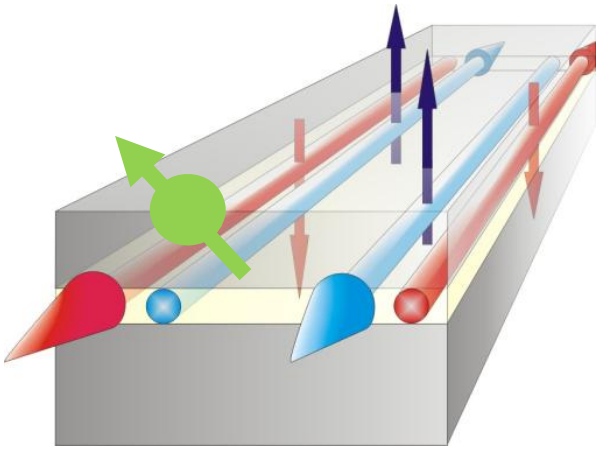

Shindou-Furusaki-NN
PRB Rapid Comm. 2010

$$2\hat{s}_z(\boldsymbol{r}) = \psi^\dagger_\uparrow \psi_\uparrow - \psi^\dagger_\downarrow \psi_\downarrow = 0,$$

$$\hat{s}_+(\boldsymbol{r}) = \begin{cases} -e^{2i\theta}\hat{s}_-(\boldsymbol{r}) & (\text{chiral}), \\ -e^{2i(\theta\pm\phi)}\hat{s}_-(\boldsymbol{r}) & (\text{helical}). \end{cases}$$

$$\Longrightarrow \quad \hat{\boldsymbol{s}}(\boldsymbol{r}) \propto \begin{cases} \boldsymbol{d_k} & (\text{chiral}), \\ \boldsymbol{d_k}|_{\boldsymbol{k}\cdot\boldsymbol{n}_\parallel=0} & (\text{helical}), \end{cases}$$

We call it z-axis or ||-direction
Ising-like coupling !

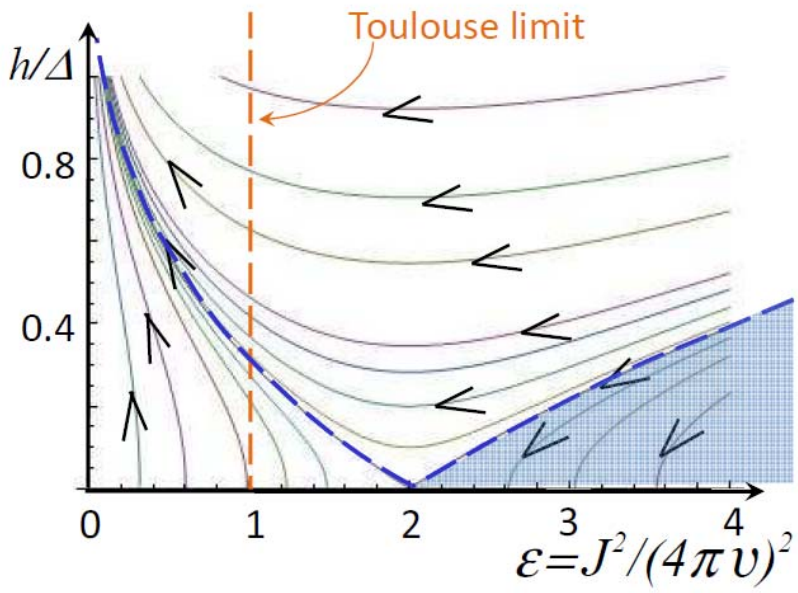

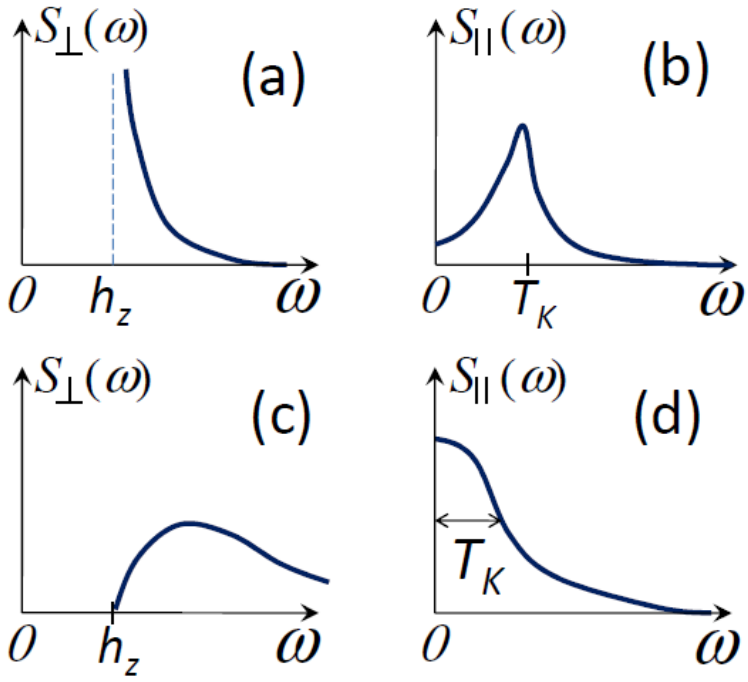

Strongly anisotropic magnetic properties

Transverse magnetic field induces the tunneling and the system becomes equivalent to anisotropic Kondo model

dissipation	$0<\epsilon<1$	$1<\epsilon<2$	$2<\epsilon$
$\chi_{xx\|h=h'=0}(T)$	$T^{-(1-\epsilon)}$	const.	const.
$\chi_{zz\|h=h'=0}(T)$	T^{-1}	T^{-1}	T^{-1}
$\chi_{xx\|T=h=0}(h')$	$h'^{-(1-\epsilon)}$	const.	const.
$\chi_{zz\|h'=T=0}(h)$	T_K^{-1}	T_K^{-1}	$T_K^{-1\,a}$
$\chi_{xx\|h'=T=0}(h)$	$h^{\frac{2(\epsilon-1)}{2-\epsilon}}$	const.	const.
$\chi_{zz\|h=0}(h',T)$	T^{-1}	T^{-1}	T^{-1}
$\omega_0(T)$	$T^{\epsilon-1}$	$T^{\epsilon-1}$	$T^{\epsilon-1}$
QPT under h	N/A	N/A	$\surd$

[a] only at $h>h_c$

Thermal transport properties of topological superconductors

Streda formula for Hall conductivity

$$\sigma_H = ec\frac{\partial M^z}{\partial \mu} \qquad \boldsymbol{j} = \sigma_H \boldsymbol{E} \times \hat{\mathbf{z}}$$

$$\boldsymbol{j} = c\nabla \times \boldsymbol{M} = -c\,\partial \boldsymbol{M}/\partial\mu \times \nabla\mu$$

How about the thermal response ?

Gravitational response
J.M. Luttinger

$$\boldsymbol{E}_g = -T^{-1}\nabla T \qquad \boldsymbol{B}_g = (2/v)\boldsymbol{\Omega}$$

$$dF = -SdT - \boldsymbol{M}_E \cdot d\boldsymbol{B}_g$$

$$\kappa_H = \frac{v^2}{2}\left(\frac{\partial L^z}{\partial T}\right)_{\Omega^z} = \frac{v^2}{2}\left(\frac{\partial S}{\partial \Omega^z}\right)_T$$

	TI	TSC
2d	$\sigma_H = ec\dfrac{\partial M^z}{\partial \mu} = ec\dfrac{\partial N}{\partial B^z}$	$\kappa_H = \dfrac{v^2}{2}\dfrac{\partial L^z}{\partial T} = \dfrac{v^2}{2}\dfrac{\partial S}{\partial \Omega^z}$
3d	$\chi_\theta^{ab} = \dfrac{\partial M^a}{\partial E^b} = \dfrac{\partial P^a}{\partial B^b}$	$\chi_{\theta,g}^{ab} = \dfrac{\partial L^a}{\partial E_g^b} = \dfrac{\partial P_E^a}{\partial \Omega^b}$

$$\boldsymbol{B}_g = (2/v)\boldsymbol{\Omega}$$

$$\boldsymbol{E}_g = -T^{-\bar{1}}\nabla T \qquad S_\theta^{\mathrm{EM}} = \int dt d^3\boldsymbol{x}\, \frac{e^2}{4\pi^2\hbar c}\theta \boldsymbol{E}\cdot\boldsymbol{B}$$

$$U_\theta = -\int d^3\boldsymbol{x}\, \frac{2}{v^2}\kappa_H \nabla T\cdot\boldsymbol{\Omega} = \int d^3\boldsymbol{x}\, \frac{k_B^2 T^2}{24\hbar v}\theta \boldsymbol{E}_g\cdot\boldsymbol{B}_g$$

$$\boldsymbol{B}_g = (2/v)\boldsymbol{\Omega}$$

2d

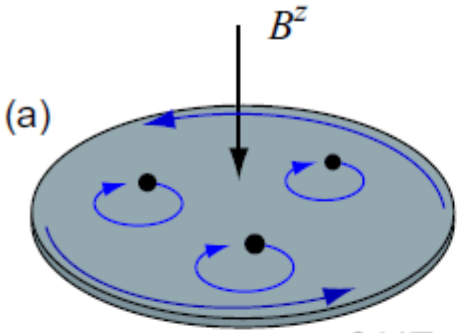

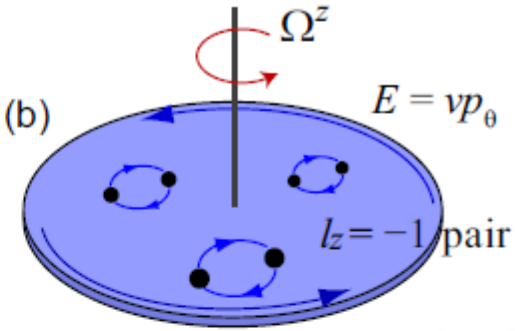

$$\kappa_H = \frac{\partial \langle j_E \rangle}{\partial T} = \frac{\pi^2 k_B^2 T}{6h}$$

3d

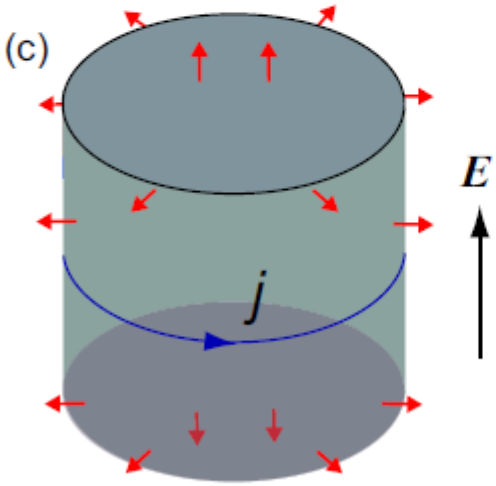

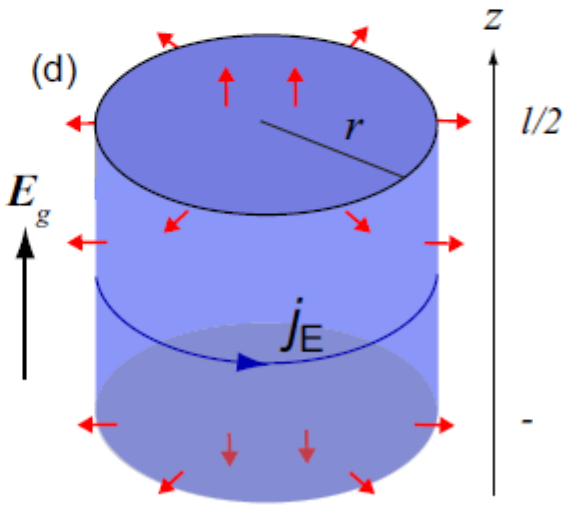

$$\kappa_H = \mathrm{sgn}(m)\frac{\pi^2}{6}\frac{k_B^2}{2h}T$$

$$\cdot \; L^z|_{\Omega^z} = \frac{rP_\varphi}{\pi r^2 \ell} = \frac{2}{v^2}\kappa_H \partial_z T$$

$$\boldsymbol{E}_g = -T^{-\bar{1}}\nabla T$$

Topological Periodic Table

Ten-fold way
general classification of gapped topological states

Schnyder et al. 2008

		TRS	PHS	SLS	$d=1$	$d=2$	$d=3$
Standard	A (unitary)	0	0	0	-	$\mathbb{Z}$	-
(Wigner-Dyson)	AI (orthogonal)	+1	0	0	-	-	-
	AII (symplectic)	−1	0	0	-	$\mathbb{Z}_2$	$\mathbb{Z}_2$
Chiral	AIII (chiral unitary)	0	0	1	$\mathbb{Z}$	-	$\mathbb{Z}$
(sublattice)	BDI (chiral orthogonal)	+1	+1	1	$\mathbb{Z}$	-	-
	CII (chiral symplectic)	−1	−1	1	$\mathbb{Z}$	-	$\mathbb{Z}_2$
BdG	D	0	+1	0	$\mathbb{Z}_2$	$\mathbb{Z}$	-
	C	0	−1	0	-	$\mathbb{Z}$	-
	DIII	−1	+1	1	$\mathbb{Z}_2$	$\mathbb{Z}_2$	$\mathbb{Z}$
	CI	+1	−1	1	-	-	$\mathbb{Z}$

Discrete symmetries of the Hamiltonian

3 symmetries which are robust against the disorder

Anti-unitary symmetry

Time-reversal symmetry Θ $\mathcal{H}(\mathbf{k},\mathbf{r}) = \Theta\mathcal{H}(-\mathbf{k},\mathbf{r})\Theta^{-1}$

Particle-hole symmetry Ξ $\mathcal{H}(\mathbf{k},\mathbf{r}) = -\Xi\mathcal{H}(-\mathbf{k},\mathbf{r})\Xi^{-1}$

Unitary symmetry

Chiral symmetry Π $\mathcal{H}(\mathbf{k},\mathbf{r}) = -\Pi\mathcal{H}(\mathbf{k},\mathbf{r})\Pi^{-1}$

$\Theta^2 = \pm 1 \qquad \Xi^2 = \pm 1$

$\Pi = e^{i\chi}\Theta\Xi \quad \Rightarrow \quad \Pi^2 = 1$

Ten-fold way
general classification of gapped topological states

Schnyder et al. 2008

		TRS	PHS	SLS	$d=1$	$d=2$	$d=3$
Standard	A (unitary)	0	0	0	-	$\mathbb{Z}$	-
(Wigner-Dyson)	AI (orthogonal)	+1	0	0	-	-	-
	AII (symplectic)	−1	0	0	-	$\mathbb{Z}_2$	$\mathbb{Z}_2$
Chiral	AIII (chiral unitary)	0	0	1	$\mathbb{Z}$	-	$\mathbb{Z}$
(sublattice)	BDI (chiral orthogonal)	+1	+1	1	$\mathbb{Z}$	-	-
	CII (chiral symplectic)	−1	−1	1	$\mathbb{Z}$	-	$\mathbb{Z}_2$
BdG	D	0	+1	0	$\mathbb{Z}_2$	$\mathbb{Z}$	-
	C	0	−1	0	-	$\mathbb{Z}$	-
	DIII	−1	+1	1	$\mathbb{Z}_2$	$\mathbb{Z}_2$	$\mathbb{Z}$
	CI	+1	−1	1	-	-	$\mathbb{Z}$

Generalization to include spatially dependent cases

Teo-Kane 2010

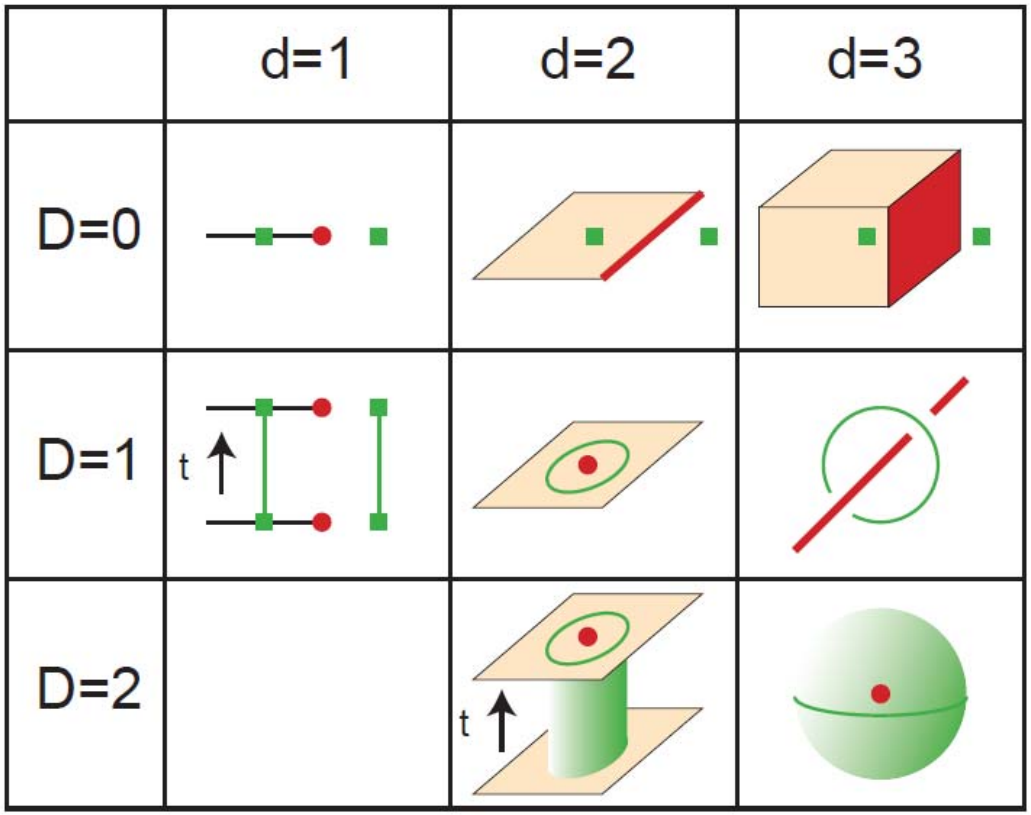

FIG. 1: Topological defects characterized by a D parameter family of d dimensional Bloch-BdG Hamiltonians. Line defects correspond to $d - D = 2$, while point defects correspond to $d - D = 1$. Temporal cycles for point defects correspond to $d - D = 0$.

Symmetry					$\delta = d - D$							
s	AZ	Θ^2	Ξ^2	Π^2	0	1	2	3	4	5	6	7
0	A	0	0	0	$\mathbb{Z}$	0	$\mathbb{Z}$	0	$\mathbb{Z}$	0	$\mathbb{Z}$	0
1	AIII	0	0	1	0	$\mathbb{Z}$	0	$\mathbb{Z}$	0	$\mathbb{Z}$	0	$\mathbb{Z}$
0	AI	1	0	0	$\mathbb{Z}$	0	0	0	$2\mathbb{Z}$	0	$\mathbb{Z}_2$	$\mathbb{Z}_2$
1	BDI	1	1	1	$\mathbb{Z}_2$	$\mathbb{Z}$	0	0	0	$2\mathbb{Z}$	0	$\mathbb{Z}_2$
2	D	0	1	0	$\mathbb{Z}_2$	$\mathbb{Z}_2$	$\mathbb{Z}$	0	0	0	$2\mathbb{Z}$	0
3	DIII	-1	1	1	0	$\mathbb{Z}_2$	$\mathbb{Z}_2$	$\mathbb{Z}$	0	0	0	$2\mathbb{Z}$
4	AII	-1	0	0	$2\mathbb{Z}$	0	$\mathbb{Z}_2$	$\mathbb{Z}_2$	$\mathbb{Z}$	0	0	0
5	CII	-1	-1	1	0	$2\mathbb{Z}$	0	$\mathbb{Z}_2$	$\mathbb{Z}_2$	$\mathbb{Z}$	0	0
6	C	0	-1	0	0	0	$2\mathbb{Z}$	0	$\mathbb{Z}_2$	$\mathbb{Z}_2$	$\mathbb{Z}$	0
7	CI	1	-1	1	0	0	0	$2\mathbb{Z}$	0	$\mathbb{Z}_2$	$\mathbb{Z}_2$	$\mathbb{Z}$

TABLE I: Periodic table for the classification of topological defects in insulators and superconductors. The rows correspond to the different Altland Zirnbauer (AZ) symmetry classes, while the columns distinguish different dimensionalities, which depend only on $\delta = d - D$.

K-Theory Bott periodicity

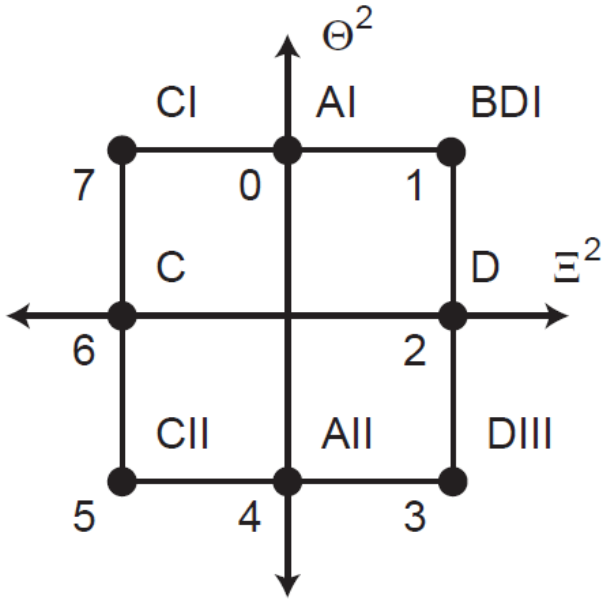

Symmetry clock

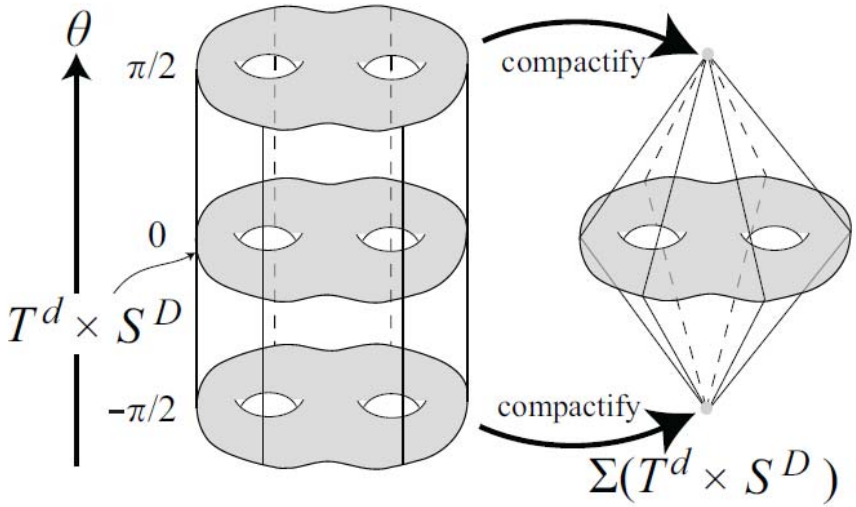

FIG. 11: Suspension $\Sigma(T^d \times S^D)$. The top and bottom of the cylinder $\Sigma(T^d \times S^D) \times [-\pi/2, \pi/2]$ are identified to two points.

Suspension to deform H

$$\mathcal{H}_{nc}(\mathbf{k}, \mathbf{r}, \theta) = \cos\theta \mathcal{H}_c(\mathbf{k}, \mathbf{r}) + \sin\theta \Pi$$

$$\mathcal{H}_c(\mathbf{k}, \mathbf{r}, \theta) = \cos\theta \mathcal{H}_{nc}(\mathbf{k}, \mathbf{r}) \otimes \tau_z + \sin\theta \mathbb{1} \otimes \tau_a$$

$$\theta = r_{D+1} : \; D \to D+1$$

or $$\theta = k_{d+1} : \; d \to d+1$$

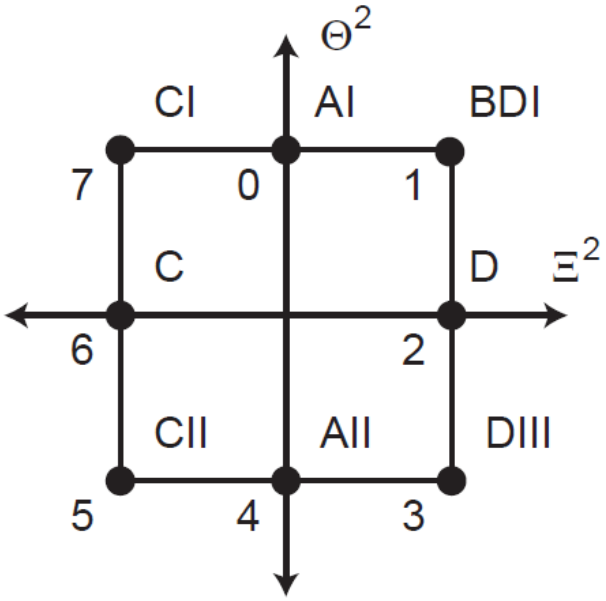

$$[\Theta, \Xi] = 0$$

$$(\Theta\Xi)^2 = \Theta^2\Xi^2 = (-1)^{(s-1)/2}$$

$$\Pi = i^{(s-1)/2}\Theta\Xi$$

$$\mathcal{H}_{nc}(\mathbf{k}, \mathbf{r}, \theta) = \cos\theta\mathcal{H}_c(\mathbf{k}, \mathbf{r}) + \sin\theta\Pi$$

$$s = 1 \bmod 4 \qquad \Pi = \pm\Theta\Xi$$

$$\theta = k_{d+1} \Rightarrow \Theta H_{nc}\Theta^{-1} = \cos k_{d+1} H_c + \sin(-k_{d+1})\Theta(\pm\Theta\Xi)\Theta^{-1} \neq H_{nc}$$

$$\Xi H_{nc}\Xi^{-1} = -\cos k_{d+1} H_c + \sin(-k_{d+1})\Xi(\pm\Theta\Xi)\Xi^{-1} = -H_{nc}$$

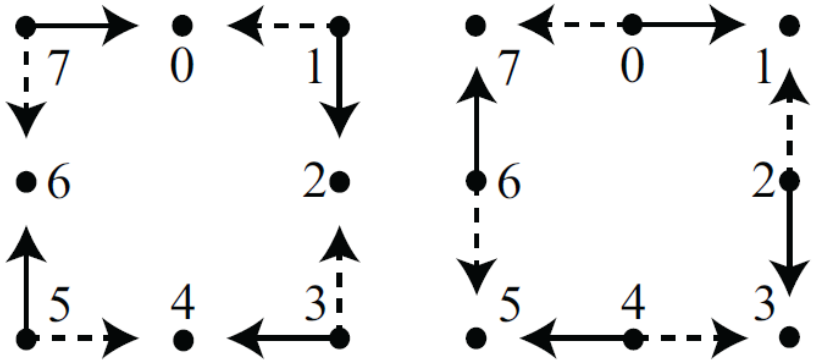

$\theta = k_{d+1}$ →

$\theta = r_{D+1}$ ←

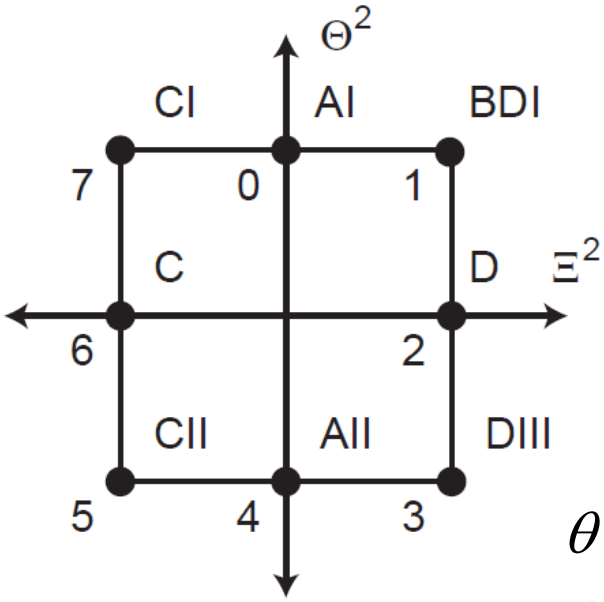

$$\mathcal{H}_{nc}(\mathbf{k},\mathbf{r},\theta) = \cos\theta\mathcal{H}_c(\mathbf{k},\mathbf{r}) + \sin\theta\Pi$$

$$\mathcal{H}_c(\mathbf{k},\mathbf{r},\theta) = \cos\theta\mathcal{H}_{nc}(\mathbf{k},\mathbf{r}) \otimes \tau_z + \sin\theta\mathbb{1} \otimes \tau_a$$

$$\theta = k_{d+1} \quad K_{\mathbb{F}}(s;D,d) \longrightarrow K_{\mathbb{F}}(s+1;D,d+1)$$

$$\theta = r_{D+1} \quad K_{\mathbb{F}}(s;D,d) \longrightarrow K_{\mathbb{F}}(s-1;D+1,d)$$

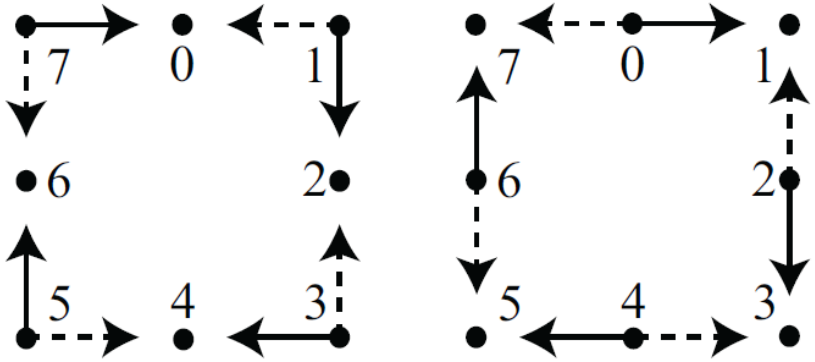

$$K_{\mathbb{F}}(s;D,d+1) = K_{\mathbb{F}}(s-1;D,d)$$

$$K_{\mathbb{F}}(s;D+1,d) = K_{\mathbb{F}}(s+1;D,d)$$

$$K_F(s+1;D-1,d) = K_F(s+1;D,d+1)$$

$$\delta = d - D \qquad K_F(s;\delta) = K_F(s+1;\delta+1)$$

Symmetry					$\delta = d - D$							
s	AZ	Θ^2	Ξ^2	Π^2	0	1	2	3	4	5	6	7
0	A	0	0	0	$\mathbb{Z}$	0	$\mathbb{Z}$	0	$\mathbb{Z}$	0	$\mathbb{Z}$	0
1	AIII	0	0	1	0	$\mathbb{Z}$	0	$\mathbb{Z}$	0	$\mathbb{Z}$	0	$\mathbb{Z}$
0	AI	1	0	0	$\mathbb{Z}$	0	0	0	$2\mathbb{Z}$	0	$\mathbb{Z}_2$	$\mathbb{Z}_2$
1	BDI	1	1	1	$\mathbb{Z}_2$	$\mathbb{Z}$	0	0	0	$2\mathbb{Z}$	0	$\mathbb{Z}_2$
2	D	0	1	0	$\mathbb{Z}_2$	$\mathbb{Z}_2$	$\mathbb{Z}$	0	0	0	$2\mathbb{Z}$	0
3	DIII	-1	1	1	0	$\mathbb{Z}_2$	$\mathbb{Z}_2$	$\mathbb{Z}$	0	0	0	$2\mathbb{Z}$
4	AII	-1	0	0	$2\mathbb{Z}$	0	$\mathbb{Z}_2$	$\mathbb{Z}_2$	$\mathbb{Z}$	0	0	0
5	CII	-1	-1	1	0	$2\mathbb{Z}$	0	$\mathbb{Z}_2$	$\mathbb{Z}_2$	$\mathbb{Z}$	0	0
6	C	0	-1	0	0	0	$2\mathbb{Z}$	0	$\mathbb{Z}_2$	$\mathbb{Z}_2$	$\mathbb{Z}$	0
7	CI	1	-1	1	0	0	0	$2\mathbb{Z}$	0	$\mathbb{Z}_2$	$\mathbb{Z}_2$	$\mathbb{Z}$

TABLE I: Periodic table for the classification of topological defects in insulators and superconductors. The rows correspond to the different Altland Zirnbauer (AZ) symmetry classes, while the columns distinguish different dimensionalities, which depend only on $\delta = d - D$.

K-Theory Bott periodicity

Strong and Weak Z2 numbers in topological insulators

Fu-Kane

Symmetry					$\delta = d - D$							
s	AZ	Θ^2	Ξ^2	Π^2	0	1	2	3	4	5	6	7
0	A	0	0	0	$\mathbb{Z}$	0	$\mathbb{Z}$	0	$\mathbb{Z}$	0	$\mathbb{Z}$	0
1	AIII	0	0	1	0	$\mathbb{Z}$	0	$\mathbb{Z}$	0	$\mathbb{Z}$	0	$\mathbb{Z}$
0	AI	1	0	0	$\mathbb{Z}$	0	0	0	$2\mathbb{Z}$	0	$\mathbb{Z}_2$	$\mathbb{Z}_2$
1	BDI	1	1	1	$\mathbb{Z}_2$	$\mathbb{Z}$	0	0	0	$2\mathbb{Z}$	0	$\mathbb{Z}_2$
2	D	0	1	0	$\mathbb{Z}_2$	$\mathbb{Z}_2$	$\mathbb{Z}$	0	0	0	$2\mathbb{Z}$	0
3	DIII	−1	1	1	0	$\mathbb{Z}_2$	$\mathbb{Z}_2$	$\mathbb{Z}$	0	0	0	$2\mathbb{Z}$
4	AII	−1	0	0	$2\mathbb{Z}$	0	$\mathbb{Z}_2$	$\mathbb{Z}_2$	$\mathbb{Z}$	0	0	0
5	CII	−1	−1	1	0	$2\mathbb{Z}$	0	$\mathbb{Z}_2$	$\mathbb{Z}_2$	$\mathbb{Z}$	0	0
6	C	0	−1	0	0	0	$2\mathbb{Z}$	0	$\mathbb{Z}_2$	$\mathbb{Z}_2$	$\mathbb{Z}$	0
7	CI	1	−1	1	0	0	0	$2\mathbb{Z}$	0	$\mathbb{Z}_2$	$\mathbb{Z}_2$	$\mathbb{Z}$

d=2 d=3

4	AII	−1	0	0	$2\mathbb{Z}$	0	$\mathbb{Z}_2$	$\mathbb{Z}_2$	$\mathbb{Z}$	0	0	0

$\nu_0 : \nu_1, \nu_2, \nu_3 \quad \vec{M}_\nu = \frac{1}{2}(\nu_1 \vec{G}_1 + \nu_2 \vec{G}_2 + \nu_3 \vec{G}_3)$

$\vec{B} \cdot \vec{M}_\nu = \pi \,(\mathrm{mod}\, 2\pi)$

Burger's vector

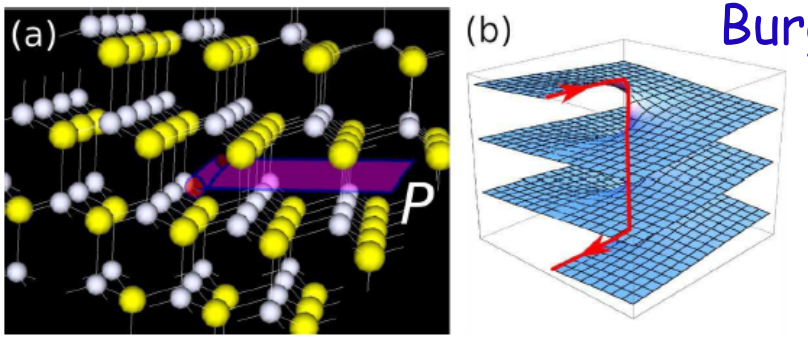

Y.Ran et al. 2009

Gapless 1d mode along the dislocation

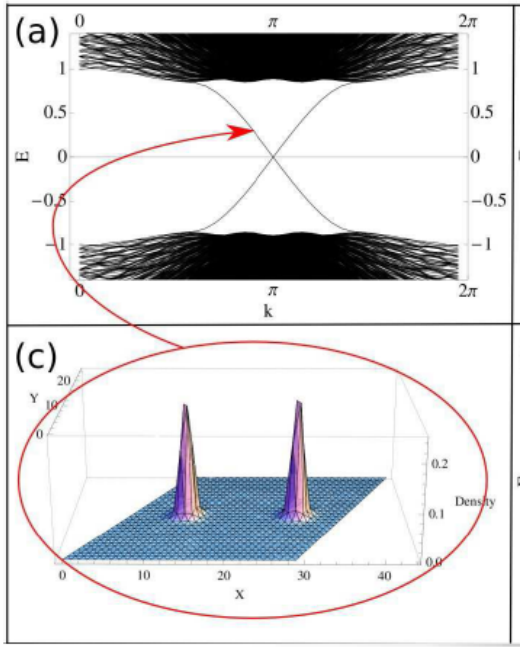

Physics of Noncollinear Magnetism

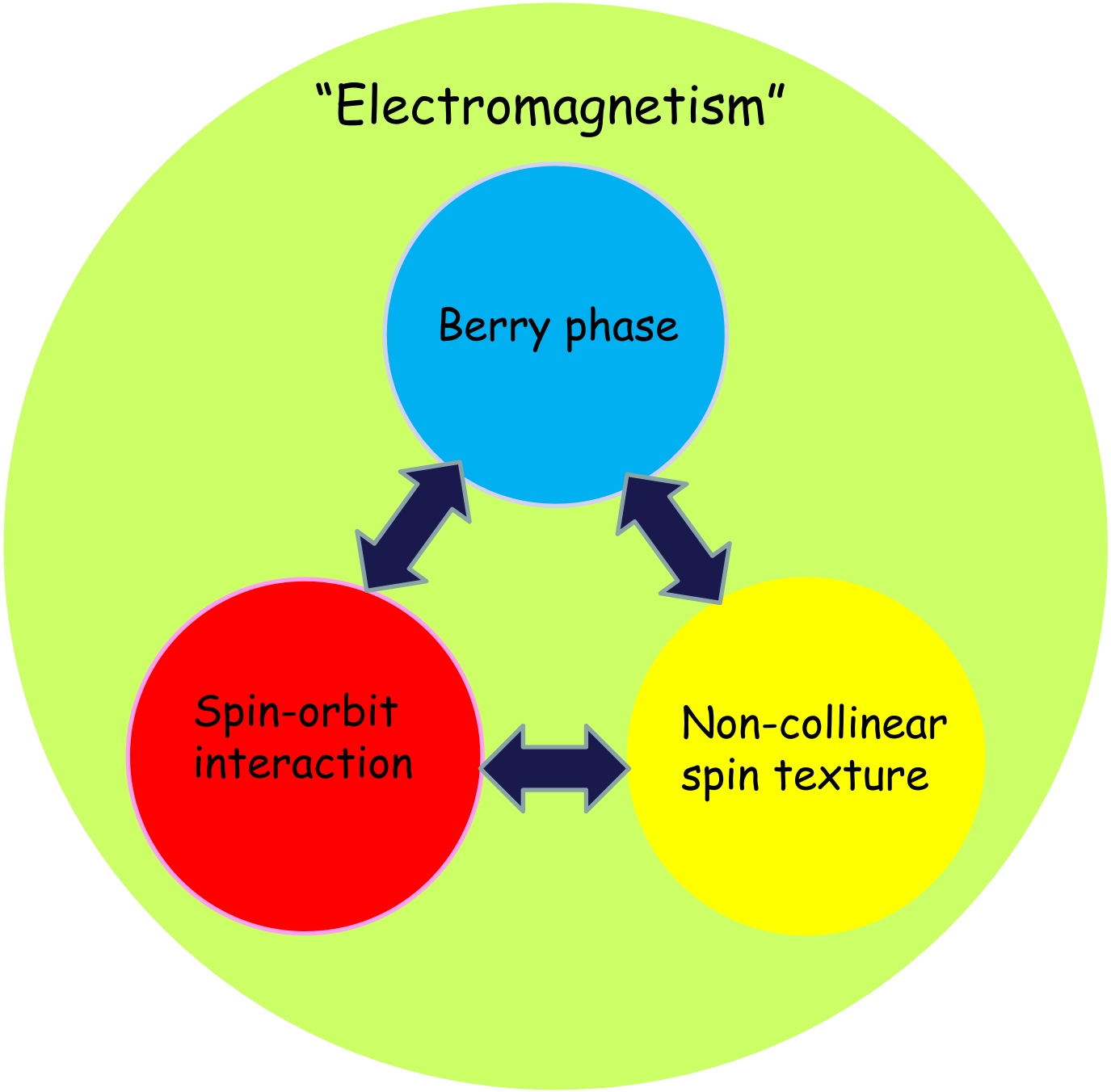
"Electromagnetism"
Berry phase
Spin-orbit interaction
Non-collinear spin texture

Multiferroics

Mott insulator
Low-energy charge dynamics is quenched ?

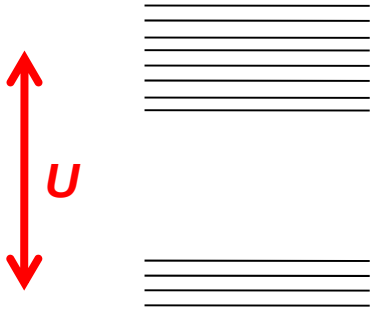

charge transfer states

spin states

$\mathrm{Im}\,\varepsilon(\omega)$

requires the real transitions between the spin states

Spin Charge Separation

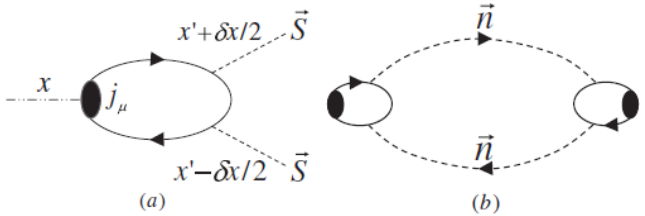

$$\varepsilon(q,\omega) = \varepsilon_c + \frac{(\varepsilon_c - 1)^2 (Dq^2 + i\omega)}{4\pi\sigma_{s,\|}}$$

Ng, Lee

Triangular process

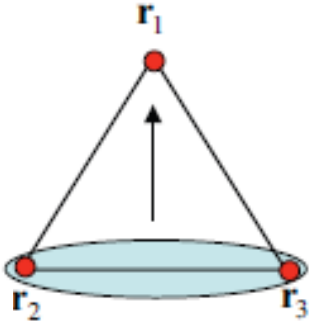

$$\delta\tilde{n}_1 =$$

$$8\frac{t_{12}t_{23}t_{31}}{U^3}\left[\mathbf{S}_1\cdot(\mathbf{S}_2+\mathbf{S}_3) - 2\mathbf{S}_2\cdot\mathbf{S}_3\right]$$

Bulaevskii,Batista
Mostovoy, Khomiskii

Spin-orbit interaction

?

gauge field coupled to spin current

Aharonov-Casher effect

$$L_{\text{int}} = \vec{j}_{spin} \cdot \vec{A}_{spin}$$

$$\vec{A}_{spin} = \lambda(\vec{E} \times \vec{S})$$

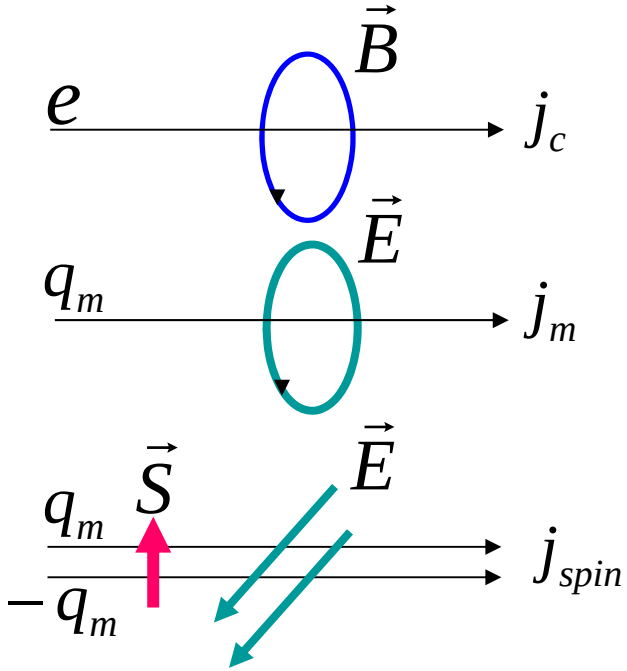

Spin-orbit interaction

$$H_{SO} = \lambda(\vec{S} \times \nabla V) \cdot \vec{p}$$

$$\approx \lambda'(\vec{S} \times \vec{r}) \cdot \vec{p} = \vec{A}_{SO} \cdot \vec{p}$$

toroidal moment

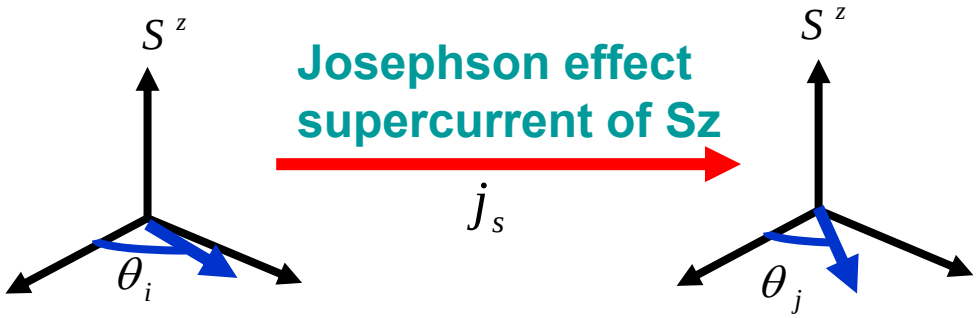

$$[\theta, S^z] = i$$

Orders of magnitudes enhancement in condensed matter !! (~10^6)

Helimagnets

Frustrated Heisenberg model (Yoshimori 1950)

$$H = \sum_{ij} J_{ij} \vec{S}_i \cdot \vec{S}_j \qquad J(q) = \sum_j e^{iq(R_i - R_j)} J_{ij}$$

$$\vec{S}_i = \vec{S}_Q e^{iQR_i} + \vec{S}_{-Q} e^{-iQR_i}$$

$$|\vec{S}_i| = \text{const} \rightarrow |\vec{S}_Q| = |\vec{S}_{-Q}| = \text{const}$$

$$\vec{S}_Q \cdot \vec{S}_{-Q} = 0$$

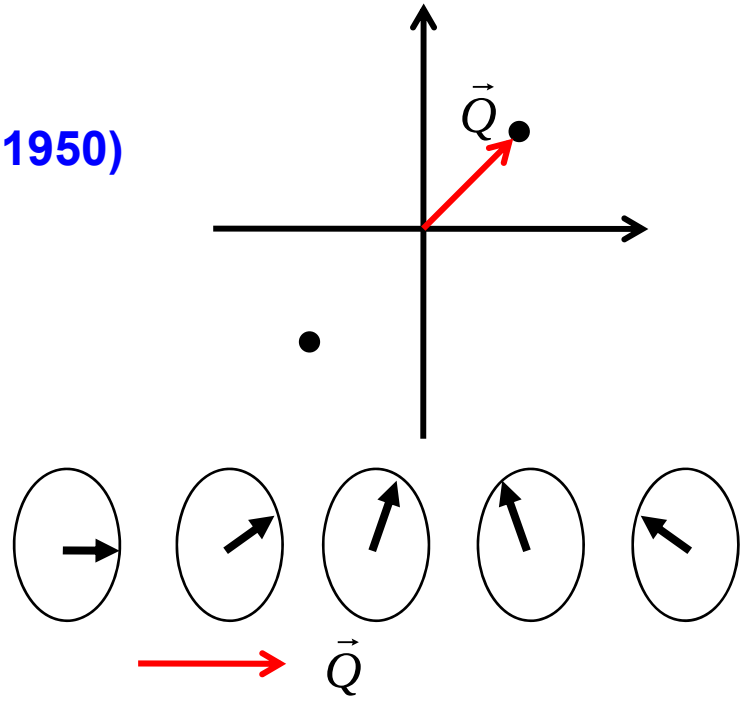

Electric Polarization due to spin current

Double exchange interaction (1 hole)	Super exchange interaction (2 holes)
$\vec{P} \cong -\frac{eV}{3\Delta} I \frac{\vec{e}_{12} \times (\vec{e}_1 \times \vec{e}_2)}{\lvert \cos \frac{\theta_{12}}{2} \rvert}$	$\vec{P} \cong -\frac{4e}{9} (\frac{V}{\Delta})^3 I \vec{e}_{12} \times (\vec{e}_1 \times \vec{e}_2)$

$(\cos\theta_{12} = \vec{e}_1 \bullet \vec{e}_2)$

$$\vec{P} \propto \vec{e}_{12} \times (\vec{S}_1 \times \vec{S}_2) \propto \vec{e}_{12} \times \vec{j}_s$$

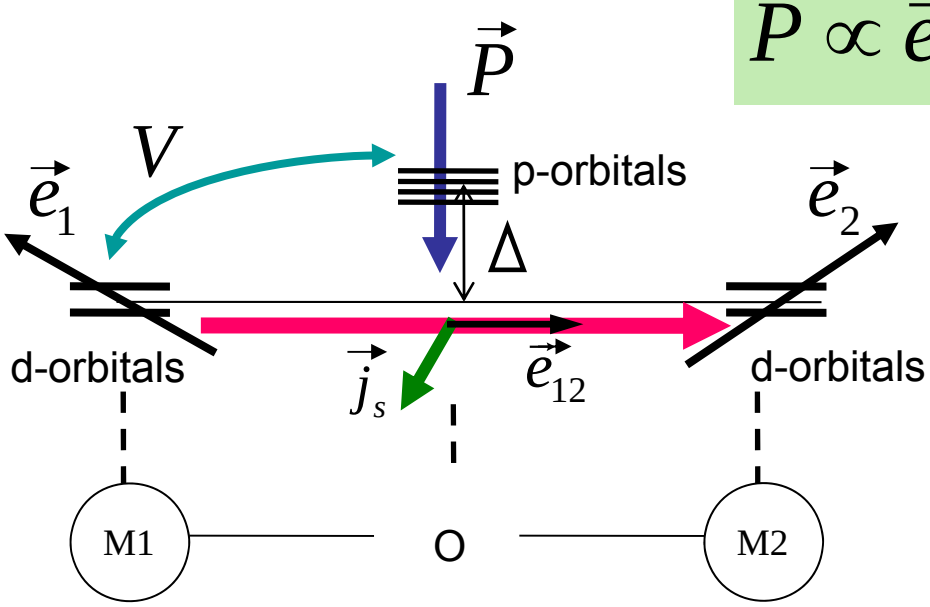

Js : spin current

Δ : d－p energy difference

V : transfer integral

I : constant $\propto a_0$ (Bohr radius)

Katsura-Nagaosa-Balatsky PRL05
Mostovoy, Dagotto

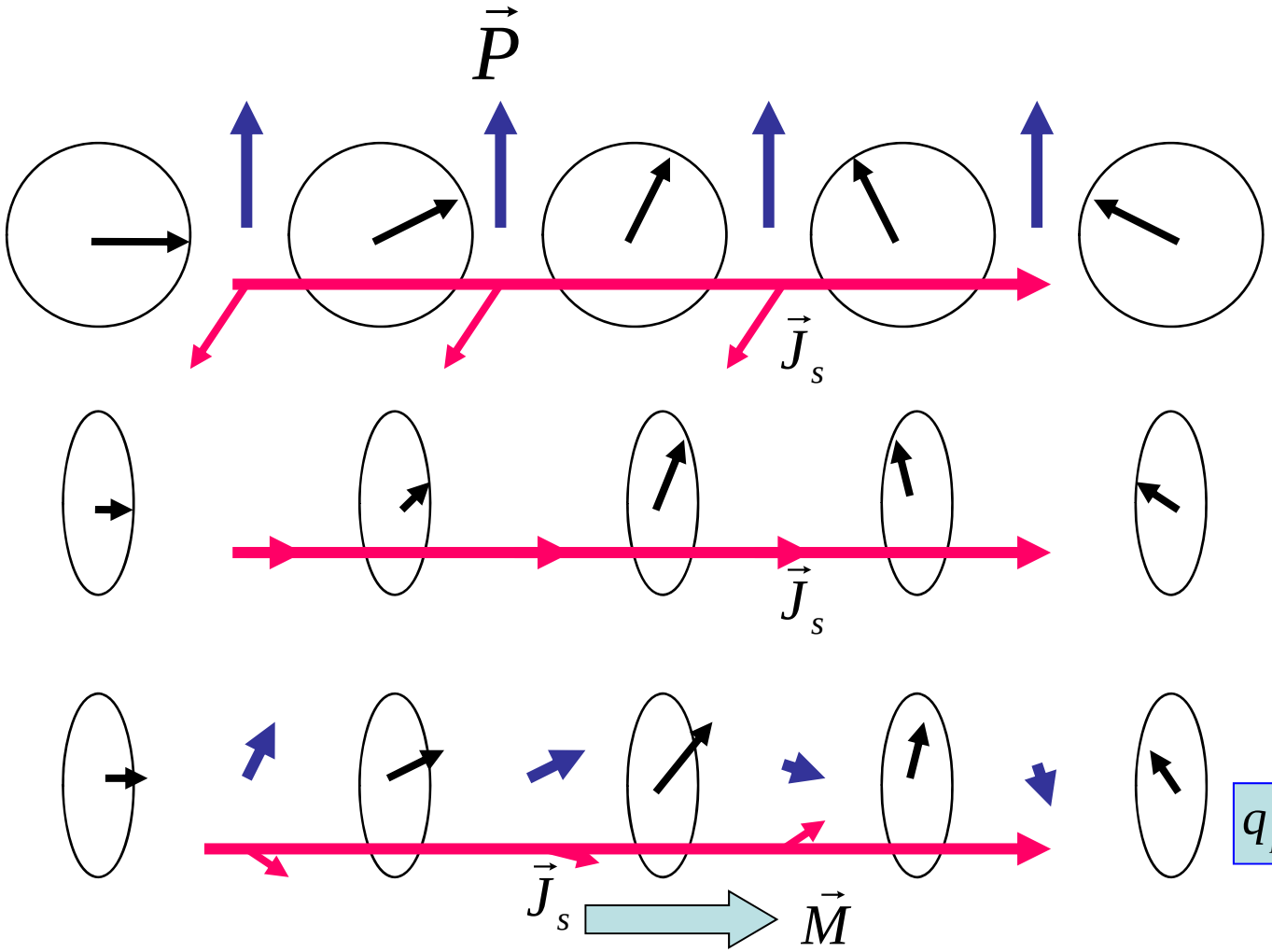

Uniform P even with *Incommensurate* spiral

No ME effect

Transverse ME effect

$q_{pol} = q_{mag}$ component

ZnCr2Se4(spinel): screw spin structure
Akimitsu et al.

GaFeO3: only transverse due to **toroidal moment**
Popov et al.

Multiferroic behavior in perovskite oxides

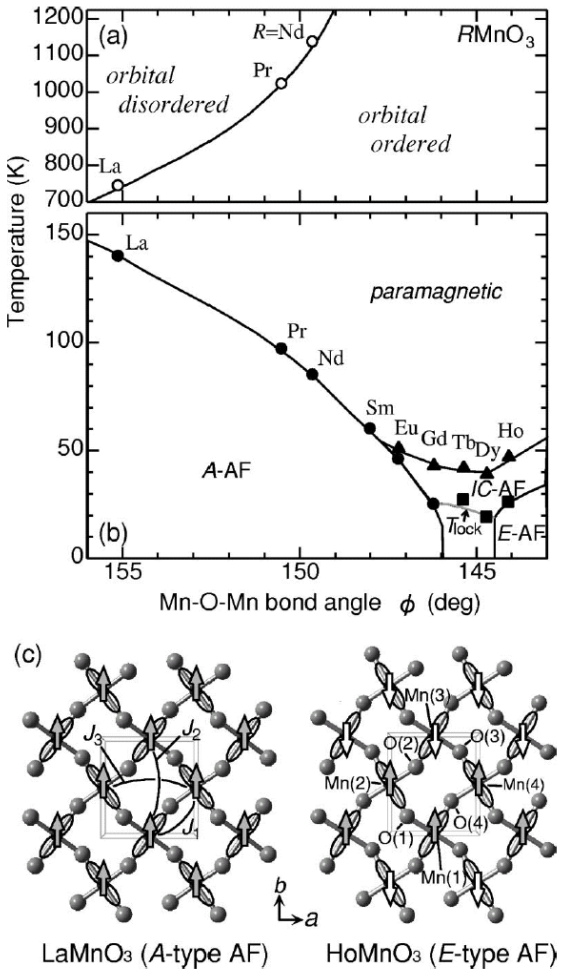

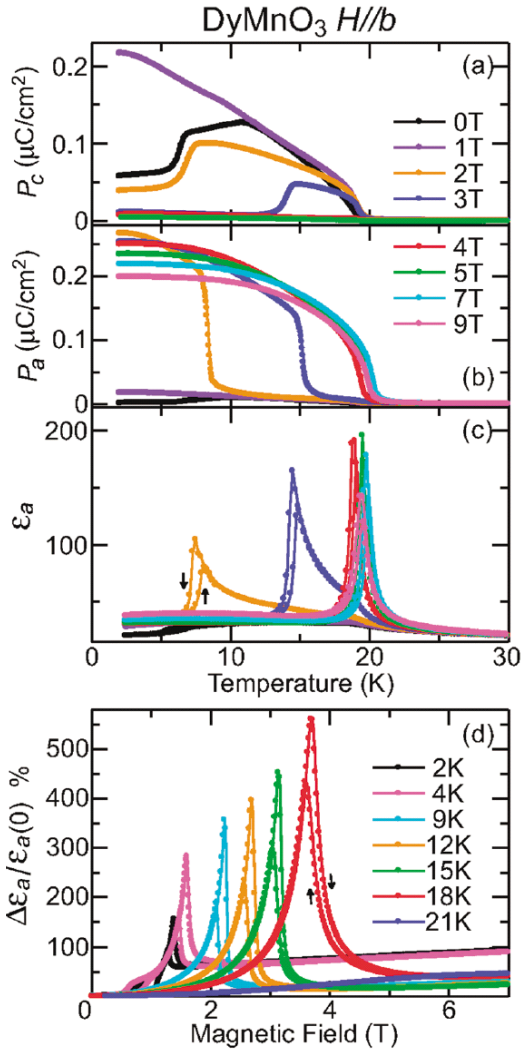

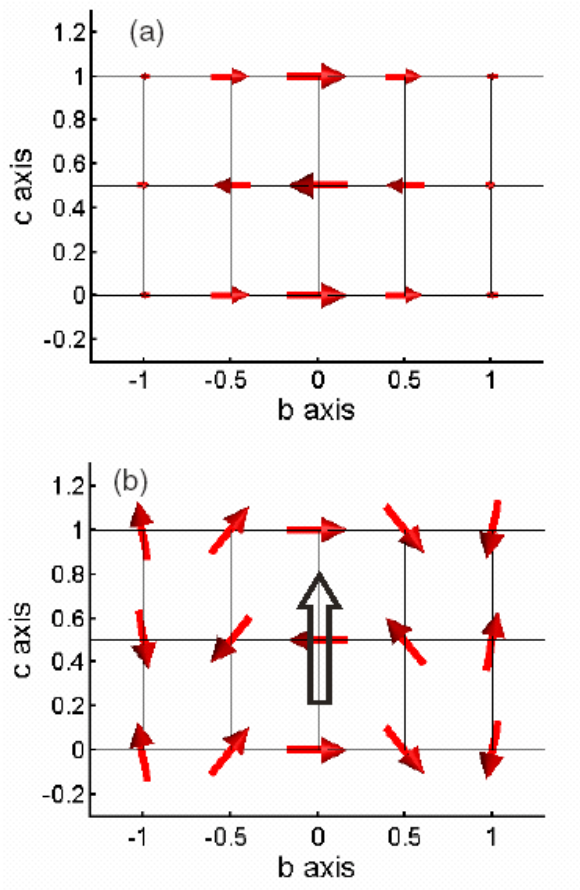

Tokura-Kimura group

Kenzelman et al.
Arima et al.

Gauge theory of spin current in magnets

$$L = |(\partial_\mu - ia_\mu - i\vec{\sigma}\cdot\vec{A}_\mu)z_\alpha|^2 + \lambda|z_\sigma|^2$$

$$\vec{A}_\mu \propto \vec{e}_\mu \times \vec{E}$$

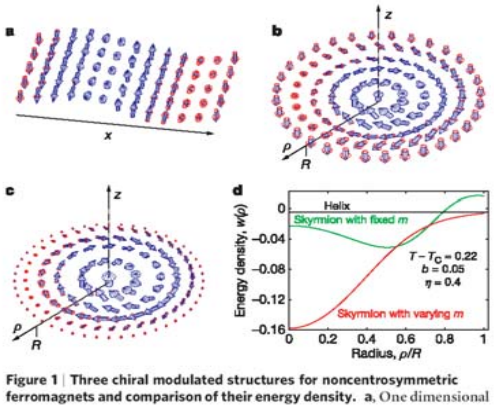

Figure 1 | Three chiral modulated structures for noncentrosymmetric ferromagnets and comparison of their energy density. a, One dimensional

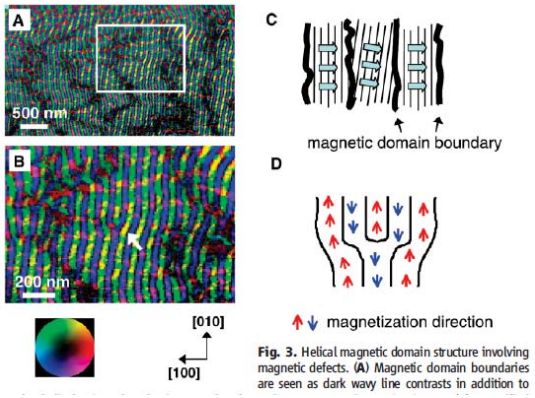

Fig. 3. Helical magnetic domain structure involving magnetic defects. (A) Magnetic domain boundaries are seen as dark wavy line contrasts in addition to

various spin textures in polar magnets analogous to vortex in superconductors

Rossler et al. Nature 2006 *Uchida et al. Science 2006*

$$\varepsilon_{xx}(\omega) \propto < j_y^z j_y^z + j_z^y j_z^y - j_y^z j_z^y - j_z^y j_y^z >$$

$$\varepsilon(\omega) \propto i\omega\sigma_{spin}(\omega) \propto \omega^2 \varepsilon_{spin}(\omega)$$

spin current dynamics can be studied by the dielectric properties of magnets.

$$C_{m_\alpha m_\alpha}(\vec{k}, \omega) = \frac{2\chi k_B T[c^2 Dk^4 + \chi^{-1}\kappa k^2(\omega^2 - c^2k^2)]}{[(\omega - ck)^2 + (\frac{1}{2}Dk^2)^2][(\omega + ck)^2 + (\frac{1}{2}Dk^2)^2]}$$

Hydrodynamic theory of spin glass (Halperin-Saslow)

Helimagnets

Frustrated Heisenberg model (Yoshimori 1950)

$$H = \sum_{ij} J_{ij} \vec{S}_i \cdot \vec{S}_j \qquad J(q) = \sum_j e^{iq(R_i - R_j)} J_{ij}$$

$$\vec{S}_i = \vec{S}_Q e^{iQR_i} + \vec{S}_{-Q} e^{-iQR_i}$$

$$|\vec{S}_i| = \text{const} \rightarrow |\vec{S}_Q| = |\vec{S}_{-Q}| = \text{const}$$

$$\vec{S}_Q \cdot \vec{S}_{-Q} = 0$$

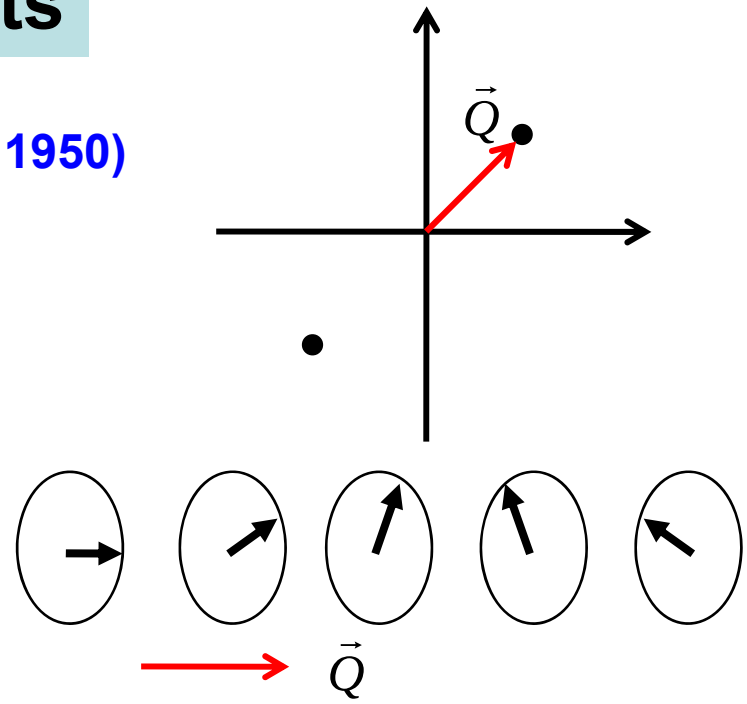

Dzyaloshinskii-Moriya interaction

$$H = \sum_{ij} J_{ij} \vec{S}_i \cdot \vec{S}_j + \sum_{ij} D_{ij} \cdot (\vec{S}_i \times \vec{S}_j)$$

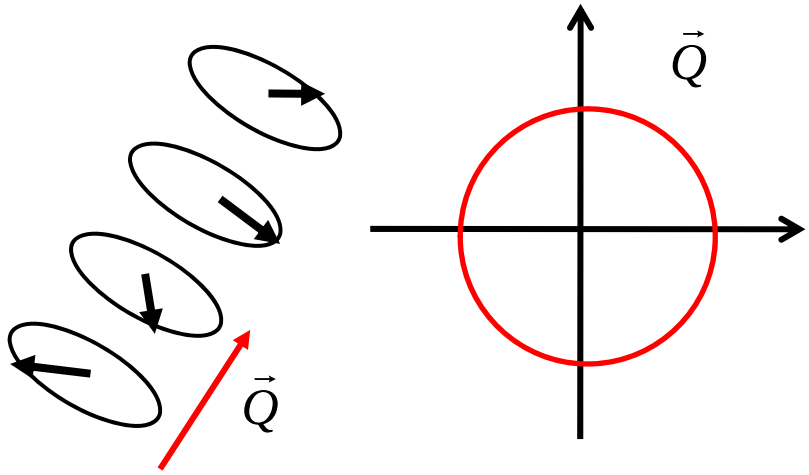

Structure

MnSi(B20 structure)

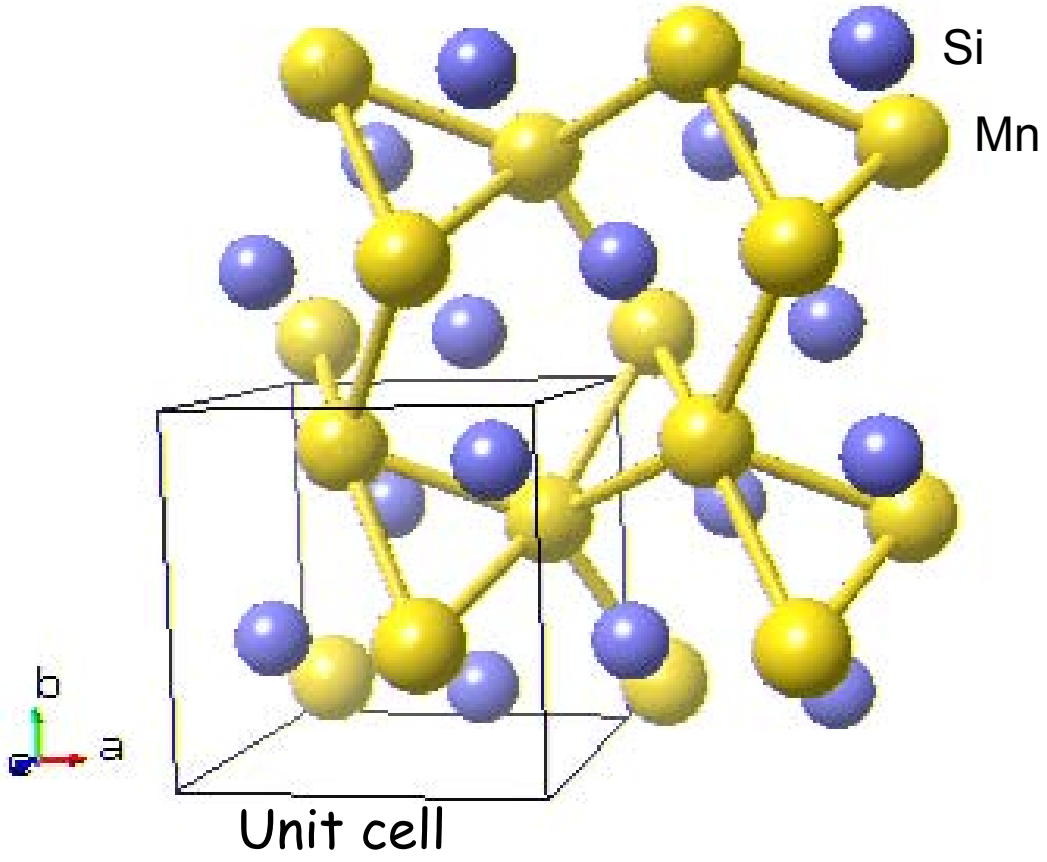

Real Space Observation of Helical Structure

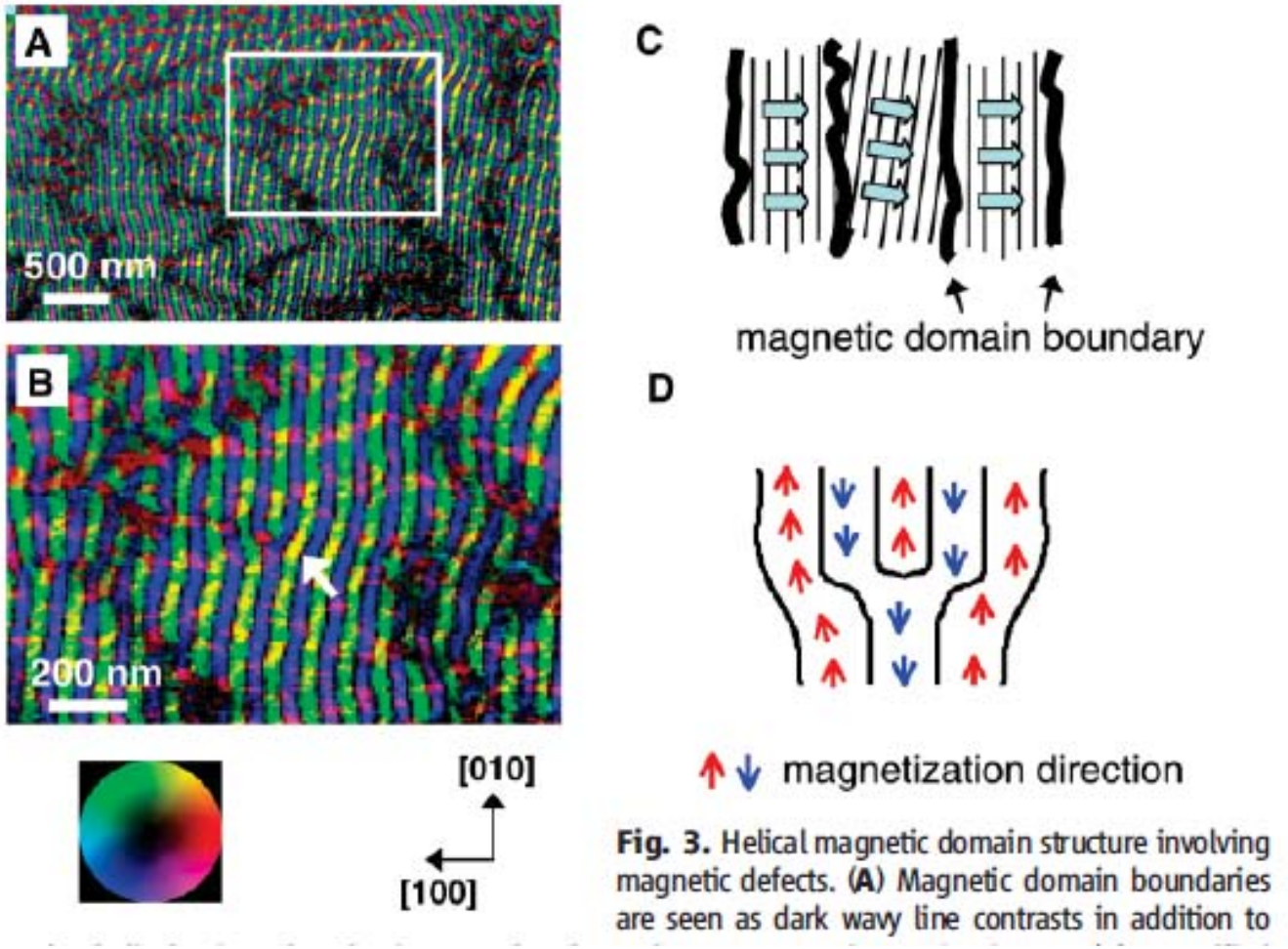

Fig. 3. Helical magnetic domain structure involving magnetic defects. (**A**) Magnetic domain boundaries are seen as dark wavy line contrasts in addition to

(Fe,Co)Si

Uchida et al. Science 2006

Skyrmions

Skyrmion and spin Berry phase in real space

Skyrmion configuration

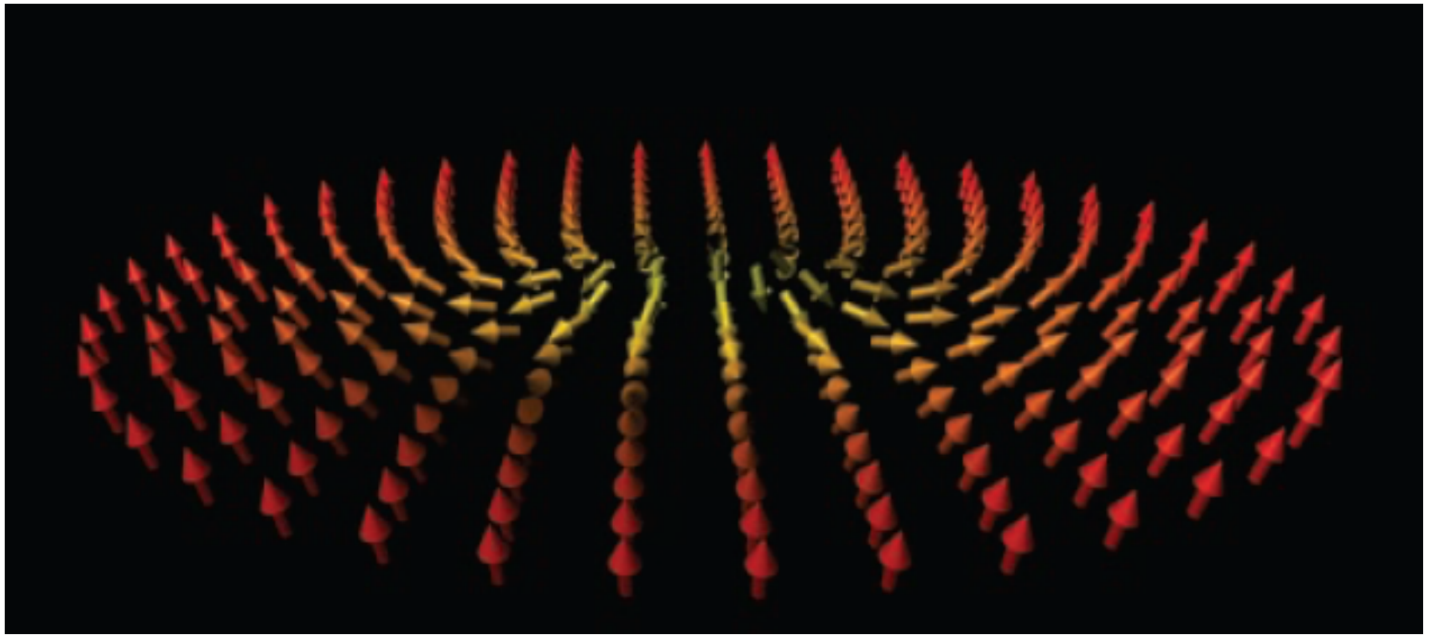

From Senthil et al.

$$L_z = \sum_{\alpha=1}^{N} |(\partial_\mu - i a_\mu) z_\alpha|^2 + s|z|^2 + u(|z|^2)^2 + \kappa(\epsilon_{\mu\nu\kappa}\partial_\nu a_\kappa)^2$$

Solid angle acts as a fictitious magnetic field for carriers

$$\vec{S}_i \cdot (\vec{S}_j \times \vec{S}_k) \approx \nabla \times \vec{a}$$

Solid angle by spins acting as a gauge field

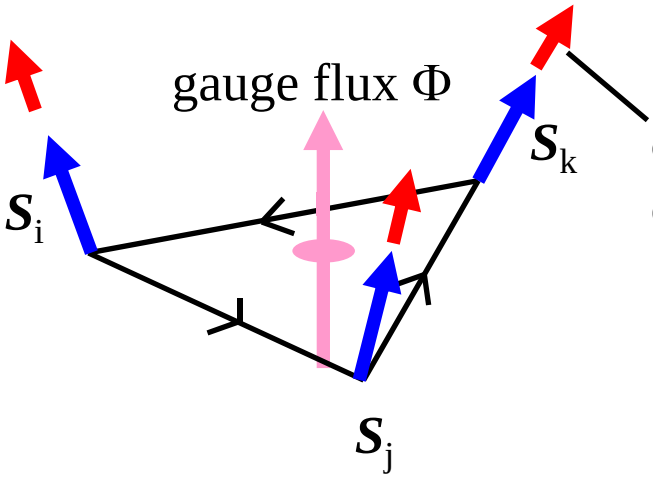

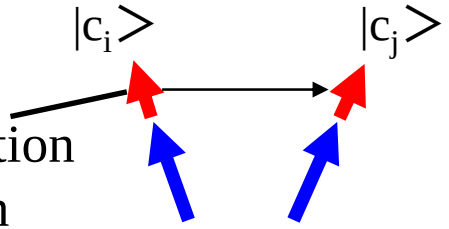

conduction electron

$$
\begin{aligned}
t_{ij} &= t\langle\chi_j|\chi_i\rangle \\
&= t\left(\cos\frac{\theta_i}{2}\cos\frac{\theta_j}{2} + \sin\frac{\theta_i}{2}\sin\frac{\theta_j}{2}\exp(i(\phi_j-\phi_i))\right) \\
&= t\cos\frac{\theta_{ij}}{2}\exp(ia_{ij})
\end{aligned}
$$

acquire a phase factor

Fictitious flux (in a continuum limit)

$$\Phi \propto \frac{\mathbf{S}_i \cdot (\mathbf{S}_j \times \mathbf{S}_k)}{2} = \frac{\Omega}{2}$$

scalar spin chirality

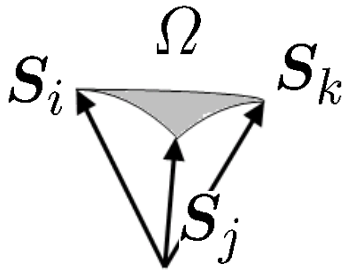

Pyrochlore $Nd_2Mo_2O_7$

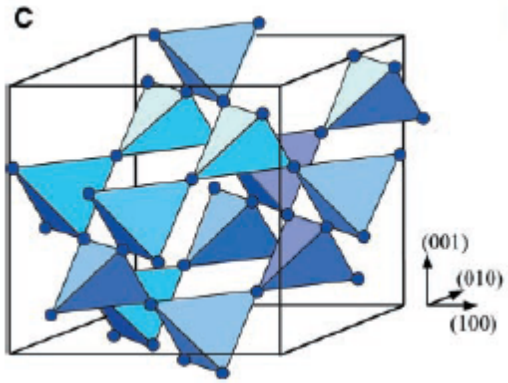

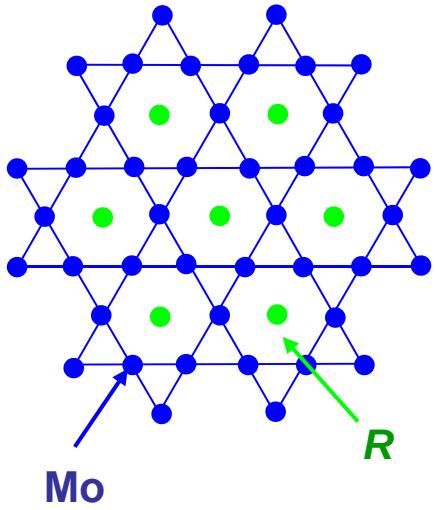

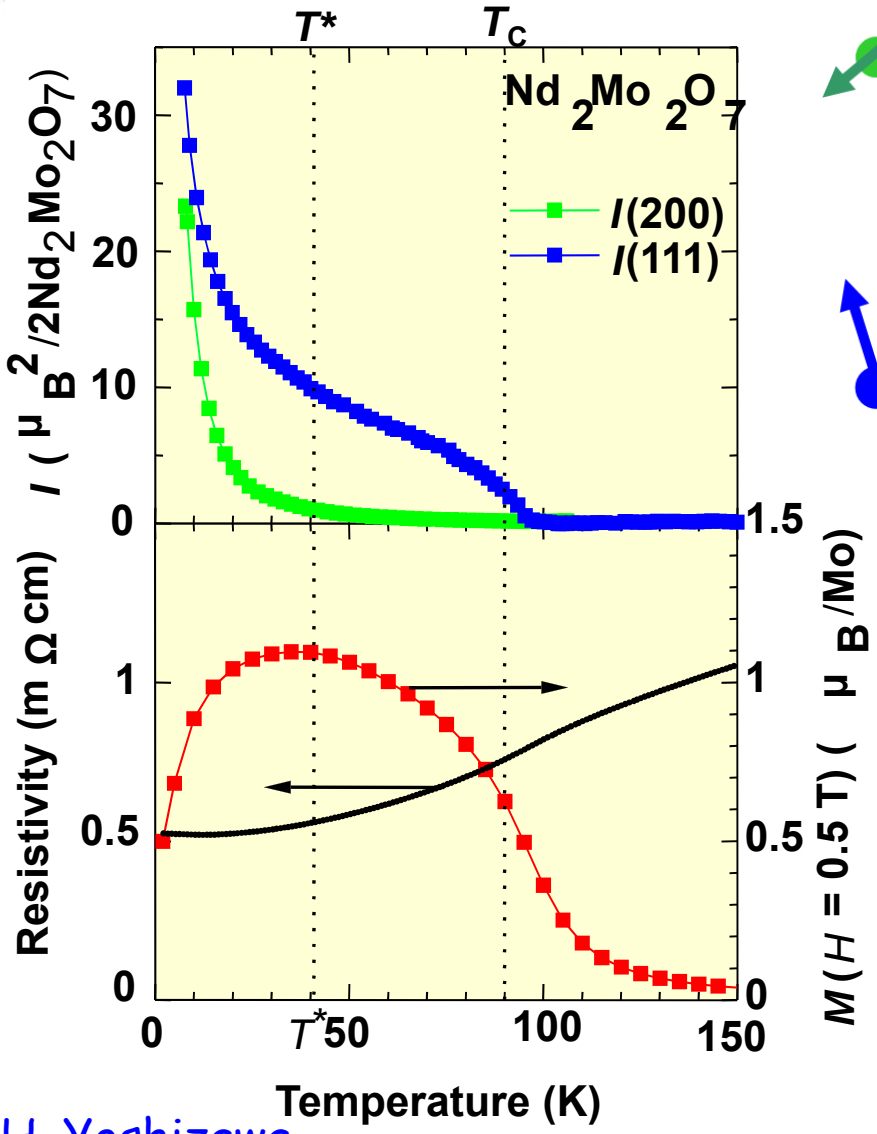

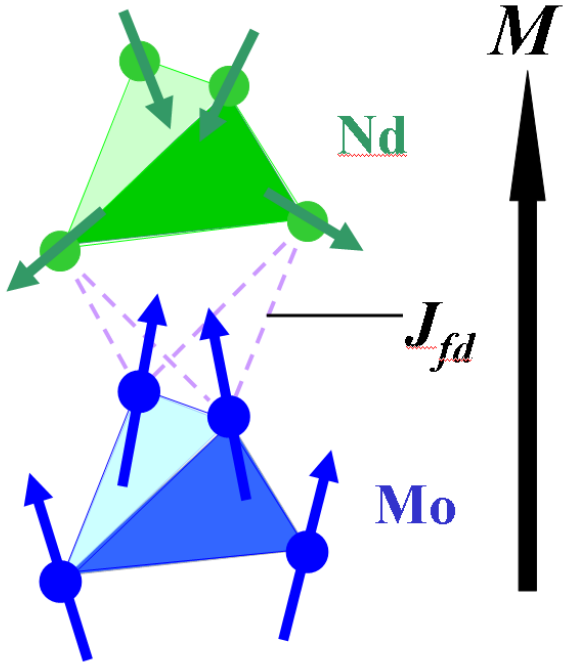

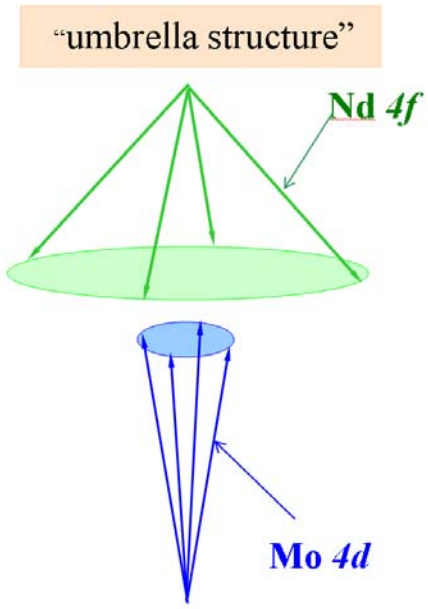

Y. Taguchi, Y. Oohara, H. Yoshizawa,
N. Nagoasa, and Y. T., Science 2001

Equation of motion

$$\frac{d\mathbf{x}}{dt} = \frac{\partial \varepsilon}{\partial \mathbf{k}} + \frac{dk}{dt} \times \mathbf{B}_{\mathrm{k}}$$

$$\frac{d\mathbf{k}}{dt} = -e\left(-\frac{\partial \varphi}{\partial \mathbf{r}} + \frac{dr}{dt} \times \mathbf{B}_{r} \right)$$

one flux quantum/(nm)^2~4000T !

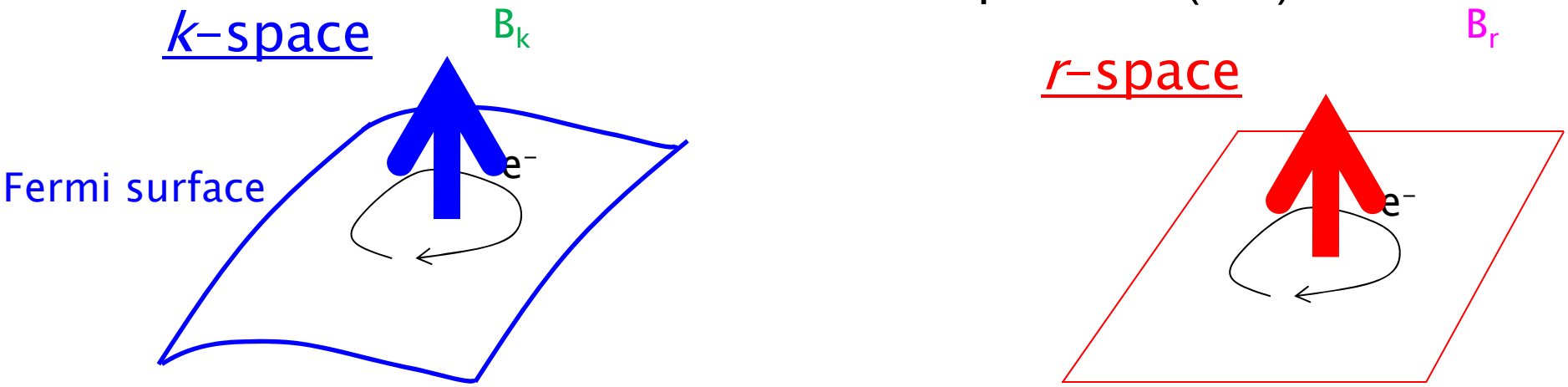

B_{k} induced AHE

$$\sigma_{xy} \propto \tau^{0}, \rho_{xy} \propto \tau^{-2}$$

"dissipationless" nature

B_{r} induced AHE

$$\sigma_{xy} \propto \tau^{2}, \rho_{xy} \propto \tau^{0}$$

Cf. normal HE

$$\rho_{xy} = B/ne, \sigma_{xy} \approx \sigma_{xx}{}^{2} B/ne$$

Helimagnets

Frustrated Heisenberg model (Yoshimori 1950)

$$H = \sum_{ij} J_{ij} \vec{S}_i \cdot \vec{S}_j \qquad J(q) = \sum_j e^{iq(R_i - R_j)} J_{ij}$$

$$\vec{S}_i = \vec{S}_Q e^{iQR_i} + \vec{S}_{-Q} e^{-iQR_i}$$

$$|\vec{S}_i| = \text{const} \rightarrow |\vec{S}_Q| = |\vec{S}_{-Q}| = \text{const}$$

$$\vec{S}_Q \cdot \vec{S}_{-Q} = 0$$

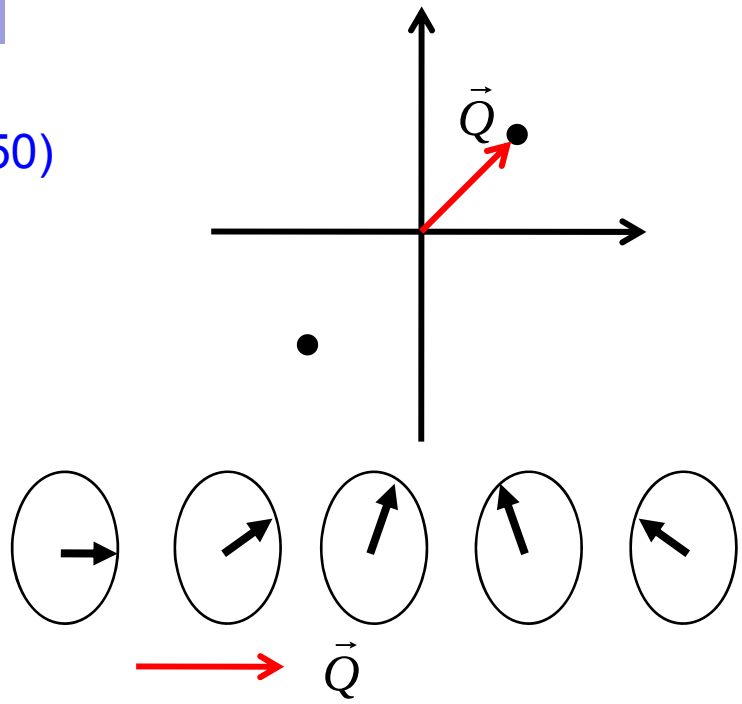

Dzyaloshinskii-Moriya interaction

$$H = \sum_{ij} J_{ij} \vec{S}_i \cdot \vec{S}_j + \sum_{ij} D_{ij} \cdot (\vec{S}_i \times \vec{S}_j)$$

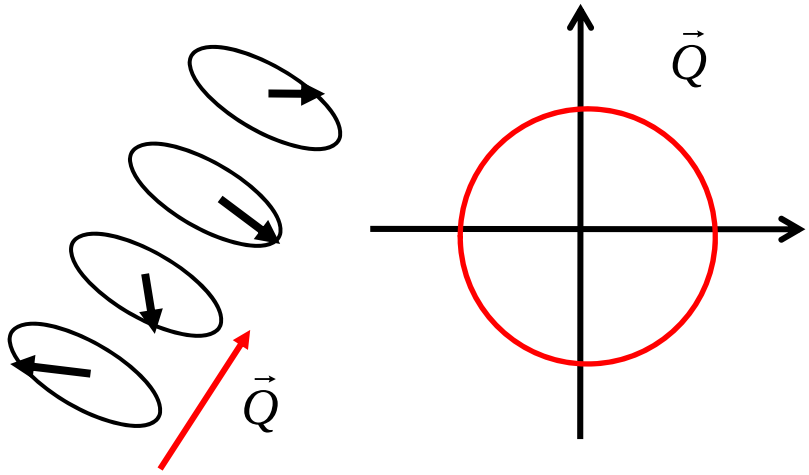

Quantum Phase Transition in MnSi

Pfleiderer, Rosch, Lonzarich et al

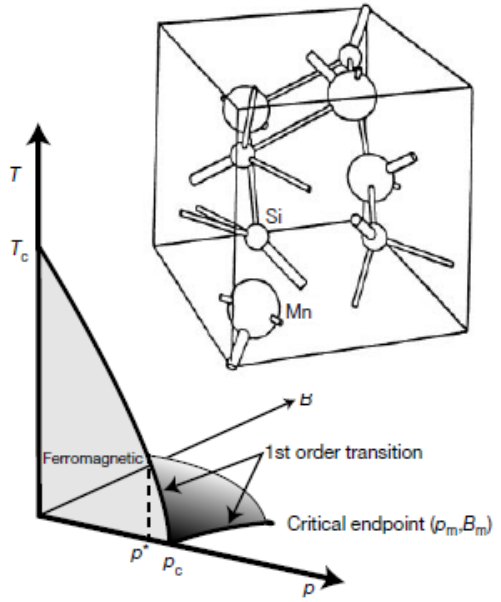

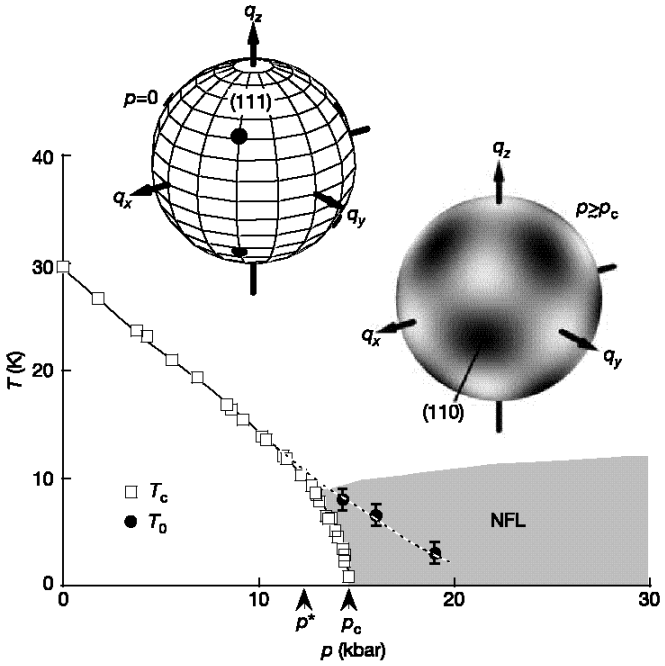

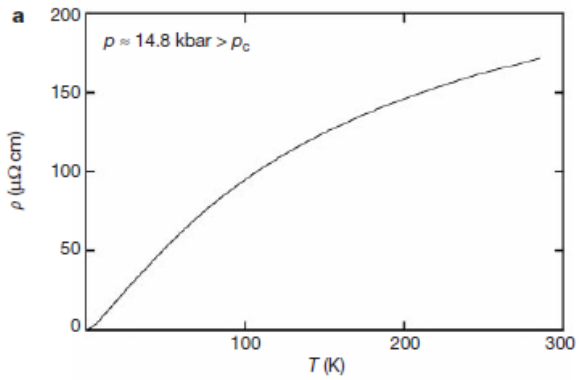

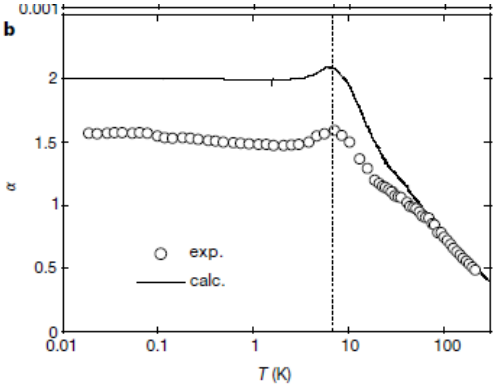

Spin fluctuation on a sphere in Momentum space

Non-Fermi liquid charge transport

Small angle neutron scattering for Skyrmion Xtal

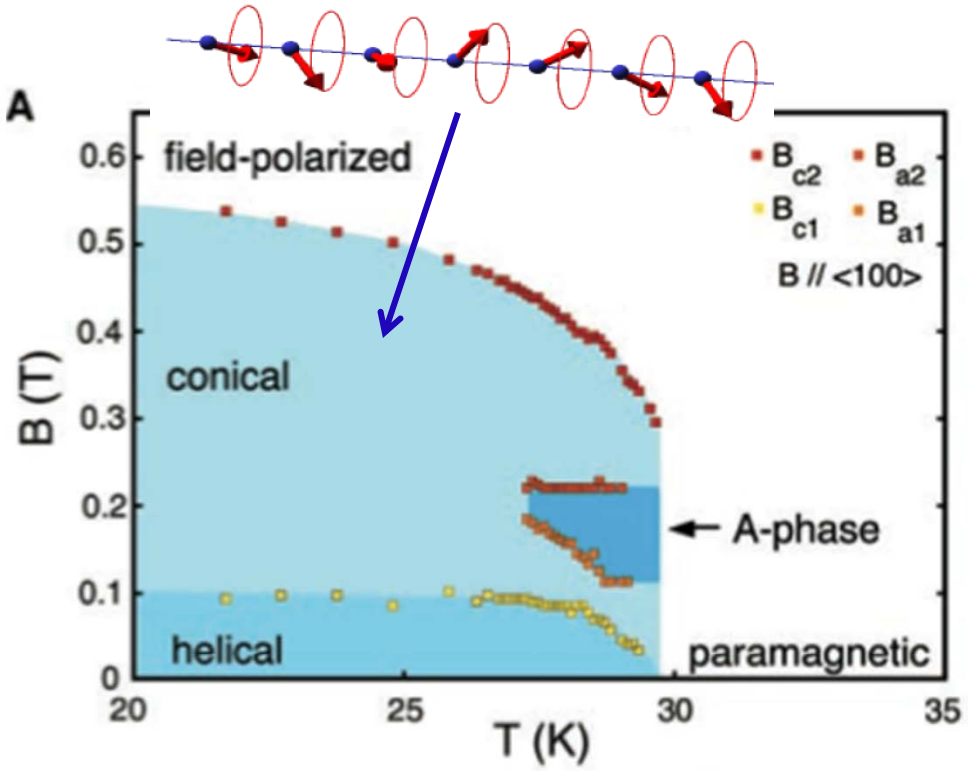

MnSi

S. Mühlbauer *et. al.*, Science 323 915 (2009)

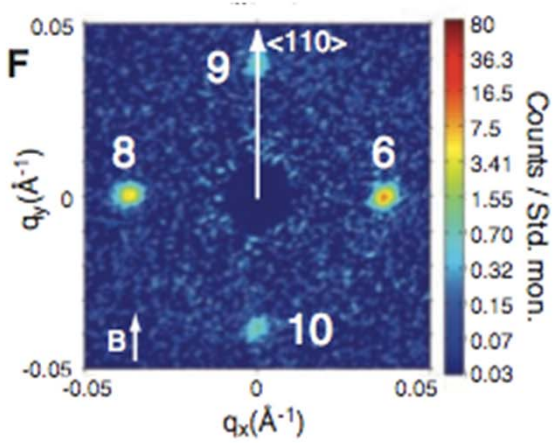

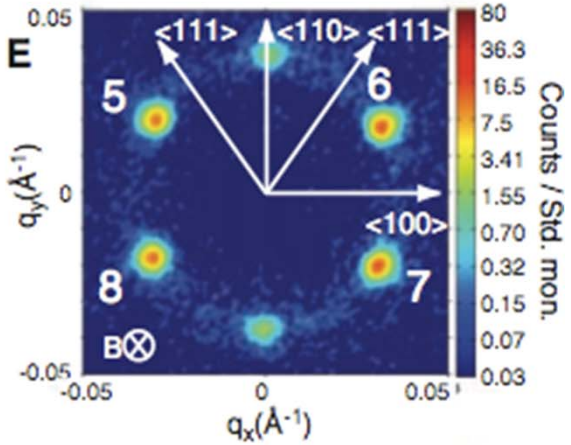

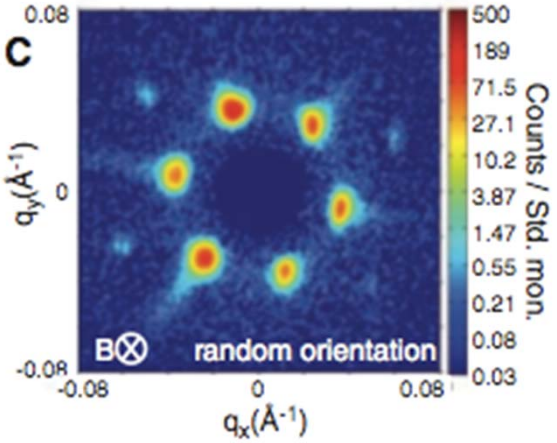

Skyrmion Crystal

Superposition of three Helix without phase shift

$$M(r) \approx M_f + \sum_{i=1}^{3} M_{Q_i}(r + \Delta r)$$

$$M_{Q_i}(r + \Delta r) = A[n_{i1}\cos(Q_i \cdot r) + n_{i2}\sin(Q_i \cdot r)]$$

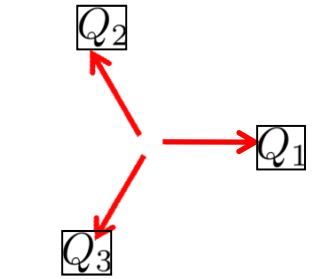

$$Q_1 + Q_2 + Q_3 = 0$$

Skyrmion

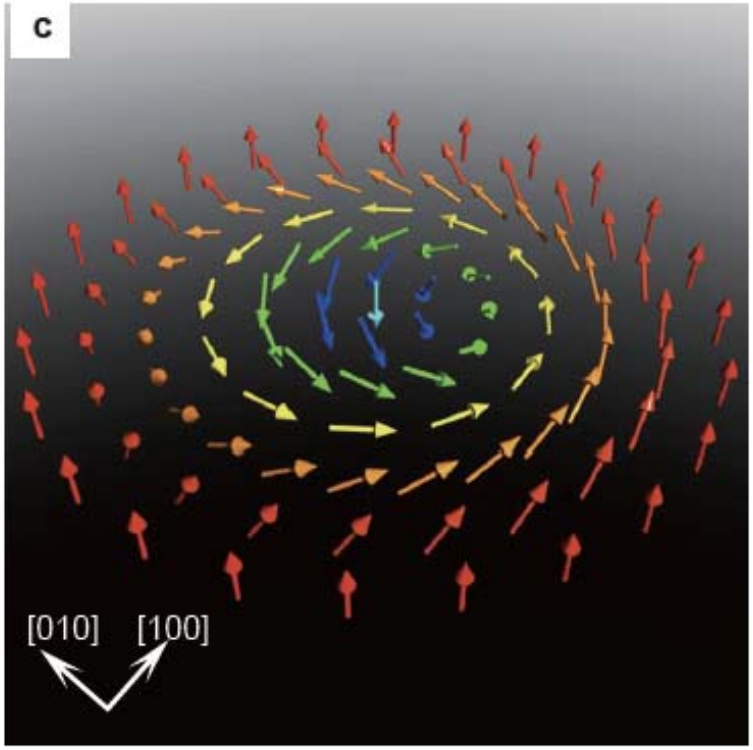

Skyrmion crystal

3-flod-Q

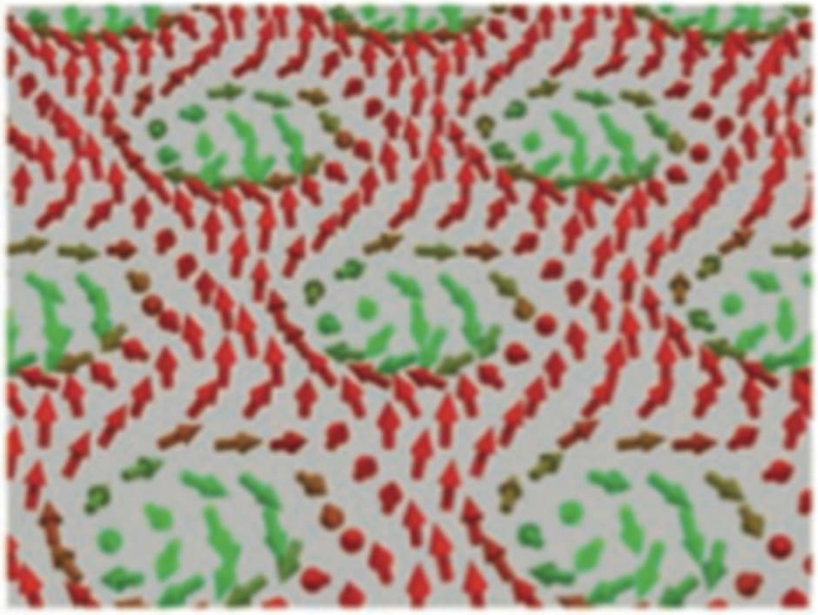

S. Muhlbauer et al. Science 323, 915 (2009).

Monte Carlo simulation for 2D helimagnet

J. H. Park, J. H. Han, S. Onoda and N.N.

$$H_S = -J\sum_{\mathbf{r}} \mathbf{S}_{\mathbf{r}} \cdot (\mathbf{S}_{\mathbf{r}+\hat{x}} + \mathbf{S}_{\mathbf{r}+\hat{y}} + \mathbf{S}_{\mathbf{r}+\hat{z}})$$

$$-K\sum_{\mathbf{r}} (\mathbf{S}_{\mathbf{r}} \times \mathbf{S}_{\mathbf{r}+\hat{x}} \cdot \hat{x} + \mathbf{S}_{\mathbf{r}} \times \mathbf{S}_{\mathbf{r}+\hat{y}} \cdot \hat{y} + \mathbf{S}_{\mathbf{r}} \times \mathbf{S}_{\mathbf{r}+\hat{z}} \cdot \hat{z})$$

$$+ A_1 \sum_{\mathbf{r}} \left((S^x_{\mathbf{r}})^4 + (S^y_{\mathbf{r}})^4 + (S^z_{\mathbf{r}})^4 \right)$$

$$-A_2 \sum_{\mathbf{r}} \left(S^x_{\mathbf{r}} S^x_{\mathbf{r}+\hat{x}} + S^y_{\mathbf{r}} S^y_{\mathbf{r}+\hat{y}} + S^z_{\mathbf{r}} S^z_{\mathbf{r}+\hat{z}} \right) - \mathbf{H} \cdot \sum_{\mathbf{r}} \mathbf{S}_{\mathbf{r}}.$$

$$\sigma_{xy} \approx \vec{S}_i \cdot (\vec{S}_j \times \vec{S}_k)$$

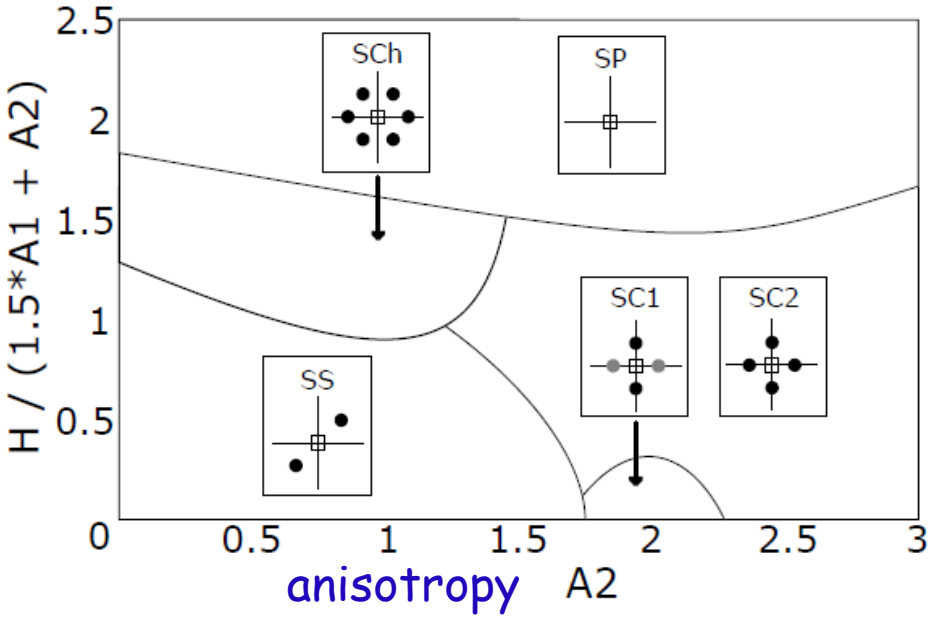

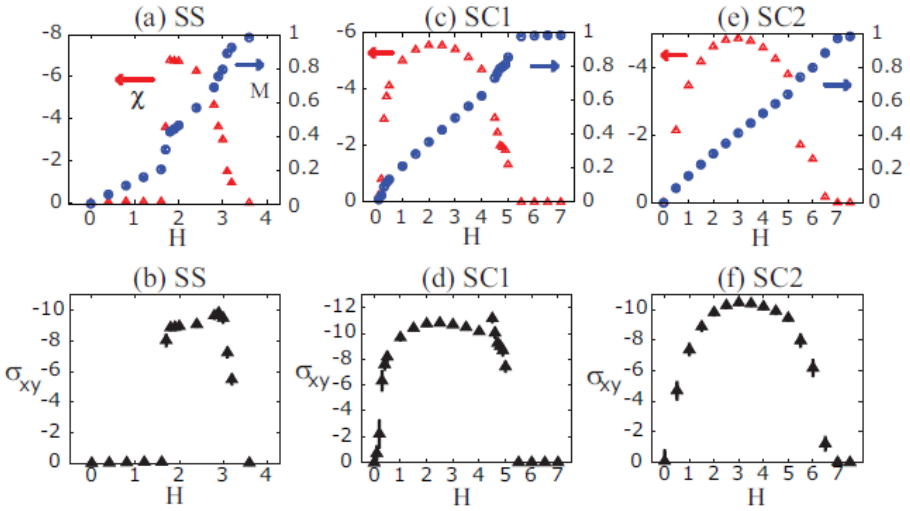

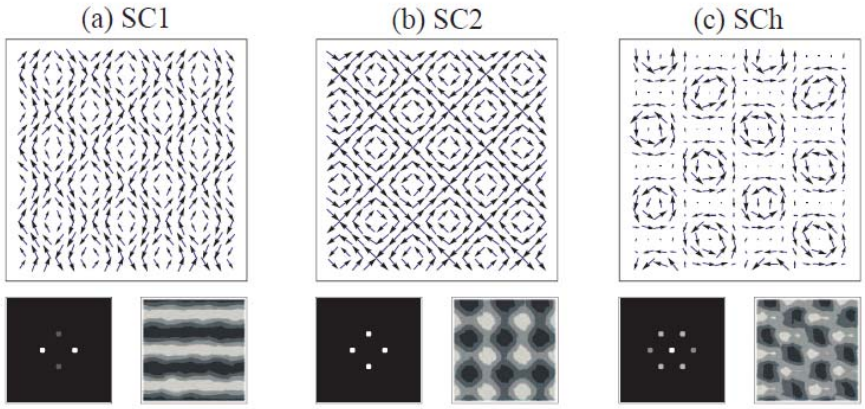

Lorentz TEM observation of Skyrmion crystal in (Fe,Co)Si

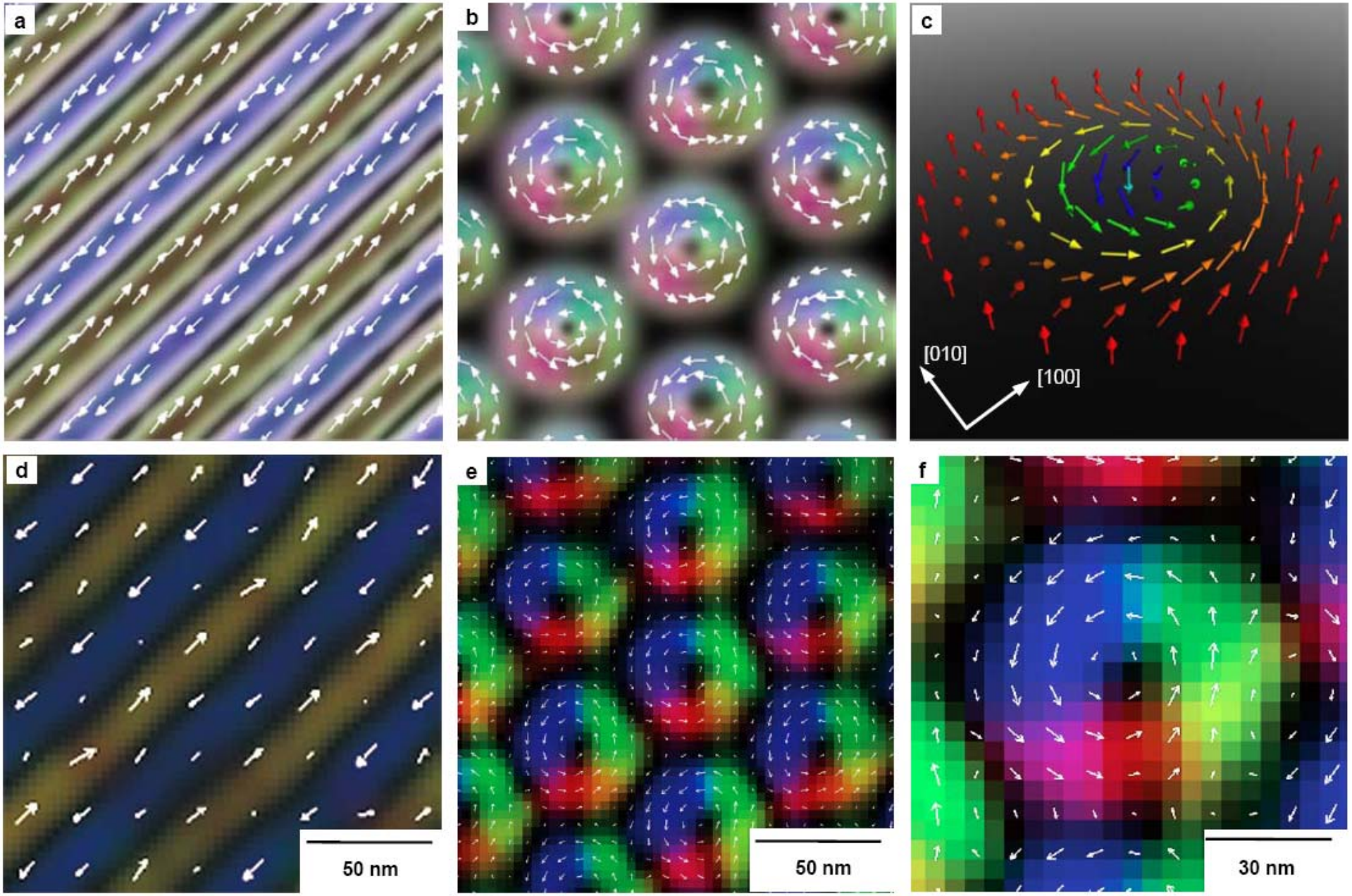

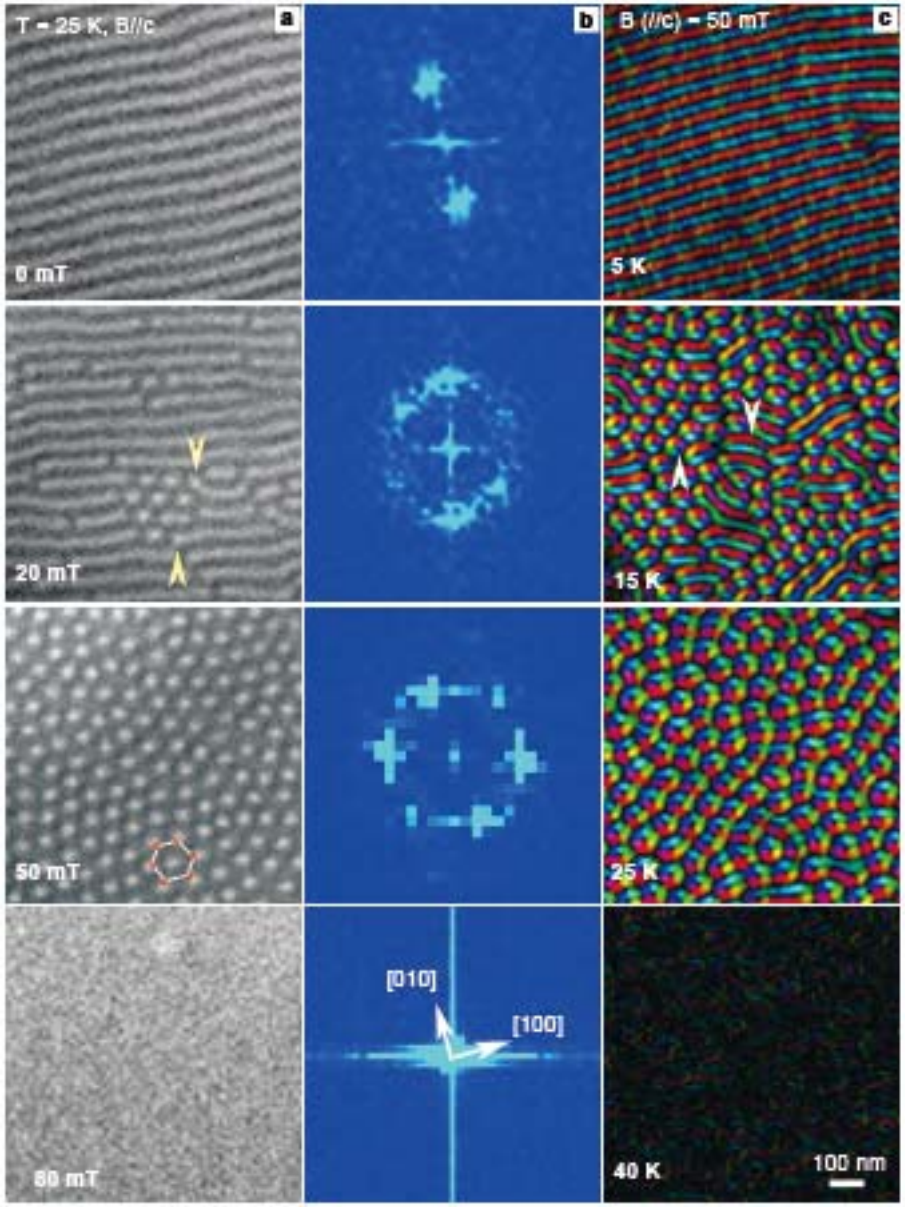

Figure 2 **(a) Magnetic field dependence of real-space Lorentz TEM images of the magnetic structure in $Fe_{0.5}Co_{0.5}Si$. (b) The corresponding fast Fourier transform (FFT) patterns of (a). (c) Temperature profiles of the magnetization distribution map with a external magnetic field of 50 mT.** The external magnetic field was applied along the c-axis. The color map represents the magnetization direction at every point.

Experiment

Theory

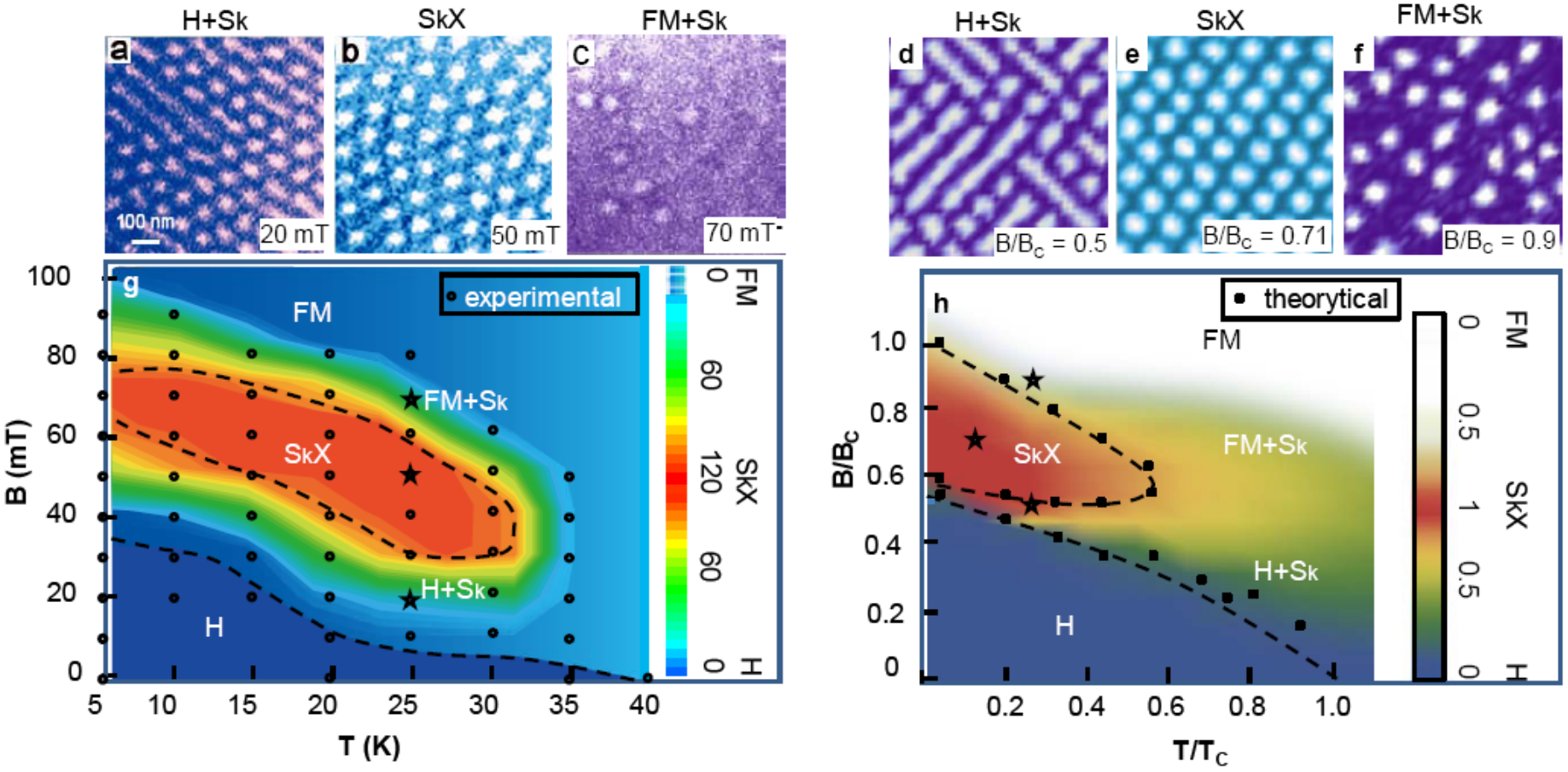

X. Z. Yu, Y. Onose, N. Kanazawa[2], J. H. Park, J. H. Han, Y. Matsui, N. N. Y. Tokura

Nature (2010)

Analogy to Abrikosov vortex lattice in superconductor

J. Han, J.Zang et al. PRB2010 c.f. A.N. Bogdanov

$$\mathcal{F}[\mathbf{z}] = 2J\sum_{\mu}\left(\mathbf{D}_\mu \mathbf{z}\right)^{+}\left(\mathbf{D}_\mu \mathbf{z}\right) - \mathbf{B}\cdot\mathbf{z}^{+}\boldsymbol{\sigma}\mathbf{z}.$$

$$\mathbf{D}_\mu = \partial_\mu - iA_\mu - i\kappa\sigma_\mu$$

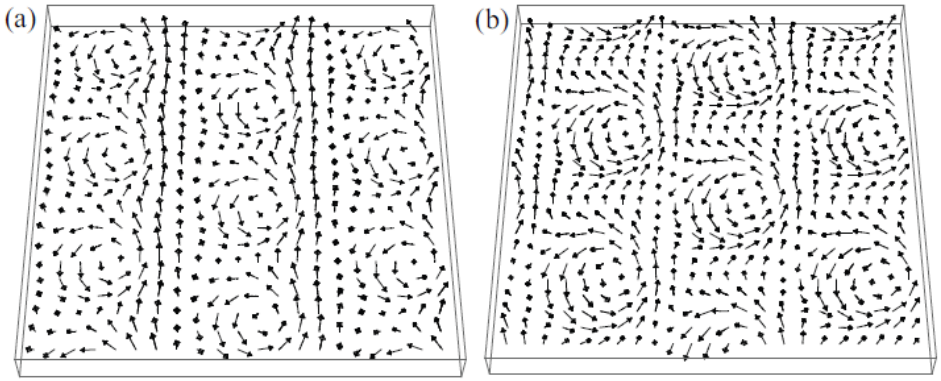

Vortex Lattice MC

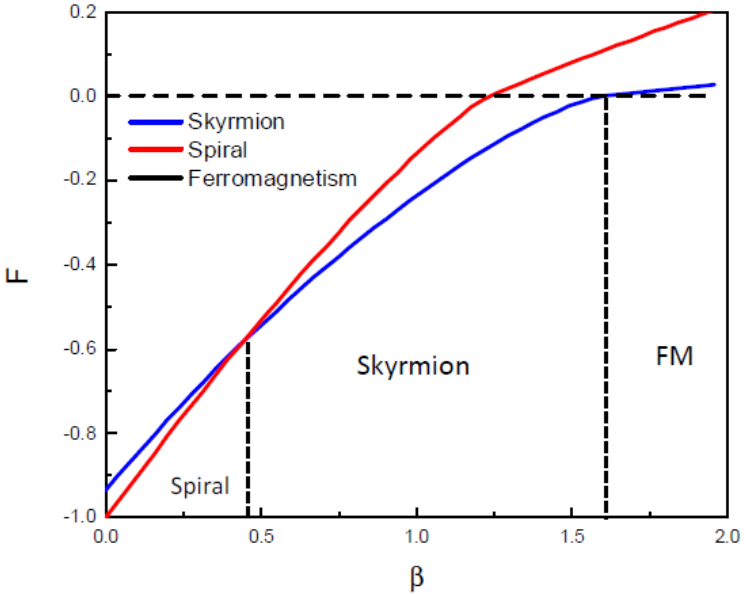

Magnetic field

Energy $\approx \kappa^2 / J$

Size $\approx J / \kappa$

Some considerations

Order estimation

$a \sim 4.5\text{Å} \quad D/J = 2\pi(a/\lambda) \approx 1/30$

$J \approx T_c \sim 30\text{K}$

$D^2/J = J(D/J)^2 \sim J/900 \sim 30\text{K}/900 \sim (1/30)\text{K}$

$\sim B_c \sim$ 40-80 mT

Thermal fluctuation and Lindeman criterion

$$\sqrt{<(\text{displacement})^2>} \approx (J/D)a \Rightarrow T_{\text{melting}} \approx J$$

Dynamics of SkX crystal

Acoustic mode of crystal $[X, Y] = i \Rightarrow \omega = ck^2$

Coupling to the current of conduction electrons $\vec{j} \cdot \vec{a}$

Coupled dynamics of conduction electrons and SkX

J.D.Zang, J.H. Han, M.Mostovoy, and N.N.

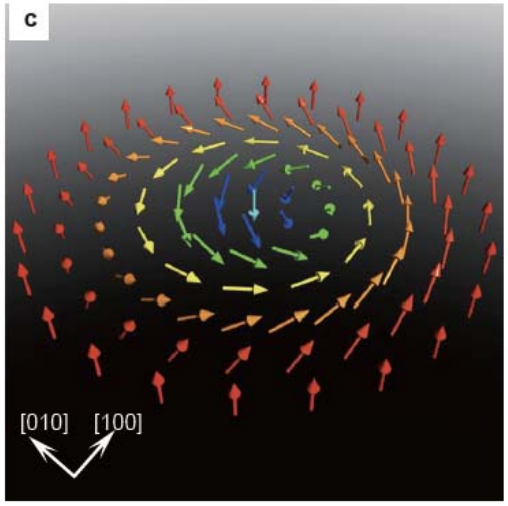

Effective EMF due to spin texture acting on conduction electrons

$$\begin{cases} e_i &= -\partial_i a_0 - \frac{1}{c}\dot{a}_i = \frac{\hbar}{2e}\left(\mathbf{n}\cdot\partial_i\mathbf{n}\times\dot{\mathbf{n}}\right), \\ h_i &= [\boldsymbol{\nabla}\times\mathbf{a}]_i = \frac{\hbar c}{2e}\delta_{iz}\left(\mathbf{n}\cdot\partial_x\mathbf{n}\times\partial_y\mathbf{n}\right), \end{cases}$$

$$\hat{H}_{\rm int} = -\frac{1}{c}\int d^3x \mathbf{j}\cdot\mathbf{a}$$ Coupling term

Lorentz force

$$\frac{\partial n}{\partial t} + \mathbf{v}\cdot\frac{\partial n}{\partial \mathbf{x}} - e\left(\mathbf{E} + \mathbf{e} + \frac{1}{c}[\mathbf{v}\times(\mathbf{H}+\mathbf{h})]\right)\cdot\frac{\partial n}{\partial \mathbf{P}} = -\frac{\delta n}{\tau}$$

Boltzmann equation

$$\dot{\mathbf{n}} = \frac{\hbar\gamma}{2e}(\mathbf{j}\cdot\boldsymbol{\nabla})\mathbf{n} - \gamma\left[\mathbf{n}\times\frac{\delta H_S}{\delta\mathbf{n}}\right] + \alpha\left[\dot{\mathbf{n}}\times\mathbf{n}\right]$$

LLG equation

Skyrmion-induced AHE (MnSi)

A. Neubauer et al, PRL 102 186602 (2009)

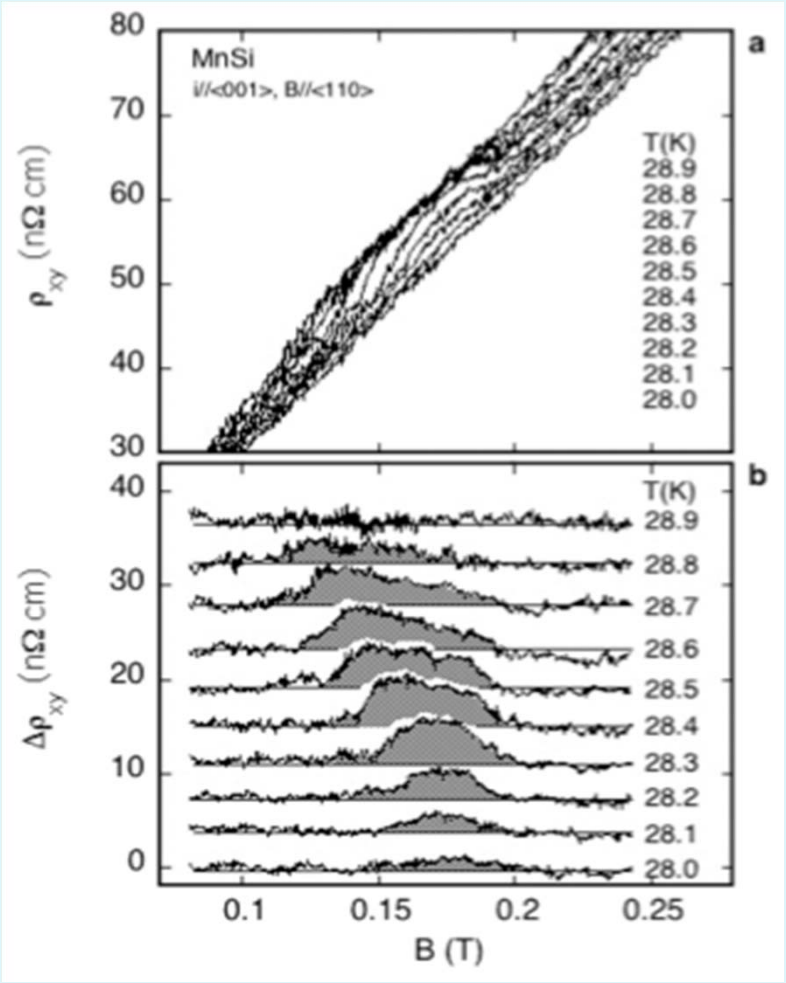

Finite but quite small

M. Lee, W. Kang, Y. Onose, Y. Tokura, and N. P. Ong, PRL (2009).

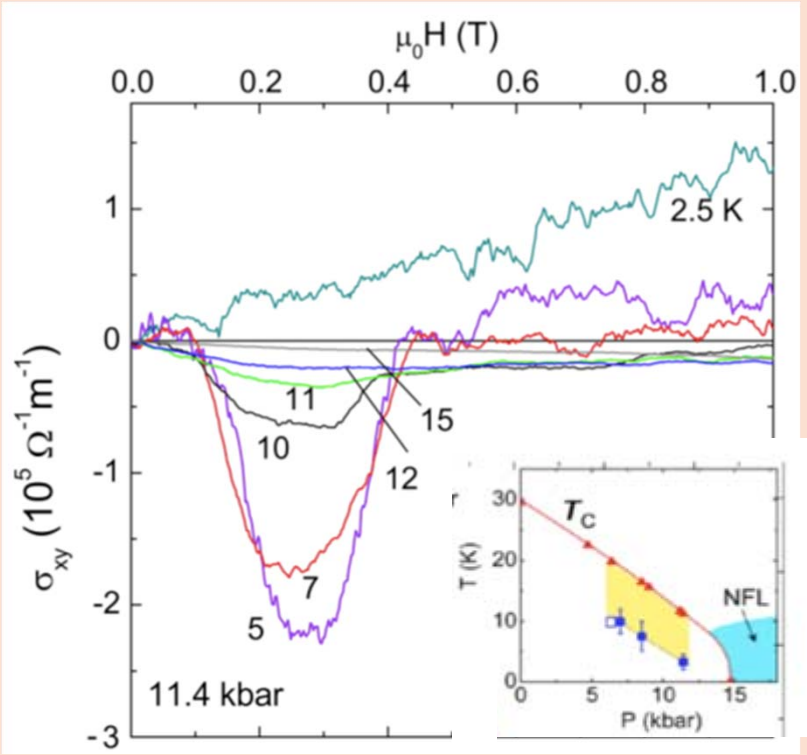

Relation to the magnetic structure??

Fictitious magnetic flux

©Y. Tokura

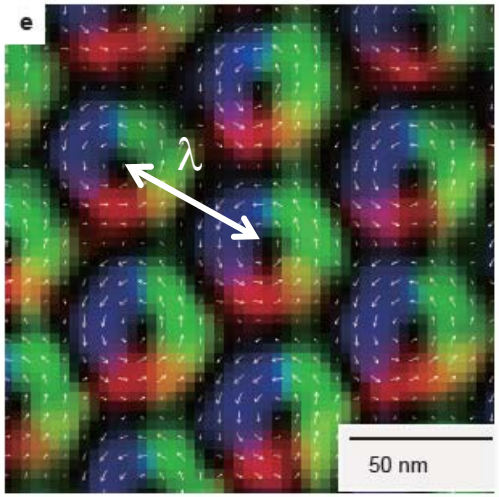

one flux quantum/(nm)^2~4000T !
(double-excahnge model)

$\Delta\rho_{yx} \propto \Phi$ (Sk density)

	λ(magnetic) [nm]	Φ(cal.) [T]		$\Delta\rho_{yx}$(topological) [nΩcm]
FeGe	70	1		indiscernible
MnSi	18	28		5
MnGe	3.0	1100	⇔	200
$Nd_2Mo_2O_7$ (reference)	~0.5	~40000		6000

Spin Transfer Torques in MnSi at Ultralow Current Densities

F. Jonietz,[1] S. Mühlbauer,[1,2] C. Pfleiderer,[1*] A. Neubauer,[1] W. Münzer,[1] A. Bauer,[1] T. Adams,[1] R. Georgii,[1,2] P. Böni,[1] R. A. Duine,[3] K. Everschor,[4] M. Garst,[4] A. Rosch[4]

17 DECEMBER 2010 VOL 330 SCIENCE

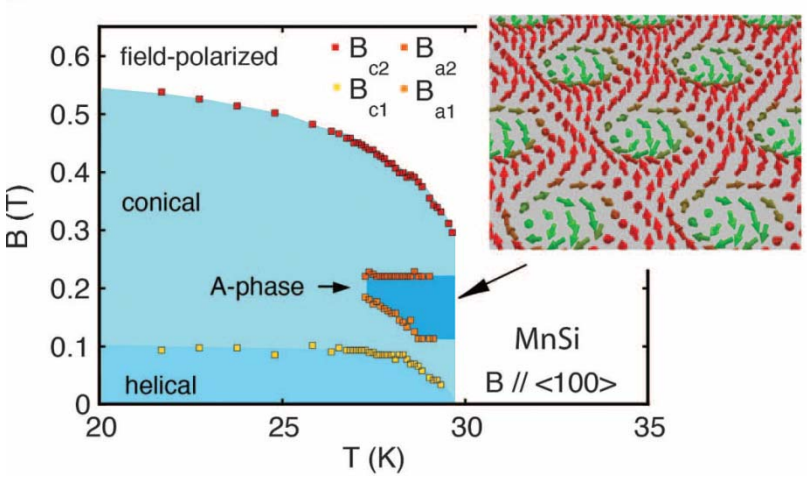

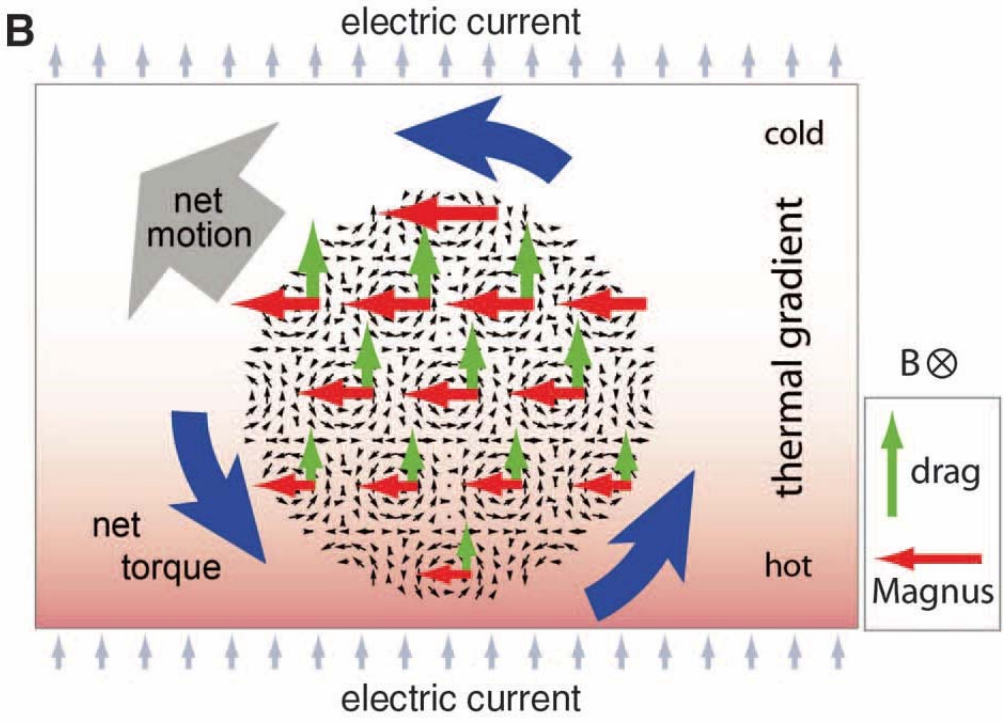

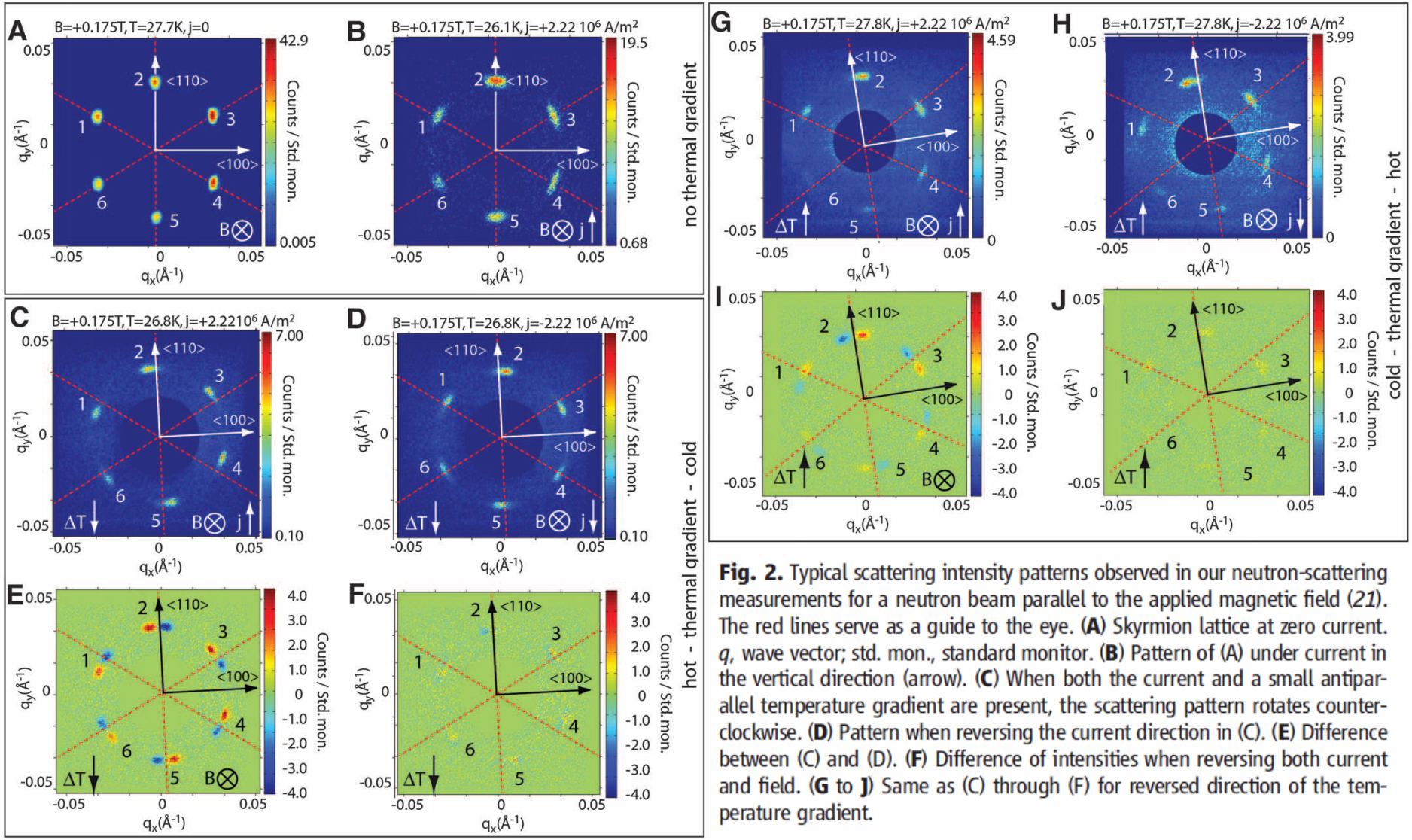

Fig. 2. Typical scattering intensity patterns observed in our neutron-scattering measurements for a neutron beam parallel to the applied magnetic field (*21*). The red lines serve as a guide to the eye. (**A**) Skyrmion lattice at zero current. *q*, wave vector; std. mon., standard monitor. (**B**) Pattern of (A) under current in the vertical direction (arrow). (**C**) When both the current and a small antiparallel temperature gradient are present, the scattering pattern rotates counterclockwise. (**D**) Pattern when reversing the current direction in (C). (**E**) Difference between (C) and (D). (**F**) Difference of intensities when reversing both current and field. (**G** to **J**) Same as (C) through (F) for reversed direction of the temperature gradient.

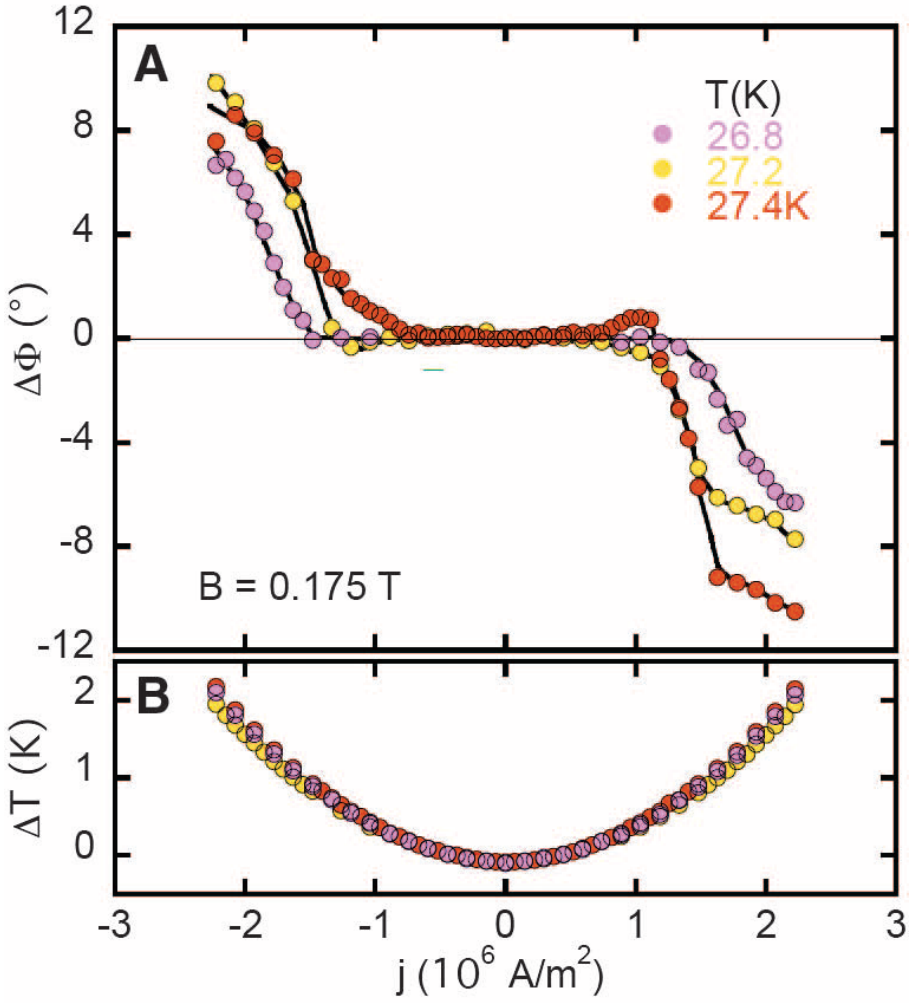
A
B
T(K)
26.8
27.2
27.4K
B = 0.175 T
ΔΦ (°)
ΔT (K)
j (10^6 A/m^2)
12
8
4
0
-4
-8
-12
2
1
0
-3
-2
-1
0
1
2
3

"Electromagnetic induction"

Moving magnetic flux produces the transverse electric field

$$\mathbf{e} = -\frac{1}{c}\left[\mathbf{V}_{\parallel} \times \mathbf{h}\right]$$

$$\Rightarrow \quad \frac{\Delta\sigma_{xy}}{\sigma} \approx -\frac{x}{2S+x}\frac{e\langle h_z\rangle\tau}{mc}$$

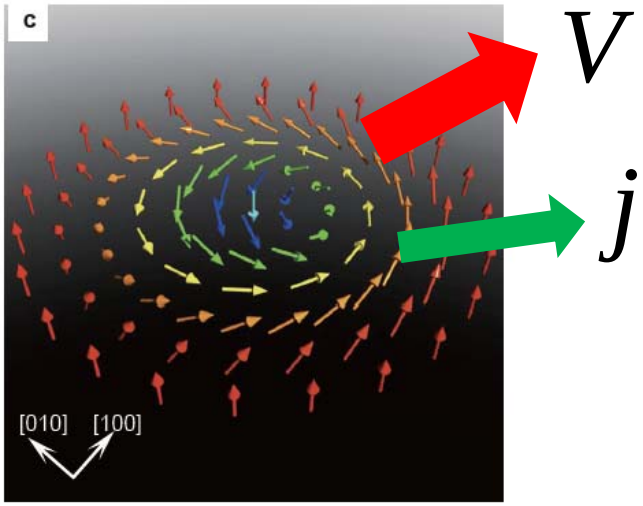

x Conduction electron number per site

S Spin quantum number

c.f. $\dfrac{\sigma_{xy}^{top}}{\sigma} = \dfrac{e < h_z > \tau}{mc}$

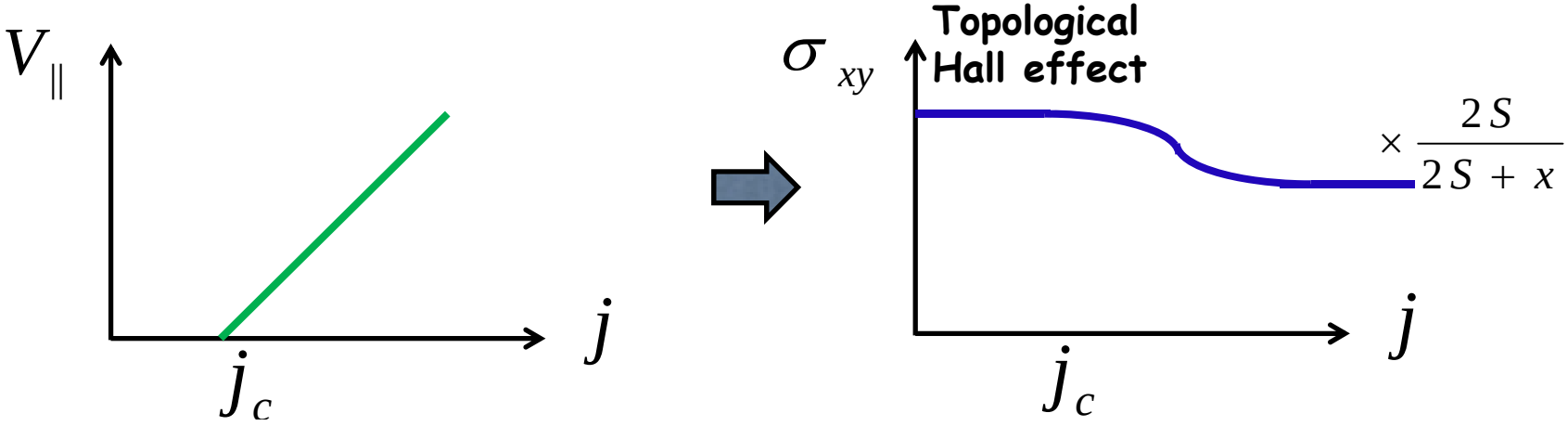

New dissipative mechanism for spin texture

$$\delta\dot{\mathbf{n}} = \frac{\hbar\gamma\sigma}{2e}(\mathbf{e}\cdot\boldsymbol{\nabla})\mathbf{n} = \frac{\hbar^2\gamma\sigma}{4e^2}\left(\mathbf{n}\cdot\partial_i\mathbf{n}\times\dot{\mathbf{n}}\right)\partial_i\mathbf{n}.$$

moving flux → electric field → induced current → dissipation

$$\Rightarrow \quad \alpha' = \frac{1}{(2S+x)}\frac{a^3\sigma}{\alpha_{\mathrm{fs}}\xi^2 c} \approx (k_F l)(a/\xi)^2$$

mean free path $l << \xi$ size of Skyrmion

α' does not require spin-orbit int. and can be as large as ~1
But ξ is determined by DM interaction.

Skyrmion Hall effect

Transverse motion of the Skyrmion as a back-action to the "electromagnetic induction"

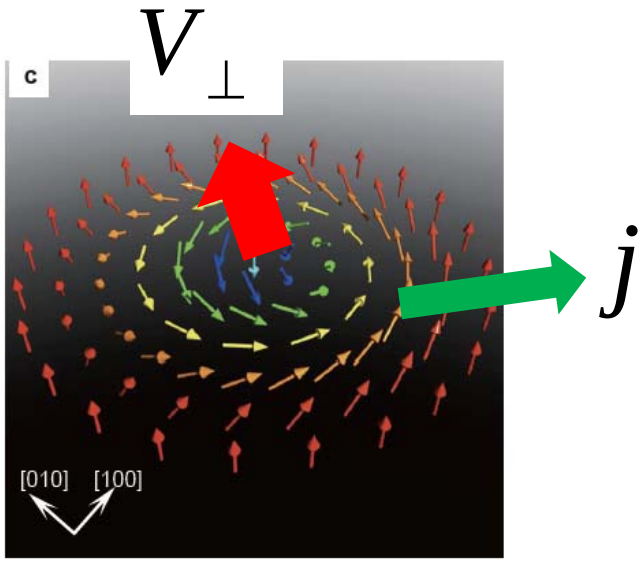

$$V_\perp \approx Q(\alpha + \alpha')(V_\parallel \times e_z)$$

$Q = \pm 1$ Skyrmion charge determined by the direction of the external magnetic field

"Hall angle" $\tan \theta_H \approx \alpha + \alpha'$

Collective dynamics of Skyrmion crystal

$$H_S = \int d^3x \left[\frac{J}{2a} (\nabla \mathbf{n})^2 + \frac{D}{a^2} \mathbf{n} \cdot [\nabla \times \mathbf{n}] - \frac{\mu}{a^3} \mathbf{H} \cdot \mathbf{n} \right]$$

$$\tilde{\mathbf{n}}(\mathbf{x}, t) = \mathbf{n}(\mathbf{x} - \mathbf{u}(\mathbf{x}, t))$$ u displacement field

$$H_{\rm lat} = d\eta J \int \frac{d^2x}{\xi^2} [(\nabla u_x)^2 + (\nabla u_y)^2]$$ elastic energy

$$S_{\rm BP} = \frac{dQ}{\gamma} \int dt \frac{d^2x}{\xi^2} (u_x \dot{u}_y - u_y \dot{u}_x)$$ Berry phase term

u_x and u_y are canonical conjugate

$$H_{\rm int} = d\frac{\hbar Q}{e} \int \frac{d^2x}{\xi^2} (u_x j_y - u_y j_x)$$ coupling to current

$$\Rightarrow \hbar\omega = \frac{\eta J}{(S + \frac{x}{2})} \frac{(ka)^2}{\left[1 + i\left(\frac{\alpha}{\eta} + \frac{\alpha'}{\eta'}\right)\right]}$$

"phonon" of SkX
- only one branch
- k^2 dispersion
- k^2 damping

Collective pinning of Skyrmion crystal

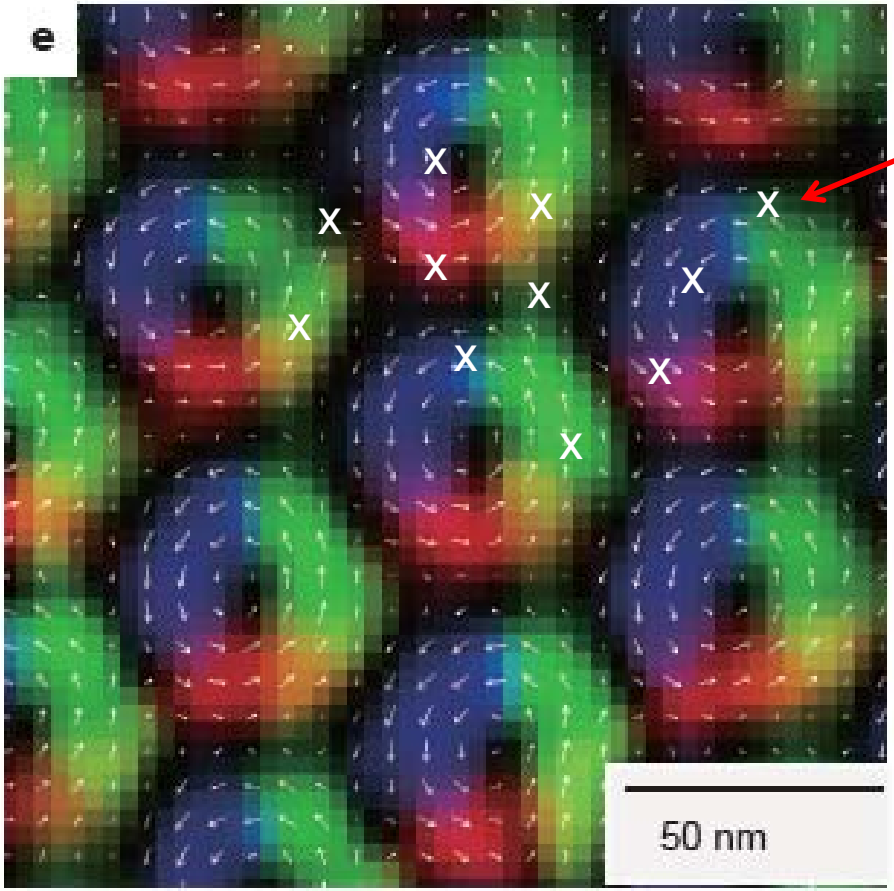

impurity

Inhomogeneity of
Impurity and skyrmion X-tal

→ Pinning and distortion

Theory of collective pinning

$E_S \sim \langle J \rangle \frac{d}{a}$ ene. of one Skyrmion $\delta J \sim J \frac{\delta n_i}{n_e}$ variation of kin. ene.

N_1 : # of impurities in a Sk $\langle N_1 \rangle = n_i 2\pi\xi^2 d$ d : film thickness

$\Rightarrow$ $\delta N_1 = \sqrt{N_1}$ Variation of #

$\Rightarrow$ $V_1 \sim \frac{J}{n_e 2\pi\xi^2 d}\sqrt{N_1} = \frac{J}{n_e a\xi}\sqrt{\frac{n_i d}{2\pi}}.$ Variation of one Skyrmion energy

$\Rightarrow$ $L \sim \frac{Jd}{aV_1}$ Competition between pinning and elastic energy determines the size L of domain for collective pinning

$\Rightarrow$

$$\hbar\omega_{\rm pin} \sim \frac{\hbar\gamma\xi^2}{d}\left\langle\frac{\partial^2 V}{\partial \mathbf{u}^2}\right\rangle \sim \frac{\hbar\gamma\xi^2}{d}\frac{V_0 L}{L^2\xi^2} = \frac{a^3}{dS}\frac{V_0}{L} \qquad V_0 = V_1/(2\pi\xi^2)$$

Pinning freq. of phonon

$$j_c \sim \frac{e}{\hbar}\frac{\xi^2}{d}\left\langle\frac{\partial V}{\partial \mathbf{u}}\right\rangle_{\rm steady\ state} \sim \frac{e}{\hbar}\frac{\xi V_0}{dL}$$

Critical current density for SkX motion

Estimates (for MnSi)

$n_e = 3.78 \cdot 10^{22}$ $x = n_e a^3 \sim 0.9$ $0.4\mu_B$ per Mn ion $S + \frac{x}{2} = 0.5$

$\frac{D}{J} = aQ \sim 0.1$ $J \sim 3\text{meV}$ $\xi \sim 77\text{Å}$

$\rho(0\text{K}) = 1.85\mu\Omega \cdot \text{cm}$ $d = 10\text{nm}$ $\langle N_1 \rangle \sim 700$

$$V_1 = 2\pi\xi^2 V_0 = \frac{J}{x}\frac{a}{\xi}\sqrt{\frac{x_i d}{2\pi a}} \sim 2 \cdot 10^{-2}\text{meV}$$

$$L \sim 5 \cdot 10^3$$

$$\alpha' \sim \frac{\hbar^2 \gamma \sigma}{4e^2}\frac{4\pi}{2\pi\xi^2} = \frac{1}{2\alpha_{\text{fs}}(S + x/2)}\frac{\sigma}{c}\frac{a^3}{\xi^2} \sim 0.1$$

$$\frac{e h_z \tau}{mc} = \frac{1}{\alpha_{\text{sf}} n_e \xi^2}\frac{\sigma}{c} = \frac{2(S + x/2)}{x}\alpha' \sim 0.09$$

$h_z \approx 6T$

$\hbar\omega_{\text{pin}} \sim 5 \cdot 10^{-11}\text{meV}$ $j_c \sim 0.2\text{A} \cdot \text{cm}^{-2}$

very small !!

Gauge field of spin textures in insulating magnets

M.Mostovoy, K.Nomura and N.N. PRL2011

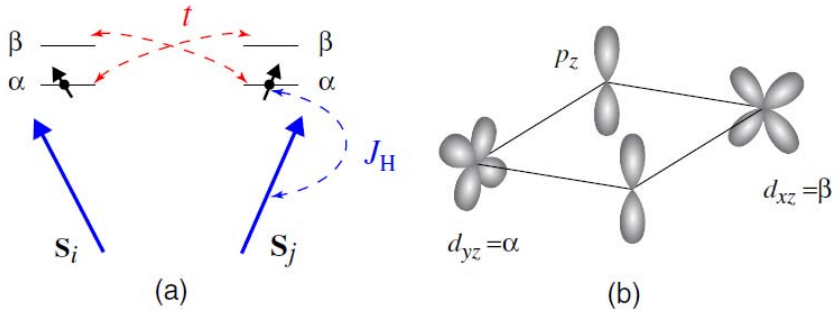

Spin dynamics in the intermediate virtual states of the exchange int.
→ Coupling between gauge field e and E
→ Multi-orbital Mott insulator

$$L_E = -\int d^3x T^{ab} E_a e_b(\mathbf{x}, t),$$

$$T^{ab} = \frac{e}{(U')^3}\frac{1}{v}\sum_j |t_{j\beta,i\alpha}|^2 (x_j^a - x_i^a)(x_j^b - x_i^b)$$

Finite even without inversion asymmetry or spin-orbit interaction

A physical consequence

Moving spin texture produces the electric polarization $\mathbf{P} \propto gQ[\hat{\mathbf{z}} \times \dot{\mathbf{R}}]$

Example: a Skyrmion in a confining potential $U = \frac{K}{2}(R_x^2 + R_y^2)$

$$G_{ij}\left(\dot{R}_j + \frac{g}{\tilde{S}}\dot{E}_j\right) + \alpha\Gamma_{ij}\dot{R}_j = -\frac{\partial U}{\partial R_i} \qquad G_{xy} = -G_{yx} = 4\pi Q$$

Applying a rotating electric field $\mathbf{E}(t) = E_\omega(\cos\omega t, -\sigma \sin\omega t)$

⇨ Different resonant response at $\Omega = \frac{K}{4\pi|Q|}$

$$X_\Omega = \frac{gE_\Omega}{2\tilde{S}} \begin{cases} \frac{i}{\Omega\tau} & \text{for } \sigma = +q \\ -\frac{1}{2-i\Omega\tau} & \text{for } \sigma = -q, \end{cases}$$

Topological phenomena associated with emergent electromagnetism

Theory

Experiment

Anomalous Hall effect (AHE)

E.Hall (1881)

Karplus -Luttinger (1954)

Berry Phase (2002)

QAHE (2003)

Spin Hall effect (SHE)

D'yakonov-Perel (1971) extrincis

Intrinsic SHE (2003)

Awschalom (2004)

Topological Insulators

Kane-Mele (2005)

L.Molenkamp -S.C.Zhang (2007)

Correlated TI in oxide Superlattice (2011)

Rashba TI (2012)

Hall effect of light

(2004)

Hosten-Kwiat(2008)

Deformed X-tal(2006)

(2010)

Multiferroics

T.Kimura (2003)

Spin current (2005)

M.Kenzelmann (2005)

Skyrmion X-tal

A.N.Bogdanov(1989)

C.Pfleiderer (2009)

2D SkX(2009)

X.Z.Yu (2010)

Magnon Hall effect

(2010)

Tokura (2010)

Left-handed magnon

(2008)

Spin-orbit Echo

(2012)

Conclusions
- Emergent electromagnetism

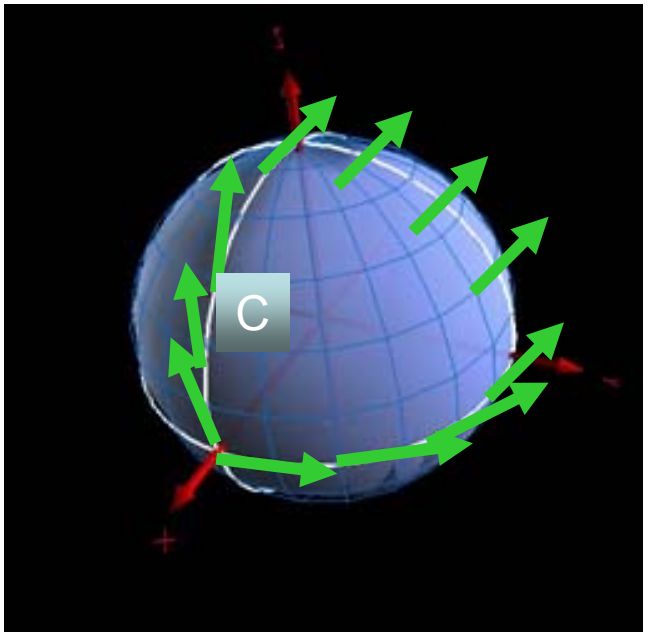

1. Projection onto Hilbert sub-space

   → Berry phase and gauge field

   → spin-orbit, spin current physics,

   3 sources of U(1) e.m.f.

2. Various Hall effects driven by

   Berry curvature

3. Global topological structures Topological materials

   edge/surface physics electron fractionalization